IDAHO TRANSPORTATION DEPARTMENT

RESEARCH REPORT

Development of Gyratory Stability Index to Evaluate Variation of RAP Content and Rutting Resistance of Asphalt Mixtures

RP 280

By

Emad Kassem
Fouad Bayomy
Mohammed Abu Saq
Ahmed Muftah
Austin Corley
University of Idaho

Prepared for

Idaho Transportation Department
ITD Research Program, Contracting Services
Highways Construction and Operations

August 2021

Disclaimer

This document is disseminated under the sponsorship of the Idaho Transportation Department and the United States Department of Transportation in the interest of information exchange. The state of Idaho and the United States Government assume no liability of its contents or use thereof.

The contents of this report reflect the view of the authors, who are responsible for the facts and accuracy of the data presented herein. The contents do not necessarily reflect the official policies of the Idaho Transportation Department or the United States Department of Transportation.

The state of Idaho and the United States Government do not endorse products or manufacturers. Trademarks or manufacturers' names appear herein only because they are considered essential to the object of this document.

This report does not constitute a standard, specification, or regulation.

Technical Report Documentation Page

1. Report No. FHWA-ID- 21-280	2. Government Accession No.	3. Recipient's Catalog No.
4. Title and Subtitle Development of Gyratory Stability Index to Evaluate Variation of RAP Content and Rutting Resistance of Asphalt Mixtures		5. Report Date August 2021 6. Performing Organization Code
7. Author(s) Emad Kassem, https://orcid.org/0000-0002-4331-6692 Fouad M.S. Bayomy, Mohammed Abu Saq, Ahmed Muftah, and Austin Corley.		8. Performing Organization Report No. [Billing code]
9. Performing Organization Name and Address University of Idaho 875 Perimeter Drive MS 1022, Moscow, ID 83844-1022		10. Work Unit No. (TRAIS) 11. Contract or Grant No. UI-19-03
12. Sponsoring Agency Name and Address Idaho Transportation Department (SPR) Highways Construction and Operations, Contracting Services, Research Program POBox 7129 Boise, ID 83707-7129		13. Type of Report and Period Covered Final Report 01/01/2019 - 08/31/2021 14. Sponsoring Agency Code RP 280
15. Supplementary Notes Project performed in cooperation with the Idaho Transportation Department and Federal Highway Administration.		

16. Abstract

ITD Research Report RP 175 developed an algorithm for determining a Gyratory Stability (GS) for asphalt mixtures based on the Servopac gyratory compactor. The GS describes the ability of asphalt mixtures to resist rutting, and it can be determined during the mix design stage using the gyratory compaction data. This study developed a modified algorithm for GS applicable to Pine Gyratory compactor model AFG2AS which is used by ITD districts. In addition, this study investigated the use of the GS, other gyratory compaction indices, and performance tests to detect the variations in mix composition. The researchers prepared and tested laboratory-mixed laboratory-compacted (LMLC) mixes and plant-mixed laboratory-compacted (PMLC) mixes obtained from new paving projects. The LMLC and PMLC were selected to cover a wide range of variables including aggregate type, binder type and content, RAP content and source, and mix design. The researchers conducted performance testing including cracking, rutting, and moisture damage. The GS, construction densification index (CDI), and laboratory compaction index (LCI) were found sensitive to the binder content; however, all the compaction indices were less sensitive to the change in the RAP content and binder grade. The GS and CDI decreased with the increase in binder content while the LCI increased with the increase in binder content which indicates less energy is needed for compaction. There were fair correlations between the APA rut depth and both GS and CDI; however, the LCI showed better correlation with the APA rut depth. Mixtures with higher resistance to densification (low LCI) were found to have higher resistance to rutting. The cracking performance results demonstrated that the $IDT_{Modulus}$ and $IDT_{Strength}$ indicators were able to capture the change in binder content, binder grade, and RAP content. The source of RAP was found to have a significant impact on cracking resistance. The cracking performance of mixtures prepared with stiffer RAP materials can be improved by adjusting the binder content.

17. Key Words Reclaimed Asphalt Pavement, RAP, APA, and Hamburg, Rutting, Cracking, Moisture Damage		18. Distribution Statement Copies available from the ITD Research Program	
19. Security Classification (of this report) Unclassified	20. Security Classification (of this page) Unclassified	21. No. of Pages 187	22. Price None

Acknowledgments

This project is funded by Idaho Transportation Department (ITD) from SPR funds. It is performed in cooperation with ITD. The authors would like to acknowledge all members of the research project Technical Advisory Committee (TAC) for their valuable feedback and cooperation all over the project tasks. The authors would like also to acknowledge the support from the National Institute for Advanced Transportation Technology (NIATT) and the Department of Civil and Environmental Engineering at the University of Idaho. We also acknowledge the help of Mr. Dio Permadi in sieving materials and preparing samples in the laboratory.

Technical Advisory Committee

Each research project is overseen by a Technical Advisory Committee (TAC), which is led by an ITD project sponsor and project manager. The TAC is responsible for monitoring project progress, reviewing deliverables, ensuring that study objectives are met, and facilitating implementation of research recommendations, as appropriate. ITD's Research Program Manager appreciates the work of the following TAC members in guiding this research study.

- Project Sponsor: John P. Bilderback, P.E.
- Project Manager: John P. Bilderback, P.E. (formerly Mark Wheeler, P.E., retired)
- TAC Members: Mark Wheeler (retired), Kyle Holman, Chad Clawson, Eric Kokernak
- FHWA-Idaho Advisor: Kyle Holman, P.E.

Table of Contents

List of Tables

List of Figures

List of Abbreviations and Acronyms

AASHTO..... American Association of State Highway and Transportation Officials

APA ..... Asphalt Pavement Analyzer

CDI ..... Construction Densification Index

CEI..... Compactability Energy Index

CFI..... Compaction Force Index

COV..... Coefficient of Variation

FHWA..... Federal Highway Administration

FI..... Flexibility Index

FN ..... Flow Number

GS ..... Gyratory Stability

Gf..... Fracture Energy

Gsb..... Bulk specific Gravity of Aggregates

Gmm ..... Maximum Specific Gravity of Asphalt Mixture

Gmb ..... Bulk Specific Gravity of Asphalt Mixture

HMA..... Hot Mix Asphalt

IDEAL-CT ..... Indirect Tensile Asphalt Cracking Test

IDT ..... Indirect Tensile

ITD ..... Idaho Transportation Department

LCI..... Laboratory Compactability Index

LMLC ..... Laboratory-Mixed Laboratory-Compacted

LP ..... Locking Point

NMAS..... Nominal Maximum Aggregate Size

PG ..... Performance Grade

PLMLC ..... Plant-Mixed Laboratory-Compacted

RAP ..... Recycled Asphalt Pavement/Reclaimed Asphalt Pavement

SCB..... Semi-Circular Bending

SD ..... Standard Deviation

TAC ..... Technical Advisory Committee

TSR..... Tensile Strength Ratio

UI ..... University of Idaho

VFA ..... Voids Filled with Asphalt

VMA..... Voids in Mineral Aggregate

WEI ..... Workability Energy Index

WeibullCRI..... Weibull Cracking Resistance Index

Executive Summary

ITD Research Report RP 175 developed an algorithm for determining a Gyratory Stability (GS) index for asphalt mixtures based on the Servopac gyratory compactor. The GS describes the ability of asphalt mixtures to resist rutting, and it can be determined during the mix design stage using the gyratory compaction data. The GS was recommended as a screening tool during the mix design to evaluate the resistance of asphalt mixtures to rutting. However, the current GS algorithm was developed for the Servopac gyratory compactor. This study developed a modified algorithm for GS applicable to Pine Gyratory compactor model AFG2AS, which is now used by ITD districts. In addition, this study investigated the use of the GS, other gyratory compaction indices, and performance tests to detect the variability in mix composition (e.g., RAP content, RAP source, binder content, binder grade). Several stability and compaction indices including the GS, laboratory compaction index (LCI), construction densification index (CDI), compaction force index (CFI), locking point (LP), compactability energy index (CEI), and workability energy index (WEI) were examined.

The researchers prepared and tested laboratory-mixed laboratory-compacted (LMLC) mixes and plant-mixed laboratory-compacted (PMLC) mixes obtained from new ITD paving projects. The LMLC and PMLC were selected to cover a wide range of variables including aggregate type, binder type and content, RAP content and source, mix design, etc. Several different batches of loose mix were sampled throughout construction to examine changes in mix performance.

The researchers conducted performance testing on LMLC and PMLC mixes including mix stability, cracking, rutting, and moisture damage. Cracking resistance was evaluated using several monotonic cracking indicators used to analyze the load-displacement curve from the indirect tension (IDT) test. These cracking performance indicators included IDEAL-CT_{Index}, cracking resistance index (CRI), N_{flex}, $Weibull_{CRI}$, fracture energy (G_f), $IDT_{Strength}$, $IDT_{Modulus}$, and flexibility index (FI). In addition, the researchers conducted the Hamburg wheel tracking test (HWTT) and asphalt pavement analyzer (APA) to evaluate the rutting resistance of the asphalt mixes. In addition, this study evaluated the moisture susceptibility using the Lottman procedure to examine the effect of change in mix composition and the use of anti-stripping agents on moisture damage of selected mixtures.

Key Findings

The key findings of this study are summarized below:

- Based on a comprehensive evaluation of the results of stability and compaction indices examined in this study, the GS, CDI, and LCI were found sensitive to binder content; however, all the compaction indices were less sensitive to the change in the RAP content and binder grade. The GS and CDI decreased with the increase in binder content while the LCI increased with the increase in binder content which indicates less energy is needed for compaction.

- The results demonstrated that there were changes in the CDI, GS, and LCI among various batches of some PMLC mixes which indicates variations in mix characteristics due to segregation or adjustment during mix production.

- The researchers developed an Excel spreadsheet to facilitate the calculations of the GS and LCI and incorporated these calculations into the Pine *PineShear+* Excel spreadsheet. The utility allows the user to import the compaction data collected from the Pine compactor and provides charts for the GS and LCI like the ones included in the *PineShear+* Excel spreadsheet.

- The rutting performance evaluation using the APA rut test and HWTT showed that all LMLC and PMLC mixes had good resistance to rutting. The APA and HWTT rut depth increased with the increase in binder content, as expected. However, there was a statistically significant difference in the APA rut depth results, while the difference in the HWTT results was not statistically significant over the range of binder content considered in this study (i.e., 4.25 percent to 5.75 percent).

- There were fair correlations between the APA rut depth and both GS and CDI. Higher GS and CDI values indicate higher resistance to densification and were found to be associated with less rutting. The LCI showed a better correlation with the APA rut depth (R^2 = 0.64). Mixtures with higher resistance to densification (low LCI) were found to have higher resistance to rutting.

- The use of RAP had an overall negative effect on moisture susceptibility and resulted in lower tensile strength ratio (TSR) values which can be improved by adding liquid anti-stripping agents.

- The cracking performance results demonstrated that the $IDT_{Modulus}$ and $IDT_{Strength}$ indicators were able to capture the change in binder content, binder grade, and RAP content. Other indices including IDEAL-CT_{Index}, $Weibull_{CRI}$, CRI, and N_{flex} factor were sensitive to binder content and RAP content from the second source of RAP. Overall, the cracking resistance improved with the increase in binder content as expected.

- All mixtures prepared at different RAP contents (up to 50 percent) from a first source of RAP had good resistance to cracking; however, mixtures prepared with a second source of RAP did not show this trend. The cracking resistance decreased with an increase in RAP content for mixtures prepared with virgin binders of different grades. The source of RAP was found to be a significant factor in this study, which agrees with the findings of previous research (Sabahfar et al. 2014; Shu et al. 2008).

- The results illustrated that the cracking performance of mixtures prepared with RAP (up to 50 percent) from a second source of RAP can be improved by increasing the virgin binder content. This indicates the importance of conducting a balanced mix design when incorporating RAP materials in asphalt mixes.

- The cracking resistance evaluation of all PMLC mixes showed good performance. Also, there were some variations in the cracking resistance among PMLC batches and in some cases such variation was

statistically significant. The variation in cracking resistance could be an indication of change in mix properties due to segregation or adjustments during mix production.

1. Introduction

Problem Statement

ITD Research Report RP 175 developed an algorithm for determining an index called GS for asphalt mixtures based on the Servopac gyratory compactor. The GS describes the ability of asphalt mixtures to resist rutting, and it can be determined during the mix design stage using the gyratory compaction data. The GS was found to have good correlation with rutting resistance and was recommended as a screening tool during mix design. However, the current GS algorithm was developed for the Servopac gyratory compactor. Feedback from experts indicated that the GS value as determined when using the Servopac is not a unique number for the mix, but rather dependent on the type of compactor. Currently, ITD has adopted the use of Pine gyratory compactor in all districts as well as at headquarter laboratories. Therefore, there is a need to modify the existing algorithm for GS to make it applicable to the Pine gyratory compactor.

This study also examined the sensitivity of various compaction and stability indices including GS to the change in mix composition (e.g., RAP content, RAP source, binder content, binder grade). Such indices can be used as quick indicators of changes in mix production in the field. In addition, this study examined the sensitivity of various cracking and rutting tests and performance indicators to the change in mix composition and studied the variability and correlation between different performance indicators. Furthermore, the team evaluated the moisture susceptibility of asphalt mixtures using the Lottman procedure to study the effect of change in mix properties and the use of anti-stripping agents on moisture damage.

Project Goal and Objectives

The main goal of this study is to investigate the use of the GS, other gyratory compaction indices, or performance tests to detect the variability in mix composition (e.g., RAP content, RAP source, binder content, binder grade). There are five specific objectives that are identified as follows:

- Develop a Gyratory Stability index for asphalt mixtures using the Pine compactor.
- Evaluate the sensitivity of the GS and other compaction indices to variations in mix composition.
- Examine the sensitivity of various cracking and rutting tests and performance indicators to the change in mix composition.
- Study the variability and correlation between various cracking and rutting performance indicators.
- Develop an Excel spreadsheet to facilitate the calculations of GS and other promising compaction and stability indices.

Research Tasks

Six tasks were performed to achieve the above-mentioned research objectives. The tasks performed in the study are described in the following section.

Task 1: Literature Review

Under this task, the research team conducted a thorough review to document the findings of recent studies on the following topics:

- Different stability and compaction indices used to analyze the laboratory compaction data of asphalt mixes and correlation with mix performance.
- Sensitivity of various stability and compaction indices to mix composition (e.g., RAP content, RAP source, binder content, binder grade, aggregate size).
- Incorporating reclaimed asphalt pavement (RAP) in asphalt mixtures and its impact on pavement performance.
- Characterization of RAP and design criteria of mixes with low and high RAP content.
- Laboratory and field performance of mixes contain high RAP content.
- Current practice of different DOTs on incorporating RAP in HMA.

Task 2: Development of Testing Matrix and Asphalt Mixture Preparation

In this study, the researchers prepared and tested laboratory-mixed laboratory-compacted (LMLC) mixes and plant-mixed laboratory-compacted (PMLC) mixes obtained from new ITD paving projects. The LMLC and PMLC were selected to cover a wide range of variables including aggregate type, binder type and content, RAP content and source, mix design, etc. The LMLC mixes were tested to evaluate the mix performance in terms of mix stability, cracking and rutting resistance, and moisture damage. Several batches of loose mix were sampled throughout the construction of each project. Each batch was collected at different times during construction to examine changes in mix production using the stability and compaction indices as well as rutting and cracking performance tests. These PLMC mixes included different mix designs, nominal maximum aggregate sizes (NMAS), binder grades, binder contents, and RAP contents. The researchers prepared and compacted 6-inch diameter and 4-inch-thick gyratory specimens for GS and compaction indices calculations and other samples for rutting (APA and HWTT) and cracking performance tests. During laboratory compaction, the researchers recorded and obtained the compaction curves (change of density versus number of gyrations) and measured the percent air void of each test sample after compaction. This data was used to calculate the GS and other compaction indices.

Task 3: Develop Algorithm for Calculating the Gyratory Stability (GS)

The researchers developed an algorithm to calculate the GS index from the compaction curve data specific to Pine SGC. Previous studies divided the compaction curve into two parts; Part A and Part B (Bayomy et al. 2002; Bahia et al.; 2003; Dessouky et al. 2004; Abu Abdo et al. 2010). Part A of the compaction curve has a steeper slope compared to Part B. The energy applied during Part A is consumed in increasing the density of the mix while most of energy applied in Part B is used in increasing the shear strength of the materials by adjusting the aggregate orientation. Therefore, the mix stability is assessed by calculating the accumulated shear energy that is dissipated in the sample during Part B of the compaction curve. The GS is calculated as a function of shear force at mid-height of the test sample and the change in sample height and over a range of number of gyrations. The GS is developed for the Pine SGC model AFG2AS that is used by most of ITD districts and the central materials laboratory.

Task 4: Conduct Laboratory Performance Tests

The researchers conducted several performance tests to evaluate the rutting and cracking performance as well as moisture susceptibility of asphalt mixtures. The rutting tests included both the APA rut test and the HWTT. The materials laboratory at the University of Idaho has a new APA Jr that was used to conduct both tests. The HWTT is used to evaluate rutting resistance and moisture susceptibility of asphalt mixes. The HWTT specimens are submerged in a water bath at a controlled temperature of 50^{o}C. The rut depth is measured along the roller path during the test, and generally the test is performed for 20,000 passes. Many states have adapted the AASHTO T324, Standard Method of Test for Hamburg Wheel-Track Testing of Compacted Asphalt Mixtures. In addition, The APA Jr was also used to measure the rutting in accordance with AASHTO T340, Standard Method of Test for Determining Rutting Susceptibility of Hot Mix Asphalt (HMA) using the Asphalt Pavement Analyzer. The test specimen is preheated before testing at least for 6 hours and the test temperature is selected based on the performance grading (PG) temperature of the virgin binder. The rut depth is recorded after each cycle and the average rut depth is reported after 8,000 cycles.

The research team also evaluated the cracking resistance of the test samples using the Indirect Tension (IDT) test in accordance with ASTM D693, Standard Test Method for Indirect Tensile (IDT) Strength of Asphalt Mixtures. In this test, a vertical compressive load is applied on a cylindrical test specimen at a constant rate of 50 plus/minus 5 mm per minute until failure. Several monotonic cracking performance indicators can be calculated from the IDT load-displacement curve including IDEAL-CT_{Index}, Cracking Resistance Index (CRI), N_{flex} factor, $Weibull_{CRI}$, Fracture Energy (G_f), $IDT_{Strength}$, $IDT_{Modulus}$, and Flexibility Index (FI). In addition, the researchers tested selected samples in wet condition to calculate the tensile strength ratio (TSR) and evaluate the moisture susceptibility of the test mixtures. The test samples were conditioned in accordance with the Lottman procedure (AASHTO T 283).

Task 5: Develop Software to Calculate Gyratory Stability (GS)

Under this task, the researchers developed an Excel spreadsheet to facilitate the calculations of the GS and LCI, which was found to have a good correlation with APA rutting. These two spreadsheets were added to the current Excel spreadsheet used to analyze the compaction data from Pine SGC. The Excel-based utility allows the user to import the compaction data collected from the Pine SGC and enter required information (e.g., weight of the sample, diameter of the sample, theoretical maximum specific gravity of the mix, and bulk specific gravity). The Excel spreadsheet provides charts for the GS and LCI like the ones included in the Pine Excel spreadsheet. These charts enable the user to compare various groups of mixtures to assess any changes in GS and LCI which may trigger change in mix production or segregation. Also, the user can compare the GS and LCI values for up to four different mixes in the same plot.

Task 6: Analyze Laboratory Test Results and Develop Recommendations

Under this task, the researchers evaluated sensitivity of various compaction and stability indices including the GS to mix composition (e.g., RAP content, RAP source, binder content, binder grade). This assessment provided comprehensive evaluation of the applicability of using the compaction and stability indices to detect variation in mix production or segregation during the plant production and placement in the field. In addition, they examined the correlation between APA and HWTT rut depth and the compaction and stability indices. The selected indices can be used as indicators of rutting resistance of asphalt mixture during the mix design stage.

The researcher team also examined the sensitivity of various cracking and rutting tests and performance indicators to the change in mix composition and studied the variability and correlation between various cracking and rutting performance indicators. They also assessed the cracking and rutting performance of mixes currently produced in Idaho and examined variation in mix production during project construction. Furthermore, the TSR results were analyzed to study the effect of mix properties and the use anti-stripping agents on moisture damage in accordance with the Lottman procedure.

Report Organization

This report documents the research methodology, presents the results and analysis, summarizes the findings, and provides recommendations for future studies and implementation. The report has seven chapters. Chapter 1 provides background and problem statement, project goal and objectives, research tasks, and report organization. Chapter 2 presents the main findings of the literature review on the performance of mixes with high RAP contents, mix stability indices, current practice of using RAP in HMA. Chapter 3 presents the methodology and testing protocols, testing matrix and design criteria of the test mixtures. Chapter 4 discusses the development of a mathematical model to calculate the GS from the compaction curve data specific to Pine SGC Model AFG2. In addition, this chapter investigates the sensitivity of various compaction and stability indices to mix composition. Also, it discusses the development of the Excel spreadsheets to facilitate the GS and LCI calculations.

Chapter 5 presents the results of rutting performance measured using the APA rut test and HWTT for the LMLC and PMLC. It examines the sensitivity of these tests to the change in mix characteristics and the correlation between the rutting performance and mix stability and compactability. Furthermore, it evaluates the moisture susceptibility of selected test mixtures. Chapter 6 provides comprehensive evaluation of cracking performance of the test mixtures and examines the sensitivity of various cracking performance indicators to the change in mix composition and the variability and correlation between various cracking and performance indicators. Finally, Chapter 7 summarizes the findings and conclusions of this study and provides recommendations for future research and implementation.

2. Literature Review

This chapter presents a summary of the main findings of the literature review of relevant studies on incorporating RAP in HMA and its impact on pavement performance. The topics reviewed included characterization of RAP, design criteria of mixes with low and high RAP content, and laboratory and field performance of mixes contain high RAP content. In addition, the researchers reviewed several research studies on asphalt mix stability, evaluation of different compaction indices, and effect of NMAS, RAP content, asphalt binder content and grade on mix characteristics during compaction.

Introduction

In the United States (U.S.), RAP has been widely used as a recycled material for its environmental and economic benefits. The asphalt pavement industry has a prolonged history of integrating RAP and other recycled materials in pavement construction. A recent survey conducted in a partnership between the National Asphalt Pavement Association (NAPA) and Federal Highway Administration (FHWA), showed a remarkable impact of RAP on cutting costs and reducing the greenhouse gas emissions (NAPA 2018). The survey revealed that more than 89.2 million tons of RAP used in asphalt mixes in 2019. As a result, about 2.4 million metric tons of carbon dioxide (CO_2) spared from the atmosphere. This survey has been conducted on annual bases since 2009, and the data shows that there is an increasing implementation of RAP in HMA by state highway agencies. Figure 1 shows a timeline of the total estimated amount of RAP and the average percentage of RAP used by various transportation agencies from 2009 to 2018. The average percentage of RAP used by all industry sectors increased to 21.1 percent in 2018 which is the max percentage since the survey was initiated in 2009 (NAPA 2018).

Several studies evaluated the amount of RAP that can be incorporated in HMA without compromising the performance. McDaniel et al. (2012) suggested that mixes with high RAP content up to 50 percent can be achieved under Superpave design criteria (McDaniel et al. 2012). The challenging part for designing high RAP mixes is to meet the specifications for the volumetric mix design criteria due to the presence of significant amount of fine aggregate materials in the RAP. A higher percentage of fines in RAP, triggered by the crushing and milling process of old pavements, could lead to aggregate degradation (McDaniel et al. 2012). Asphalt mixes with high RAP contents require adjustments in the PG of the virgin binder in the mix due to the stiffer RAP binder caused by aging. McDaniel et al. (2012) also noted that, based on indirect tensile strength testing, mixes with more than 20 percent RAP content tend to have increased stiffness which may reduce the resistance of the mix to cracking at low temperatures (McDaniel et al. 2012).

Beeson et al. (2011) conducted a study to determine the maximum amount of RAP that can be added to the HMA. The researchers investigated 33 samples of asphalt binder that were recovered from RAP mixes taken across the state of Indiana. The samples were characterized for low temperature and high temperature grade. In addition, new asphalt binder properties were obtained from more than 200 Quality Acceptance (QA) samples that covered three -22 grades and three -28 grades. The data concluded that up to 22 percent RAP can be added to asphalt mixtures before changing the low temperature grade of a -22

binder and up to 40 percent RAP can be added to a mixture if the virgin binder grade is one grade lower than what is required per traffic and environmental demands. It was also concluded that it is important to evaluate high RAP mixes in terms of virgin binder replacement rather than the percent of the aggregate weight added. For instance, if the amount of recycled binder from the RAP materials exceeds 20 percent of the total asphalt binder, the Iowa DOT requires that the designated virgin binder grade to be reduced by one temperature grade (Sondag et al. 2002). Idaho Transportation Department (ITD) implements a similar procedure regarding to the virgin binder grade adjustment based on the amount of RAP replacement and limits the maximum RAP content to 30 percent by weight of RAP binder as discussed later in this chapter.

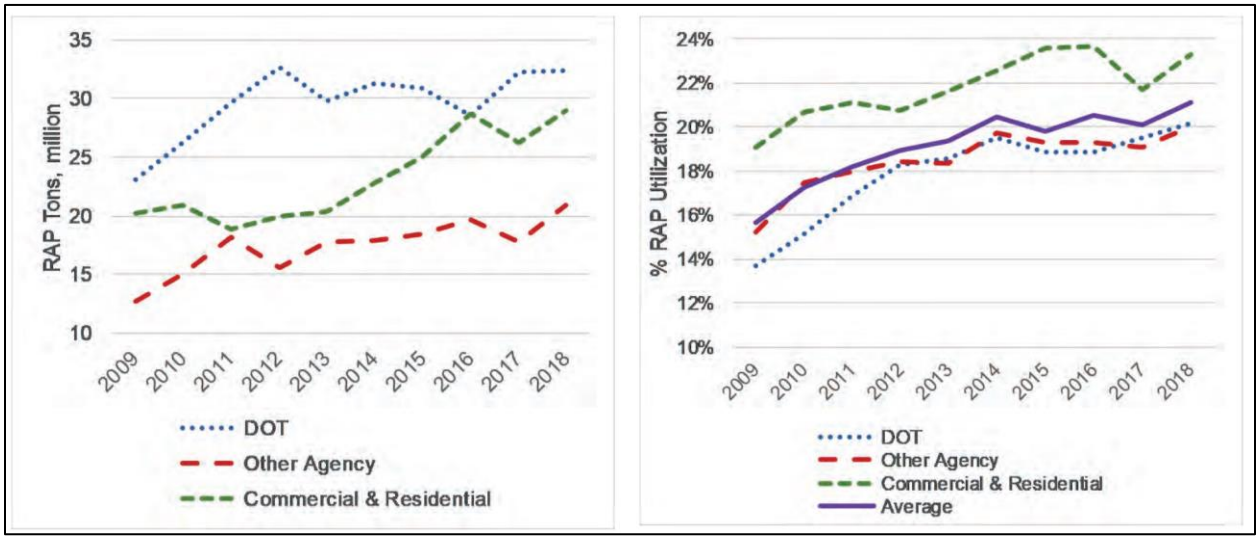

Figure 1. RAP Use by Sector (Million Tons) and Average Percent RAP Used by Sector (NAPA 2018)

Characterization of RAP

Flexible pavements at the end of their service life or even earlier, can be milled and reused. The recycled materials (i.e., asphalt binder and aggregates) are valuable, but the quality of both could be altered during the lifetime of the pavements due to oxidation and other degradation that occurs due to exposure to the environment and traffic loading. To prevent the negative impact of using high RAP contents on the performance of asphalt mixtures, specific considerations must be taken (McDaniel et al. 2012). RAP materials should be fully characterized before they are used in the mix. Binder content in the RAP, RAP aggregate gradation, bulk specific gravity (Gsb) of RAP aggregates, and PG of recovered RAP binder should be determined. A blending chart is used when high RAP content is considered.

The quantity and the properties of the asphalt binder in the RAP have a significant impact on the selection of the virgin binder used in the mix. The residual asphalt binder in the RAP contributes to the total binder content in the mix. Furthermore, the physical and rheological properties of RAP binder could be altered due to oxidative aging, and this should be considered in the mix design. The RAP binder can be quantified

or extracted from the recycled materials. The ignition furnace in accordance with AASHTO T 308 (AASHTO 2018) is used to quantify the RAP binder content. The second method is conducted in accordance with AASHTO T164 (AASHTO 2018) and AASHTO T319 (AASHTO 2018) using solvent extraction. Hajj et al. (2012) and McDaniel and Anderson (2001) evaluated the difference between these two methods and their effect on the binder content and aggregate gradation of the RAP materials using laboratory produced mixes. They found that RAP binder content evaluated after solvent extraction was lower than actual values since the binder around the RAP aggregates could not be thoroughly removed by solvent extraction. In addition, the RAP binder content determined by ignition oven, without considering correction factors, was close to the actual binder content of laboratory simulated RAP materials. Both the ignition oven and solvent extraction methods have no effect on the coarse portion of RAP aggregates (retained on Sieve No. 4); however, there was a change in the size distribution of the fine portion of RAP aggregates (passing Sieve No. 4). This effect was dependent on aggregate type as some aggregates were lost when exposed to extreme temperatures in the ignition furnace.

The Gsb of RAP aggregate is another property that is used in the mix design. A small error in Gsb would affect the Voids in Mineral Aggregates (VMA) to be off by plus/minus 0.4 percent when the RAP content in the mix approaches 50 percent (Hajj et al. 2012; Kvasnak et al. 2010). Currently, there are three methods that can be used to evaluate Gsb of RAP aggregates. The first method uses extraction procedures, either by the ignition oven or solvent extraction, to generate clean aggregates and determine the Gsb of the resulting coarse and fine aggregates following AASHTO T85 (AASHTO 2018) or T84 (AASHTO 2018), respectively. Prowell and Carter (2000) and Hajj et al. (2012) examined the effect the extraction procedures on calculated specific gravity results. They found that the ignition oven had a higher effect on Gsb when compared to the solvent extraction method. However, both extraction methods likely cause small errors in Gsb of RAP materials. Alternatively, the second method is to use the effective specific gravity (Gse) of the RAP aggregate instead of Gsb in VMA calculations; however, this is not recommended since it may result in considerably inaccurate value of VMA (Prowell and Carter 2000; Hajj et al. 2012). The third method is also an indirect approach that is based on maximum specific gravity (Gmm) testing and the asphalt absorption in RAP materials. Practicing engineers can use this approach, but only if they have a good estimate of asphalt absorption (West et al. 2013; Hajj et al. 2012).

The blending chart is used to select the virgin binder grade when the RAP binder content exceeds 30 percent of total binder weight in the mix. At higher RAP contents (greater than 30 percent) and as per the blending chart, the grade of recovered RAP binder also needs to be evaluated. Table 1 and 2 present the grade adjustment for RAP content and the typical adjustment of binder grades as per ITD specifications (ITD 2018).

Table 1. Grade Adjustment for RAP (ITD Specification 2018)

Level	RAP binder content by weight of the total binder in the mixture, percent	Binder Grade Adjustment to compensate for the stiffness of the asphalt binder in the RAP
1	0 to 17	No binder grade adjustment is made.
2	> 17 to 30	The selected binder grade adjustment for the binder grade specified on the plans is one grade lower for the high and the low temperatures designated. Or determine the asphalt binder grade adjustment using a blending chart. Note: See AASHTO M 323 for recommended blending chart procedure.

Table 2. Typical Adjusted Binder Grades (ITD Specification 2018)

Binder Grade Specified in Contract	Adjusted Binder Grade (Level2)	Adjusted Binder Grade (Level1)
58-28	58-34	No Adjustment Needed
58-34	No Adjustment Needed	No Adjustment Needed
64-28	58-34	No Adjustment Needed
64-34	58-34	No Adjustment Needed
70-28	64-34	No Adjustment Needed
76-28	70-34	No Adjustment Needed

Mix Design Considerations with RAP

The inconsistency of RAP material gradation or its binder content, which may be a combination of different RAP sources, may make it difficult for RAP mixes to meet mix design specifications and, subsequently, many agencies limit the quantity of RAP in the mix (McDaniel and Anderson 2001). The inconsistency of RAP materials could lead to a higher variation in binder content during the mixing at the hot mix plant (Solaimanian and Tahmoressi 1996). The procedures for managing RAP stockpiles and processing RAP materials were proposed to control the RAP variability (West et al. 2013; Zhou et al. 2010; West, R.C. 2010; West, R.C. 2009). The best practices typically involved fractionation, not over-crushing

RAP, avoiding contamination by keeping deleterious materials out of RAP stockpiles, ceasing processing during rain, and reducing moisture in RAP stockpile by covering it. More details of these precautions are available in the Appendix D of report for NCHRP 9-46 project (West et al. 2013). RAP variability could be controlled by managing RAP stockpiles well, as indicated by a survey conducted by NCAT during 2007 and 2008. The standard deviation of binder content in individual RAP stockpiles ranged from 0.1 percent to 1.5 percent and the standard deviation of percentages passing median sieve and 75-micron sieve ranged from 0.78 percent to 9 percent and 0.3 percent to 3.0 percent, respectively (West R. C. 2008). Furthermore, RAP stockpiles could be less variable than virgin aggregates (Estakhri et al. 1999; Nady R. M. 1997).

The design procedure for mixes with high RAP contents is similar to that of virgin mixes using the Superpave specifications. Once the RAP is characterized, it can be blended with the virgin aggregates to produce a blend gradation that satisfies the mix design specifications. The RAP mix should meet the volumetric requirements such as voids in the mineral aggregate (VMA), voids filled with asphalt (VFA), density, and dust proportion at N_{design}. Generally, RAP materials contain large quantity of fines (passing Sieve No. 200) because of RAP processing. This may limit the amount of RAP materials that can be added to the mix to satisfy the volumetric requirements. In addition, RAP materials should be heated separately at lower temperatures than that required for mixing and compaction to avoid further aging of the recycled binder. To meet the mixing requirements, virgin aggregates can be heated at higher temperatures so when blended with the RAP materials heated at lower temperatures, the mixing temperature of the mix would be within the acceptable range. In summary, mixes with high RAP content should meet all testing and design criteria like the virgin mix, and no special mix design requirements are needed (Brown et al. 2009; Al-Qadi et al. 2007).

Blending at known RAP Content

There are many factors that limit the amount of RAP in asphalt mixtures including RAP variability, RAP availability, specification limits, properties of RAP binder, availability of softer virgin binders, and capability of the hot mix asphalt plant to handle RAP materials for drying and heating, etc. (Advanced Asphalt Technologies 2011). Fractionation (separate the material in different sizes) of RAP can reduce variability in the gradation and binder content of RAP materials. The limitation of using high percentage of RAP mainly depends on the selection of virgin binder in RAP mixtures to offset the effect of the aged binder in the RAP on the performance of the produced mixtures.

AASHTO M323 and NCHRP 9-12 provided binder selection guidelines for RAP mixtures. If the percentage of RAP is less than 15 percent (17 percent for ITD specifications), there is no requirement to change the virgin binder grade. For RAP percentage between 15 percent to 25 percent (17 percent to 30 percent per ITD specifications), the virgin binder must be one grade lower than targeted grade on both low and high temperature PG. For RAP percentage greater than 25 percent, a blending chart is required for binder grade selection. Based on the targeted blended binder grade, the preferred RAP percentage, and the recovered RAP binder properties, the required virgin binder grade is determined using Equation 1.

$$T_{virgin} = \frac{T_{blend} - (\%RAP \times T_{RAP})}{(1 - \%RAP)}$$

……Eqn. 1

where,

T_{virgin} = Critical temperature of virgin asphalt binder

T_{blend} = Critical temperature of the blended asphalt binder

T_{RAP} = Critical temperature of recovered RAP binder

Percent RAP = Percentage of RAP

If a specific market available virgin binder must be used, and the targeted blended binder grade and recovered RAP properties are known, the RAP percentage that can be used in the mix is determined using Equation 2.

$$\%RAP = \frac{T_{blend} - T_{virgin}}{T_{RAP} - T_{virgin}}$$

……Eqn. 2

The process of using the blending chart is time-consuming, includes hazardous solvents, and creates disposal issues (Copeland A. 2011). The hypothesis of completed blending between the RAP and virgin aggregate might not always be reasonable in the plant field production (Mogawer et al. 2012; Yousefi 2013; Shirodkar et al. 2011). Furthermore, the degree of blending would impact the RAP mix performance, as rutting resistance could be compromised by poor blending between the virgin binder and RAP binder. Even if a softer binder is used, the final mixture may still be stiff and susceptible to low temperature cracking (Mogawer et al. 2012). Therefore, it is still a challenge to select the proper virgin binder in RAP mixtures.

Besides the mix design requirements for volumetric properties, moisture susceptibility of RAP mixes needs to be considered during the mix design. Moisture susceptibility of asphalt mixtures is commonly evaluated using AASHTO T 283, Resistance of Compacted Hot Mix Asphalt (HMA) to Moisture Induced Damage (Sondag et al. 2002). The tensile strength ratio (TSR) is used as an indicator of HMA resistance to moisture damage. In general, studies conducted on the moisture susceptibility of RAP mixes showed that the addition of RAP to a mixture had no positive or negative impact on the mixture moisture susceptibility (Li et al. 2004), and most of RAP mixes could satisfy the local requirement for minimum TSR values (Hajj et al. 2009; Al-Qadi et al. 2012). In several instances described as part of NCHRP project 9-43, the TSR values of mixes with high RAP contents were lower than those of virgin mixes or the criterion of 0.80 requirement in AASHTO M323, the addition of anti-stripping additives was found effective in improving the TSR values above 0.80 (West et al. 2013).

Laboratory and Field Evaluation of Mixes with High RAP Contents

It is essential to evaluate the performance of mixes with high RAP contents. The performance evaluation includes rutting resistance, fatigue cracking resistance and low temperature thermal cracking resistance, and moisture damage. Pavement performance in the field can be predicted using a mechanical-empirical pavement design approach that incorporates pavement structure, traffic data, weather conditions as well as pavement material properties (e.g., dynamic modulus, creep compliance, indirect tensile strength, and complex modulus of binder). The effect of RAP on the mix resistance to rutting, fatigue cracking, low temperature thermal cracking and field pavement performance is discussed in the next section.

Evaluation of Rutting Resistance

One of the most common distresses in flexible pavements is rutting, especially in hot climates. Laboratory tests such dynamic modulus (E*), which is a mix stiffness indicator, and the flow number (FN) tests can be used as indicators to the resistance of asphalt mixtures to permanent deformation. The rutting resistance of asphalt mixtures increases as the E* and FN increase. Other performance tests such as the Asphalt Pavement Analyzer (APA) and HWTT are used as a direct measurement of rutting in the laboratory.

Many studies have shown that E* and FN values increase with RAP content due to the stiffer RAP binder. Though, different testing factors such as temperature or frequency, optimum binder content (OBC), virgin binder grade, and aggregate gradation might affect the E* and FN values (Daniel and Lachance 2005; Al-Qadi et al. 2012; McDaniel et al. 2012; Putman et al. 2002). Daniel and Lachance (2005) investigated the E* values of mixes with 0 percent, 15 percent, 25 percent, and 40 percent RAP. The results showed that mixes with 15 percent RAP increased E* when compared against the control mixes (i.e., 0 percent RAP), while mixes with 25 percent and 40 percent RAP did not follow the same trend, and their E* values were close to the ones obtained for the control mix. Possible explanation of this unanticipated trend is that mix with 25 percent RAP had higher OBC and finer gradation, and the mix with 40 percent RAP had an even finer gradation as compared to the mix with 25 percent RAP. Both mixes with 25 percent and 40 percent RAP had higher VFA and VMA values when compared to the control mix and the mix with 15 percent RAP.

Li (2004) studied RAP mixes from Minnesota with 0 percent, 20 percent, and 40 percent RAP to investigate the effect of RAP content, virgin binder grade, and RAP sources on E* (Li et al. 2004). It was found that adding RAP to HMA increased E* values when compared to the ones obtained for the control mix. Though, at low temperature, E* did not always increase with added RAP content likely because of the formation of micro-cracks at the low test temperature, which possibly decreased the stiffness of the mixture. Additionally, the virgin binder grade and RAP source had a significant effect on complex modulus values. Al-Qadi (2012) examined two mixes with different RAP percentages and the impact of virgin binder grade bumping (PG 64-22, PG 58-22, and PG 58-28) on E* and FN. The results revealed that E* and FN increased with an increase in RAP content due to the aged binder in the RAP. In addition, virgin binder grade bumping reduced E* and increased the rutting potential indicated by FN and HWTT. McDaniel et al. (2012) studied plant mixes with 0 percent, 15 percent, 25 percent, and 40 percent RAP from five contractors. The relation between RAP content and E* did not follow the same trend among different contractors. For

mixes from contractor number 1, 2, and 4, the E* master curve increased as RAP content increased. For mixes for contractor number 3, the 25 percent RAP mix was stiffer than the control mix, but the 15 percent and 40 percent RAP mixes were less stiff than the control mix. The E* master curves of all mixes from contractor number 5 were close to each other.

A direct evaluation of rutting resistance could be performed using the APA and HWTT. Consistent conclusions were drawn from these direct rutting tests that mixes containing RAP performed better than virgin mixes in terms of rutting resistance (Colbert and You 2012; Putman et al. 2002; Stroup and Wagner 1999; Zhao et al. 2012; Vavrik et al. 2007; West et al. 2009). Colbert (2012) used APA at a testing temperature of 136.4°F (58°C) to evaluate the rutting resistance of mixes with 0 percent, 15 percent, 35 percent, and 50 percent RAP. The results showed that rutting depth decreased with the increase in RAP content (Colbert and You 2012). Putman et al. (2002) evaluated the effects of RAP materials and crumb rubber modified (CRM) binder on rutting resistance measuring with the APA. The results indicated that mixes containing RAP or with CRM binder had similar or better rutting resistance as compared to virgin mixes or with unmodified binder. Zhao et al. (2012) conducted laboratory performance tests to study the effect of using high percentages of RAP on warm mix asphalt (WMA) mixtures. Using the Marshall Mix design procedure, four WMA mixtures with same the aggregate gradation, different RAP contents (0 percent, 30 percent, 40 percent, and 50 percent), and a PG 64-22 virgin binder were prepared and tested. The rut depth was measured using the APA at a testing temperature of 50°C. The results showed that the rutting resistance was improved by adding RAP to the mixes, and that mixes with WMA performed better than HMA mixes. Similar conclusions were made by other researchers (Stroup and Wagner 1999; Vavrik et al. 2008; West et al. 2009).

Fatigue Cracking Resistance and Moisture Damage

Several laboratory tests such as the bending beam fatigue test, (IDT fracture energy test, Texas Overlay Tester (OT), and semi-circular bending beam (SCB) test are used to evaluate mix resistance to fatigue cracking. Many researchers evaluated the resistance of mixes with RAP to cracking and reported reduced fatigue life or more brittle behavior at high percentages of RAP. However, the fatigue cracking resistance might be improved at low percentages of RAP content (i.e., less than 20 percent) (McDaniel and Anderson 2001; Hajj et al. 2009; West et al. 2013; Kingery 2004; Vukosavljevic 2006). For instance, McDaniel and Anderson (2001) evaluated the fatigue life of mixes with various contents of RAP (0 percent, 10 percent, 20 percent, and 40 percent) from three different sources. The researchers evaluated the cracking resistance using the beam fatigue test in accordance with AASHTO TP 8 at 400 and 800 micro strains at 68°F (20°C) (McDaniel and Anderson 2001). The results demonstrated a decrease in fatigue life due to the increase in stiffness caused by higher RAP contents when no adjustment was made in the virgin binder grade. West et al. (2013) tested mixes from Utah, New Hampshire, Florida, and Minnesota to evaluate mix resistance to fatigue cracking. They measured the IDT fracture energy at a temperature of 10°C. The fracture energy results from all of four mixes showed that RAP mixes had significantly lower fatigue resistance as compared to virgin mixes. All virgin mixes had better fracture energy than high RAP mixes.

Hajj et al. (2009) conducted beam fatigue tests to evaluate fatigue resistance of mixtures with 0 percent, 15 percent, and 30 percent RAP from three different sources and two types of virgin binders (PG 64-28, and PG 64-22) were used in the testing matrix. For the PG 64-22 binder, adding 15 percent RAP to the mix resulted in either an equivalent or better resistance to fatigue cracking as compared to the virgin mix regardless of the source of RAP. The addition of 30 percent RAP to a mix improved the resistance to fatigue cracking. However, RAP mixtures performed better than the virgin mix only for a given RAP source. For the PG 64-28 binder, the addition of 15 percent or 30 percent RAP to the mixes resulted in a substantial decrease in fatigue resistance regardless of RAP source. Kingery (2004) and Vukosavljevic (2006) used sSCB, IDT strength, and beam fatigue tests to evaluate mixes with 0 percent, 10 percent, 20 percent, and 30 percent of screened RAP materials satisfying Tennessee mix design criteria. The outcome of this study revealed that, in general, adding RAP up to 20 percent in HMA increased the stiffness and fatigue resistance; however, at a higher percentage of RAP (i.e., 30 percent), some fatigue characteristics were compromised. Thus, no more than 20 percent RAP was advised for use in Tennessee surface mixes.

A few studies have shown that the fatigue cracking resistance of RAP mixtures depends on RAP sources or test methods (Shu et al. 2008; Sabahfar et al. 2014). Shu et al. (2008) used different testing methods to assess the fatigue characteristics of HMA with 0 percent, 10 percent, 20 percent, and 30 percent RAP. They examined fatigue parameters including failure strain, IDT strength, resilient modulus, toughness index, dissipated creep strain energy threshold, plateau value, energy ratio, and load cycles to failure. It was found that the inclusion of RAP in HMA mixture generally increased the IDT strength and reduced the post-failure tenacity in IDT strength test. However, the dissipated creep strain energy threshold and energy ratio decreased with the increase in RAP content which indicated reduced fatigue life. The fatigue resistance results from the plateau values obtained by the beam fatigue test showed that higher RAP contents were more resistant to fatigue. The number of cycles to attain a 50 percent-decrease in stiffness was also greater for mixes with higher RAP contents than for virgin mixes. Sabahfar et al. (2014) conducted SCB and Texas OT tests at 77^{o}F (25^{o}C) to study the cracking resistance of mixtures with 20 percent, 30 percent, and 40 percent RAP from two regions in Kansas. The cracking test results did not follow the same trend for the two sources of RAP. For the mixes with RAP from the Shilling area, the cracking resistance declined as the percentage of RAP in the mix increased, while for the mix with RAP from the Konza area, good cracking resistance was achieved even at the highest RAP content of 40 percent.

Some studies have found that mixes with moderate to high RAP contents had equivalent or better fatigue life when compared against the performance of virgin mixes (Santos et al. 2010; Al-Qadi et al. 2012). For instance, Santos et al. (2010) conducted beam bending testing and considered 50 percent loss of initial stiffness modulus as the fatigue resistance criterion to evaluate mixes with 0 percent, 20 percent, 30 percent, and 40 percent RAP from batch plant and laboratory mixing. Both the plant and laboratory mixtures with RAP showed better fatigue performance than the reference or control mixture (i.e., 0 percent RAP). Al-Qadi et al. (2012) conducted the beam fatigue test at 68^{o}F (20^{o}C) and various levels of 1000, 800, 700, 500, 400 and 300 microstrains to evaluate cracking performance of eight mixtures with different RAP contents (i.e., 0 percent, 30 percent, 40 percent, and 50 percent RAP) from two regions (District 1 and 5). The failure criterion was the traditional 50 percent reduction in initial stiffness. Based on the slope parameter of the fatigue curve, the fatigue life of the asphalt mixtures was slightly improved

with the addition of RAP. A single or double bump in the virgin binder grade also improved fatigue behavior of RAP mixtures as compared to the control mixture.

Field Evaluation

McDaniel et al. (2002) evaluated the use of RAP in HMA considering Superpave specifications. They included three sources of RAP from Indiana, Michigan, and Missouri. A comparison was performed between the laboratory and plant-produced mixes with 15 percent to 25 percent RAP content. The findings of the study showed that Superpave mixtures with 50 percent RAP were achievable. The laboratory mixtures had similar stiffness to the plant-produced mixes at the same RAP content. In addition, the stiffness increased, and shear strain decreased (i.e., increased resistance to rutting) with the increase in RAP content. It was concluded that asphalt mixtures with RAP could provide good performance under Superpave specifications (McDaniel et al. 2002).

The Louisiana Transportation Research Center (LTRC) examined the performance of five projects constructed using RAP over six years. The field evaluation of the study included field distress, serviceability, and structural investigation. The findings showed that the performance of the pavements with 20 percent to 50 percent RAP content was similar to the pavements without RAP, and there was no significant difference in terms of serviceability rating and pavement condition (Paul et al. 1995).

Carvalho et al. (2010) investigated the short and long-term performance of RAP mixes used in overlays compared to control HMA. The study included records of 18 projects from the long-term pavement performance (LTPP) program in United States and Canada. The history of data collection ranged from 8 to 17 years. The performance evaluation included three main distress parameters (i.e., rutting, roughness, and fatigue cracking). An analysis of variance (ANOVA) performed on these results showed that the performance of RAP overlays was comparable to the virgin mix. In addition, the performance of RAP overlays showed structural improvements equivalent to the control HMA in terms of deflection (Carvalho et al. 2010).

The effect of increased RAP content on pavement performance and cost were evaluated by Virginia Department of transportation (VDOT) in 2007. Projects from three VDOT districts using more than 20 percent RAP were included in the study. A mix containing less than 20 percent RAP was also sampled and tested for comparison purposes. The results of laboratory tests revealed that no significant difference between mixes with high RAP contents and the control mix in terms of rutting, fatigue, and moisture susceptibility. Furthermore, no construction problems were associated with the use of high RAP mixes (Maupin et al. 2008).

In a research project in Georgia (1995), another comparison was conducted between the performance of recycled pavement and control asphalt pavements (Kandhal et al. 1995). The Georgia Department of Transportation (GDOT) constructed five projects, each of which had a recycled section and a control section. The recycled sections contained RAP contents between 10 percent to 25 percent. The performance evaluation showed no significant differences between the test sections of recycled mix pavements and virgin mixes in terms of rutting, fatigue cracking, and raveling over 18 to 27 months.

A study in Virginia by Apeagyei et al. (2011) focused on evaluating the rut resistance of RAP mixes. The study included 19 plant-produced asphalt mixtures with up to 25 percent RAP content. The results showed that the stiffness of the control mixes was the same as the stiffness of the mixes with 25 percent RAP. The FN test was conducted at 129.2°F (54°C) showed that mixes with moderate RAP contents (10 percent and 15 percent) had better rut resistance when compared to mixes with high RAP content and control mixtures. A statistical analysis indicated RAP content was the most relevant factor affected the rutting resistance in the selected mixes. The authors suggested that the reason for the decrease in FN values at high RAP contents could be linked to the practice of using a softer virgin binder on these mixes.

Another study included 18 plant-produced asphalt mixes with up to 40 percent RAP. The mixes had NMAS of 9.5 mm and 12.5 mm (Mogawer et al. 2012). Mogawer et al. (2012) studied the characteristics of these mixes which were obtained from three contractors located in the Northeastern U.S. Different binder and mix tests were performed to evaluate the effect of RAP on field performance. The investigation indicated that it was essential to document how RAP mixes were handled and produced because differences in the recorded production parameters affected the degree of blending between RAP and virgin binders. Production parameters were also found to affect workability and mix performance. The results showed that the use of softer virgin binders could improve low temperature properties of RAP mixes. Also, the results of the Texas OT indicated that the cracking resistance decreased with the increase of RAP content. These results were consistent with the results from the low-temperature tests on the recovered asphalt binder tests.

Current Practice of Different DOTs

The FHWA and NAPA have been collecting data over the past years to track the current practice of RAP use by state (NAPA 2018). In U.S., the asphalt industry continues to be the country's most consistent recycler with more than 99 percent of RAP being reused. The average RAP content utilized in asphalt mixes has increased from 15.6 percent in 2009 to 21.1 percent in 2018. The estimated RAP used in asphalt mixes was 82.2 million tons in 2018. This represents more than 23 million barrels (4.1 million tons) of asphalt binder preserved, alongside the preservation of more than 78 million tons of virgin aggregates with a total estimate of more than $2.8 billion in savings (NAPA 2018).

Figure 2 shows the average RAP content used by each state as reported by asphalt mix producers during the construction seasons from 2014 to 2018 (NAPA 2018). The data shows that the number of states using RAP contents of 20 percent or greater have been rising significantly, increasing from 10 states in 2009 to 27 states in 2014, to 24 states in 2017, and reaching a peak of 30 states in 2018. The number of states with asphalt mix producers reporting RAP contents less than 15 percent has decreased from 23 states in 2009 to just six states in 2018. Figure 2 demonstrates that the states are moving forward towards increasing RAP content in asphalt mixes. The Idaho Transportation Department (ITD) is among the leading states by currently allowing up to 30 percent RAP by weight of asphalt binder.

State	Average RAP Percent					State	Average RAP Percent				
	2014	2015	2016	2017	2018		2014	2015	2016	2017	2018
Alabama	23%	25%	24%	24%	26%	Montana	*	*	*	*	*
Alaska	*	*	*	*	*	Nebraska	33%	*	*	19%	26%
American Samoa	NCR	NCR	NCR	*	*	Nevada	18%	*	22%	12%	*
Arizona	14%	*	9%	10%	12%	New Hampshire	22%	19%	21%	22%	18%
Arkansas	14%	14%	10%	11%	12%	New Jersey	19%	*	19%	19%	18%
California	13%	16%	15%	18%	16%	New Mexico	*	NCR	22%	21%	19%
Colorado	21%	20%	24%	24%	20%	New York	14%	16%	16%	16%	17%
Connecticut	21%	*	21%	18%	15%	North Carolina	26%	26%	23%	18%	26%
Delaware	*	*	*	*	*	North Dakota	*	*	*	12%	*
Dist. of Columbia	NCR	NCR	NCR	*	*	No. Mariana Isl.	NCR	NCR	NCR	NCR	NCR
Florida	32%	33%	32%	35%	27%	Ohio	28%	28%	27%	28%	28%
Georgia	21%	*	27%	23%	25%	Oklahoma	16%	20%	17%	15%	17%
Guam	NCR	NCR	NCR	NCR	NCR	Oregon	28%	27%	22%	18%	27%
Hawaii	*	*	*	20%	23%	Pennsylvania	16%	15%	15%	15%	16%
Idaho	25%	25%	21%	27%	27%	Puerto Rico	NCR	*	NCR	NCR	NCR
Illinois	28%	25%	23%	25%	28%	Rhode Island	*	*	*	*	*
Indiana	29%	28%	22%	22%	24%	South Carolina	21%	19%	23%	21%	22%
Iowa	15%	13%	14%	11%	18%	South Dakota	*	NCR	*	*	NCR
Kansas	22%	17%	20%	19%	21%	Tennessee	14%	23%	21%	23%	18%
Kentucky	14%	15%	13%	24%	16%	Texas	15%	13%	13%	15%	17%
Louisiana	*	*	19%	21%	22%	U.S. Virgin Islands	NCR	NCR	NCR	NCR	*
Maine	21%	*	16%	20%	*	Utah	28%	25%	25%	22%	27%
Maryland	21%	23%	26%	23%	26%	Vermont	*	*	*	*	*
Massachusetts	17%	18%	18%	16%	16%	Virginia	27%	29%	28%	32%	28%
Michigan	32%	32%	32%	28%	28%	Washington	25%	25%	25%	20%	24%
Minnesota	24%	22%	21%	20%	25%	West Virginia	15%	14%	14%	18%	20%
Mississippi	17%	17%	19%	18%	20%	Wisconsin	*	16%	22%	16%	17%
Missouri	20%	23%	23%	23%	21%	Wyoming	*	*	10%	12%	*

No Company Responding	< 3 Companies Reporting	0–9%	10–14%	15–19%	20–29%	≥ 30%

Figure 2. Average Estimated RAP Content in Asphalt Mixes by State (NAPA 2018)

Figure 3 shows the percentage of RAP mixes using softer binders and/or recycling agents in each state. These results may not completely reflect practices in each state, and it is representative only of the survey participants. Although there is no strong relationship between the states using recycling agents or softer binders in RAP mixes and the amount of RAP being used by those same states, it should be noted that 22 of the 30 states using 20 percent RAP or more reported using recycling agents and/or softer binders. Eight of these states reported no use of recycling agents or softer binders in their RAP mixes (NAPA 2018).

State	Softer Binder	Recyc. Agent	State	Softer Binder	Recyc. Agent	State	Softer Binder	Recyc. Agent
Alabama	0%	0%	Kentucky	22%	18%	Ohio	33%	0%
Alaska	*	*	Louisiana	25%	0%	Oklahoma	7%	0%
American Samoa	*	*	Maine	*	*	Oregon	3%	3%
Arizona	11%	0%	Maryland	19%	4%	Pennsylvania	13%	3%
Arkansas	14%	0%	Massachusetts	2%	0%	Puerto Rico	NCR	NCR
California	28%	8%	Michigan	35%	0%	Rhode Island	*	*
Colorado	25%	0%	Minnesota	28%	1%	South Carolina	29%	0%
Connecticut	0%	0%	Mississippi	0%	1%	South Dakota	NCR	NCR
Delaware	*	*	Missouri	35%	4%	Tennessee	5%	2%
Dist. of Columbia	*	*	Montana	*	*	Texas	38%	8%
Florida	55%	12%	Nebraska	17%	0%	U.S. Virgin Isl.	*	*
Georgia	14%	0%	Nevada	*	*	Utah	40%	12%
Guam	NCR	NCR	New Hampshire	0%	0%	Vermont	*	*
Hawaii	0%	0%	New Jersey	2%	0%	Virginia	5%	1%
Idaho	79%	2%	New Mexico	0%	0%	Washington	19%	9%
Illinois	23%	3%	New York	2%	8%	West Virginia	0%	0%
Indiana	8%	8%	North Carolina	19%	0%	Wisconsin	21%	3%
Iowa	19%	3%	North Dakota	*	*	Wyoming	*	*
Kansas	68%	15%	No. Mariana Isl.	NCR	NCR			
						Average, When Used†	20%	4%

NCR No Companies Responding for the State to the Survey
* Fewer than 3 Companies Reporting
† Includes Values from States with Fewer than 3 Companies Reporting

Figure 3. Percent of RAP Mixes Using Softer Binder and/or Recycling Agents by State (NAPA 2018)

Figure 4 shows a summary of the RAP use in the state of Idaho from 2009 to 2011. Since 2011, ITD is approving RAP usage in all its new HMA mixes. In 2017, District 2 constructed a project that used as much as 45 percent RAP in the 150,000 tons of HMA produced for a series of mill and overlay projects on US 95 and US 12 nearby Lewiston, Idaho. The project was 4-miles long on US 12 and used cement-reinforced asphalt base (CRABS) stabilization. ITD and the contractor (Knife River) won a NAPA 2017 Quality in Construction Green Paving Award for the construction of this field project (NAPA 2018).

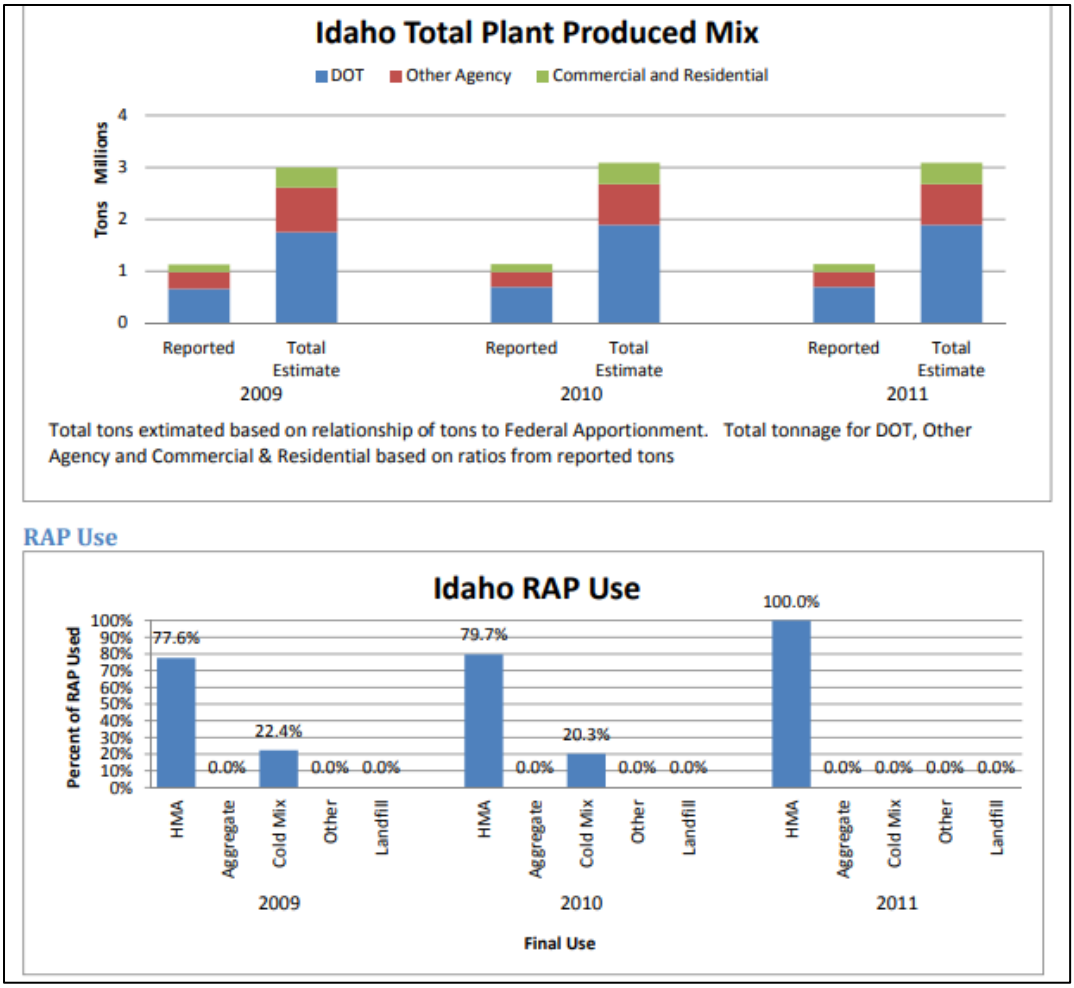

Figure 4. Summary of RAP Use in State of Idaho (NAPA 2011)

Mix Stability Indices

Since the introduction of Superpave asphalt mix design, several research studies have been conducted to improve the methodology. In general, performance tests are carried out to check the anticipated quality of the Superpave mix design at the preliminary design stage. One of these proposed methods is evaluation of GS during laboratory compaction using the Superpave Gyratory Compactor (SGC). The GS evaluates the resistance of the mix to applied loads. This method is not proposed as a replacement of performance tests; instead, it is proposed to assist in detecting weak aggregate structures at the early stage of the mix design, before further intensive performance mix evaluation takes place (e.g., cracking and rutting). In addition, the GS may be able to capture the change in mix composition, which could alter the mix performance. Several researchers calculated the shear stress during compaction through conventional static equilibrium analysis (McRae 1965; De Sombre et al. 1998; Dessouky et al. 2004; Abdo et al. 2010) to estimate the GS. Other researchers used the compaction data to develop various compaction indices and related them to mix performance (Dessouky et al. 2013; Bahia et al. 1998; Vavrik and Carpenter 1998; Faheem and Bahia 2004). The following section summarizes several compaction indices used to assess various aspects of mix stability and performance.

Construction Densification Index

Bahia et al. (1998) proposed the construction densification index (CDI) to evaluate the constructability of asphalt mixtures and the resistance to traffic loading. The CDI is defined as the area measured under the densification curve from the eighth gyration to the number of gyrations at 92 percent of the theoretical maximum specific gravity (Gmm) as presented in Equation 3.

$$CDI = \sum_{N=8}^{N_{92}} \%G_{mm}$$

……Eqn. 3

where,

Percent G_{mm} = Percent maximum density

$N_{=8}$ = Gyration number 8

N_{92} = Number of gyrations at 92 percent Gmm

Bahia et al. (2004) showed that CDI values ranged from 50 and 100 as shown in Figure 5. Also, the authors demonstrated that mixes with higher CDI required more energy for compaction. In addition, Bahia et al. (2004) proposed another index called traffic densification index (TDI) that calculates the area under the densification curve between 92 percent Gmm to 98 percent Gmm . The TDI values ranged from 500 and

2000 (Figure 6). Based on the findings of this study, the authors envisioned that controlling the CDI and TDI values could allow for optimization of HMA construction and traffic requirements.

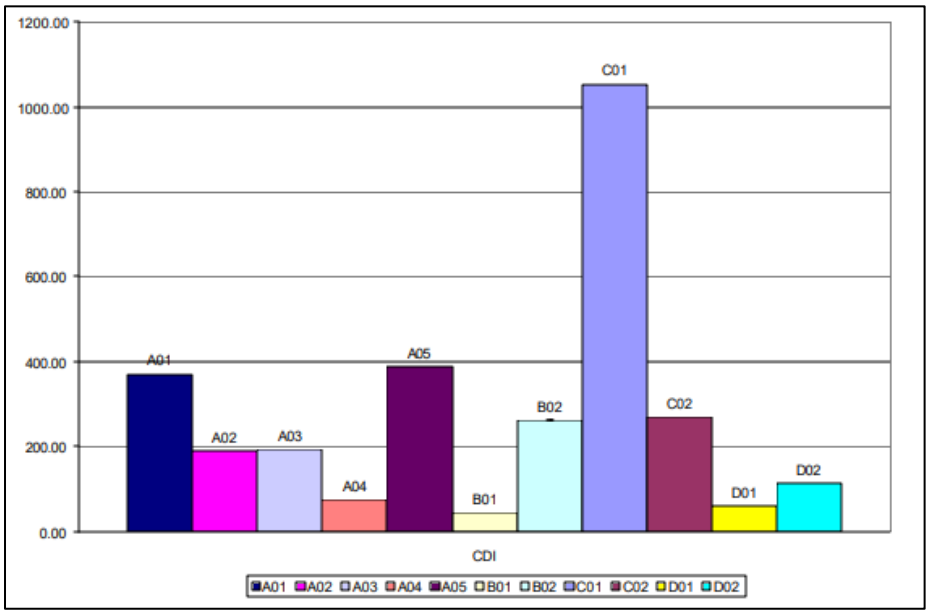

Figure 5. Averages CDI Values for Different Mixes (Bahia et al. 2004)

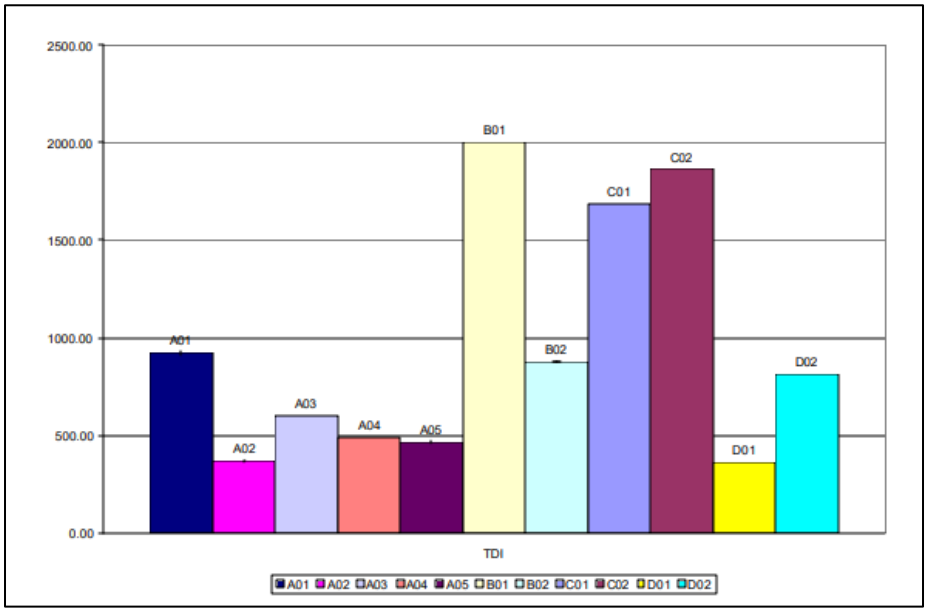

Figure 6. Averages TDI Values for Different Mixes (Bahia et al. 2004)

Mohammed et al. (2007) calculated CDI and TDI for mixes prepared with different aggregate types (limestone, sandstone, and granite) and three aggregate gradations (coarse, intermediate, and fine) as shown in Figure 7. The results showed that the coarse mixes required more energy in the first part of the densification curve and were less desirable for construction. The variation in TDI was less compared to CDI. Overall, the results of their study showed that the higher the TDI, the lower the rut depth; however, at some point, the rut depth increased with the increase of TDI a shown in Figure 8. The study related the sudden trend shifting to the fact that the mix was confined in a mold, which prevented lateral movement.

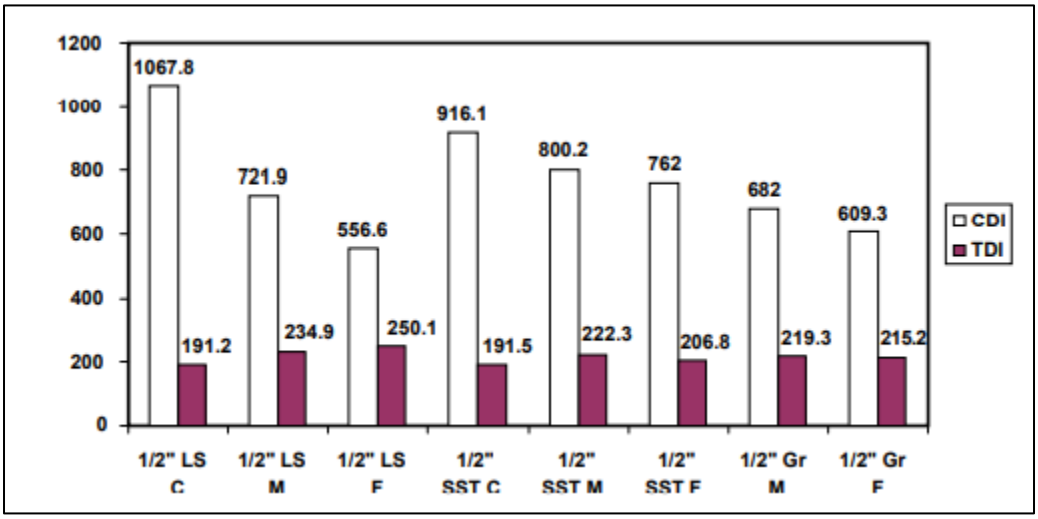

Figure 7. CDI and TDI for Different Asphalt Mixes (Mohammed et al. 2007)

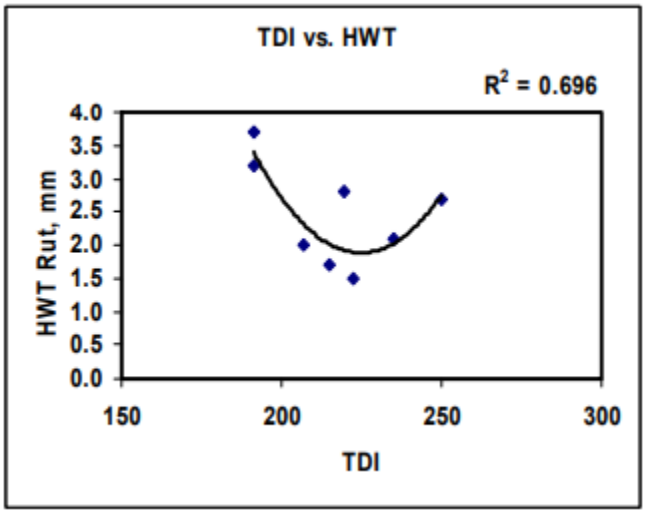

Figure 8. TDI vs. HWTT Rut Depth for Different Asphalt Mixes (Mohammed et al. 2007)

Locking Point

Vavrik and Carpenter (1998) proposed an index called Locking Point (LP) to evaluate compaction characteristics of asphalt mixes. The LP is defined when the mixture exhibits a noticeable increase in resistance to further densification. The LP concept was adopted by two transportation agencies. GDOT uses LP in the design of HMA mixes. The department defines the locking point as the number of gyrations at which the same height is recorded for three times in the first occurrence (GDOT, 2003). In addition, the Alabama Department of Transportation (ALDOT) defines the locking point as the point at which the sample being compacted drops less than 0.1 mm in height between successive gyrations (Delage 2000). However, in general, LP is determined when the height of the sample does not change within two consecutive gyrations. Mohammed et al. (2007) studied the LP for mixes prepared using three aggregate types (limestone, sandstone, and granite) and three aggregate gradations (coarse, intermediate, and fine) as shown in Figure 9. They observed that the LP for coarse mixes was higher than for mixes with intermediate aggregate gradations.

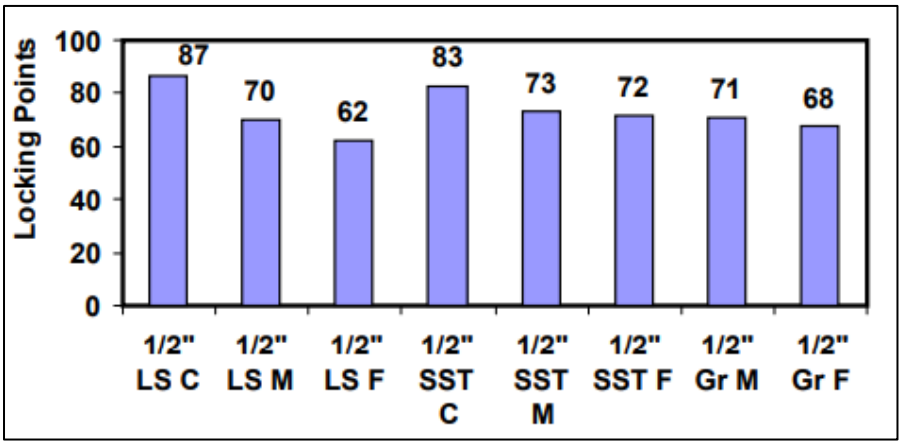

Figure 9. Locking Point of Asphalt Mixtures with Different Aggregate Gradations (Mohammed et al. 2007)

Workability Energy Index

Dessouky et al. (2013) demonstrated that the compactability of asphalt mixes was affected by several factors including binder grade and content, aggregate gradation and size, temperature, and type of compactor. They found that the mechanical characteristics of asphalt mixes could I improve by using polymer-modified binder, but such binder could also have a significant effect on asphalt pavement compaction in the field. Therefore, they proposed and developed compaction indices to evaluate the workability and compactability of asphalt mixes during the design process and prior to lay down operations. The Workability Energy Index (WEI) is defined as the energy required to compact a sample from zero gyrations to the number of gyrations corresponding to 92 percent Gmm. A higher WEI indicates that the mix is easy to compact(Dessouky et al. 2013). WEI is calculated using Equation 4 which represents the amount of effort needed to compact a sample to a density of 92 percent Gmm.

Workability refers to the ease of blending the mix components using typical construction equipment. To identify adequate thresholds for the compactability indices, performance testing was required to validate the long-term behavior of these mixes. This was accomplished in two phases: laboratory performance testing and field performance testing. The former was conducted using HWTT and E* tests, whereas the latter phase was accomplished through accelerated pavement testing. The authors also studied the effect on the internal structure of the test mixes in terms of aggregate orientation and number of contacts (Dessouky et al. 2013). The results shown in Figure 10a demonstrate that mix workability decreased with a decrease in binder content. In addition, they found that the plant mixes had similar trends to that of lab mixes. Figure 10b shows that mixes with higher binder content such as N4 and D(WMA) had the highest WEI among all mixes. Also, the author proposed a minimum value of 4.5 for WEI that reflected: "the minimum compaction effort for the mixes to be workable".

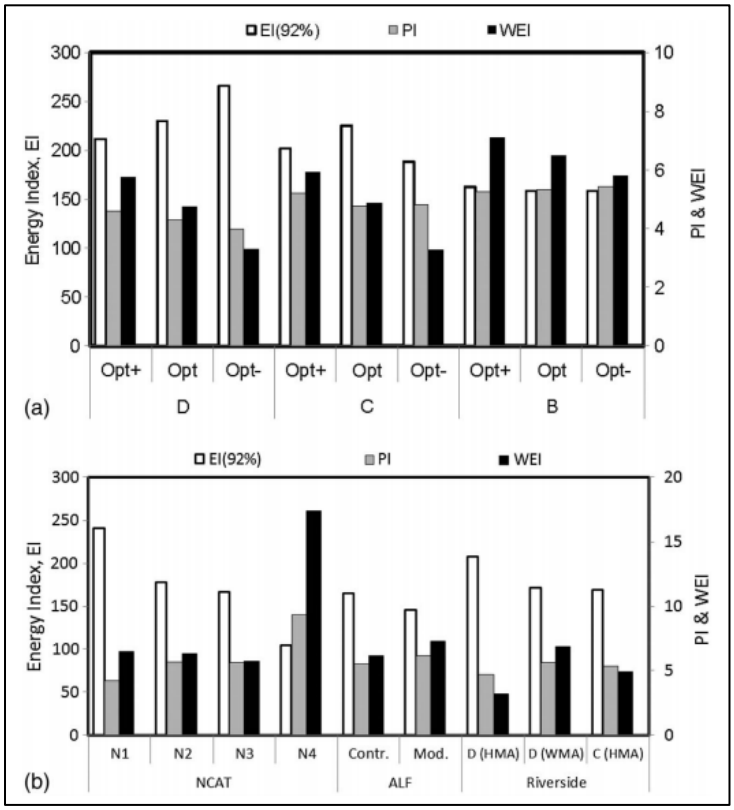

Figure 10. Workability Indices of (a) Lab mixes; (b) Plant Mixes (Dessouky et al. 2013)

$$WEI = \frac{\frac{\pi d^2}{4} P(h_{n=0} - h_{n=92})}{N_{92} - N_{n=0}}$$

…… Eqn. 4

where,

P = Compaction pressure

d = The diameter of the specimen

$h_{n=0}$ = Initial height of the specimen at gyration 0

$h_{n=9}$ = Height of the specimen

$N_{=0}$ = Gyration 0

N_{92} =Number of gyrations at 92 percent G_{mm}

Compactability Energy Index

Dessouky, et al. (2013) also proposed the CEI to evaluate the stability of asphalt mixes during the compaction stage. The CEI is a function of change in height between the number of gyrations corresponding to 92 percent Gmm and the one corresponding to 96 percent Gmm as given in Equation 5. Dessouky et al. (2013) investigated the effect of the asphalt content and aggregate gradation on CEI. The results in Figure 11 show that CEI decreased with the decrease in binder content. A TxDOT type C mix with at optimum binder content was more stable when compared to type B and type D mixes (Figure 11). Mixes with lower CEI exhibited higher stability when subjected to traffic loads. Also, the authors found a strong correlation between CEI and rate of rutting or RR (Figure 12). The rate of rutting increased with CEI. Finally, the researchers proposed an initial threshold (CEI ≤ 0.5) to ensure that mix stability.

$$CEI = \frac{\frac{\pi d^2}{4} P(h_{92} - h_{96})}{N_{96} - N_{92}} \quad \text{..... Eqn. 5}$$

where,

P = Compaction Pressure

d = Diameter of specimen

h_{92} = Height of the specimen at 92 percent G_{mm}

h_{96} = Height of the specimen at 96 percent G_{mm}

N_{92} = Number of gyrations at 92 percent G_{mm}

N_{96} = Number of gyrations at 96 percent G_{mm}

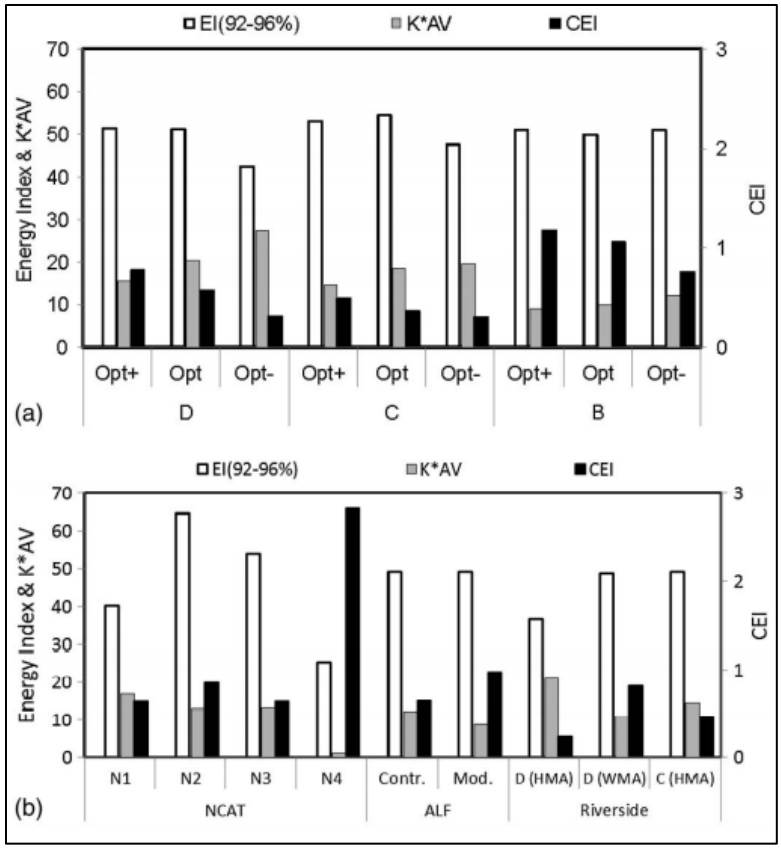

Figure 11. Compactability Energy Indices of (a) Lab mixes; (b) Plant mixes (Dessouky et al. 2013)

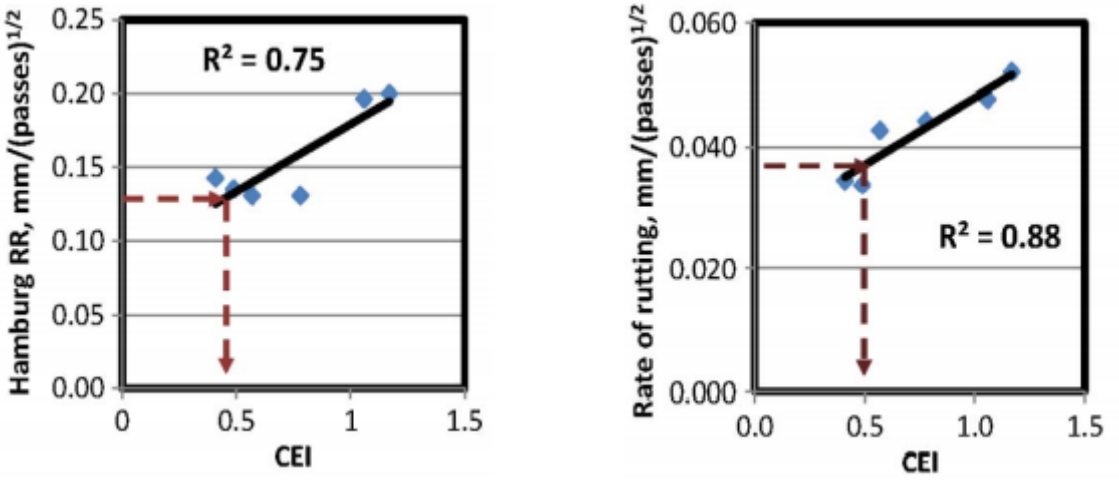

Figure 12. Relationship between CEI versus HWTT Rutting Rate (Dessouky et al. 2013)

Resistive Effort and Compaction Force Index

Faheem and Bahia (2004) proposed two indices calculated from the laboratory compaction data: resistive effort (w) and CFI. The index w is a measure of the mix resistance to compaction, and it is calculated using Equation 6. Higher w values indicate stiffer mix (Faheem and Bahia 2004).

$$w = \frac{4Fe\theta}{Ah} \quad \text{.....Eqn. 6}$$

where,

Fe = Resultant moment (M)

θ = Internal angle of tilting (rad)

A = Cross sectional area of the specimen

h = Height of the specimen at each gyration

The CFI is the summation of the resistive effort from the second gyration to the number of the gyrations corresponding to 92 percent Gmm as presented in Equation 7. Higher CFI indicates higher resistance of the mix to deformation. Faheem and Bahia (2004) found that the values of CFI ranged from 100 to 1000 as shown in Figure 13. They suggested that a lower resistive effort was desirable under 92 percent Gmm and higher resistive effort was desirable for values above 92 percent Gmm.

$$CFI = \sum_{N_{=2}}^{N_{92}} w \quad \text{.....Eqn. 7}$$

where,

w = Resistive effort $\left(\frac{4Fe\theta}{Ah}\right)$

$N_{=2}$ = Gyration 2

N_{92} = Number of gyrations at 92 percent G_{mm}

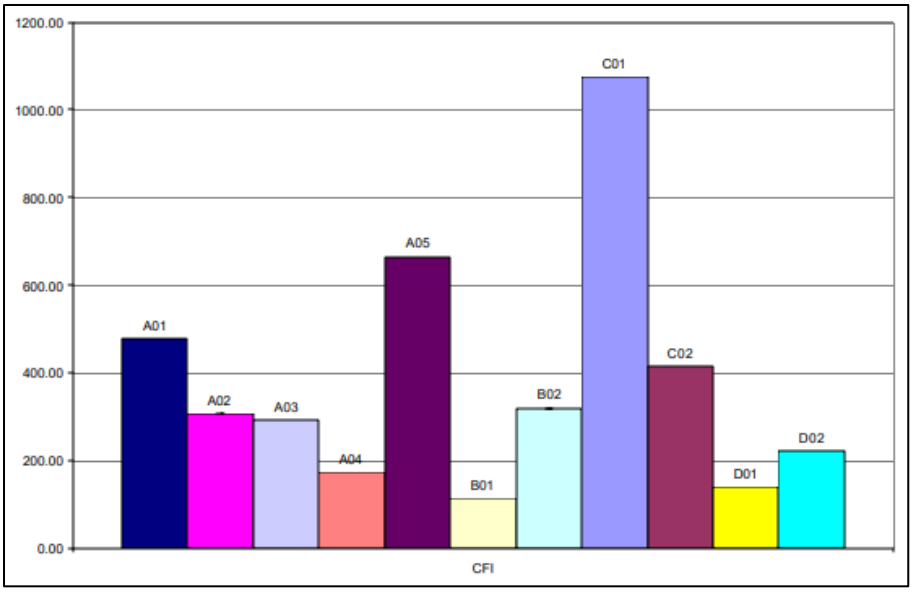

Figure 13. CFI of Different Asphalt Mixes (Faheem and Bahia 2004)

Laboratory Compatibility Index

Kassem et al. (2012) developed an index called LCI calculated from the SGC compaction data to evaluate the compactability of asphalt mixtures in the laboratory. In addition, they examined the correlation between LCI and field compaction. The LCI is a function of the absolute value of the slope (a) and intercept (b), of the laboratory compaction curve as presented in Equation 8 (Kassem et al. 2012).

$$LCI = 100 * \frac{b^{1.2}}{a} \quad \text{.....Eqn. 8}$$

where,

b =The intercept of the compaction curve

a =The slope of the compaction curve (absolute value)

The LCI index was found to have a fair correlation with field compaction (number of passes to achieve a certain density) as presented in Figure 14. The correlation coefficient (R^2) of this relationship was considered acceptable since field compaction is affected by several factors including mix temperature, air temperature, wind speed, and roller speed and weight. The LCI was used to assess the compactability level (i.e., easy, moderate, or difficult) of asphalt mixtures during the mix design stage. Mixes with higher LCI values are easier to compact when compared to mixes with lower LCI values.

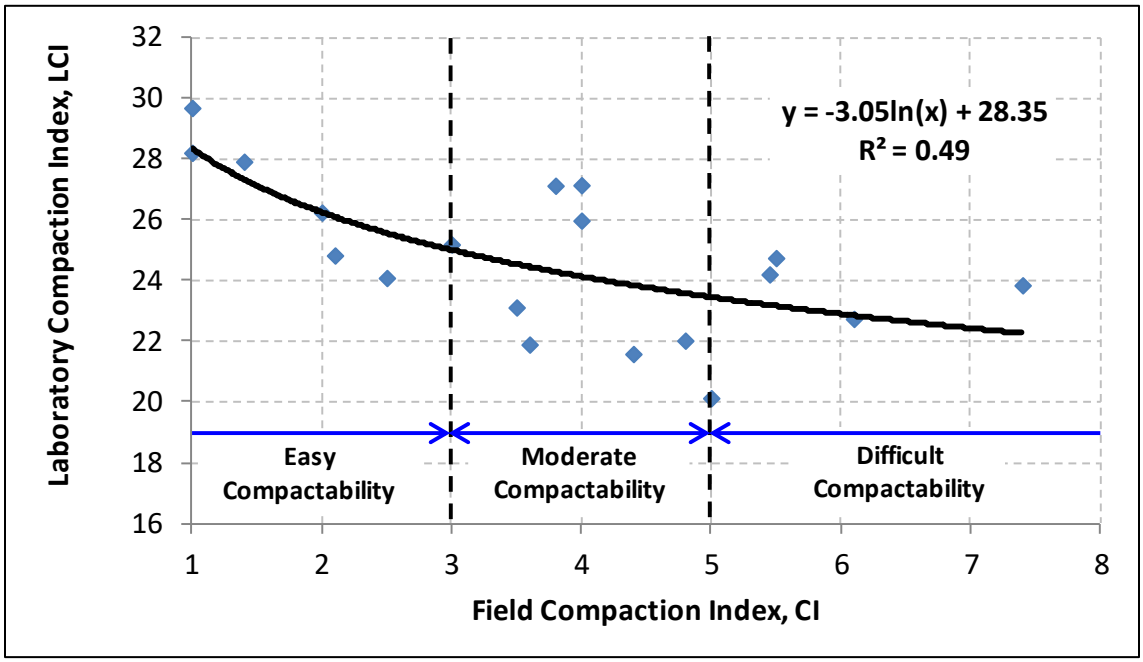

Figure 14. Relationship between Laboratory and Field HMA Compaction Index (Kassem et al. 2012)

Gyratory Stability

McRae (1962 and 1965) developed an equation to determine the shear stress in HMA during compaction, and several researchers used this equation to predict mix stability and performance (Mallick et al. 1999; Kumar et al. 1974; Sigurjonsson et al. 1990; Ruth et al. 1991). Butcher et al. (1998) used the same equation with data from the Australian SGC (Servopac) and found that the shear stress was sensitive to changes in binder type. Dessouky et al. (2004) proposed a modified formula to assess the mix stability during laboratory compaction at the mix design stage. They proposed a new stability index called contact energy index (CEI-2). The CEI-2 reflects the mix resistance to deformation during compaction until the maximum number of gyrations (N_{max}). Abdo et al. (2010) proposed the GS index which is a modification to CEI-2 to evaluate the mix stability. This section discusses the development of CEI-2 and GS and the effect of mix composition on these indices.

Laboratory compaction curves can be divided into two parts: Part A and Part B (Figure 15) (Bayomy et al. 2004; Bahia et al. 2003; Dessouky et al. 2004). The first part (i.e., Part A) shows steep change in slope with number of gyrations. This part represents the densification of loose mixes. As a result, percent air voids in the mix drops quickly. In this part, aggregates in the mix do not experience significant amount of shear forces. Therefore, reorientation or sliding of aggregates is not observed. Whereas, in the second part (i.e., Part B) aggregates experience more particle-to-particle contact and higher shear stresses. Most of the energy is dissipated through aggregate sliding (Dessouky et al. 2004). Consequently, it increases the shear strength. In Part B of the compaction curve, the sample height does not change significantly, while there

is a small decrease in air voids. Therefore, Part B is of interest to calculate the mix stability at ambient temperature (Bahia et al. 2004).

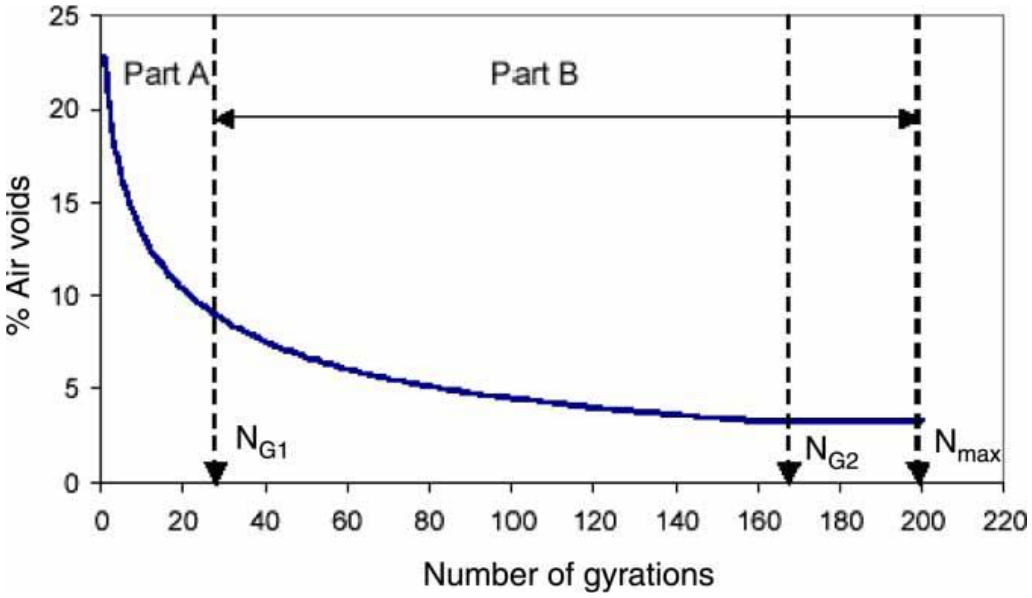

Figure 15. Typical Compaction Curve (Dessouky et al. 2004)

Dessouky et al. (2004) and Abdo et al. (2010) analyzed the forces acting on the SGC samples during compaction (Figure 16) and calculated the internal shear force at mid-height (S_i) of the sample at any number of gyrations (i). The shear force can be determined using Equations 9 through 11.

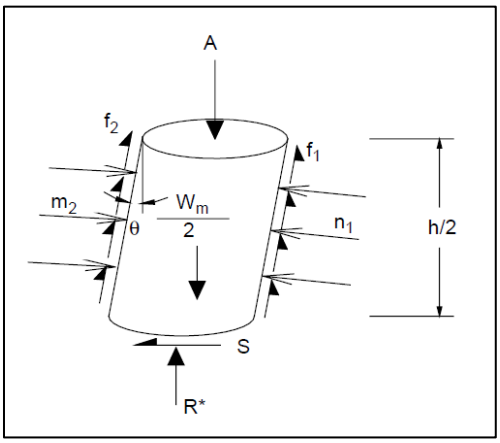

Figure 16. Forces Acting on the Specimen at θ Angle of Gyration (Dessouky et al. 2004)

$$S_i = (n_2 - n_1)\cos\theta + \frac{1}{2}.(\sum P - W_d)\,.\tan\theta$$

…… Eqn. 9

$$n_2 - n_1 = \frac{\left(F_v + \frac{W_m}{2}\right)\left(x_\theta - \frac{h}{2}\tan\theta\right) - \frac{1}{2}(\sum P - W_d)(x_\theta - \frac{r}{\mu}\tan\theta)}{\frac{h}{4\cos\theta} + \mu.r.\cos\theta - \frac{r\sin^2\theta}{\mu.\cos\theta}}$$

…… Eqn. 10

$$\sum p = \frac{\text{Area}.h.r}{2.L}$$

…… Eqn. 11

where,

S_i = Shear force at mid height of sample, kN

F_v = Resultant force of the applied pressure, kN

W_m = Weight of the asphalt sample, kN

W_d = Weight of the mold, kN

θ = Angle of gyration, degrees

h = Height of sample at any gyration

r = Sample radius

n_1 & n_2 = Normal forces acting on the half sample surface due to friction

x_θ = The distance from the center to the point where the resulting force is acting

μ = The distance from the center to the point where the resulting force is acting

ΣP = Average force on the three actuators, kN

τ = Shear Stress given by the Superpave gyratory compactor, kPa

L = Radial distance to the point of application of the actuator load, it is equal to 165 mm

The calculated shear forces were utilized to calculate CEI-2 using Equation 12. CEI-2 reflects the ability of the aggregate structure to develop contacts among the particles when subjected to shear force. The term CEI-2 was introduced to specify the accumulated shear energy increments that are dissipated in the sample during Part B of the compaction process (Abdo et al. 2010).

$$CEI = \sum_{N_{G1}}^{N_{G2}} S_i \Delta d_i$$ ..... Eqn. 12

where,

S_i = Shear force at mid height of sample, kN

Δd_i = The change in sample height in meters between number of gyrations (i) and (i-1)

The CEI-2 is calculated over a range of number of gyrations from N_{G1} to N_{G2} (Figure 15) where N_{G1} is the number of gyrations at which the compaction curve is linear. This point defines the starting of Part B of the compaction curve in Figure 15. After this point (i.e., N_{G1}), the mix starts to gain shear resistance up to N_{G2} where it reaches a maximum value. The shear strength remains almost the same from N_{G2} to N_{max}. However, if compaction continues beyond the maximum number of gyrations (i.e., N_{max}), the sample may lose its shear strength due to micro fractures at the particle contacts.

Bayomy et al. (2007) defined N_{G2} as N_{design} rather than N_{max} on the compaction curve since the samples are typically produced at N_{design} (Abdo et al. 2010). The summation of shear energy increments between N_{G1} and N_{design} is referred to as GS as presented in Equation 13.

$$GS = \sum_{N_{G1}}^{N_{design}} S_i \Delta d_i$$ ..... Eqn. 13

Several studies investigated the sensitivity of CEI-2 or GS to mix components including aggregate type, aggregate size and texture, binder content, and binder grade; compaction variables including angle of gyration and pressure; as well as mechanical properties, compactor type, and method of measuring compaction force (Dessouky et al. 2003; Dessouky et al. 2004; Abdo et al. 2005; Abdo et al. 2010). The following section provides a brief discussion of the effects of some of these factors on mix stability.

Effect of Binder Content

Dessouky et al. (2004) showed that CEI-2 decreases with binder content. To investigate the effect of binder content on CEI-2, the researchers used two different binder contents in 16 mixes. The first binder content was an optimum value determined from the Superpave mix design procedure. The second binder content was 0.8 percent higher than the OBC value which was referred as optimum plus. The results shown in Figure 17a revealed that CEI-2 was higher for mixes with OBC. The reason was stated as mixes at OBC require higher compaction forces to cause aggregate sliding (Dessouky et al. 2004).

A similar observation was reported by Abdo et al. (2010) for GS. The researchers utilized two mixes (mix 1 and Mix 2) at three binder contents. One was optimum binder content and the other two were Optimum + 0.5 percent and Optimum – 0.5 percent. This study also found that mixes with lower binder content (i.e., Optimum – 0.5 percent) provided the highest GS values (Figure 17b). It is believed that the increase of friction between aggregate particles resulted in higher GS values for the mixes at a lower binder content. Another study by Abdo et al. (2007) provided contradictory results. It was found that higher asphalt content provided higher CEI-2 values (Figure 17c). The researchers speculated that the cause of the inconsistent results could have been due to the fact that the mixes were designed in accordance with the Hveem method, but the OBCs estimated in accordance with the Superpave PG grading system.

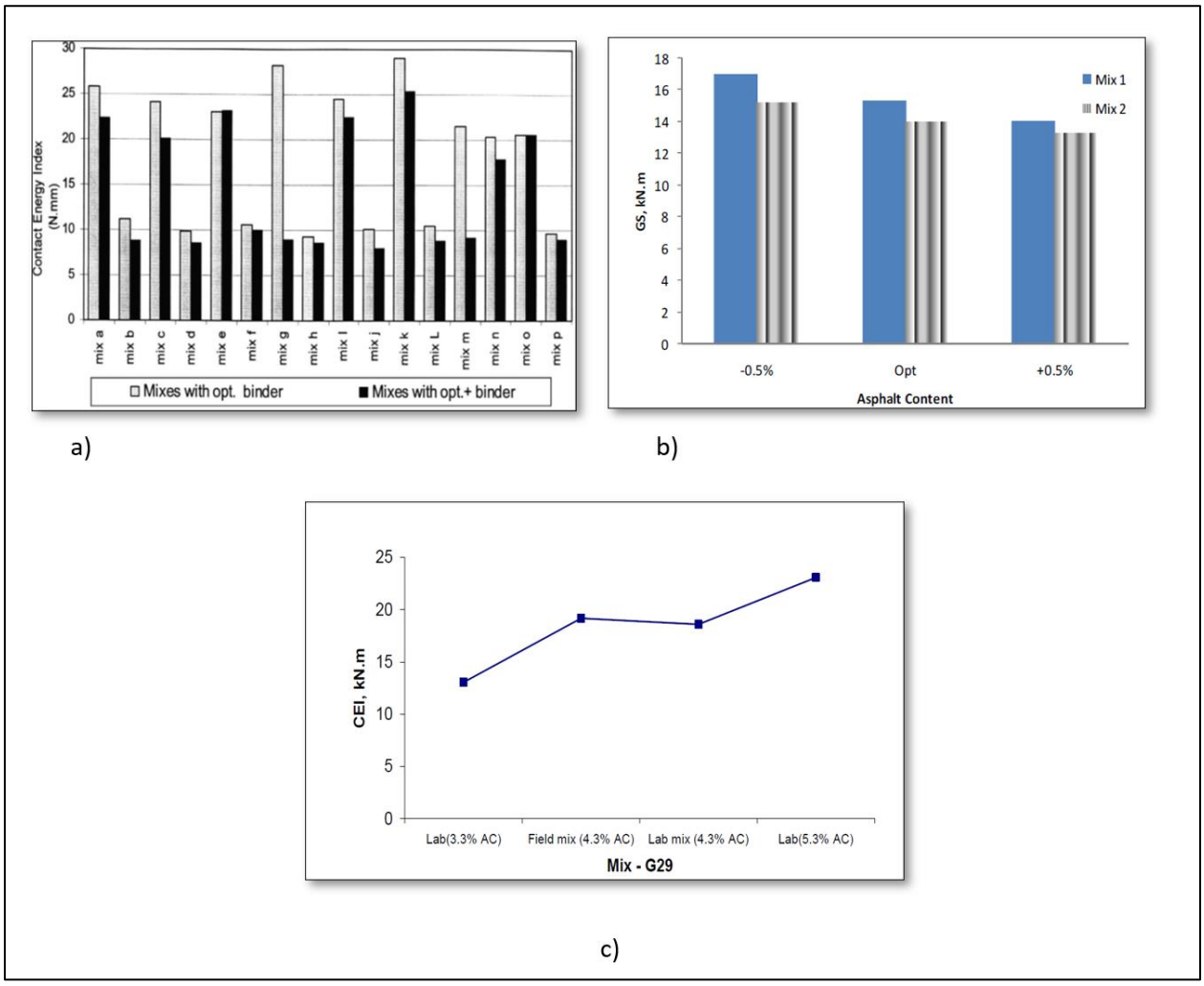

Figure 17. Effects of Binder Content on CEI-2 and GS (Dessouky et al. 2004; Abu Abdo et al. 2007)

Effect of Binder Grade

The binder grade generally does not have a significant effect on GS. The reason is that samples are compacted at different temperatures depending on the PG of the binder to achieve the same viscosity (0.28 plus/minus 0.30 Pa·s). At the compaction temperature, the binder turns into liquid and as a result, the PG binder grade doesn't make any significant difference on the resistance of the mix to the applied compaction forces. An example is depicted in Figure 18 where two mixes (i.e., Mix 1 and Mix 2) with different binder PG have similar GS average values.

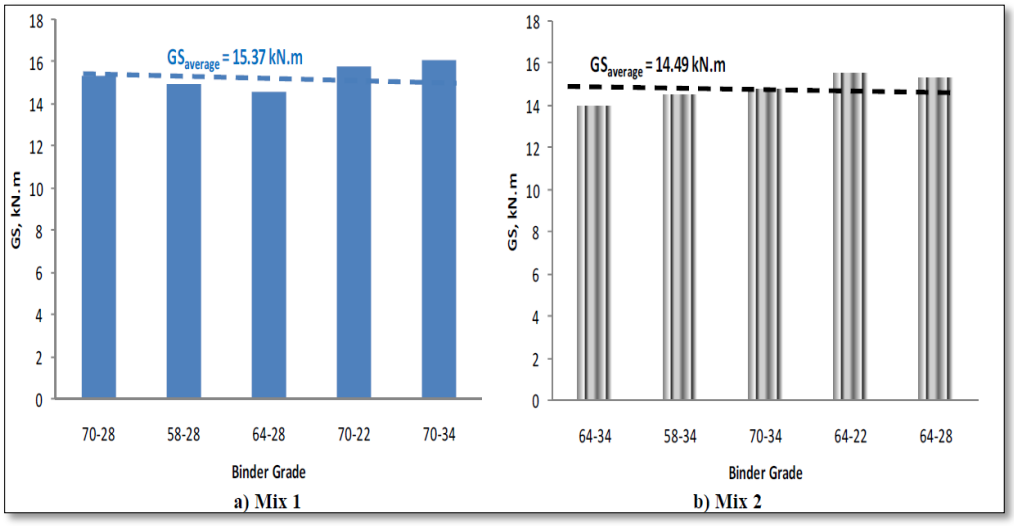

Figure 18. Effects of Binder Grade on GS (Abdo et al. 2010)

Effect of Aggregate Properties

Dessouky et al. (2004) evaluated the effect of aggregate type on the CEI-2. The researchers tested mixtures prepared with two different aggregates (i.e., gravel and limestone). The results showed that limestone mixtures provided higher CEI-2 values when compared to that of the gravel mixtures. The limestone aggregate had higher texture and angularity, so it required more energy to be compacted than that of mixes with gravel (Dessouky et al. 2004).

A study conducted by Abdo et al. (2010) demonstrated the effect of aggregate gradation on GS. Four different aggregate gradations were included: Mix 1 (25 mm mix), Mix 2 (19 mm mix), very coarse mix (25 mm mix), and fine mix (4.75 mm mix). All four mixes were prepared with the same binder grade (PG 70-28) and binder content (4.9 percent). The results revealed that the coarser mixes produced higher GS values as shown in Figure 19 (Abdo et al. 2010).

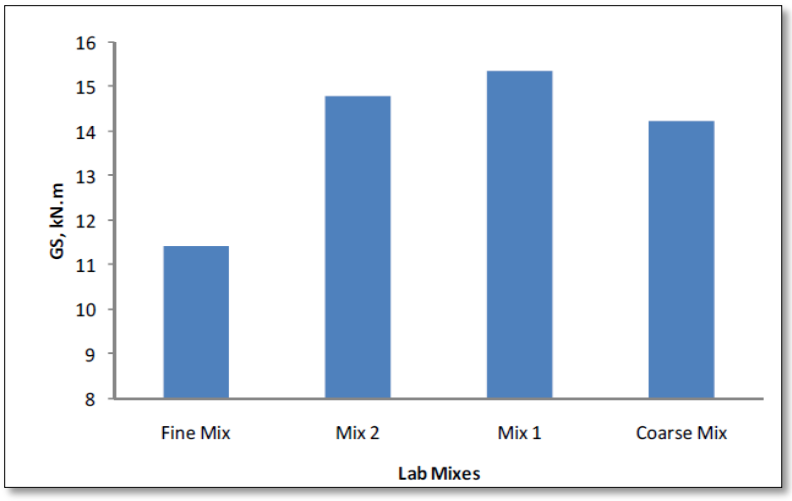

Figure 19. Effect of Aggregates Gradation on GS (Abdo et al. 2010)

Abdo et al. (2005) evaluated the effect of aggregate shape on CEI. The researchers examined three aggregate properties using the Aggregate Imaging System (AIMS) developed by Masad et al. (2003). These properties were surface texture, angularity, and sphericity. The relationship between surface texture and CEI is presented in Figure 20. It can be observed that, in general, an increase in surface texture yielded increments in CEI. This could be due to the increase in friction among aggregate particles due to the increase in surface texture. However, there was no clear relationship between angularity and sphericity with the CEI for the range of aggregates used in their mixes (Abdo et al. 2005).

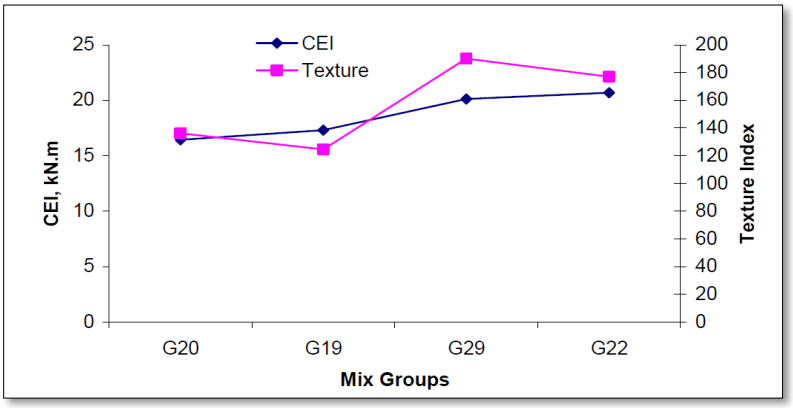

Figure 20. Relationship between Aggregate Surface Texture and CEI (Abdo et al. 2005)

Effect of Natural Sand

Dessouky et al. (2004) also investigated the effect of inclusion of natural sand in asphalt mixtures. The researchers tested 16 different mixes without natural sand (i.e., 0 percent) and with 40 percent natural sand. The results presented in Figure 21 revealed that mixes without natural sand yielded higher CEI-2

values when compared to their counter mixes with 40 percent natural sand. Natural sand has rounded shape with low texture; therefore, mixes with natural sand do not have high resistance to deformation, subsequently yielding mixes with low stability (Dessouky et al. 2004).

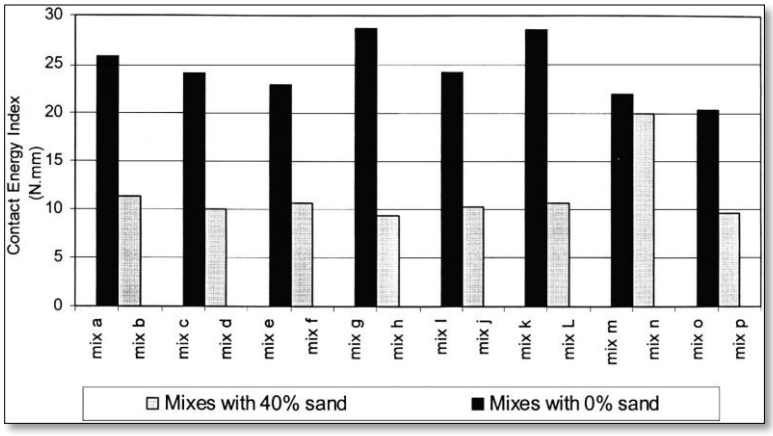

Figure 21. Effects of Natural Sand on CEI-2 (Dessouky et al. 2004)

Effect of Compaction Variables

The angle of gyration and pressure are the two main compaction variables considered in the SGC. Dessouky et al. (2004) evaluated the effect of various compaction parameters on mix stability using a Servopac compactor. They selected four mixes (C, D, K, and L) prepared with different component materials. Five specimens were prepared from each mix and compacted under five different angles of gyrations (i.e., 0, 0.75, 1.5, 2.25, and 3.0^{o}). The results showed that samples gained more shear strength with the increase in angle of gyration (Figure 22). Test samples compacted at 0 ^{o}, collapsed right after they were extracted from the compaction mold as contacts between particles were not developed through shear action induced by the angle of gyration.

To evaluate the effect of applied pressure on mix stability, Dessouky et al. (2004) considered three pressures (i.e., 450, 600, and 750 kPa). In addition, they considered two different angles of gyration (1.5 and 2.25 ^{o}). The results showed that the CEI-2 increased with the increase in applied pressure. However, at different combinations of pressure and angle of gyration, the rank of the mixes in terms of CEI-2 values remained almost the same.

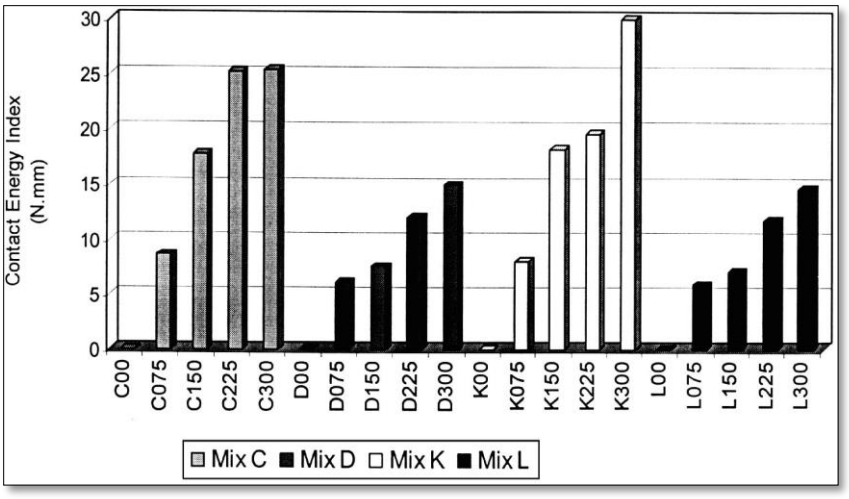

Figure 22. Effects of Angle of Gyration on CEI-2 (Dessouky et al. 2004)

Effect of Compactor Type

Abdo et al. (2005) evaluated the effect of compactor type on the CEI. Twelve mixes were prepared and compacted using a Servopac gyratory compactor and a Troxler gyratory compactor (Model 4140) equipped with a pressure distribution analyzer (PDA) plate. The results demonstrated good correlation between CEI-2 values calculated from Servopac and Troxler compactors as shown in Figure 23.

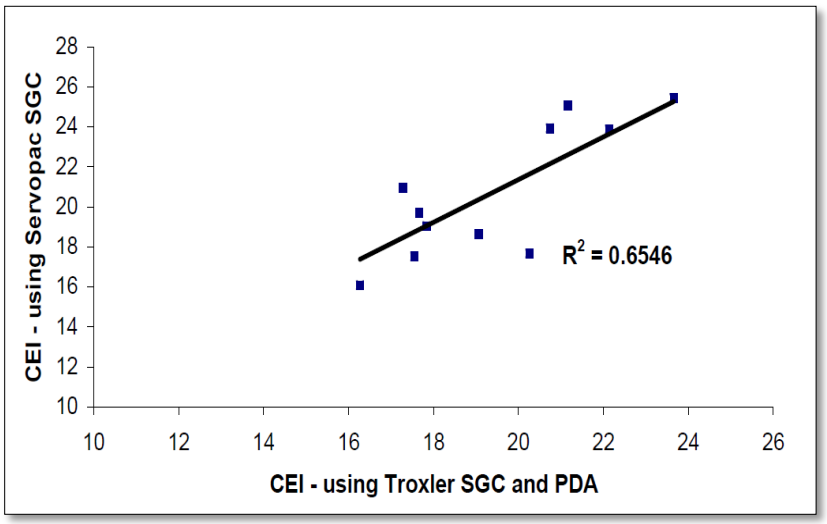

Figure 23. Effects of Compactor Type on CEI-2 (Abdo et al. 2005)

Gyratory Stability of Laboratory versus Field Mixes

Abdo et al. (2010) compared the GS for mixes produced in the laboratory with the same mix design of mixes sampled from the field. They evaluated two mixes: Mix 1 and Mix 2. They found a small difference in GS between the mix produced in the lab and field for Mix 1, while the there was no difference in GS for Mix 2 as presented in Figure 24.

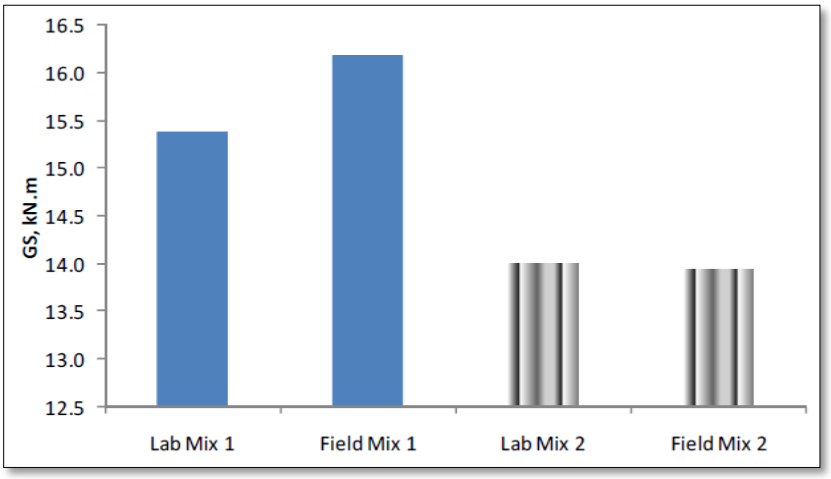

Figure 24. Comparison between GS of Lab and Field Mixes (Abdo et al. 2010)

Relationship between CEI and Rut Depth

Abdo et al. (2005) examined the relationship between the CEI-2 and permanent deformation or rut depth. They examined 16 mixes of different binder grades and measured the rutting using the APA. Each mix had three replicates. The comparison results between the CEI and the rut depth revealed that there was no clear relationship between CEI and rut depth for all test binders. When the researchers compared the CEI to the rut depth for each binder PG, they found good correlation between APA and CEI-2 for PG 58-28 and PG 58-34 but not for PG 64-28 and PG 64-34 (Figure 25).

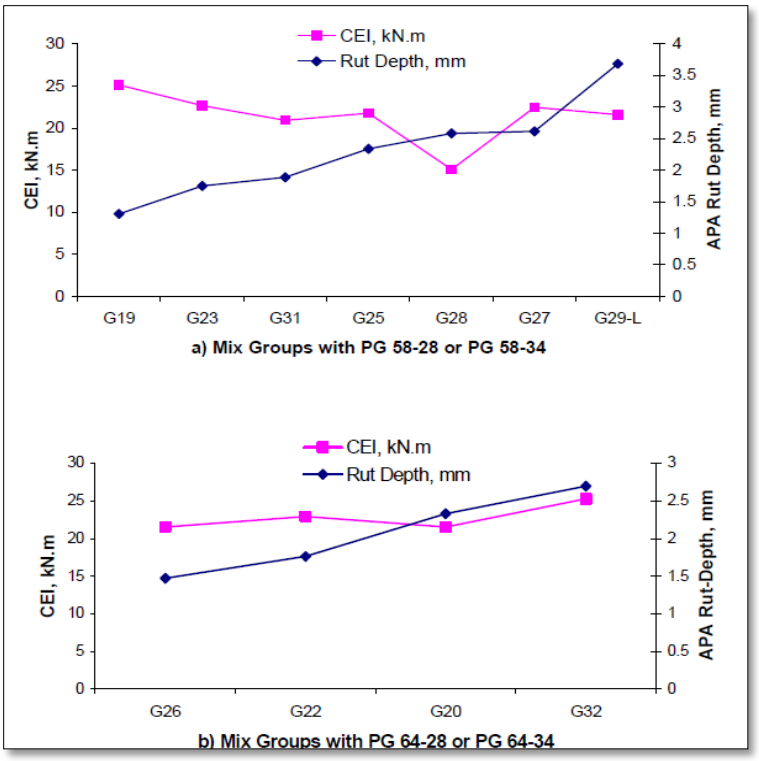

Figure 25. Comparison between CEI-2 and APA Rut Depth (Abdo et al. 2005)

3. Materials Description and Experimental Design

Chapter 3 provides information about asphalt mixes and field projects evaluated in this study. It also discusses the current ITD specifications for HMA mixes and documents methods and standard protocols used to evaluate the performance of laboratory and field produced mixes. The laboratory tests included rutting resistance, cracking resistance, moisture damage, and mix stability during compaction.

Materials Description

RAP and Aggregate Characterization

Two different sources of RAP were used in this project. The first source (i.e., RAP No. 1) was obtained from an asphalt plant in Pullman, WA, while the second source of RAP (RAP No. 2) was acquired from an asphalt plant in Lewiston, ID. To control the variability of the RAP materials, the research team fractionated the RAP materials into coarse (retained on Sieve No. 4) and fine (passing Sieve No. 4) sizes and incorporated both sizes into the mix in accordance with the job mix formula. Figure 26 shows the RAP binder content for the two sources of RAP using the ignition oven method. RAP No. 2 had higher binder content (i.e., 5.7 percent) compared to RAP No. 1 which had 4.3 percent binder content. Figure 27 shows the gradation of RAP materials from the two sources. In addition to the RAP materials, two types of virgin aggregates (i.e., basalt and river gravel) were obtained and used in this study. The basalt rock was acquired from an asphalt plant in Pullman, WA, while the river gravel was obtained from an asphalt plant in Lewiston, ID.

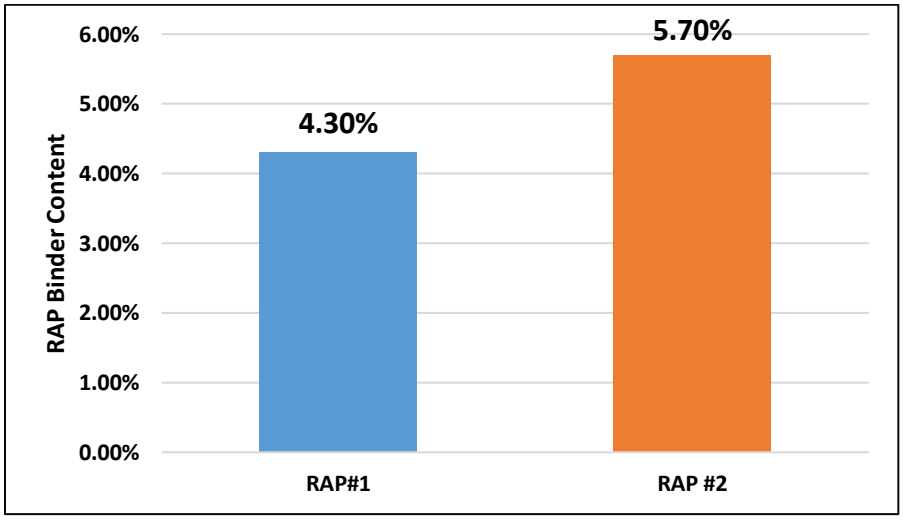

Figure 26. Binder Content of RAP No. 1 and RAP No. 2

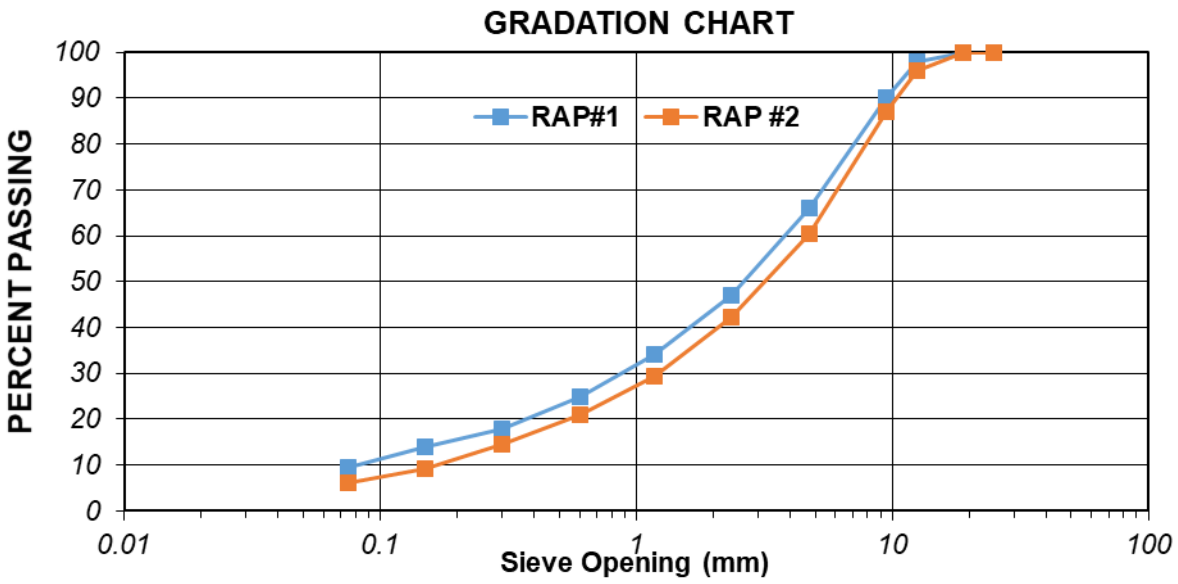

Figure 27. Aggregate Gradation of RAP No. 1 and RAP No. 2

Laboratory-Mixed Laboratory-Compacted Mixes

The researchers prepared LMLC mixes. The LMLC included several variables including aggregate type, binder type and content, RAP content, percent air voids, and mix design. LMLC mixes were tested to evaluate the performance in terms of mix stability, cracking and rutting resistance, and moisture damage. In addition, the research team evaluated the applicability and sensitivity of GS index and other compaction parameters to capture the change in mix composition (e.g., RAP content, binder content, binder grade) during the laboratory compaction of the LMLC. Table 3 summarizes the main variables of the testing matrix of LMLC and PMLC mixes. Three binder grades (i.e., PG 58-34, PG 64-28, and PG 76-22) at three different binder contents (OBC, OBC+0.75 percent, and OBC-0.75 percent) were included in preparing the LMLC mixes. The testing matrix also included two types of aggregates (i.e., basalt rock and river gravel) and two RAP sources (i.e., RAP No. 1 and RAP No. 2) with various RAP contents (i.e., 0 percent, 25 percent, and 50 percent). Some LMLC samples were tested at 4 percent air voids and others were tested at 7 percent air voids for various tests as discussed in detail later in this chapter.

Table 3. Testing Matrix of LMLC Asphalt Mixture

Mix type	SP5	SP3	-
RAP	0 percent	25 percent	50 percent
RAP Sources	1	2	-
AV percent	4 percent	7 percent	-
Aggregate Type	Basalt	River Gravel	-
Binder Grade	PG 76-22	PG 64-28	PG 58-34
Binder Content	OBC	OBC+0.75 percent	OBC-0.75 percent
Anti-Stripping agent	0 percent	1.50 percent	-

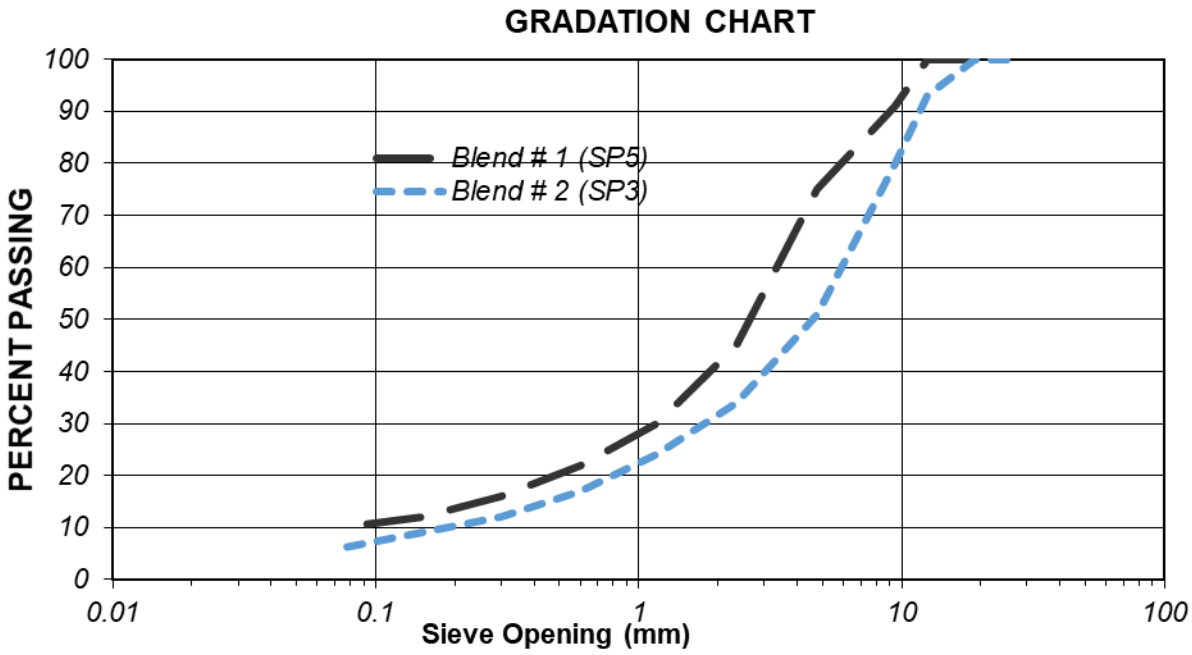

Figure 28. SP3 & SP5 Aggregate Gradation

Plant-Mixed Laboratory-Compacted Mixes

In addition to the LMLC mixes, the research team evaluated PMLC mixes obtained from new ITD paving projects. Several different batches of loose mix were sampled throughout the construction of each project. PMLC from three batches (i.e., Batch No. 1, Batch No. 2, Batch No. 3) from each project were obtained and tested to evaluate the variability in mix performance during production. Each batch was collected at different times during project construction. The laboratory performance evaluation included mix stability during compaction as well as resistance to cracking, rutting, and moisture damage. The team

examined six PMLC mixes distributed across the state as presented in Table 4. PMLC samples were prepared from 18 batches of loose mix as summarized in Table 6. The plant loose mixes were sampled and delivered in 50-pound boxes to the materials laboratory. Each box was clearly labeled with information about the project including project/key number, milepost (MP), and binder content and other mix properties. The Job Mixes Formulas (JMFs) for all PLMC mixes are provided in Appendix A. Table 5 summarizes the main properties of PMLC mixes. The PLMC mixes included two mix designs (SP3 and SP5), two NMAS (12.5 mm and 19.0 mm), three binder grades (PG 64-28, PG 64-34, PG 70-28), six binder contents (5.1 percent, 5.2 percent, 5.3 percent, 5.4 percent, 5.9 percent, and 6.2 percent), and three RAP contents (0 percent, 17 percent, and 30 percent).

Table 4. PMLC Project Information

Mix #	Project ID	District	Construction Year	Project Key No.	Location
1,2,3	D1-P1-b1,2,3	1	2020	20794	US-95, JCT SH-53 OIC, UPRP BR Kooteai Co.
4,5,6	D3-P5-b1,2,3	3	2020	21858	US20/26, SH16 to Linder Road, sh55 Marsing to SR
7,8,9	D6-P1-b1,2,3,	6	2019	19711	US-Ashton Bridge to Dumpground Road
10,11,12	D1-P2-b1,2,3	1	2020	20795 & 19794	US-95, Garwood Rd GS 4 Frontage Rds & H-57, Priest River Boat Access
13,14,15	D4-P1-b1,2,3,	4	2020	18881	I-84/I-86 Interchange System
16,17,18	D4-P2-b1,2,3	4	2020	20170	Sh-81, Declo to Burley

Table 5. PMLC Mix Properties

Project #	District	Project ID	Mix Type	Specified Binder PG	Virgin Binder PG	Binder Content Pb (percent)	RAP (percent)	NMAS	Theoretical Specific Gravity (Gmm)	Bulk Specific Gravity (Gsb)
1	D1	D1-P1	SP3	PG64-28	PG 58-34	5.2	30	1/2”	2.473	2.646
2	D3	D3-P5	SP3	PG64-34	N/A	5.4	0	1/2”	2.430	2.571
3	D6	D6-P1	SP5	PG64-34	PG64-34	5.9	16	3/4”	2.382	2.481
4	D1	D1-P2	SP3	PG64-28	PG 58-34	5.3	30	1/2”	2.476	2.654
5	D4	D4-P1	SP5	PG70-28	N/A	5.1	17	3/4”	2.414	2.559
6	D4	D4-P2	SP3	PG64-28	N/A	6.2	17	1/2”	2.293	2.417

Testing Protocols

Evaluation of Rutting Resistance

The rutting resistance of the test mixtures were evaluated using two performance tests: the APA rut test and the HWTT. The APA rut test and HWTT were conducted in accordance with AASHTO T 340 and AASHTO T 324, respectively. The HWTT is conducted in wet condition; therefore, it can be used to assess moisture susceptibility in addition to rutting resistance. Conversely, the APA rut depth in conducted in dry condition. Both tests can be conducted using the APA device (Figure 29). The APA device is an accelerated laboratory loading equipment that simulates traffic using loaded steel wheels. The rut depth is measured at five locations in the APA rut test, while it is measured at 11 locations in the HWTT. The average rut depth is calculated and reported for both tests as recommended by AASHTO T 340 and AASHTO T 324. The APA test is terminated after 8,000 cycles, while the HWTT is terminated after 20,000 passes or after a rut depth of 20 mm is achieved.

In both tests, the samples are subjected to accelerated reciprocating wheel loading to simulate traffic loading repetitions in the field. Table 6 summarizes the test conditions, sample dimensions, conditioning time, test duration, and other relevant information for both tests (i.e., APA rut test and HWTT). Both tests are performed on cylindrical specimens that are 2.5 in (150 mm) in diameter and 2.95 in and 2.36 in (75 mm and 60 mm) thick for APA and HWTT, respectively. The test specimens are compacted to achieve 7 plus/minus 0.5 percent air voids. Four cylindrical specimens are used for each test. The HWTT test specimens are submerged in water at a temperature of 122^{o}F (50^{o}C) and conditioned for one hour before the start of the test. The APA samples are conditioned in air at a temperature equal to the higher binder PG for six hours.

As per the standards, the APA rut test wheels apply 578 N load on pressurized rubber hoses that have a constant pressure of 690 kPa at a constant rate of 60 pass/minute. The HWTT wheels apply 705 N load directly on the surface of the test specimens at a constant rate of 52 pass/minute. Both tests collect the rut depth measurements with number of cycles or passes until the test is terminated.

Table 6. Testing Protocols for Rutting Evaluation (Kassem et al. 2019)

Test	APA rut test	HWTT
Testing Standards	AASHTO T 340	AASHTO T 324
Specimen shape	Cylindrical	Cylindrical or
Specimen replicates	4	4
Specimen diameter (mm)	150	150
Specimen thickness (mm) for lab prepared	75	60
Specimen thickness (mm) for field Projects	38 -75	38 - 60
Test temperature (°C)	High binder PG	50°C
Specimen conditioning	Air chamber	Water bath
Conditioning time (hour)	6 – 24	1
Testing time (hour)	≈ 2	≈10
Wheel type	Concave wheel	Solid steel
Wheel speed (Pass/minute)	50 ± 5	52
Load (N)	578	705 ± 4.5
Number of data collection locations	5 locations	11 locations
Test output	Cycle-deformation curve	Passes-deformation curve
Distress assessed	Rutting	Rutting and moisture susceptibility

Figure 29. APA and HWTT Rutting Test in the Asphalt Pavement Analyzer

Typically, the rut depth measurements obtained from the APA rut test are different from those obtained using the HWTT since both tests are conducted at different conditions. In the APA rut test, there are only two phases: primary (pre-consolidation) and secondary phase. In HWTT, the rut depth follows an S-curve shape, where three phases can be identified: primary (pre-consolidation), secondary, and tertiary (AASHTO T 340). The primary phase shows a high deformation rate per pass due to initial specimen consolidation. This stage is usually completed within the first 1,000 cycles (AASHTO T 340). In the secondary phase, the deformation continues to increase but at a smaller constant rate (creep slope). The deformation in the secondary phase is due to plastic flow. The tertiary phase exhibits a rapid increase in the rate of deformation (stripping slope). The deformation in the tertiary phase could be due to both rutting plastic flow and moisture damage. Figure 30 and Figure 31 show typical rut depth measurements from the APA rut test and HWTT, respectively.

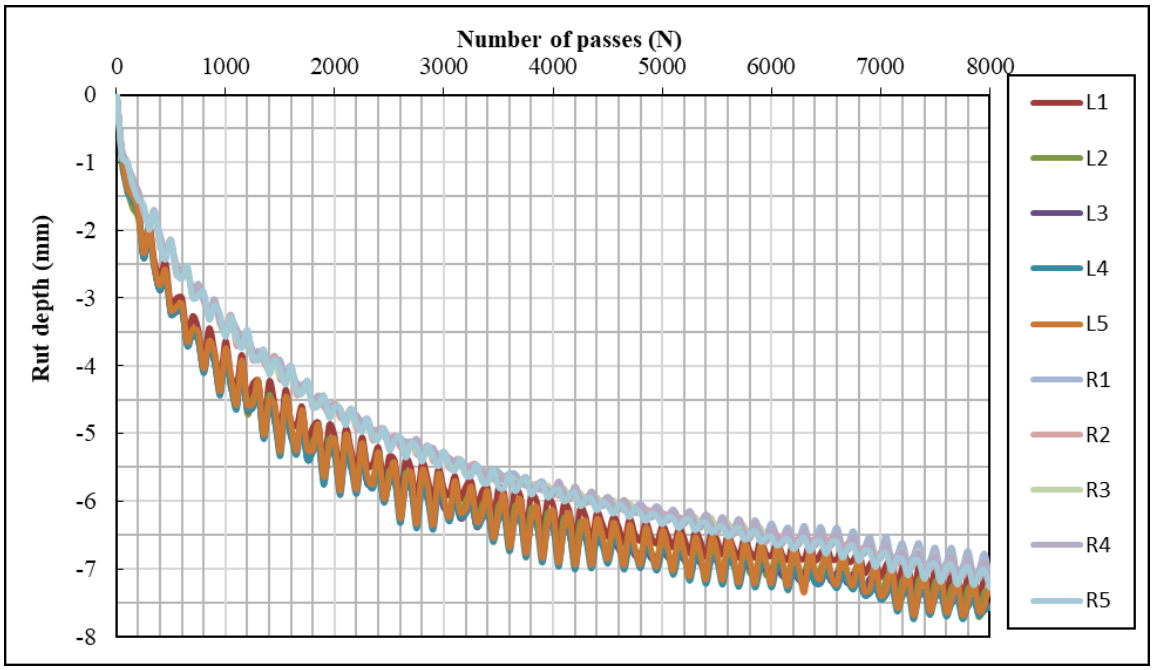

Figure 30. APA Rut Test Left Wheel (L1- L5) and Right Wheel (R1-R5) Deformation Measurement

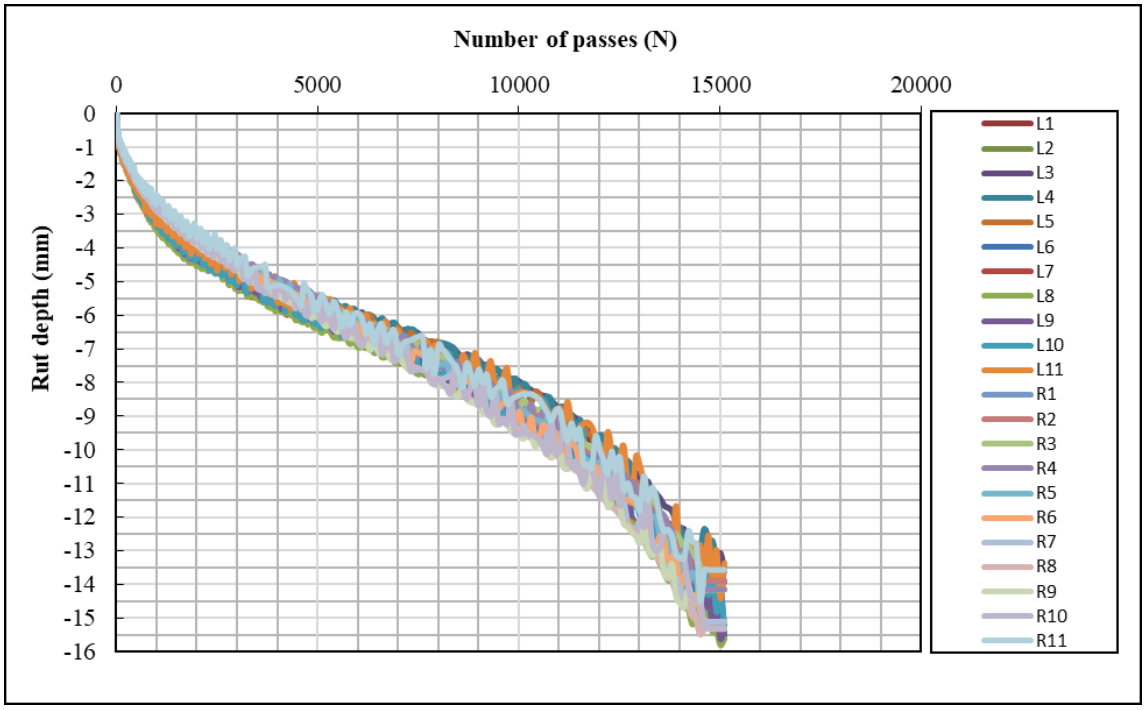

Figure 31. HWTT Left Wheel (L1- L11) and Right Wheel (R1-R11) Deformation Measurement

Evaluation of Cracking Resistance

The research team evaluated the cracking resistance of the test samples using the IDT test in accordance with ASTM D693, Standard Test Method for Indirect Tensile (IDT) Strength of Asphalt Mixtures" In this test, a vertical compressive load is applied on a cylindrical test specimen at a constant rate of 50 plus/minus 5 mm per minute until failure. The applied load and corresponding axial displacement measurements were recorded and analyzed to calculate various cracking performance indicators such as IDEAL-CT_{Index}, CRI, N_{flex} factor, $Weibull_{CRI}$, G_f, $IDT_{Strength}$, $IDT_{Modulus}$, and FI to evaluate the cracking resistance of the test samples.

A servo-hydraulic Material Testing System (MTS-810) equipped with an environmental chamber and data acquisition was used in this study (Figure 32). The test was conducted at a constant temperature of 77°F (25°C). The IDT test specimens are 6 inches (150 mm) in diameter and 2.45 inches (62 mm) thick and compacted to have 7 plus/minus 0.5 percent air voids. The test specimen was placed inside the temperature chamber at 77°F (25°C) for two hours for conditioning before testing. Table 7 summarizes the testing conditions for the IDT test. Figure 32 shows the IDT testing setup and a typical load-deformation curve obtained from the IDT test. At least three replicates were tested from each mix.

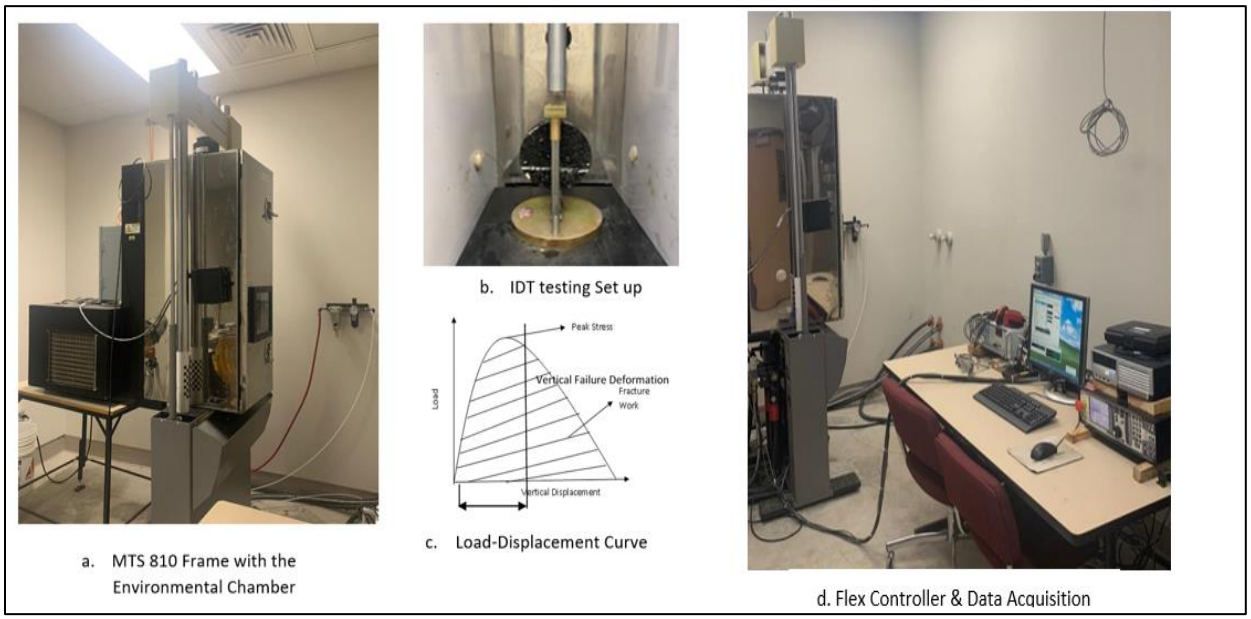

Figure 32. Indirect Tensile Test Setup and Load-Displacement Curve

Table 7. Testing Protocols for IDT and Moisture Damage

Test	IDT	Moisture Damage (Lottman)
Testing Standards	ASTM D6931	AASHTO 283 & ASTM D6931
Specimen Diameter (mm)	150 mm	150mm
Specimen thickness (mm)	minimum of 62 mm	minimum of 63.5 mm
Test temperature (°C)	25	25
Loading rate (mm/min)	50 ± 5	50 ± 5
Air voids	7 ± 0.5 percent	7 ± 0.5 percent
Test output	Load-displacement curve	Peak Load

Moisture Damage

The researchers conducted the modified Lottman test in accordance with AASHTO T 283, Resistance of Compacted Bituminous Mixture to Moisture-Induced Damage, and ASTM D6931, Standard Test Method for Indirect Tensile (IDT) Strength of Asphalt Mixtures to evaluate the moisture susceptibility of selected asphalt mixtures. The testing procedure requires six specimens that are 6 inches (150 mm) in diameter and 2.5 inches (63.5 mm) thick at 7 plus/minus 0.5 percent air voids. The samples were divided into two groups, three samples each. The first group was tested in without conditioning, while the second group was moisture conditioned before testing. The following procedure was followed to moisture condition the test samples:

- The test sample was placed in a water container and subjected to a vacuum of 13 to 67 kPa absolute pressure (10 to 26 in Hg) for 5 to 10 minutes until a saturation level between 70 and 80 percent was achieved.
- The saturated samples were wrapped with plastic saran and placed in a heavy-duty leak-proof bag that contains 10 plus/minus 0.5mL of water and kept in a freezer at 0 plus/minus 5°F (-18°C) for 24 hours.
- The test samples were then removed from the freezer and placed in a distilled water bath at 135 plus/minus 5°F (60°C) for 24 hours.
- The test samples were then transferred to another water at 77°F (25°C) for a minimum of 2 hours before the test.
- The IDT test was conducted on both unconditioned and conditioned samples at a constant compressive axial loading rate of 2 inches per minute (50 plus/minus 5 mm per minute) as shown in Table 7.

The tensile strength of each sample was calculated using Equation 14. The average IDT strength of the unconditioned or dry samples and conditioned or wet samples was calculated, and the TSR was calculated using Equation 15. Asphalt mixes with a TSR of 0.8 or higher were considered to have good resistance to

moisture damage (NCHRP 175). Antistripping agents are often used to improve the resistance to moisture damage, as needed.

$$S_t = \frac{2P}{\pi t D}$$

……..Eqn. 14

where:

St = tensile strength (psi)

P = maximum load (lb)

t = sample thickness (inches)

D = sample diameter (inches)

$$TSR = \frac{S_2}{S_1}$$

…… Eqn. 15

where:

TSR = tensile strength ratio

S1 = average tensile strength of unconditioned samples

S2 = average tensile strength of conditioned samples

Mix Stability Evaluation

The researchers evaluated several compaction indices including the GS, CDI, LP, WEI) w and CFI, and LCI. Test samples that are 6 inches (150 mm) in diameter and 4 inches (100 mm) in height were prepared and compacted using the Pine SGC, Model AFG2 (Figure 33a). The Pine SGC applies a constant pressure of 600 kPa at a gyration angle of 1.16 degrees and a rate of 30 rpm. The test specimens used to assess mix stability and various compaction indices were compacted to have 4 percent air voids. The compaction data including number of gyrations, specimen height, gyration angle, and moment are recorded by the compactor and stored during the compaction process. The Pine SGC provides an Excel-based utility called *PineShear+* to import and analyze the compaction data to calculate several compaction indices such as

CDI, CEI, WEI, LP, and resistive effort. Figures 33b and 34 show a sample of the compaction data and a snapshot of the *PineShear+* (version 15.6) spreadsheet, respectively.

The current *PineShear+* spreadsheet does not include the GS and LCI calculations, and the research team integrated the calculations of these indices in a revised spreadsheet. More information about the GS and LCI are provided in Chapter 4.

a. Pine AFG2 Compactor

Example: Pine AFG2A Data File Format

File Name: SEP14_04.DAT
Time: 14:36
Date: 04/14/07
Diameter: 150 mm
S/N: 8001

Gyration (#)	Height (mm)	Angle (deg Int)	Pressure (kPa)	Moment (N-m)
0	144.2	-----	576	653.6
1	140.7	1.16	576	516.8
2	137.0	1.16	587	665.4
3	134.6	1.16	589	710.9
4	132.8	1.16	590	742.7
5	131.4	1.16	590	766.5
6	130.2	1.16	593	777.1
7	129.3	1.16	593	786.9
8	128.4	1.16	592	792.1
9	127.7	1.16	593	799.4
10	127.0	1.16	591	804.0
11	126.4	1.16	593	809.0
12	125.9	1.16	594	812.4
13	125.4	1.16	595	812.8
14	124.9	1.16	596	817.7
15	124.5	1.16	595	818.6
16	124.1	1.16	595	821.9
17	123.7	1.16	596	826.3
18	123.3	1.16	592	813.5
19	123.0	1.16	599	843.0
20	122.8	1.16	597	831.1
21	122.5	1.16	595	821.6
22	122.2	1.16	598	834.9
23	121.9	1.16	597	831.3
24	121.7	1.16	598	836.3
25	121.5	1.16	598	837.4
26	121.2	1.16	599	840.8
27	121.0	1.16	599	845.3
28	120.8	1.16	599	847.9
29	120.6	1.16	600	840.7
30	120.4	1.16	600	846.5
31	120.3	1.16	600	845.1
32	120.1	1.16	600	846.9

b. Compaction Data File Formats

Figure 33. the Pine Superpave AFG2 Gyratory Compactor (SGC)

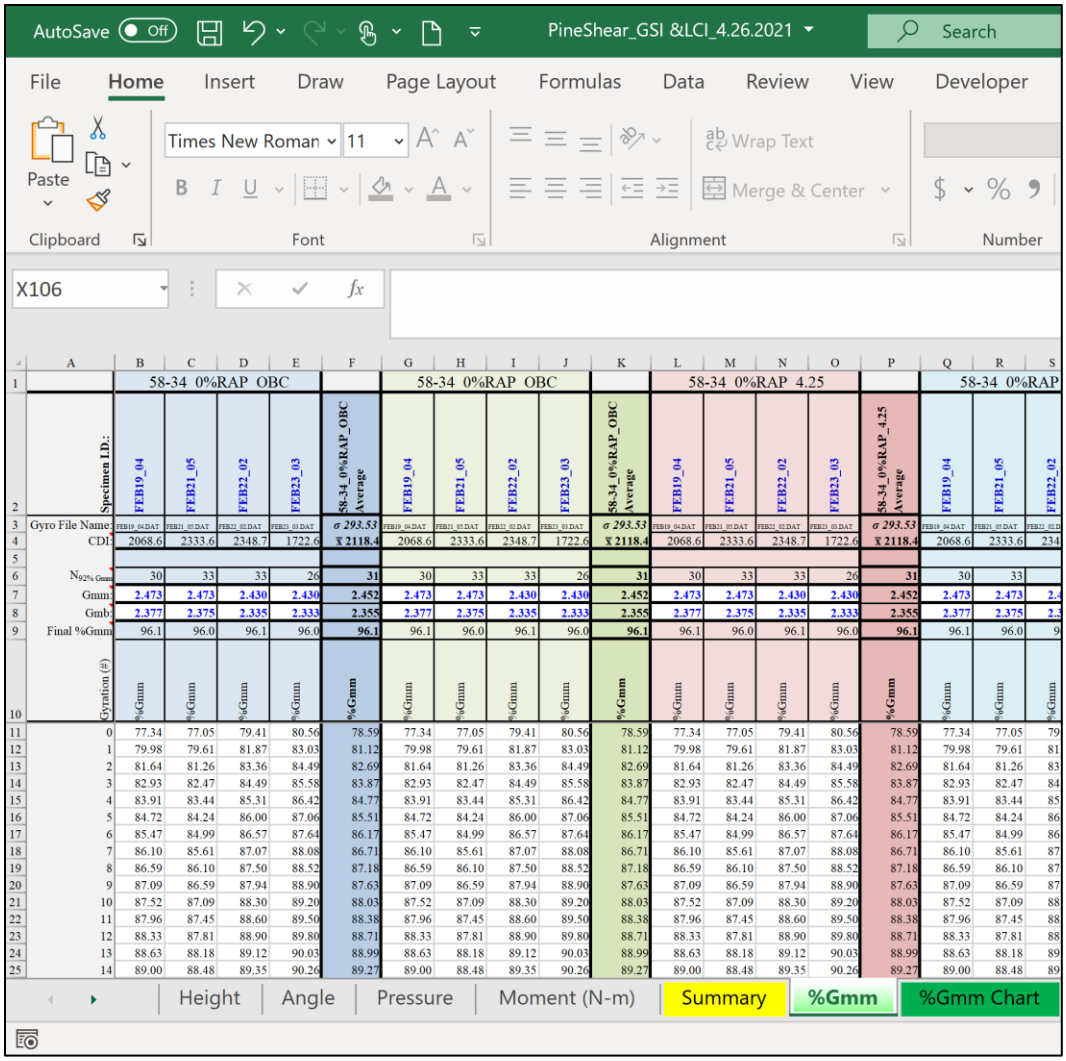

Figure 34. Compaction Data Imported to PineShear+ (V15.6)

4. Development of Gyratory Stability Algorithm and Sensitivity of Compaction Indices to Mix Composition

Chapter 4 discusses the development of the GS index from the compaction curve data specific to Pine AFG2AS gyratory compactor. In addition, this chapter investigates the sensitivity of various compaction indices, including the GS, CDI, LCI, CFI, LP, CEI, and WEI to mix composition. Furthermore, this chapter discusses the development of an Excel spreadsheet to facilitate the GS and LCI calculations.

Gyratory Stability Concept

ITD RP 175 developed an algorithm to determine the GS index for asphalt mixes based on the Servopac gyratory compactor. The GS index as determined by the Servopac is not a unique number for the mix, but rather dependent on the compactor equipment. Currently, ITD has adopted the use of the Pine gyratory compactor in all districts as well as at headquarter laboratories. Therefore, a modified algorithm to estimate GS for compaction data obtained with the Pine gyratory compactor (model AFG2AS) was developed. The GS index is calculated using the applied shear force and change in height during compaction. The incremental shear energy exerted on the sample during compaction is calculated and summed. This concept was applied and used to develop the GS for the Servopac Gyratory Compactor and was discussed in the literature review presented in Chapter 2. The next section discusses the development of the GS for Pine gyratory compactor.

Derivation of Gyratory Stability

The derivation of the GS index relies on the calculation of the maximum horizontal shear stress (S_g) generated in the sample by the gyratory compactor at any number of gyrations at mid height. Figure 35 shows the free body diagram of a specimen during compaction using a SGC Compactor. Figure 36 shows the free body diagram of half specimen and the resultant shear force at mid depth during compaction.

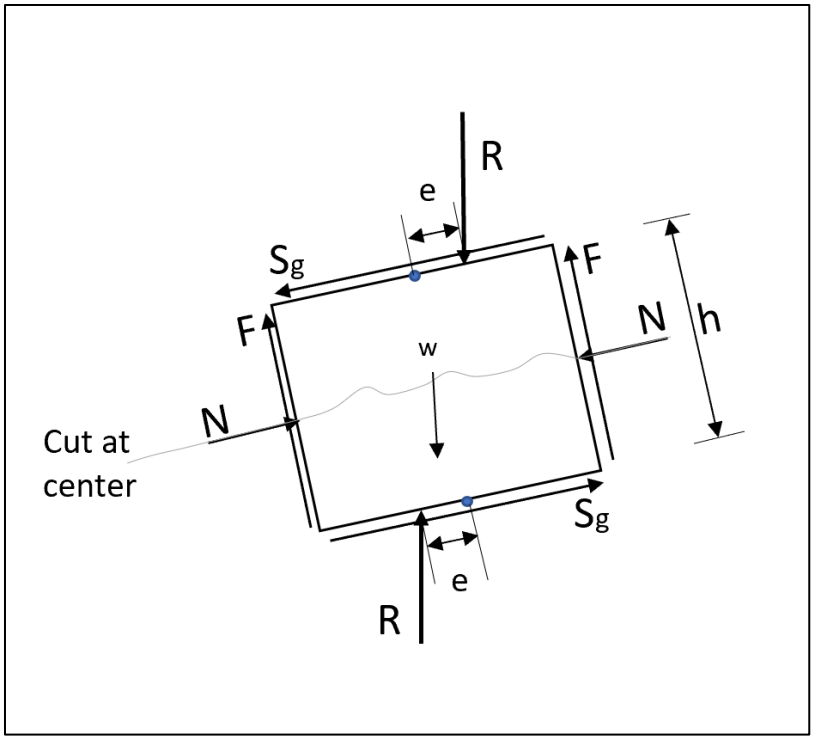

Figure 35. FBD of HMA Specimen inside the SGC Compactor

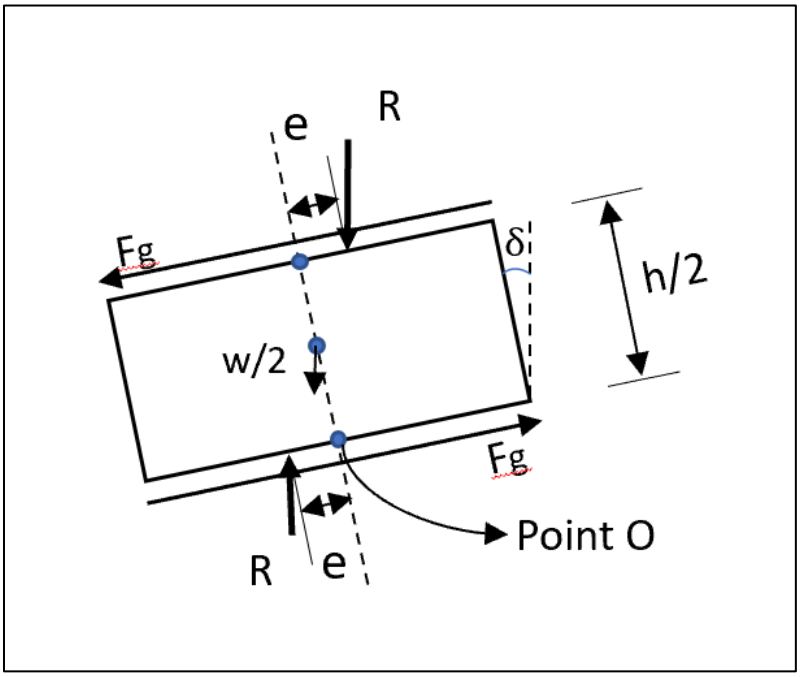

Figure 36. FBD of Half Specimen in the SGC Compactor

By studying the forces applied to the sample during the compaction, the summation of the moments at Equation 12 used to calculate the CEI-2 based on the shear force at mid height of sample and the change in the sample height. point O (Figure 36) equal zero.

$$\Sigma M_O = 0$$ ……Eqn. 16

$$2R \cdot e\cos(\delta) - (F_g \cdot {}^{h}/_{2}) - ({}^{w}/_{2} \cdot {}^{h}/_{2} \sin(\delta)) = 0$$ ……Eqn. 17

where:

R = resultant compaction force

w = weight of the sample

e = distance from the specimen axis to the point where the force is applied

δ = gyration angle

Since δ is small, we can assume $\sin(\delta) = 0$ and $\cos(\delta) = 1$, Equation 17 can be reduced to Equation 18.

$$2R \cdot e - F_g \cdot {}^{h}/_{2} - 0 = 0$$ …… Eqn. 18

The shear force (F_g) can be expressed as:

$$F_g = \frac{2R \cdot e}{{}^{h}/_{2}} = \frac{4R \cdot e}{h}$$ …… Eqn. 19

The shear stress (S_g) can be calculated using Equation 20.

$$S_g = \frac{F_g}{A} = \frac{4R \cdot e}{Ah}$$ ……..Eqn. 20

Pine Gyratory compactor uses the AFLS1 Rapid Angle Measurement (RAM) Kit to measure the tilting moment that generates the angle of gyration. The AFLS1 makes use of the Invelop Load Simulation (ILS) technology developed by Invelop Oy (Savonlinna, Finland), Pine Test Equipment, March 2017. The tilting moment (M) = 2R.e and is reported by Pine in its PineShear Excel sheet. (PineShear+ User Guide, June 2017)

Replacing 2R.e by M, Equation 20 can be written as

$$S_g = \frac{2M}{Ah}$$ …… Eqn. 21

where:

M = Tilting Moment (M) = 2 R e

A = cross-sectional area of the sample

The shear stress at any number of gyration (S_{gi}), can be calculated using Equation 22.

$$S_{gi} = \frac{2M_i}{Ah_i}$$ .....Eqn. 22

The shear force at any number of gyration (F_{gi}) can be calculated using Equation 23.

$$F_{gi} = \frac{2M_i}{h_i}$$ ..... Eqn. 23

The incremental shear energy (ΔE_i) exerted on the sample to change the sample height from h_i to h_{i+1} can be calculated using Equation 24.

$$\Delta E_i = Fg_i * \Delta h_i$$ ..... Eqn. 24

where:

Δh_i = change in height at each number of gyrations

The gyratory stability (GS) is the summation of energy incremental shear energy and calculated using Equation 25.

$$GS = \sum_{Ng_1}^{Ng_2}\{(2M_i/h_i)(\Delta h_i)\}$$ ..... Eqn. 25

where:

N_{g1} = the number of gyrations at which the second derivative of the air voids function with respect to the number of gyrations is zero. It is assumed that particle contacts are developed at N_{g1}.

N_{g2} = the gyration number corresponding to 96 percent Gmm

M_i = the moment at each gyration number, which is readily measured and provided in the Pine Excel spreadsheet.

Evaluation of Compaction Indices

The researchers evaluated the effect of mix composition on the GS and other indices measured from the compaction data recorded during compaction. The evaluation was conducted on LMLC and PMLC samples as discussed in Chapter 3. The LMLC included three distinct binder contents (4.25 percent, 5.00 percent, 5.75 percent), three RAP contents (0 percent, 25 percent, 50 percent), three binder grades (PG 58-34, PG 64-28, PG 76-22) and two types of aggregates (i.e., basalt and river gravel). The PMLC included six loose mixtures collected from the field. Three different batches were evaluated from each PMLC mix. The PMLC mixes had different characteristics (i.e., binder content, RAP content, and mix design) as discussed in Chapter 3. Various compaction indices including the GS, CDI, LCI, CFI, LP, CEI, and WEI were evaluated. The results showed that some indices are more sensitive to the change in mix composition than others. Due to the huge amount of data and to avoid repetition, the researchers focused on selected indices, and more information about other indices is provided in Appendix B.

Effect of Binder Content

Figure 37 shows the change in GS at different binder contents. The results demonstrated that the GS decreased with the increase in binder content for all mixes (with and without RAP) and for different binder grades. These results are consistent with the previous studies which indicated that stiffer mixes had higher GS values (Dessouky et al. 2004; Abdo et al. 2010). The GS represents the mix resistance to the shear force. At lower binder content, the mix is dry and hard to compact, which requires more energy to achieve 4.0 percent air voids. At higher binder content, the mix is softer, and it requires less energy to be compacted. The sensitivity of GS to binder content was examined using ANOVA and Tukey's Honestly Significant Difference (Tukey's HSD). Both tests were performed at 95 percent confidence interval (i.e., $\alpha = 0.05$). Figure 37 shows the average GS and error bars present plus/minus one standard deviation from the average value. The statistical analysis results (Tukey's HSD groups) are included in the form of small letters within each bar. The mixes that do not share the same letters in each group (e.g., 0 percent RAP PG 58-34, 0 percent RAP PG 64-28) are statistically different in terms of their GS values. The Minitab 19 software was used to conduct the statistical analysis of this study (Minitab 2019). Figure 37 shows the statistical analysis within each group at the same RAP content (i.e., 0 percent RAP, 25 percent RAP, 50 percent RAP) and performance binder grade (i.e., PG 58-34, PG 64-28, PG 76-28). The results showed that in all cases, there was statistically significant difference in GS results at different binder grades except that there was no difference between 4.25 percent and 5.00 percent binder content at 25 percent RAP for the PG 58-34 binder, but there was a significant difference between 4.25 percent and 5.75 percent and between 5.00 percent and 5.75 percent binder content. It can be concluded that the GS can capture the change in binder content in the mix.

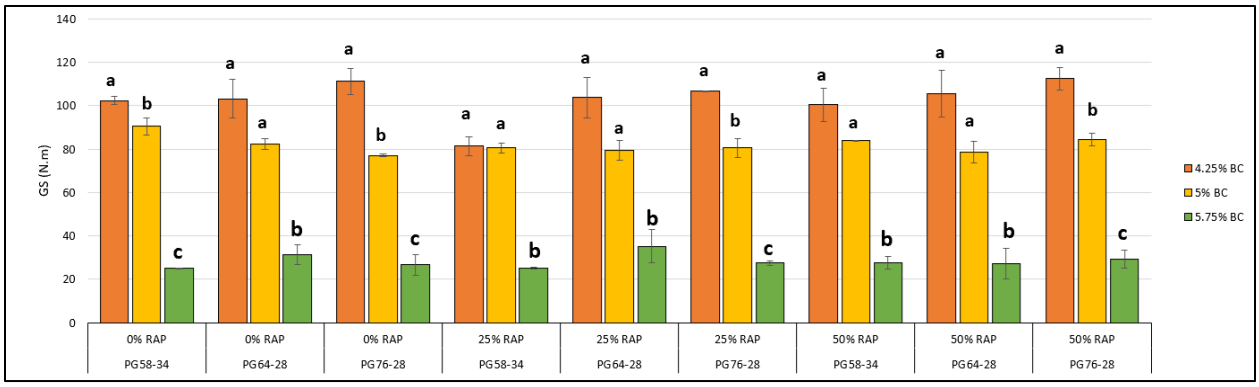

Figure 37. GS Sensitivity to Binder Content

The CDI, described in Chapter 2, is the area under the density curve between the gyration number corresponding to 8 percent Gmm and the gyration number corresponding to 92 percent Gmm. Higher CDI values indicate that the mix requires more energy to achieve 92 percent Gmm, while lower CDI values demonstrate that less energy is required. Figure 38 illustrates the CDI results at different binder contents. The CDI decreased with an increase in binder content. Asphalt mixes prepared with 4.25 percent binder content had higher CDI which indicates more energy was required to achieve 92 percent Gmm, while mixes at 5.75 percent binder content had the lowest CDI. In most cases, there was a statistically significant difference in CDI for each group, except there was no statistically significant difference between 4.25 percent and 5.00 percent binder content for two groups (i.e., 25 percent RAP PG 76-28 and 50 percent RAP PG 64-28); however, there was a significant difference between 4.25 percent and 5.75 percent and between 5.00 percent and 5.75 percent binder content for all groups.

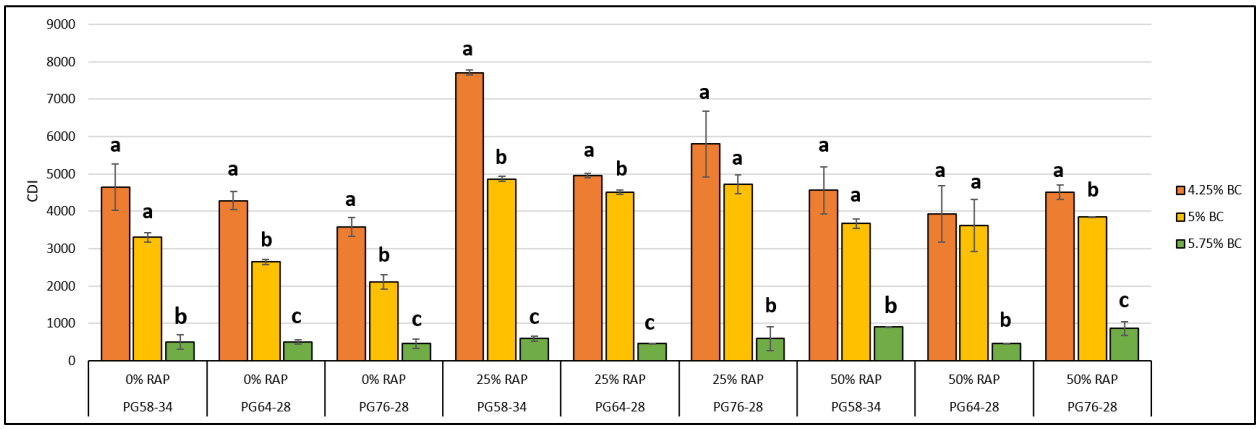

Figure 38. CDI Sensitivity to Binder Content

In a previous study by Kassem et al. (2012), LCI was found to have a fair correlation with field compaction. The LCI is calculated based on the intercept and the slope of the compaction curve as discussed in Chapter 2. Higher LCI values indicate less compaction effort is needed to compact a given mix in the laboratory and a smaller number of roller passes are needed to compact the mix in the field. Figure 39 shows LCI

values for the test mixes. In this study, the LCI was calculated to assess the sensitivity of this index to the mix composition (e.g., binder content and percent RAP in the mix) and assess the correlation with rutting resistance that will be presented and discussed in Chapter 5. The results show that mixes with 5.75 percent binder content had higher LCI values and, they were significantly different from mixes with lower binder contents (i.e., 4.25 percent). There was a statistically significant difference between 4.25 percent and 5.0 percent binder contents for the mixes without RAP but not for mixes with 25 percent or 50 percent RAP content, which could be related to the variability of RAP materials.

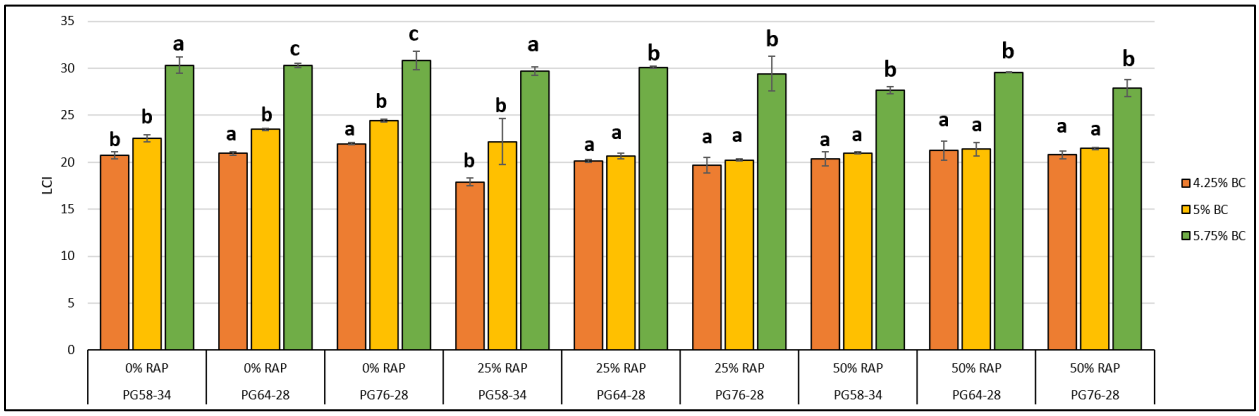

Figure 39. LCI Sensitivity to Different Binder Content

The WEI is defined as the energy required to compact the mix from the initial state (zero gyration) to the corresponding gyration number to 92 percent Gmm as discussed in Chapter 2. Higher WEI demonstrates that the mix is easy to compact and vice versa. Figure 40 shows that mixes with 5.75 percent binder content are softer binder grade and had a higher WEI when compared to those with low binder contents (i.e., 4.25 percent). For the mixes with higher RAP content (i.e., 50 percent), there was no statistically significant difference in WEI between 4.25 percent and 5.0 percent binder content except for PG 76-28. This could be also related to the variability of RAP materials.

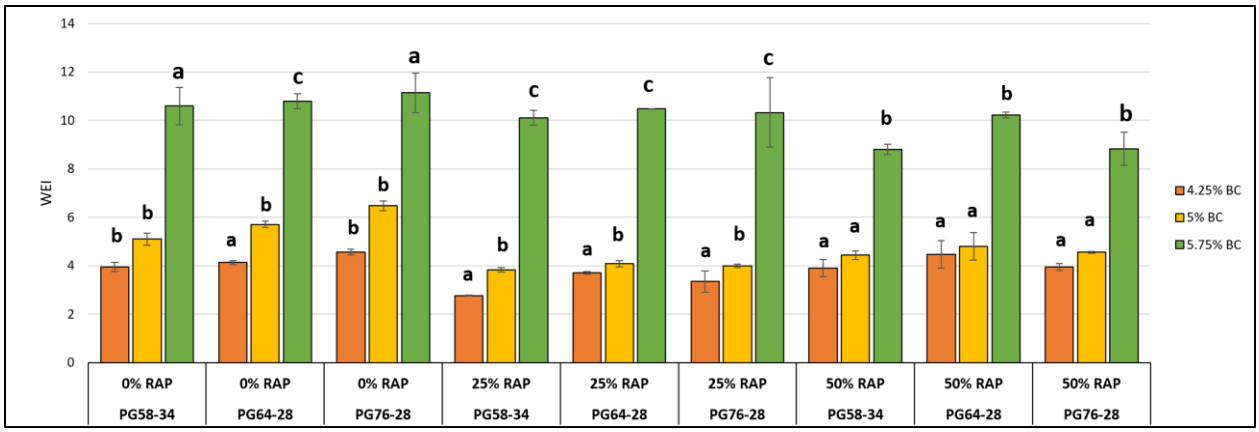

Figure 40. WEI Sensitivity to Different Binder Content

The LP is an indicator of the compaction characteristics of the mixture as explained in Chapter 2. It is identified as the point when the mixture exhibits a noticeable increase in resistance to further densification. The LP results presented in Figure 41 indicate that the LP was not able to capture the effect of binder content. Mixes with 4.25 percent and 5.0 percent binder content had no statistically significant difference in LP values. In addition, all mixes at 5.75 percent binder content had LP of zero which means it was not able to be determined from the compaction data.

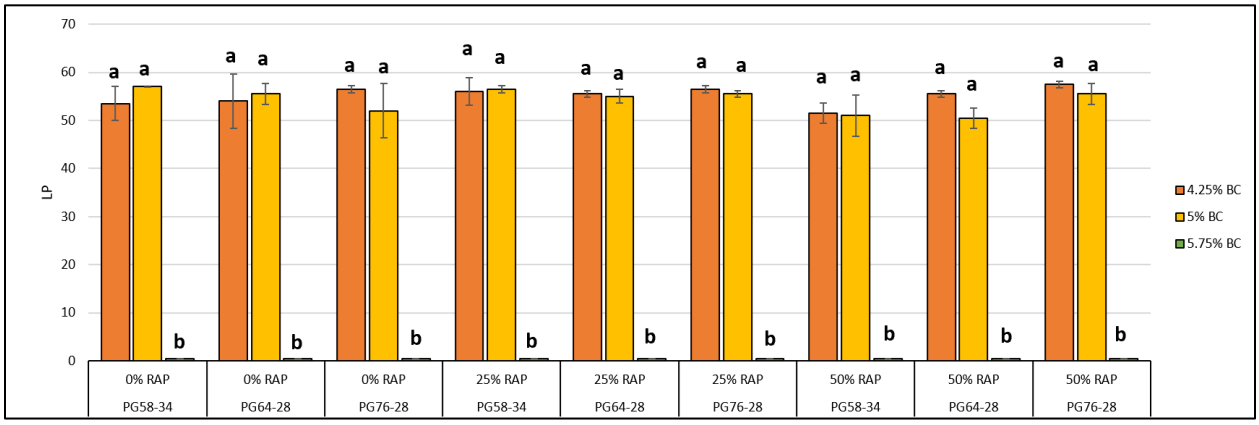

Figure 41. LP Sensitivity to Different Binder Content

Effect of RAP Content

Figure 42 shows the GS of the mixes at different RAP contents. In general, there was no clear trend for the effect of RAP content on GS, additionally there was no statistically significant difference in GS at different RAP contents for different binder types as shown in Figure 42. Possible explanation is that since GS is measured at compaction temperature, which is relatively high, the effect of higher binder stiffness

due to higher RAP content might be minor. Hence all the mixes at the compaction temperature are less viscus and it was hard to capture the increase in stiffness due to the change in RAP content or even binder grade as discussed later in this chapter.

The effect of RAP content on the CDI is depicted in Figure 43. The results also showed that there was no clear trend of the effect of RAP content on CDI values. The CDI values tended to increase for the mixes with 25 percent RAP compared to the 0 percent RAP. However, when exceeding 25 percent RAP, the CDI decreased.

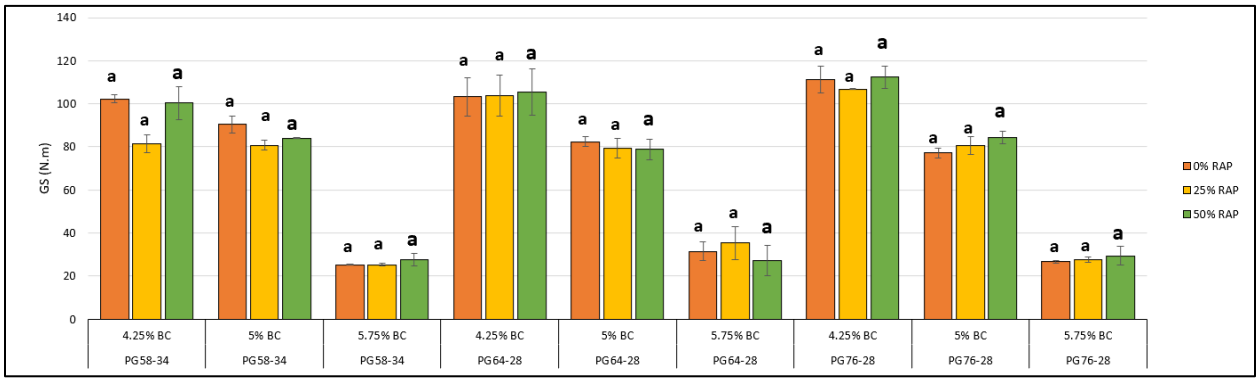

Figure 42. GS Sensitivity to Different RAP Content

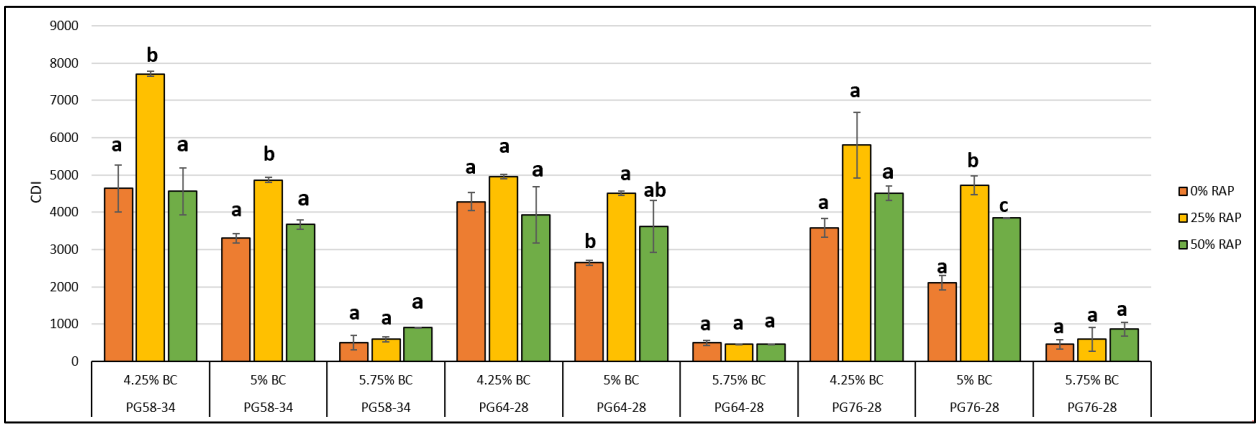

Figure 43. CDI Sensitivity to Different RAP Content

Figure 44 shows the effect of RAP content on the LCI. While there was no clear trend on the effect of RAP content on LCI, many mixes with 50 percent RAP had lower LCI, indicating more compaction effort was needed when compared to mixes without RAP content and such difference was statistically significant. Conversely, there was no statistically significant difference between 0 percent and 25 percent RAP. The results demonstrated that the LCI is less sensitive to RAP content, similar to CDI and GS, since all these indices are calculated from the compaction data, and the compaction is conducted at relatively high temperature where the binder is less viscous.

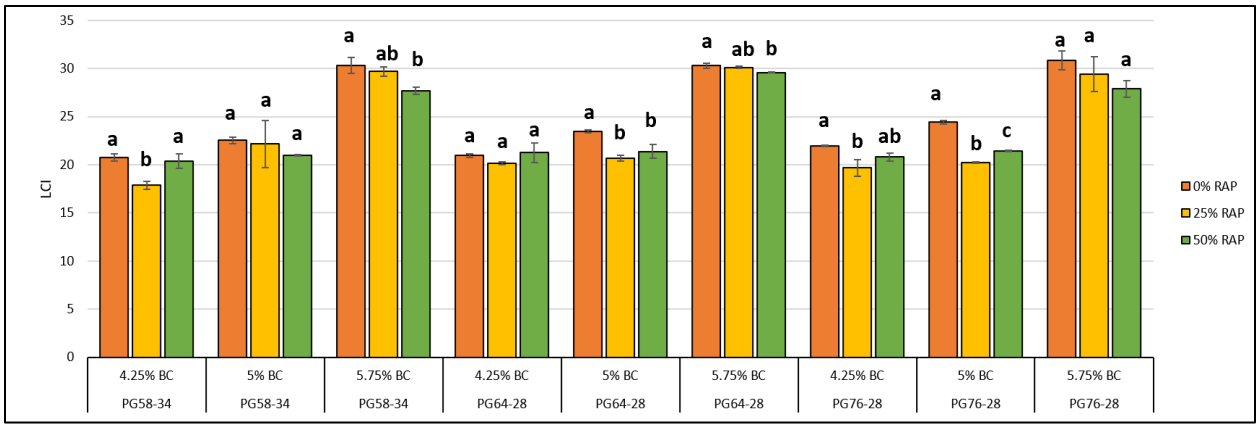

Figure 44. LCI Sensitivity to Different RAP Content

Figures 45 and 46 also show that the WEI and LP were not sensitive to the change in RAP content and there was no clear trend for the effect of RAP content on these two indices (i.e., WEI and LP).

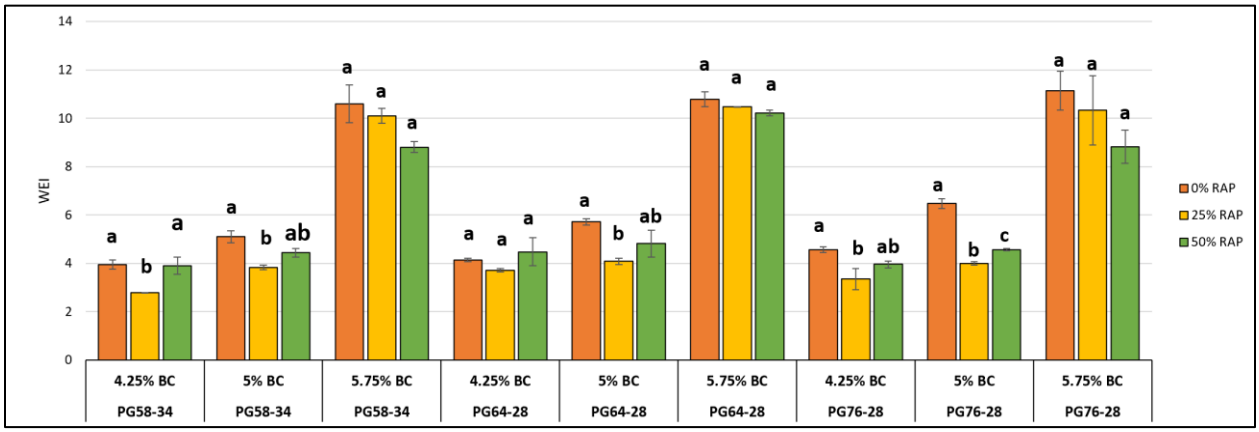

Figure 45. WEI Sensitivity to Different RAP Content

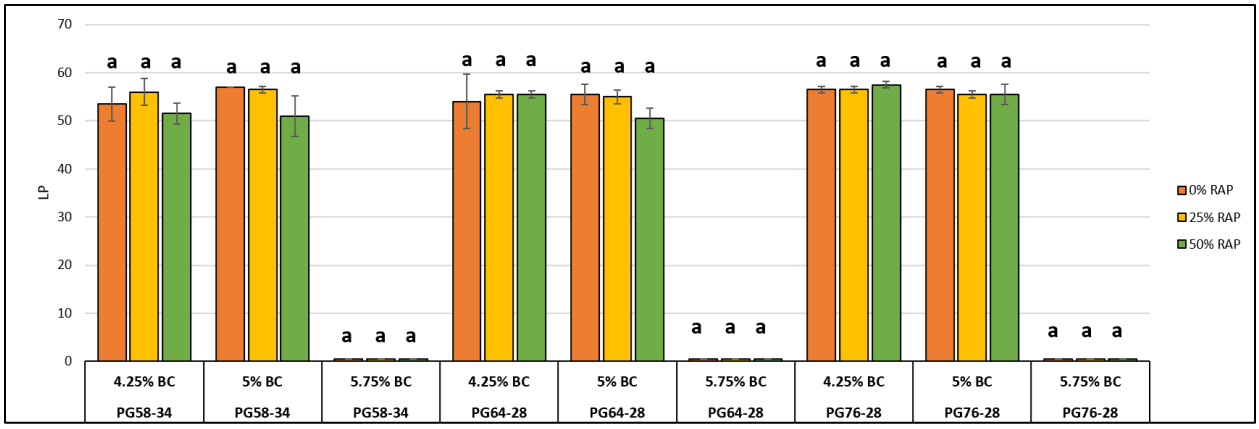

Figure 46. LP Sensitivity to Different RAP Content

Effect of Binder Grade

The researchers examined the effect of different binder grades (i.e., PG 58-34, PG 64-28 and PG 76-22) on the selected compaction and stability indices as presented in Figures 47 through 51. At low binder content (i.e., 4.25 percent), the GS tended to increase as the binder grade increased from 58 to 76; however, there was no clear trend at 5.00 percent and 5.75 percent binder content (Figure 47). Similarly, the LCI increased with the increase in binder grade for some mixes especially at low binder content, and the different was statistically significant; however, there was no similar trend for all mixes evaluated in this study (Figure 48). Furthermore, the CDI, WEI and LP were less sensitive to the change in binder grade, as presented in Figures 49, 50, and 51, respectively. The binder grade generally does not have a significant effect on laboratory compaction data since the compaction is conducted at different temperatures depending on the PG grade of the binder, where different binders are expected to achieve the same viscosity (0.28 plus/minus 0.30 Pa·s). At typical compaction temperatures, different binders have comparable viscosities; therefore, the binder grade does not affect the resistance of the mix to the applied compaction forces.

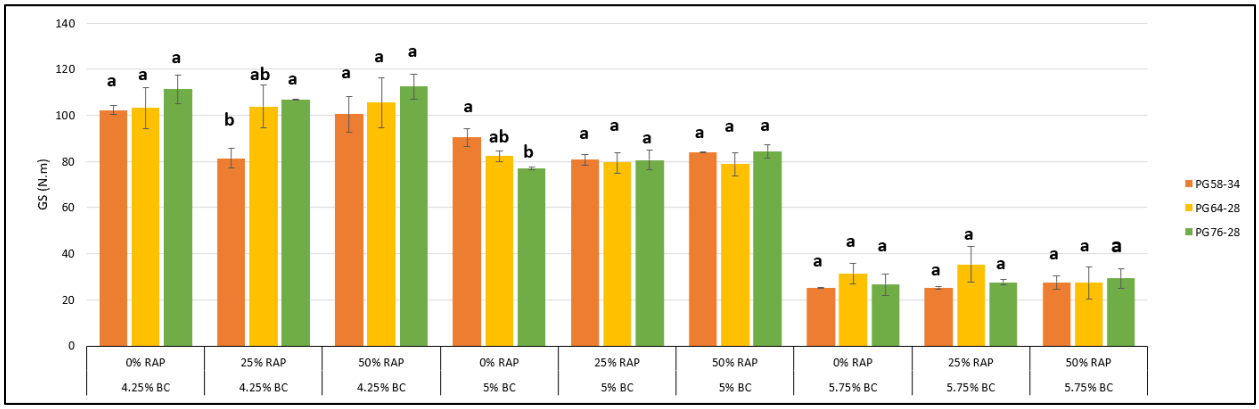

Figure 47. GS Sensitivity to Different Binder Grades

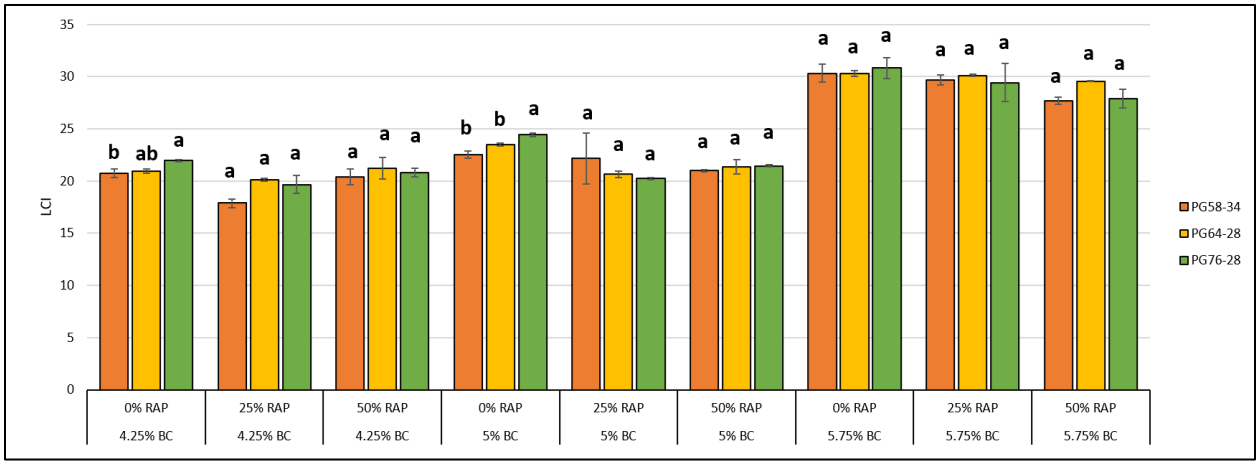

Figure 48. LCI Sensitivity to Different Binder Grades

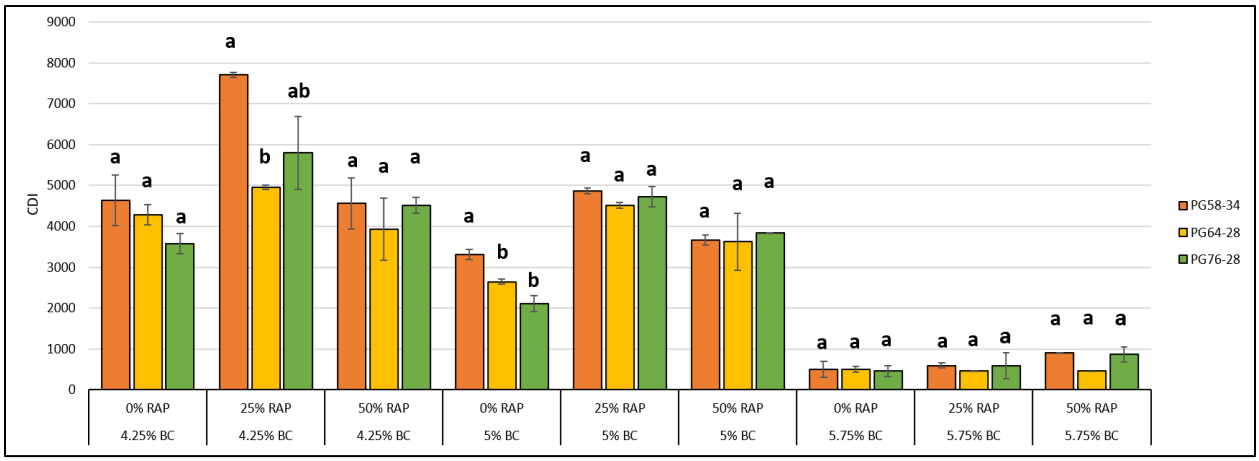

Figure 49. CDI Sensitivity to Different Binder Grades

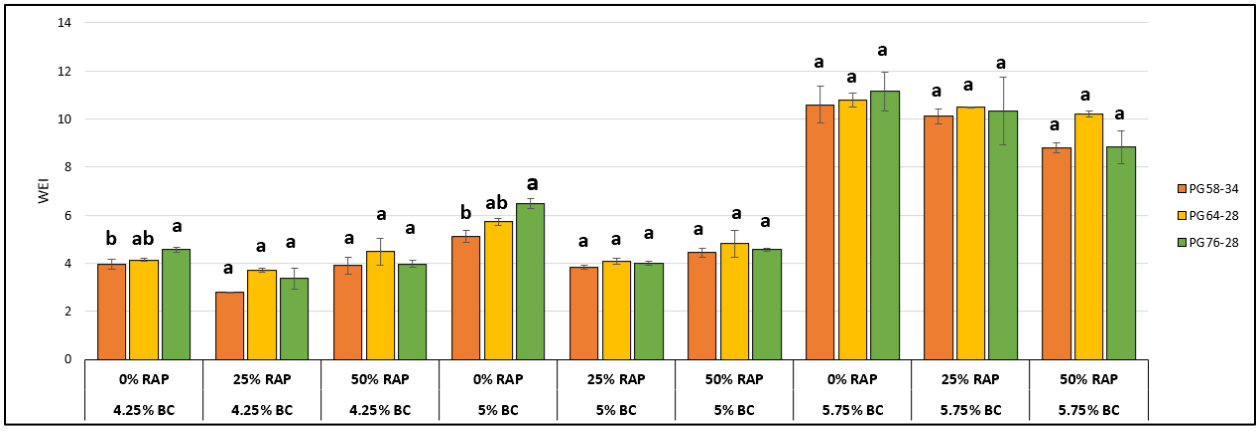

Figure 50. WEI Sensitivity to Different Binder Grades

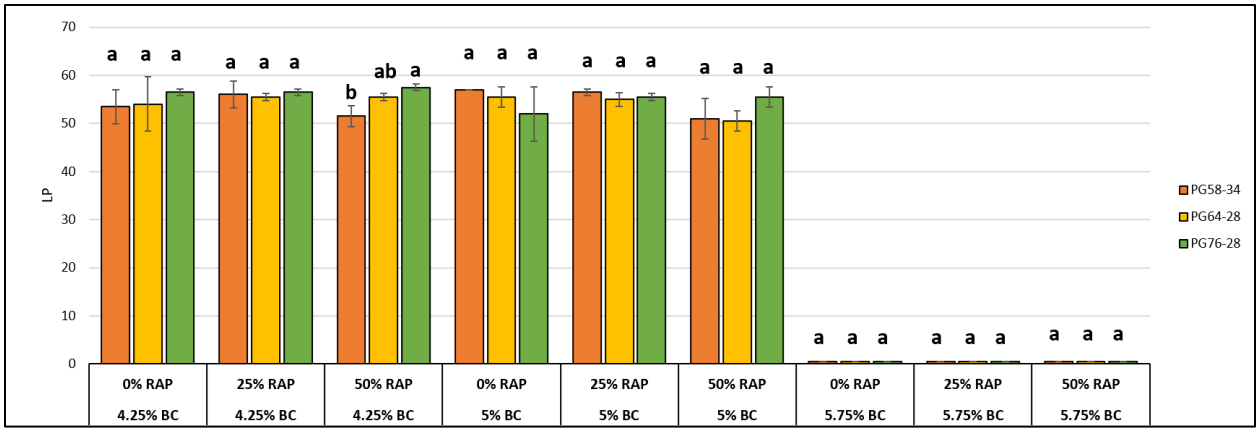

Figure 51. LP Sensitivity to Different Binder Grades

Effect of RAP Source

Two different sources of RAP (i.e., RAP No. 1 and RAP No. 2), previously discussed in Chapter 3, were used to evaluate the sensitivity of the compaction and stability indices to RAP source. Besides the source of RAP, the mixes were prepared using t three RAP contents (0 percent, 25 percent, and 50 percent), and three virgin binder contents (i.e., 4.25 percent, 5.00 percent, and 5.75 percent) of PG 58-34 asphalt binder, and one type of rock (basalt). Figures 52 through 54 demonstrate that none of the compaction and stability indices were sensitive to the change in the RAP source. Although both RAP materials have different aggregate gradations and RAP binder contents, such effect on mix characteristics is often normalized by adding virgin aggregates and binders to meet the required gradation and binder content of the mix. It is worth mentioning that both RAP No. 1 and RAP No. 2 are characterized as category two as per ITD standards. That means both sources or RAP came from a previous ITD pavement project and have good quality. When the mix design is performed per the Superpave design criteria, the RAP should not compromise the mix's volumetric properties. Figures 52 through 54 show the effect of RAP source on the GS, CDI, and LCI, respectively.

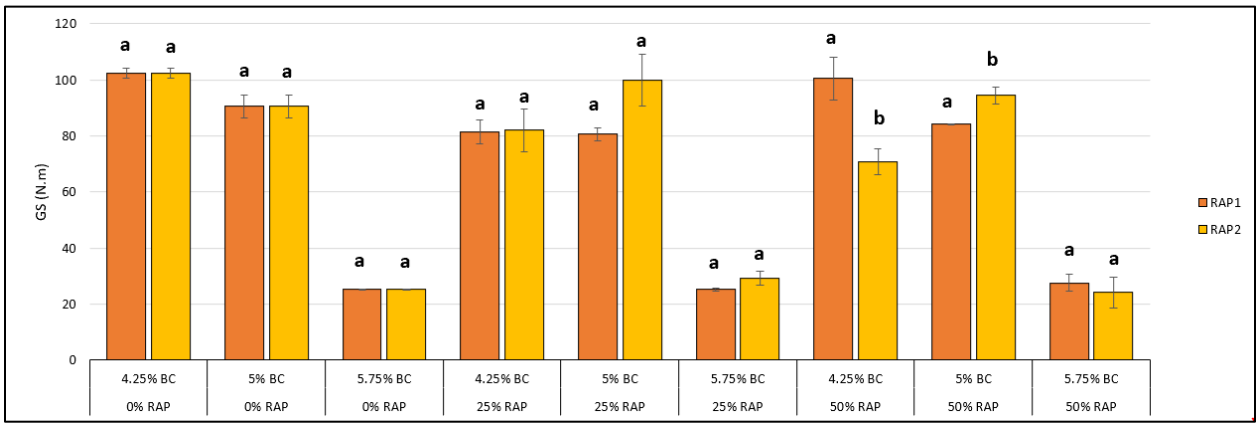

Figure 52. Gyratory Stability of RAP1 and RAP2

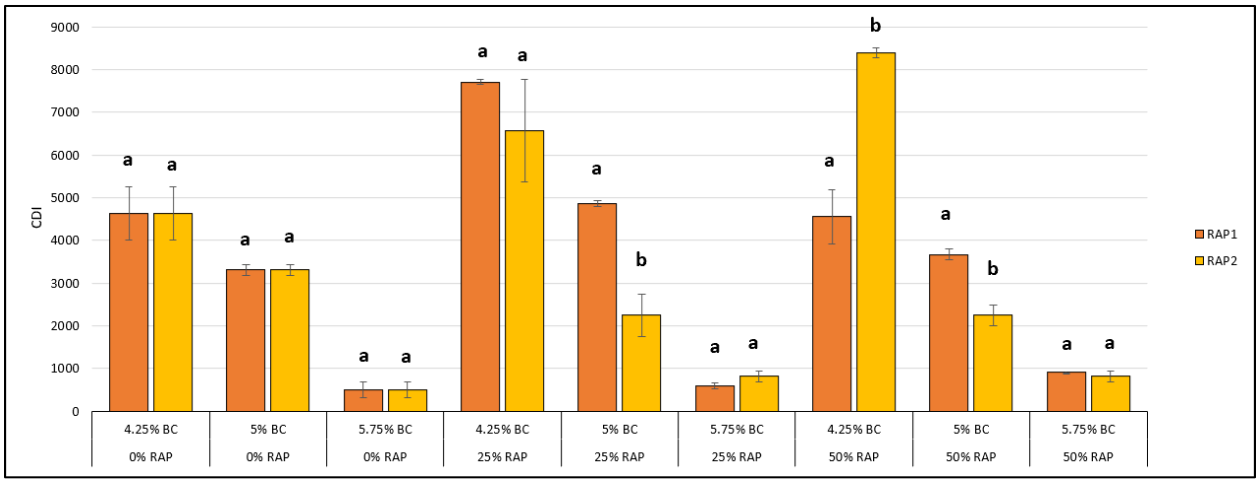

Figure 53. Construction Densification Index for RAP1 and RAP2

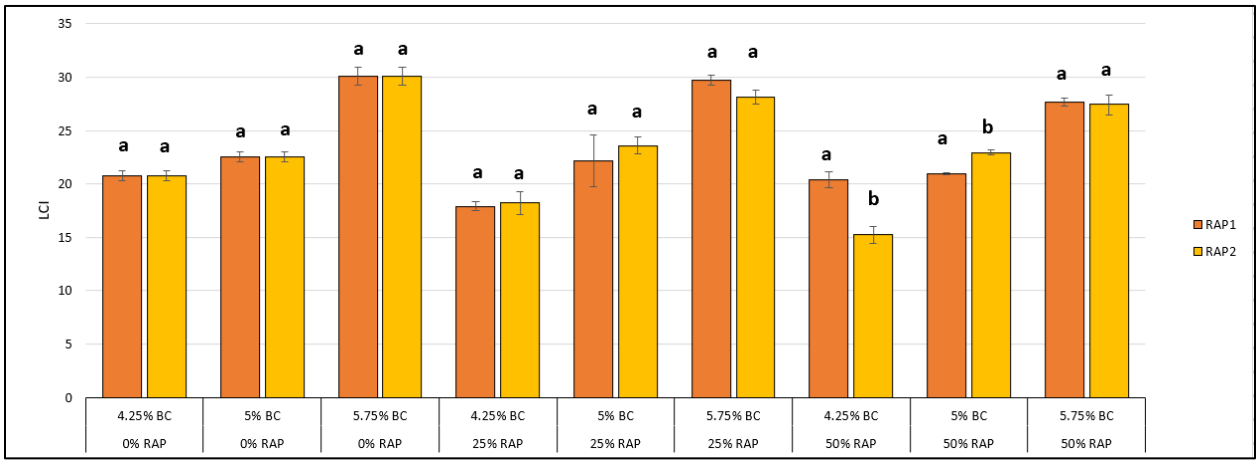

Figure 54. Laboratory Compaction Index for RAP1 and RAP2

Effect of Aggregate Type

Samples of asphalt mix were prepared using two types of aggregates (i.e., basalt and river gravel), one RAP source (RAP No. 2), three RAP contents (0 percent, 25 percent, and 50 percent), and one binder grade (PG 58-34) at OBC of 5.0 percent. A total of 12 mixes were prepared and tested to investigate the effect of aggregate type at different RAP contents on the compaction and stability indices. Figure 55 shows the effect of RAP source at various RAP contents on the GS. The results demonstrate that mixes prepared with basalt had higher GS compared to those prepared using river gravel at the corresponding RAP contents; however, there was a statistically significant difference only for mixes with at 50 percent RAP content. The basalt rock has crushed faces and high angularity which provides good aggregate interlock leading to less resistance to compaction compared to gravel which has more round faces. In addition, and like the

previous findings, the results showed that there was no clear trend for the effect of RAP content from different RAP sources on the GS values.

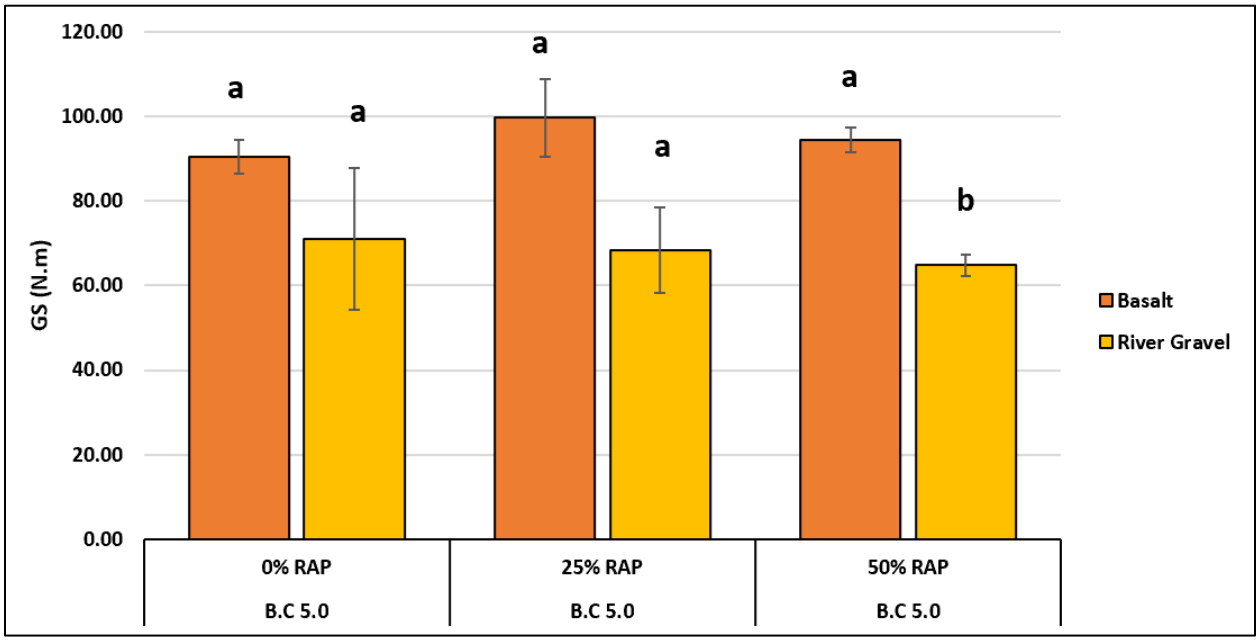

Figure 55. GS of Basalt and River Gravel Aggregates

Figure 56 shows the CDI of the test mixtures. The results clearly demonstrate that there was a statistically significant difference in the CDI results between mixes prepared with basalt and mixes prepared with river gravel. The mixes prepared with river gravel had higher CDI values compared to basalt at the corresponding RAP contents. These results demonstrated that mixtures prepared using river gravel are stiffer than those prepared using basalt at the corresponding RAP contents which implies higher energy needed to achieve 92 percent Gmm for the river gravel mixes. Similarly, the LCI results, presented in Figure 57, demonstrated that mixes prepared using basalt rock had higher LCI values compared to those prepared using river gravel at the corresponding RAP contents. Higher LCI values indicate less compaction energy is required. The LCI results are consistent with the findings of CDI and GS which demonstrated that these compaction and stability indices (i.e., GS, CDI, and LCI) are sensitive to the aggregate type regardless the RAP content in the mix.

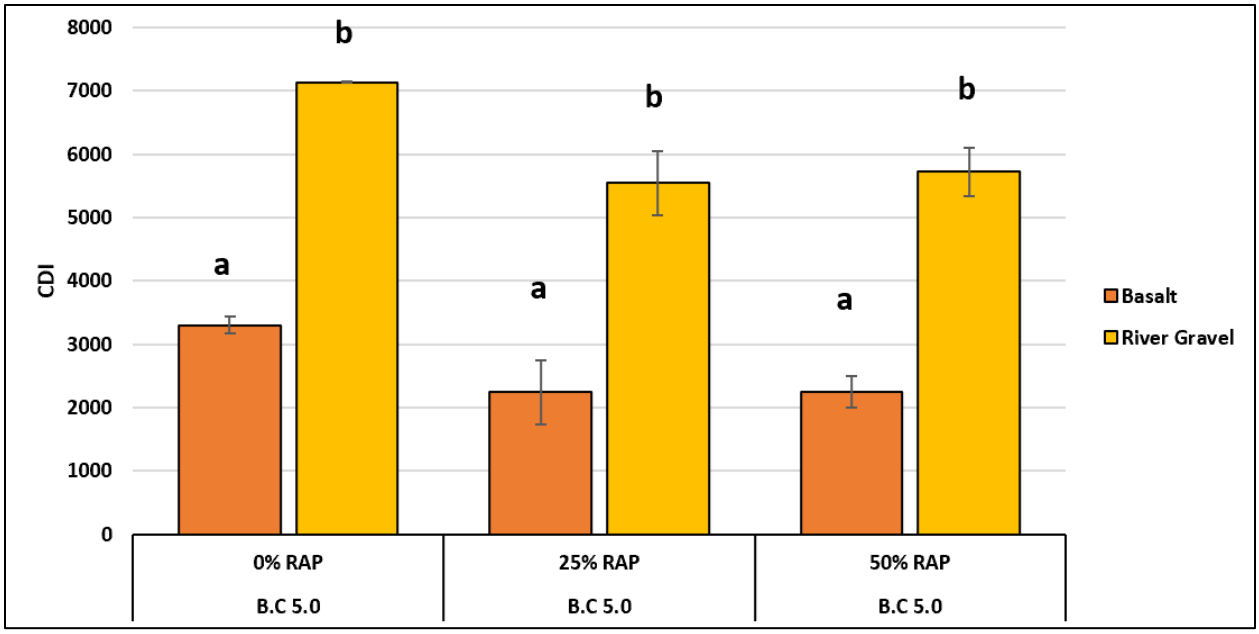

Figure 56. CDI of Basalt and River Gravel

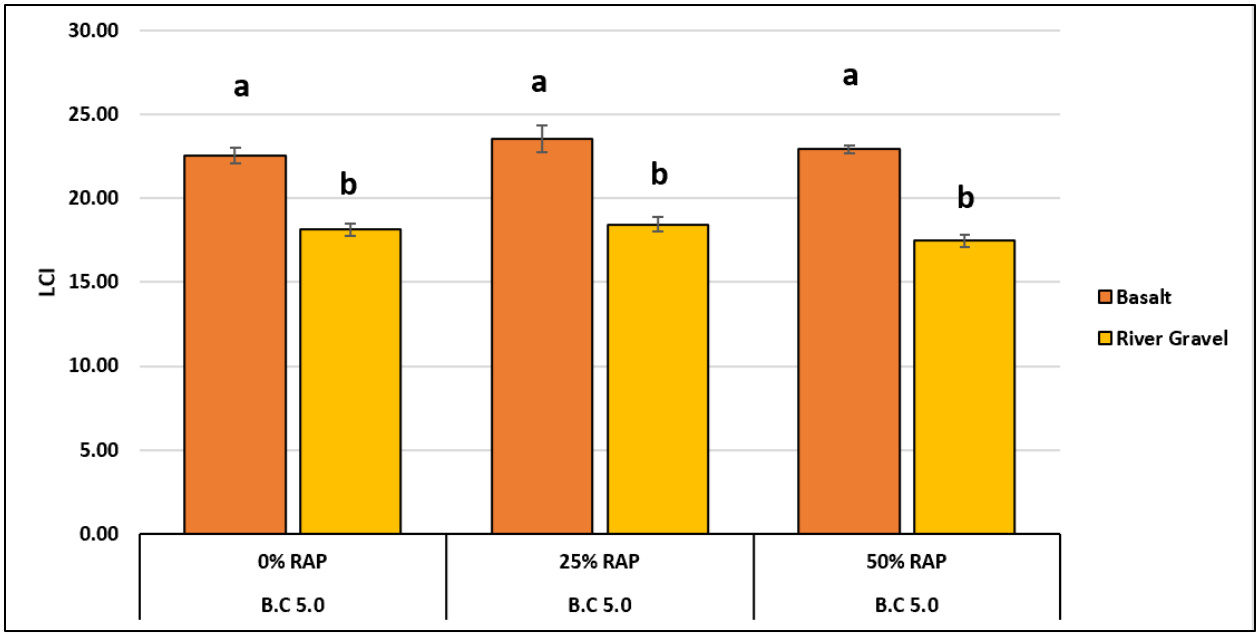

Figure 57. LCI of Basalt and River Gravel

Evaluation of Field Mix

The compaction and stability indices were also calculated for PMLC mixes collected from six field projects. These mixes had different properties including mix design (SP3 and SP5), two NMAS (12.5 mm and 19.0 mm), three binder grades (PG 64-28, PG 64-34, and PG 70-28), six binder contents (5.1 percent, 5.2 percent, 5.3 percent, 5.4 percent, 5.9 percent, and 6.2 percent), and three RAP contents (0 percent, 17 percent, and 30 percent). PMLC samples from three batches (i.e., Batch No. 1, Batch No. 2, and Batch No. 3) from each project were prepared and tested to evaluate the variability in mix performance during production. Each batch was collected at different times during construction as discussed in Chapter 3.

Figures 58 shows the CDI results of different batches of the PMLC mixes. The results demonstrate that there was a statistically significant difference among batches for some projects which indicated variations in mix characteristics due to segregation or change in mix production. The following observations can be made from Figure 58:

- There was a significant difference between Batch 1 of project D1-P1 and both Batch 2 and Batch 3, while Batch 2 had a statistically significant difference with Batch 3.
- D3-P5 and D6-P1 showed no statistically significant difference among various batches (i.e., Batch 1, Batch 2, and Batch 3); however, D6-P1 had a higher CDI compared to D3-P5. D3-P5 had higher NMAS of 3/4” while D3-P5 has a NMAS of 1/2”. Higher NMAS may require higher energy to compact the mix.
- There was a statistically significant difference in CDI between Batch 2 of D1-P2 and both Batch 1 and Batch 3, while there was no statistically significant difference between Batch 1 and Batch 3.
- In D4-P1, Batch 1 had a statistically significant difference in CDI compared to Batch 2 and Batch 3, while there was no significant difference between Batch 2 and Batch 3.
- All the three batches of D4-P2 showed a significant difference in CDI.

Tukey’s HSD was also conducted to compare the CDI values for the six field projects. If the projects share the same capital red letters (e.g., A, B, C) at the bottom of the figure, then, there was no significant difference between the projects. It should be noted that the Tukey’s HSD analysis considered the average values of CDI and standard deviation based on the three batches of each project. Based on the Tukey’s HSD analysis, all field projects had no significant difference except D6-P1 which had a significant difference in CDI with D1-P1, D3-P5, and D1-P2.

By investigating the effect of mix composition of field projects on CDI, all the projects had 1/2" NMAS except D6-P1 and D4-P1 with NMAS of 3/4”. Mixes with larger NMAS required more energy to achieve 92 percent Gmm. In addition, the RAP content was not found to affect the CDI. For example, D1-P1 had 30 percent RAP while D3-P5 had 0 percent RAP, and there was no statistically significant difference in CDI values between these two projects. Both mixes (D1-P1 and D3-P5) had the same NMAS and mix type (SP3), and close binder contents and grades. These results are consistent with the findings from LMLC where the CDI was not sensitive to the change in RAP content.

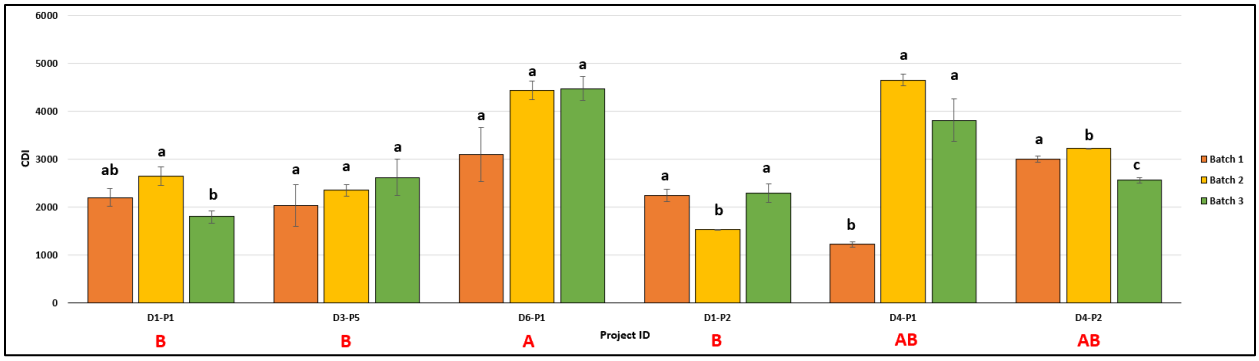

Figure 58. Construction Densification Index of Field Prepared Mixes

Figure 59 shows the GS values for various batches of the PMLC mixes. The following observations can be made:

- All the three batches of D1-P1, D6-P1, and D4-P2 showed no statistically significant difference in the GS values, while there was statistically significant difference in the other three projects (D3-P5, D1-P2, D4-P1) for some batches.
- The Tukey's HSD analysis showed that there was no statistically significant difference among projects except between D4-P1 compared to both D3-P5 and D1-P2. D4-P1 had NMAS of 3/4" and 17 percent RAP compared to D3-P5 with NMAS of 1/2" and 0 percent RAP and D1-P2 with NMAS of 1/2" and 30 percent RAP.
- Overall, all the PMLC mixes had higher GS values which indicates that all the mixes should have good stability which is examined during the laboratory compaction stage.

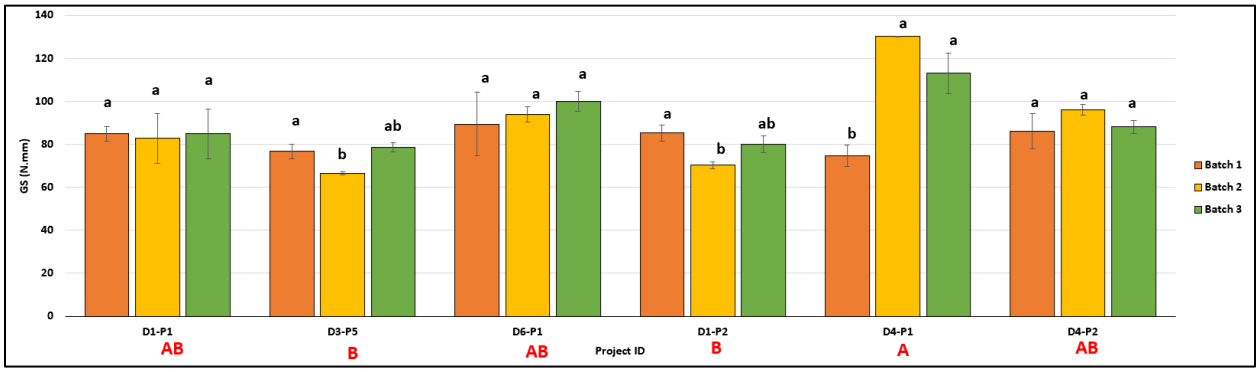

Figure 59. Gyratory Stability of Field Prepared Mixes

Figure 60 presents the LCI values for various batches of the PMLC mixes. The results showed that there was a statistically significant difference in LCI values for at least one batch in each project. For example, Batch 1 of For D4-P1 had a significant difference LCI compared to Batch 2 and Batch 3 which agrees with the results of CDI (Figure 58). Batch 1 needed less energy to achieve 4 percent air voids compared to Batch

2 and Batch 3. In addition, the Tukey's HSD analysis classified mixes into three statistical groups (A, B, and C). Three projects (D1-P1, D1-P2, and D4-P2) had higher LCI compared to the other three projects (D3-P5, D6-1, and D4-P1). Higher LCI values are associated with easy compaction and smaller number of roller passes. For example, D1-P1 had relatively higher LCI compared to D3-P5 which indicates that former is easier to compact when compared to the latter. During the laboratory compaction of D3-P5 mixes, the researchers observed that the materials were dry; therefore, it required more energy to achieve 4 percent air voids which resulted in higher CDI and lower LCI. In addition, it is believed that the use of NMAS of 3/4" in D6-P1 and D4-P1 resulted in lower LCI compared to D1-P1 and D1-P2 of NMAS of 1/2". The results of the compaction and stability indices were compared to the rutting performance and discussed in Chapter 5.

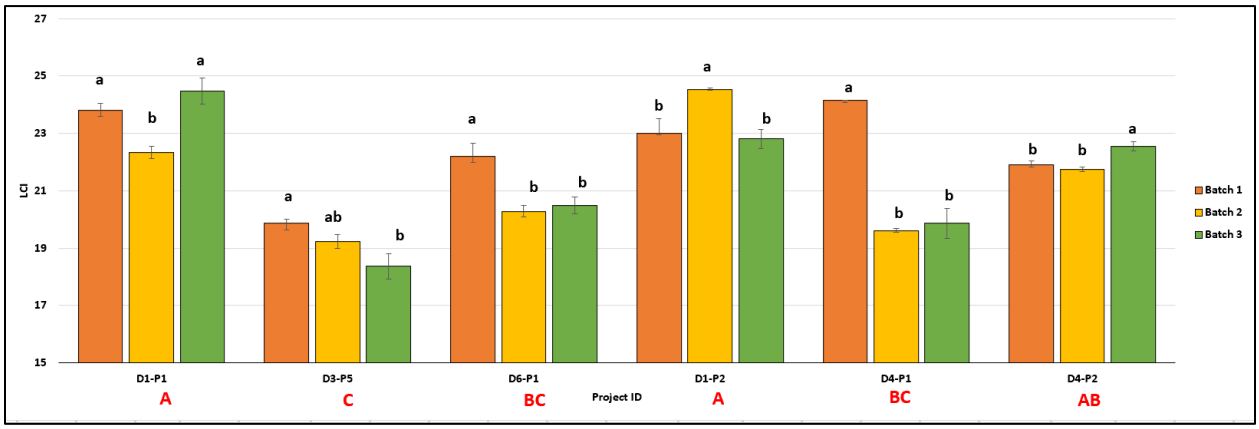

Figure 60. Laboratory Compaction Index of Field Prepared Mixes

Incorporating of GS and LCI Calculations into *PineShear+*

To facilitate the calculations of GS, the researchers incorporated an additional spreadsheet to the *PineShear+* (V15.6) Excel Spreadsheet to calculate GS. Once the compaction data are imported into *PineShear+*, the GS results are automatically populated, and a representative graph of the results is generated as shown in Figures 61 and 62. In addition, the researchers developed another spreadsheet to facilitate the calculations of LCI that was incorporated in *PineShear+*. The calculations of GS and LCI for *PineShear+* are summarized below.

Gyratory Stability Calculations

Two new Excel spreadsheets were added to the *PineShear+*. One sheet named "GS" for the calculations of the GS model, and the other "GS Bar" to provide a chart with the GS results. Figure 61 shows a screenshot for the GS Excel spreadsheet in *PineShear+*. The values of GS (N•m) for each sample are presented in Row No. 5 in the GS Excel spreadsheet as shown in Figure 61. The GS is calculated automatically once the compaction data are imported in *PineShear+* like the other compaction indices

currently included in *PineShear+* such as CDI, LP, and WEI. Figure 62 shows a graph with the GS results provided in the "GS Bar" Excel spreadsheet. Each bar presents the average GS for the selected replicates (up to four) and the error bar presents plus/minus one standard deviation (SD) from the average value. Figure 62 shows the GS values for three groups of asphalt mixtures and the Excel spreadsheet can accommodate up to four groups of asphalt mixtures. This chart enables the user to compare various groups to assess changes in GS values. For example, the user can compare the GS values for four different batches (up to four replicates or samples from each batch) from a given project and examine if there is a difference in GS values which may trigger change in mix production or indicate segregation. Also, the user can compare the GS values for up to four different projects in the same plot.

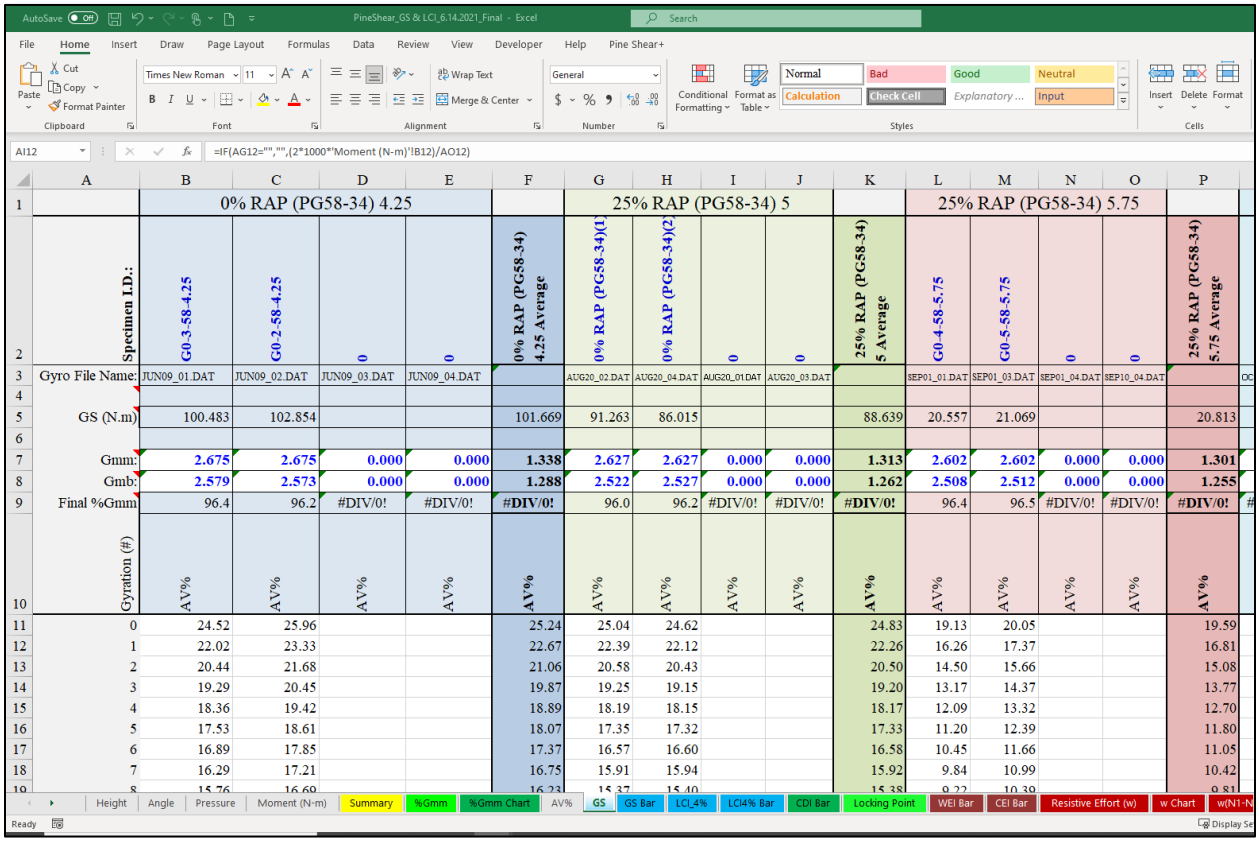

	A	B	C	D	E	F	G	H	I	J	K	L	M	N	O	P
1		0% RAP (PG58-34) 4.25					25% RAP (PG58-34) 5					25% RAP (PG58-34) 5.75				
2	Specimen I.D.:	G0-3-58-4.25	G0-2-58-4.25	0	0	0% RAP (PG58-34) 4.25 Average	0% RAP (PG58-34)(1)	0% RAP (PG58-34)(2)	0	0	25% RAP (PG58-34) 5 Average	G0-4-58-5.75	G0-5-58-5.75	0	0	25% RAP (PG58-34) 5.75 Average
3	Gyro File Name:	JUN09_01.DAT	JUN09_02.DAT	JUN09_03.DAT	JUN09_04.DAT		AUG20_02.DAT	AUG20_04.DAT	AUG20_01.DAT	AUG20_03.DAT		SEP01_01.DAT	SEP01_03.DAT	SEP01_04.DAT	SEP10_04.DAT	
4																
5	GS (N.m)	100.483	102.854			101.669	91.263	86.015			88.639	20.557	21.069			20.813
6																
7	Gmm:	2.675	2.675	0.000	0.000	1.338	2.627	2.627	0.000	0.000	1.313	2.602	2.602	0.000	0.000	1.301
8	Gmb:	2.579	2.573	0.000	0.000	1.288	2.522	2.527	0.000	0.000	1.262	2.508	2.512	0.000	0.000	1.255
9	Final %Gmm	96.4	96.2	#DIV/0!	#DIV/0!	#DIV/0!	96.0	96.2	#DIV/0!	#DIV/0!	#DIV/0!	96.4	96.5	#DIV/0!	#DIV/0!	#DIV/0!
10	Gyration (#)	AV%	AV%	AV%	AV%	AV%	AV%	AV%	AV%	AV%	AV%	AV%	AV%	AV%	AV%	AV%
11	0	24.52	25.96			25.24	25.04	24.62			24.83	19.13	20.05			19.59
12	1	22.02	23.33			22.67	22.39	22.12			22.26	16.26	17.37			16.81
13	2	20.44	21.68			21.06	20.58	20.43			20.50	14.50	15.66			15.08
14	3	19.29	20.45			19.87	19.25	19.15			19.20	13.17	14.37			13.77
15	4	18.36	19.42			18.89	18.19	18.15			18.17	12.09	13.32			12.70
16	5	17.53	18.61			18.07	17.35	17.32			17.33	11.20	12.39			11.80
17	6	16.89	17.85			17.37	16.57	16.60			16.58	10.45	11.66			11.05
18	7	16.29	17.21			16.75	15.91	15.94			15.92	9.84	10.99			10.42
19	8	15.76	16.69			16.23	15.37	15.40			15.38	9.22	10.39			9.81

Figure 61. Example of Data in GS Excel Tab in *the PineShear+* Spreadsheet

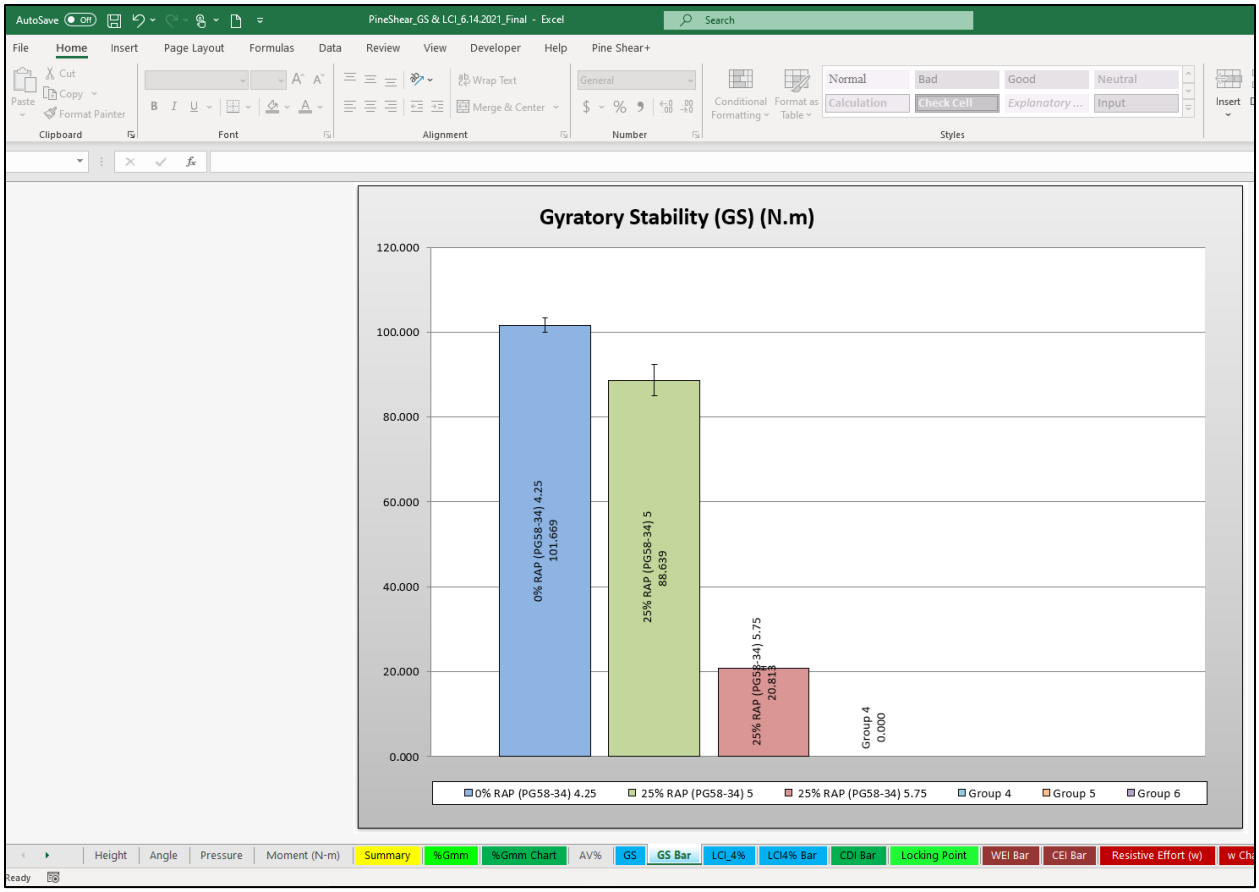

Figure 62. Gyratory Stability Bar Chart added to the *PineShear+* Spreadsheet

The following steps summarize the GS calculations in the developed GS Excel spreadsheet tabs (Figure 63).

- Column #1 (Gyrations) is the number of gyrations from the compaction data.
- Column #2 (percent AV) is the percent of air voids of the sample calculated by *PineShear+* based on the maximum specific gravity (Gmm) and the bulk specific gravity (Gmb). It should be noted that the calculations are conducted until 96 percent of Gmm or 4.0 percent air voids.
- Column #3 (Δh from Power Function) represents the difference in height between every two consecutive gyrations. To improve the accuracy of the GS calculations, the researchers fitted a power function to describe the change in height with respect to number of gyrations. The power function was used to calculate the change in height at each gyration since the recorded height has a resolution of 0.1 mm only. In some cases, it was found that this resolution limited the calculations of change in height at each gyration. Calculating the change in height from the power function at each gyration was found to improve the accuracy of the energy calculations at each gyration.
- Column #4 shows the calculations of the shear force in Newton using Equation 23.

- Column #5 (d^2y/dx^2) shows the calculations of the second derivative of a polynomial function that describes the change in air voids with number of gyrations as used in previous studies (Dessouky et al. 2004, Abdo et al. 2010). The GS is calculated between two points on the compaction curve (N_{g1} and N_{g2}). N_{g1} is defined as the gyration number at which the second derivative of the air voids function with respect to the number of gyrations is zero. It is assumed that particle contacts are developed at N_{g1}. N_{g2} is the gyration number corresponding to 92 percent Gmm.
- Column #8 (Δh*Shear Force) shows the multiplication of shear force and difference in height at each gyration (Δh).
- Column #9 (Gyratory Stability) is the shear force multiplied by change in height at each gyration between N_{g1} and N_{g2} only.
- Finally, the GS is calculated using Equation 25 which is the summation of shear force multiplied by change in height at each gyration between N_{g1} and N_{g2} only.

	b	Log (a)	a
Power Function of Hight vs Gyrations	-0.04726815	2.131879663	135.4813961

AV% vs Gyr.	b6	b5	b4	b3	b2	b1	a
6 Polyno.	1.1537E-09	-3.5948E-07	4.43217E-05	-0.00275769	0.09230653	-1.720374479	23.16556376
dy/dx	6.92219E-09	-1.7974E-06	0.000177287	-0.00827306	0.184613061	-1.720374479	0
d^2y/dx^2	3.4611E-08	-7.1897E-06	0.00053186	-0.01654612	0.184613061	0	

min(d2y/dx2)	0.000000	@ Gyration#	33	Gyra. Count	57	GS_P0-96 (N.m)	82.422

Gyrations	AV%	Δh from Power Function (m)	Shear Force (N)	d^2y/dx^2 (Polyn. AV% vs Gyrations)	Gyration	Δh *Shear F (N.m)	Gyratory Stability GS (N.m)	Sample Height from Compactor (mm)
1	22.66	0.000000	0	0.028423	1	0.00		136.7
2	20.02	0.004367	9103.497508	0.023590	2	39.75		132.2
3	18.36	0.002489	10761.47548	0.019480	3	26.78		129.5
4	17.07	0.001737	11711.0924	0.015999	4	20.34		127.5
5	16.09	0.001331	12325.884	0.013065	5	16.41		126
6	15.28	0.001077	12721.77175	0.010604	6	13.71		124.8
7	14.53	0.000904	13004.16388	0.008550	7	11.75		123.7
8	13.90	0.000778	13241.2282	0.006847	8	10.30		122.8
9	13.41	0.000682	13460.91526	0.005441	9	9.18		122.1
10	12.91	0.000607	13631.81576	0.004290	10	8.27		121.4
11	12.48	0.000546	13814.06488	0.003352	11	7.55		120.8
12	12.04	0.000496	13970.60947	0.002595	12	6.94		120.2
13	11.67	0.000455	14118.55728	0.001988	13	6.42		119.7
14	11.37	0.000420	14218.27088	0.001506	14	5.97		119.3
15	11.00	0.000389	14306.65988	0.001127	15	5.57		118.8
16	10.78	0.000363	14382.34638	0.000832	16	5.22		118.5
17	10.47	0.000340	14462.43827	0.000605	17	4.92		118.1
18	10.25	0.000320	14508.33464	0.000433	18	4.64		117.8
19	9.94	0.000302	14543.76373	0.000304	19	4.39		117.4
20	9.79	0.000285	14577.36766	0.000209	20	4.16		117.2
21	9.56	0.000271	14600.79685	0.000140	21	3.96		116.9
22	9.32	0.000258	14603.89431	0.000092	22	3.76		116.6
23	9.17	0.000246	14622.62723	0.000058	23	3.59		116.4
24	8.93	0.000235	14634.9184	0.000035	24	3.44		116.1
25	8.77	0.000225	14652.87204	0.000021	25	3.29		115.9
26	8.62	0.000216	14655.95403	0.000012	26	3.16		115.7
27	8.46	0.000207	14668.32174	0.000006	27	3.04		115.5
28	8.30	0.000199	14676.27829	0.000003	28	2.92		115.3
29	8.22	0.000192	14695.44932	0.000001	29	2.82		115.2
30	8.06	0.000185	14736.35401	0.000001	30	2.73		115

Figure 63. Steps of GS Calculations added to the *PineShear+* Spreadsheet

Laboratory Compaction Index Calculations

Like the GS spreadsheet, the researchers also developed a spreadsheet to facilitate the calculations of th LCI. The LCI spreadsheet was added to *PineShear+*. The first tab in the spreadsheet called "LCI" calculates the LCI (Figure 64), and the other tab called "LCI Bar" provides a chart with the LCI results (Figure 65). Figure 64 shows a screenshot from the *PineShear+* spreadsheet with these additions. The LCI values for each sample are presented in Row No. 6 in the LCI spreadsheet. These LCI values are automatically calculated once the compaction data are imported into *PineShear+* like the compaction indices currently included *PineShear+*. The LCI is calculated using Equation 8. The LCI model parameters (i.e., slope [b] and intercept [a]) are calculated from the compaction curves as presented in Figure 66. Figure 65 shows a graph with the LCI results provided in the "LCI Bar" tab in the *PineShear+* spreadsheet. Each bar presents the average LCI values for the selected replicates (up to four) and the error bar presents plus/minus one standard deviation (SD) from the average value. Figure 65 shows the LCI values of three groups of asphalt mixtures; the modified *PineShear+* spreadsheet can accommodate up to four groups of asphalt mixtures. The LCI tab can assist the user in comparing the LCI values for up to four groups of mixes, and four replicates from each mix can be analyzed. The LCI was found to have good correlation with the APA rut depth as further discussed in Chapter 5.

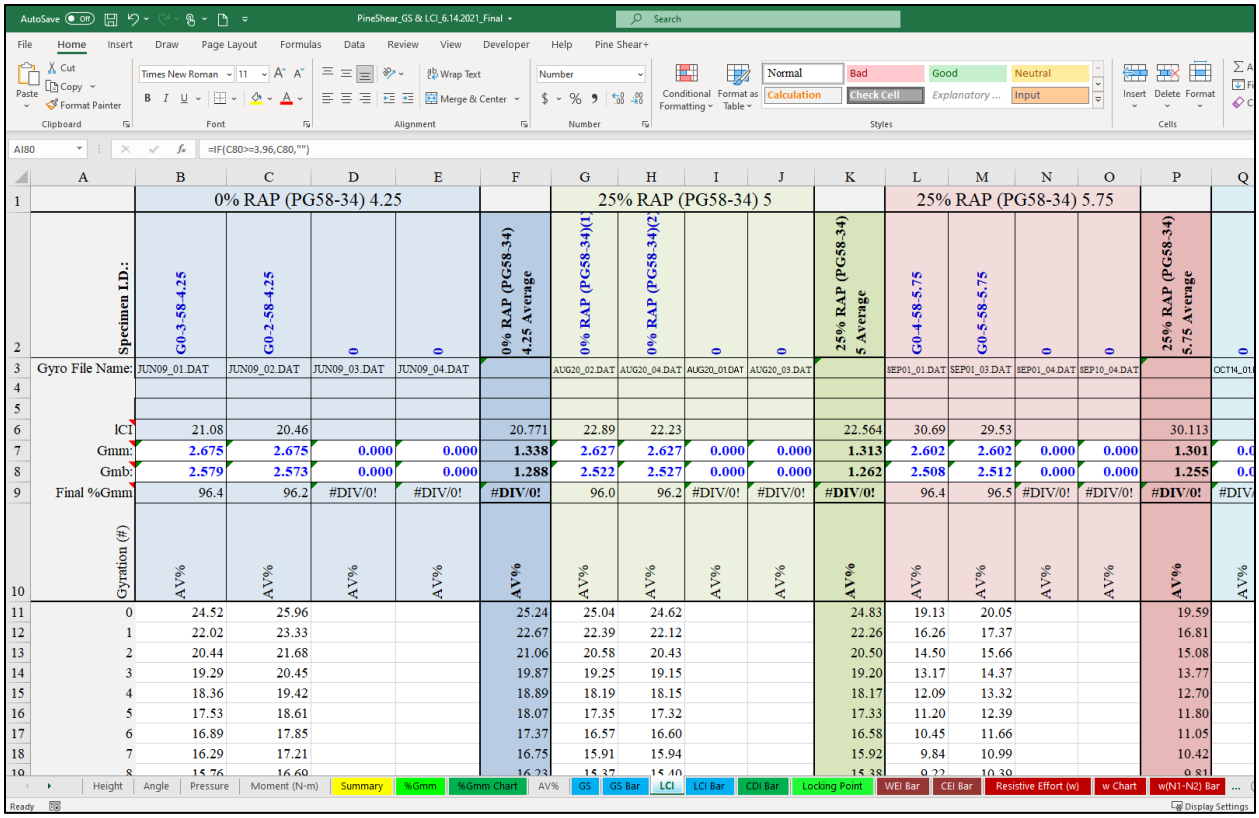

	A	B	C	D	E	F	G	H	I	J	K	L	M	N	O	P	Q
1		0% RAP (PG58-34) 4.25					25% RAP (PG58-34) 5					25% RAP (PG58-34) 5.75					
2	Specimen I.D.:	G0-3-58-4.25	G0-2-58-4.25	0	0	0% RAP (PG58-34) 4.25 Average	0% RAP (PG58-34)(1	0% RAP (PG58-34)(2	0	0	25% RAP (PG58-34) 5 Average	G0-4-58-5.75	G0-5-58-5.75	0	0	25% RAP (PG58-34) 5.75 Average	0
3	Gyro File Name:	JUN09_01.DAT	JUN09_02.DAT	JUN09_03.DAT	JUN09_04.DAT		AUG20_02.DAT	AUG20_04.DAT	AUG20_01DAT	AUG20_03.DAT		SEP01_01.DAT	SEP01_03.DAT	SEP01_04.DAT	SEP10_04.DAT		OCT4_01
4																	
5																	
6	ICI	21.08	20.46			20.771	22.89	22.23			22.564	30.69	29.53			30.113	
7	Gmm:	2.675	2.675	0.000	0.000	1.338	2.627	2.627	0.000	0.000	1.313	2.602	2.602	0.000	0.000	1.301	0.0
8	Gmb:	2.579	2.573	0.000	0.000	1.288	2.522	2.527	0.000	0.000	1.262	2.508	2.512	0.000	0.000	1.255	0.0
9	Final %Gmm	96.4	96.2	#DIV/0!	#DIV/0!	#DIV/0!	96.0	96.2	#DIV/0!	#DIV/0!	#DIV/0!	96.4	96.5	#DIV/0!	#DIV/0!	#DIV/0!	#DIV
10	Gyration (#)	AV%	AV%	AV%	AV%	AV%	AV%	AV%	AV%	AV%	AV%	AV%	AV%	AV%	AV%	AV%	AV%
11	0	24.52	25.96			25.24	25.04	24.62			24.83	19.13	20.05			19.59	
12	1	22.02	23.33			22.67	22.39	22.12			22.26	16.26	17.37			16.81	
13	2	20.44	21.68			21.06	20.58	20.43			20.50	14.50	15.66			15.08	
14	3	19.29	20.45			19.87	19.25	19.15			19.20	13.17	14.37			13.77	
15	4	18.36	19.42			18.89	18.19	18.15			18.17	12.09	13.32			12.70	
16	5	17.53	18.61			18.07	17.35	17.32			17.33	11.20	12.39			11.80	
17	6	16.89	17.85			17.37	16.57	16.60			16.58	10.45	11.66			11.05	
18	7	16.29	17.21			16.75	15.91	15.94			15.92	9.84	10.99			10.42	
19	8	15.76	16.69			16.23	15.37	15.40			15.38	9.22	10.39			9.81	

Figure 64. Example of Data in the LCI Tab of the PineShear+ Spreadsheet

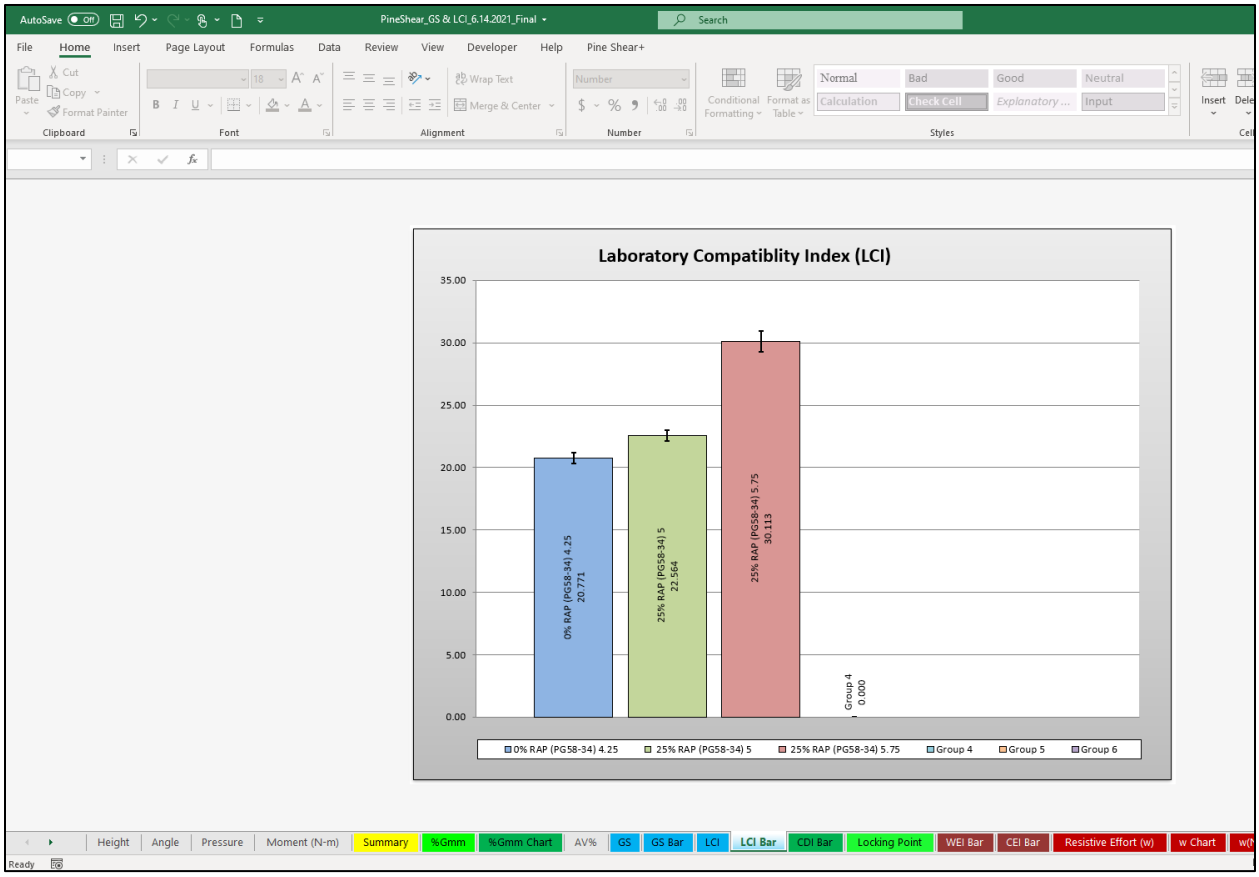

Figure 65 Laboratory Compaction Index Bar Chart tab added to the PineShear+ Spreadsheet

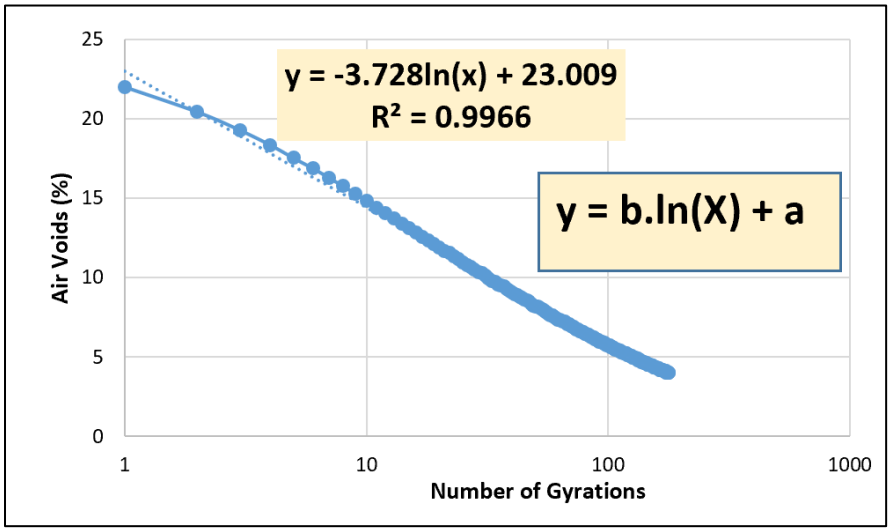

Figure 66. Calculations of LCI Parameters from the Change of Air Voids with Number of Gyrations

5. Evaluation of Rutting and Moisture Damage of RAP Mixes

Chapter 5 evaluates the rutting characteristics of LMLC and PMLC mixes. The sensitivity of the APA and HWTT tests to the change in mix characteristics such as binder content, binder grade, RAP content, and aggregate type was examined. In addition, the researchers evaluated the moisture susceptibility of selected test mixtures using the Lottman test protocol to examine the effect of mix composition on moisture susceptibility. Furthermore, Chapter 5 examines the correlation between rutting performance and mix stability and compactability.

Effect of Mix Composition on Rutting Characteristics

Effect of Binder Content

Figures 67 and 68 shows the rut depth for the LMLC mixes prepared using a PG 58-38 binder measured with the APA and HWTT, respectively. The tested samples included different RAP contents (0 percent [No RAP], 25 percent, and 50 percent), binder contents (4.25 percent, 5.00 percent, and 5.75 percent) and RAP sources (RAP No. 1 and RAP No. 2). In this study, the OBC was 5.0 percent, and the researchers evaluated the rutting performance at OBC and OBC plus/minus 0.75 percent (i.e., 4.25 percent and 5.75 percent) as discussed in Chapter 3. The results of Figures 67 show that the APA rut depth increased with an increase in binder content, as expected. There was a statistically significant difference in the rut depth between mixtures with 5.75 percent binder content and 4.25 percent binder content. Meanwhile, there was no statistically significant difference between mixtures with 4.25 percent and 5.0 percent binder contents.

Figure 68 shows the same mixes as in Figure 67, but the rut depth was obtained using HWTT. As previously mentioned, the HWTT was performed in wet conditions, where the test samples are submerged in water at 50^{o}C; therefore, the HWTT test results were used to evaluate both rutting resistance and moisture susceptibility. Overall, the HWTT rut depths were higher than the APA rut depths, which is likely related to the testing conditions and applied loads (Table 6). Like the APA test, the HWTT rut depth increased with the increase of binder content; however, the difference in the HWTT results was not statistically significant.

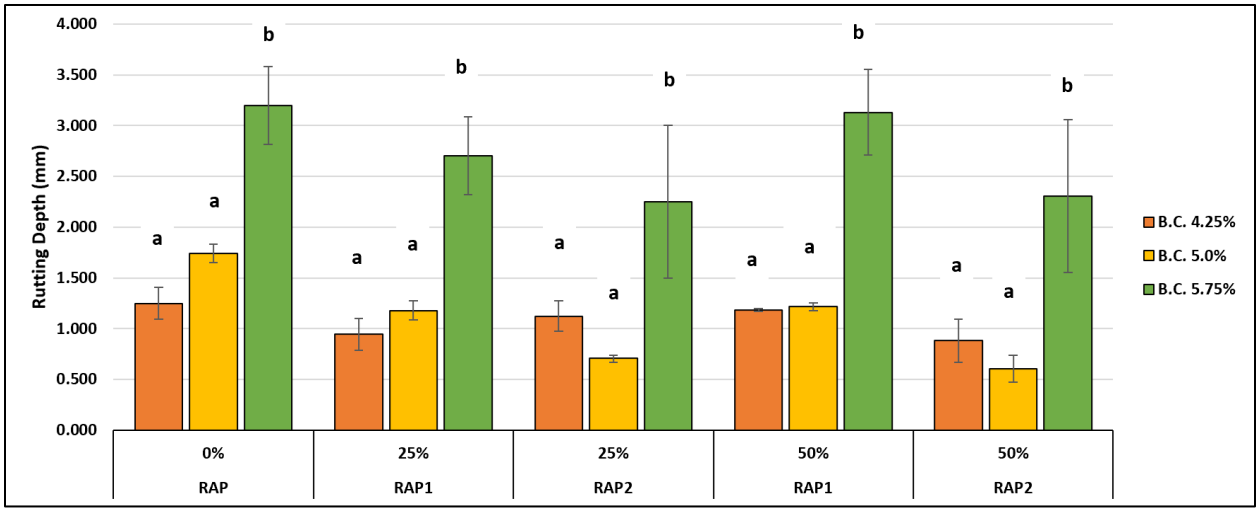

Figure 67. APA Rut Depths at Different Binder Contents (PG58-38)

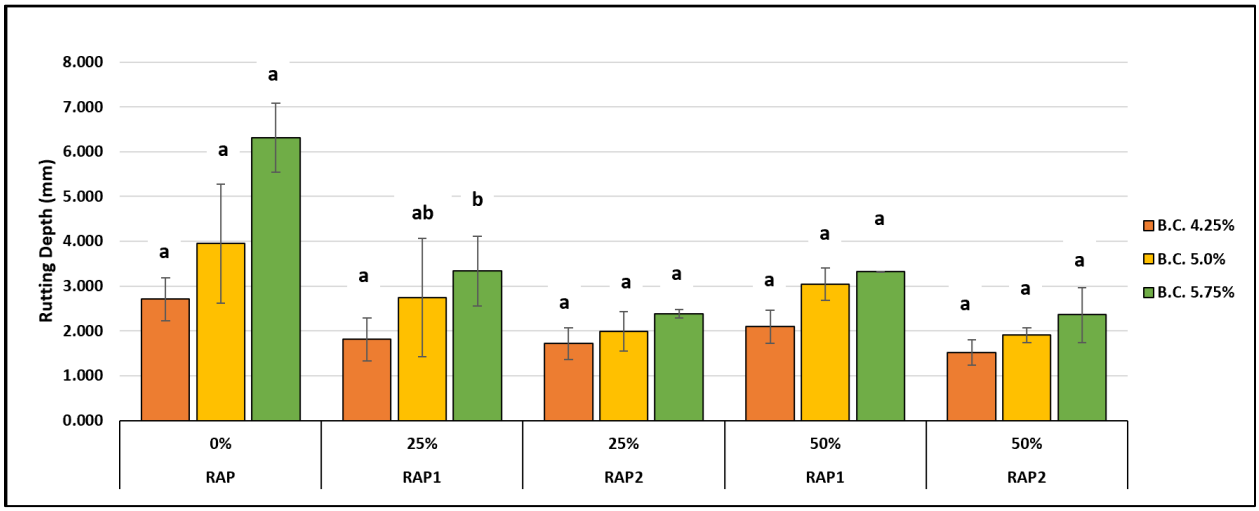

Figure 68. HWTT Rut Depths at Different Binder Contents (PG58-38)

Effect of RAP Content

Figures 69 and 70 show the effect of RAP content on rutting using the APA rut test and HWTT, respectively. For the APA, the results demonstrated that there was no clear trend between RAP content and rut depth. The expected trend is to have less deformation with the increase in RAP content since mixes with higher RAP content would be stiffer and more brittle due to using less virgin binder to replace the stiffer RAP binder. However, the results showed inconsistent trends. For the first source of RAP (i.e., RAP No. 1), most of the mixes had lower rut depth at 25 percent RAP compared to 0 percent RAP. However, at 50 percent RAP, the rutting increased slightly compared to 25 percent RAP. For the second source of RAP (i.e., RAP No. 2), there was no statistically significant difference between the rut depth at different RAP contents, except for PG 58-34 at 5.0 percent binder content where there was a statistically significant difference between 0 percent RAP and both 25 percent and 50 percent RAP contents. Also, the results demonstrated that RAP materials from the second source (RAP No. 2) were stiffer than the RAP materials from the first source (RAP No. 1), which resulted in slightly less rutting. Overall, all the samples had good rutting performance since all rut depths were below 5 mm, which is the maximum APA rut depth threshold accepted by ITD.

Figure 70 shows the HWTT rut depth for the test mixtures. The results demonstrated that mixtures with no RAP had higher rut depth than those with 25 percent and 50 percent RAP; however, such difference was not statistically significant for most of the test mixtures. Overall, all test mixtures had good resistance to rutting using the HWTT. All mixtures had a rut depth less than 12.5 mm (the failure threshold) after 20,000 of HWTT passes.

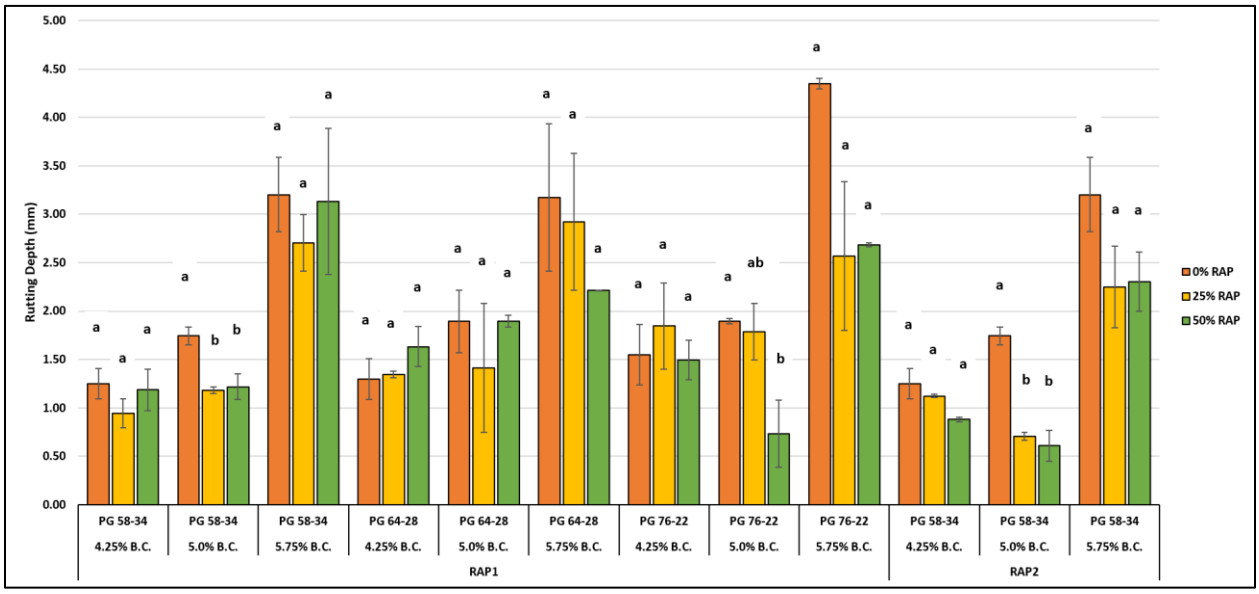

Figure 69. APA Rut Depths for Mixes with Different RAP Contents

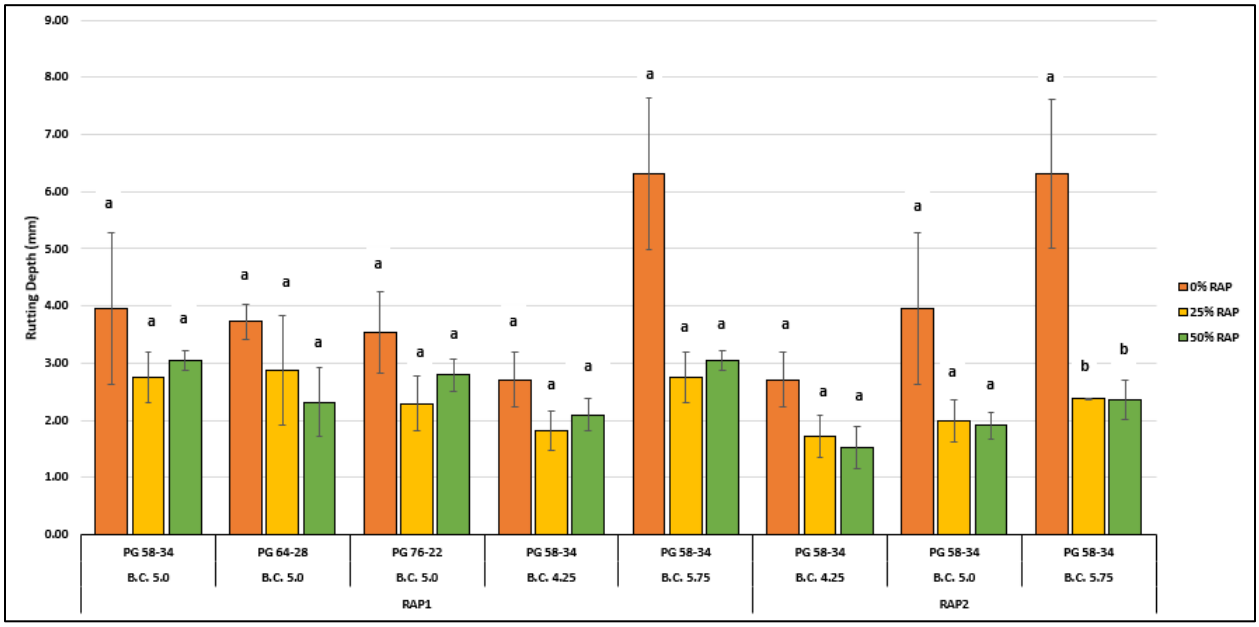

Figure 70. HWTT Rut Depths for Mixes with Different RAP Contents

Effect of Binder Grade

The researchers investigated the effect of binder grade on rutting resistance measured using APA rut test and HWTT. Three binder grades were included (i.e., PG 58-34, PG 64-28, and PG 76-22), one aggregate type (basalt), and RAP No. 1. Figures 71 through 73 show the APA rut depth for the test mixtures prepared at 4.25 percent, 5.0 percent, and 5.75 percent binder content, respectively. The results of Figure 71 showed that mixes with PG 76-22 had a slightly higher APA rut depth compared to other two binders (PG 58-34, PG 64-28), one explanation is that the APA test is conducted at an equivalent temperature to the high-performance grade (PG) of the test binder. The APA testing temperature for the mixes prepared with PG 76-22 was 168.8°F (76 °C). This could result in higher rut depth due to decreased viscosity compared to softer binder (e.g., the testing temperature of PG 58-34 mixes was 136°F [58 °C]). The rut depth was very small (less than 2 mm) for all mixes with different binder grades at 4.25 percent binder content which indicate good resistance to rutting. And the difference among all mixes was less than 1.00 mm. The statistical analysis showed that there was no significant difference among the mixes using different binder grades.

Figure 72 shows the APA rut depth for test mixes at OBC of 5.0 percent. There was a small increase in rut depth compared to mixes prepared at 4.25 percent (Figure 71). This is expected as the samples at 5.0 percent binder content are softer than those at 4.25 percent; however, there was no clear effect for the binder grade on the measured rut depth. All test samples had relatively low rut depth (less than 2.0 mm).

Figure 73 shows the APA rut depth for mixes at 5.75 percent binder content. These mixes were softer and showed higher rut depth compared to mixtures at 4.25 percent and 5.0 percent binder content. The

results showed that for mixes prepared with PG 64-28 and PG 76-22, the rut depth decreased with the increase in RAP content. However, for PG 58-34, the rut depth decreased at 25 percent RAP and slightly increased at 50 percent RAP. The binder grade was found to have no statistically significant effect on rutting at 5.75 percent binder content.

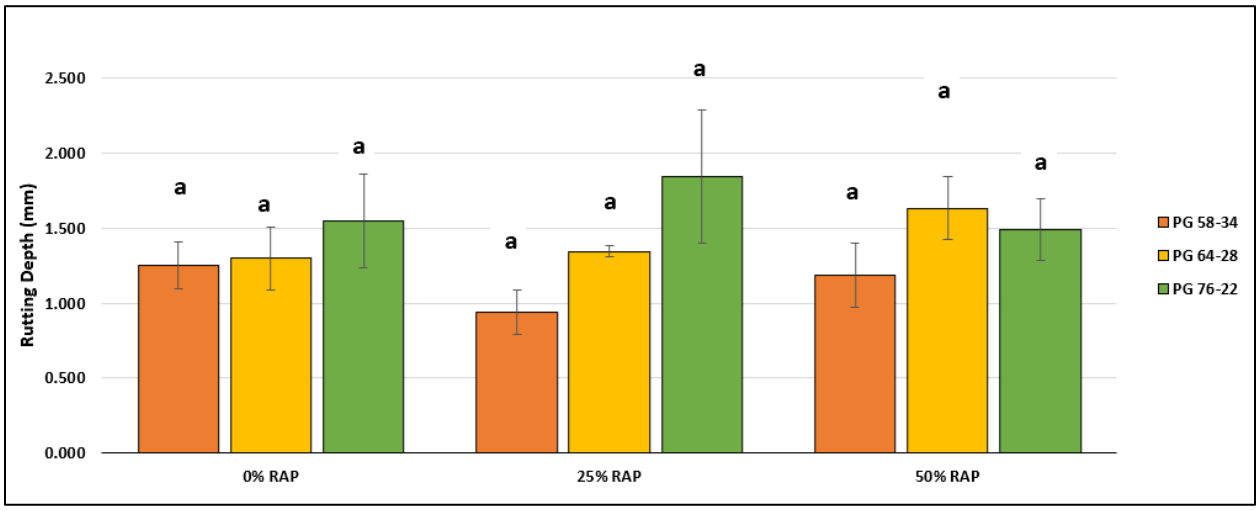

Figure 71. APA Rut Depth for Mixes with Different Binder Grades at 4.25 percent B.C.

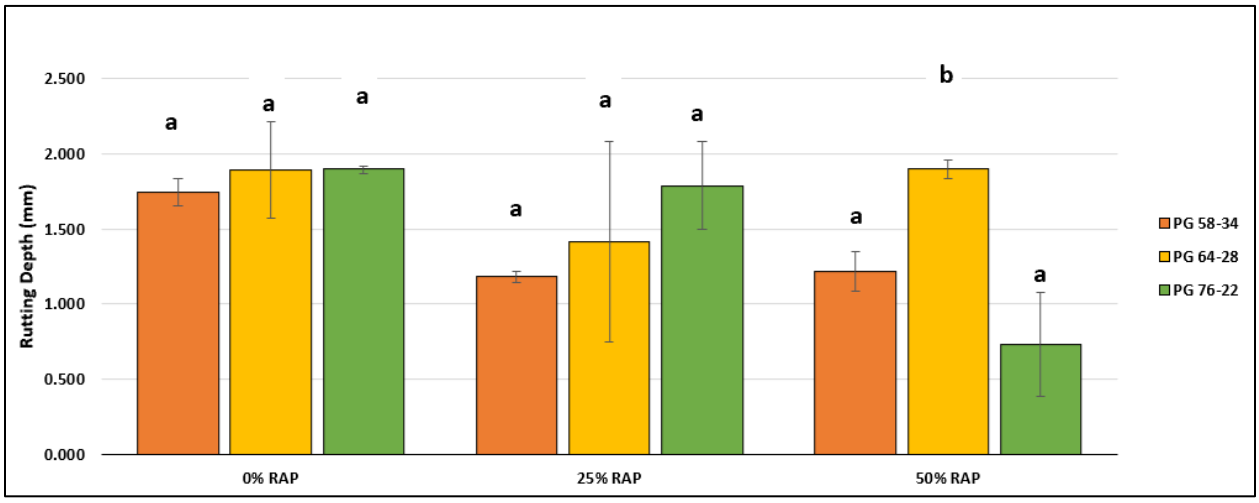

Figure 72. APA Rut Depth for Mixes with Different Binder Grades at 5.00 percent B.C.

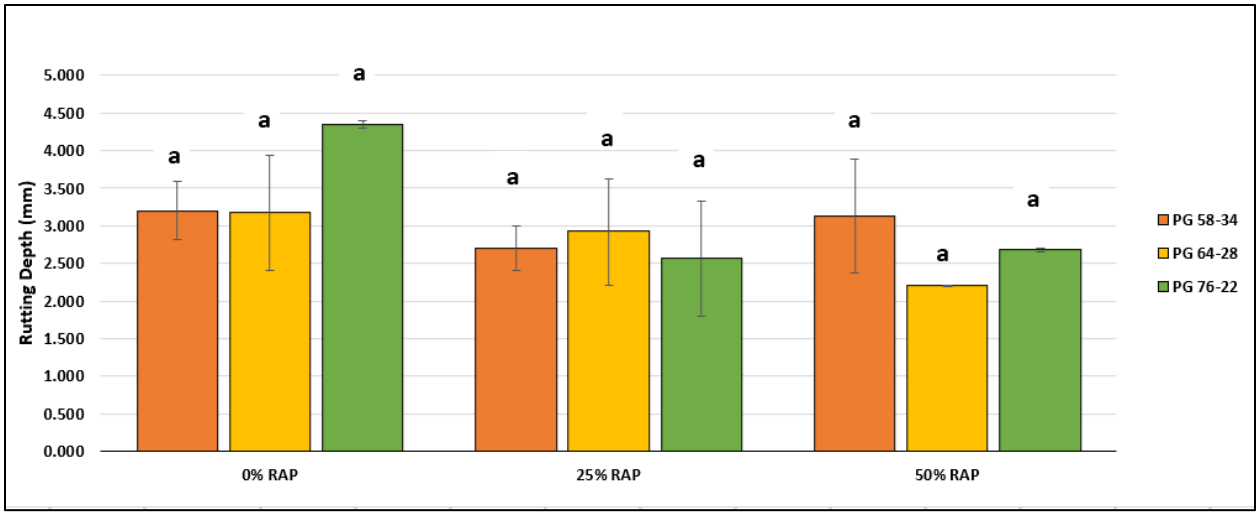

Figure 73. APA Rut Depth for Mixes with Different Binder Grades at 5.75 percent B.C.

Figure 74 shows the HWTT rut depth for test samples using different binder grades at various RAP contents and at 5.0 percent binder content. The HWTT rut depth for mixtures with no RAP had a slightly higher rut depth compared to those prepared with 25 percent and 50 percent RAP. In addition, the results demonstrated that there was no statistically significant difference in rut depth for mixtures prepared with different binder grades. All test samples showed good resistance to rutting and the HWTT rut depth was less than 4 mm.

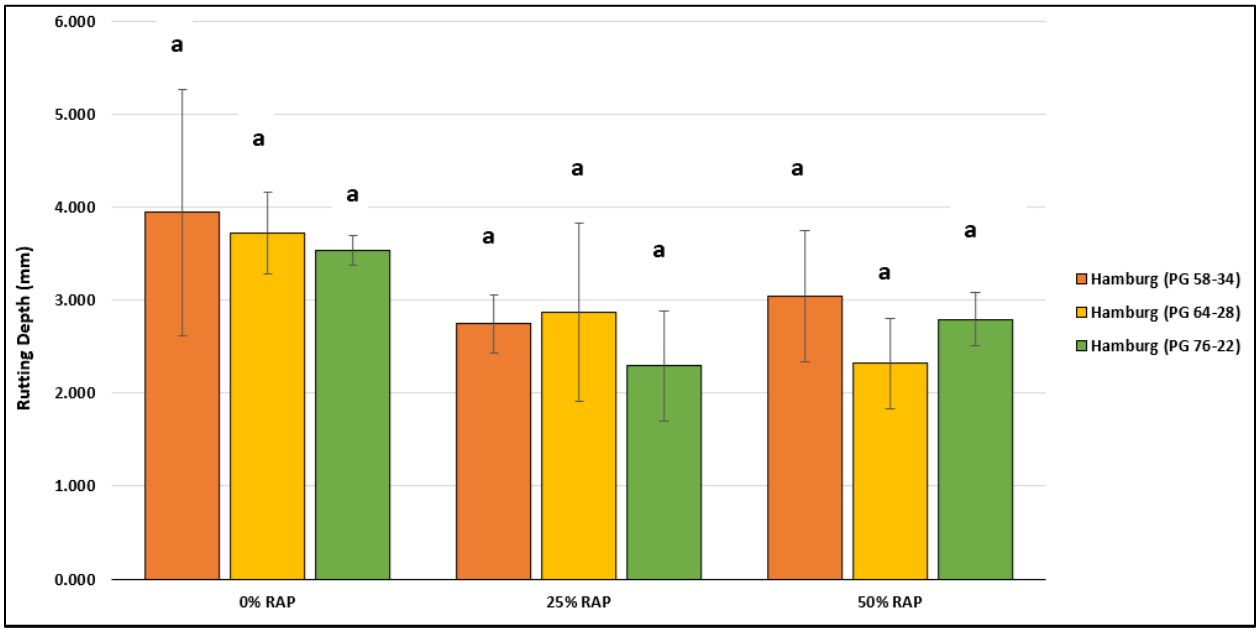

Figure 74. HWTT Rut Depth for Mixes with Different Binder Grades at 5.00 percent B.C.

Effect of Aggregate Type

A limited comparison was performed to evaluate the rutting performance of mixtures prepared using different aggregate sources. The rutting performance of test mixtures prepared using basalt and river gravel at lower and higher binder contents (4.25 percent and 5.75 percent) was evaluated. Figure 75 shows the HWTT rutting depth of test samples. The results show that there was no statistically significant difference in rut depth between basalt and river gravel mixtures at 4.25 percent binder content; however, there was a statistically significant difference in rut depth at 5.75 percent binder content. The river gravel mixtures experienced higher rutting compared to basalt mixtures, especially at the higher binder content. It should be noted that river gravel has less resistance to moisture damage compared to basalt. The river gravel was selected to study the use of anti-strip agents to improve the resistance of asphalt mixtures to stripping as discussed later in this chapter.

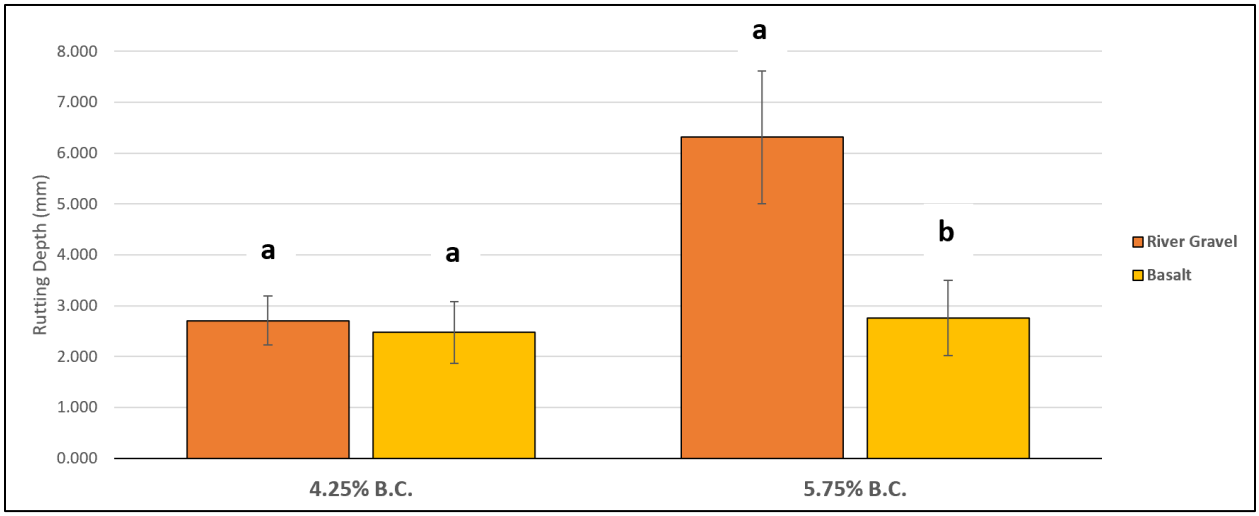

Figure 75. HWTT Rut Depth for Mixes with Two Types of Aggregates

Correlation between HWTT and APA Results

The researchers investigated the relationship between APA and HWTT rut depth for the LMLC mixes. It should be noted that the HWTT was selected to assess the PMLC mixes. Figure 76 shows the rut depth measured using APA against HWTT. A poor correlation was found between APA and HWTT rut depth results, which was not surprising since both APA and HWTT test mixes under different conditions (Table 6). The APA is performed at different temperatures based on the binder grade, while the HWTT is conducted at a constant temperature of 50°C. The testing temperature has a significant effect on rutting since the viscosity of asphalt binder decreases with the increase in temperature. Also, the HWTT is conducted in wet conditions, while the APA is performed in dry conditions. These results are consistent with the findings of RP 261 (Kassem et al. 2019).

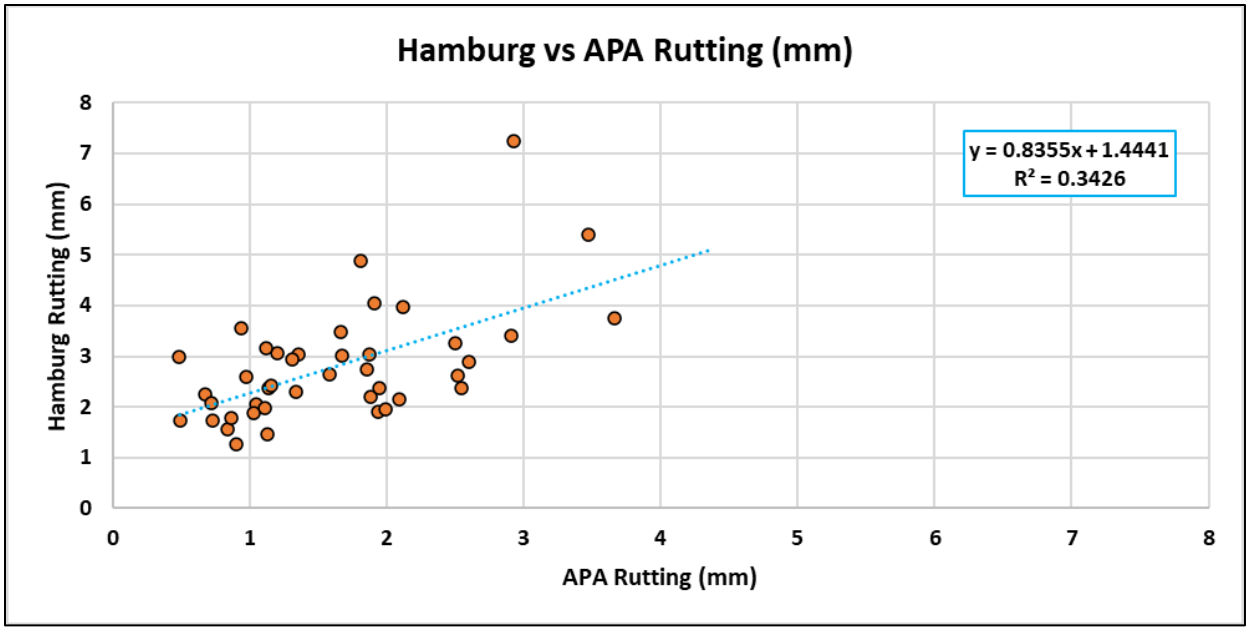

Figure 76. Correlation between APA and HWTT Rut Depth Results for LMLC Mixes

Evaluation of Rutting Resistance of Field Mixes

The researchers evaluated the rutting performance of PMLC samples prepared with mix collected from the field. These mixes had different RAP contents, binder contents, binder grades, and NMAS as discussed in detail in Chapter 3. Three batches were evaluated from each project to examine the change in rutting performance during project construction. The HWTT was used to evaluate the rutting resistance of the PMLC mixes since it can be used to assess both rutting and moisture susceptibility. In addition, ITD is planning on implementing this test to evaluate the rutting resistance of asphalt mixes in accordance with AASHTO T 324.

Figure 77 shows the HWTT rut depth for all PMLC mixes after 20,000 passes. All test batches from the six projects exhibited good resistance to rutting. The measured rut depth was less than 12.5 mm (the failure threshold) after 20,000 passes of HWTT. The rut depth of PMLC mixes ranged from 1.714 mm to 4.198 mm. There was no statistically significant difference in rut depth among the batches of the PMLC mixes for all the projects. All batches passed the HWTT rutting threshold and there was no sign of moisture damage. Therefore, it is expected that all field projects will provide good resistance to rutting.

By investigating the effect of mix composition of field projects on rutting, D4-P1 had the lowest rut depth since it had the lowest binder content (5.1 percent) among all mixes. On the other hand, D1-P1 had the highest rut depth and higher binder content of 5.9 percent. The statistical analysis confirmed that there was a significant difference between these two mixes (i.e., D4-P1 and D1-P1).

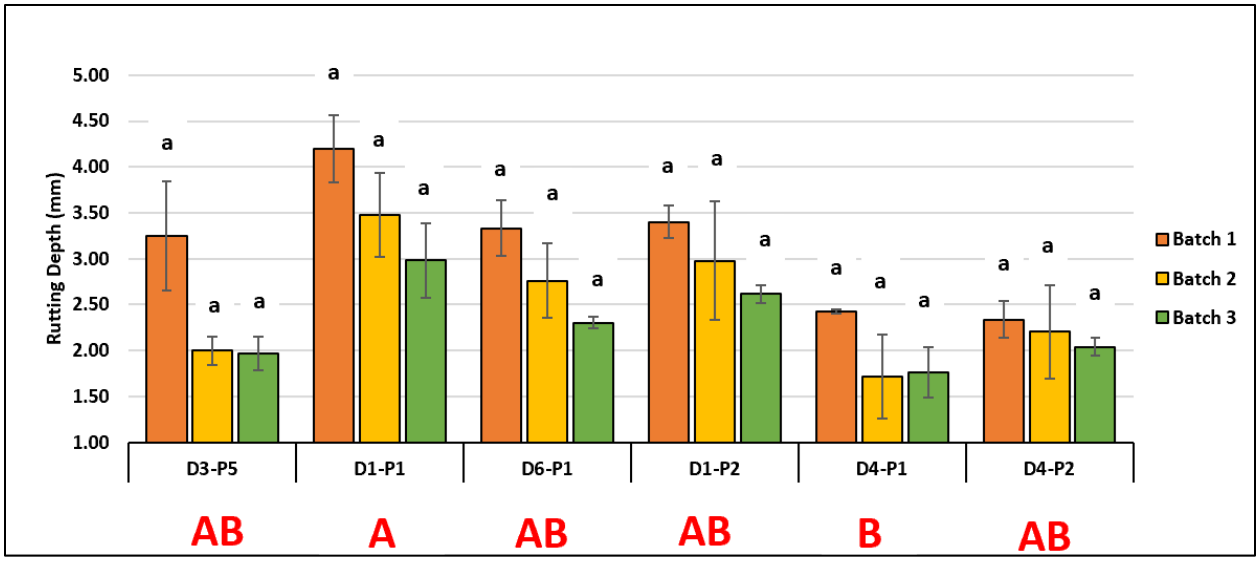

Figure 77. HWTT Rut Depth of PMLC Mixes

Correlation between Rutting and Mix Stability Indices

The researchers investigated the correlation between the rut depth, measured using the APA and HWTT, and compaction and stability indices including the GS, CDI and LCI. These correlations examine the effect of compaction and densification on rutting performance. The assumption is that mixes that require higher energy during laboratory compaction are often stiffer mixes, and thus should have higher rutting resistance. This section thoroughly investigated the relationship between APA and HWTT test results and mix stability and compactability for LMLC and PMLC mixes.

Gyratory Stability

Figure 78 shows the correlation between the GS and APA rut depth for all LMLC mixes regardless the binder grade. The results revealed that there was a fair correlation (R^2 = 0.55) between GS and APA rut depth. The R^2 of the correlation was slightly improved when the relationship between GS and APA rut depth was examined for each binder grade separately (i.e., PG 58-34, PG 64-28, PG 76-22) as shown in Figure 79. Higher GS values indicate higher energy is required to compact the samples in the laboratory to achieve the target density. Higher GS values indicate higher resistance to densification and were found to be associated with less rutting as expected.

Similarly, Figure 80 shows the correlation between the GS and HWTT rut depth for all LMLC mixes regardless the binder grade. The results revealed that there was no good correlation between the GS values and HWTT results. Also, Figure 81 shows that there was no improvement in the relationship between GS and HWTT rut depth for different binder grades. One explanation is that the GS is calculated from the compaction data which is conducted at different temperatures based on the binder grade, while

the HWTT is conducted at a constant temperature of 50°C and in wet conditions. Since the viscosity of asphalt binders change with temperature, the rutting performance also changes with temperature.

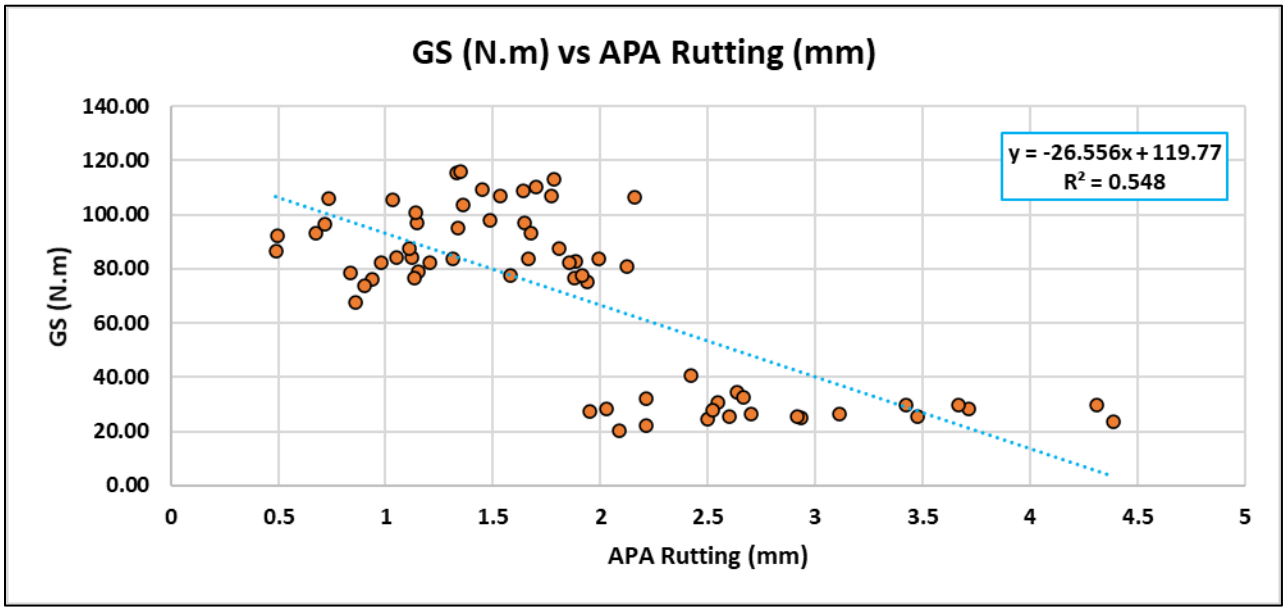

Figure 78. Correlation between GS and APA Rutting Data of LMLC Mixes

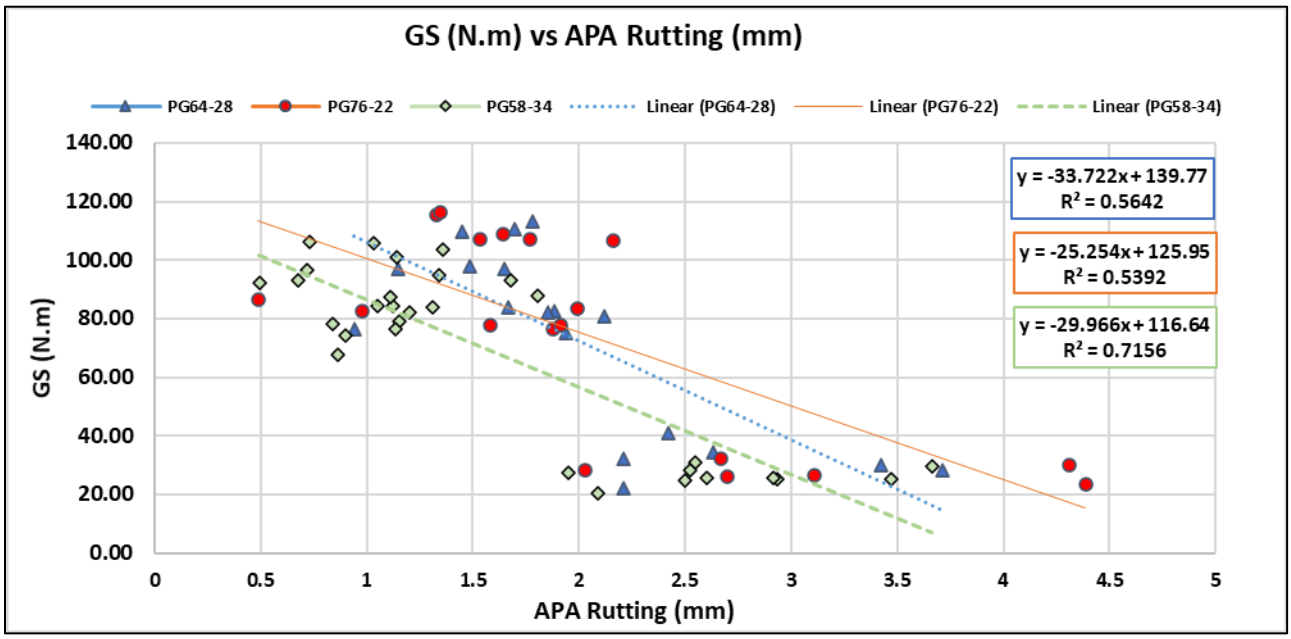

Figure 79. Correlation between GS and APA Rutting Data of LMLC Mixes

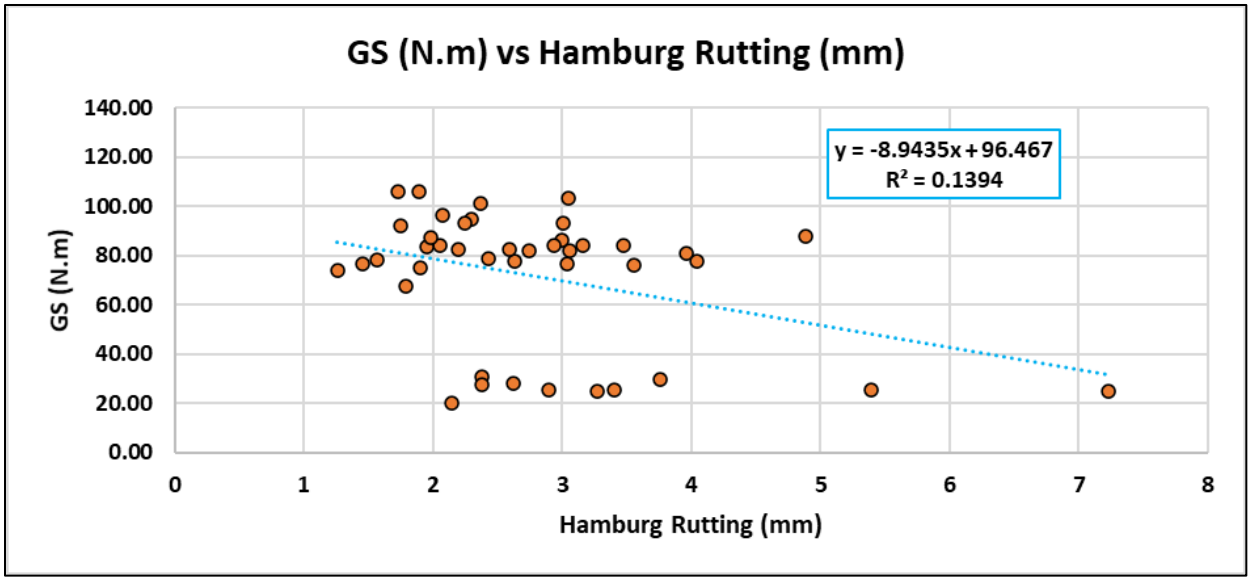

Figure 80. Correlation between GS and HWTT Rutting Data of LMLC Mixes

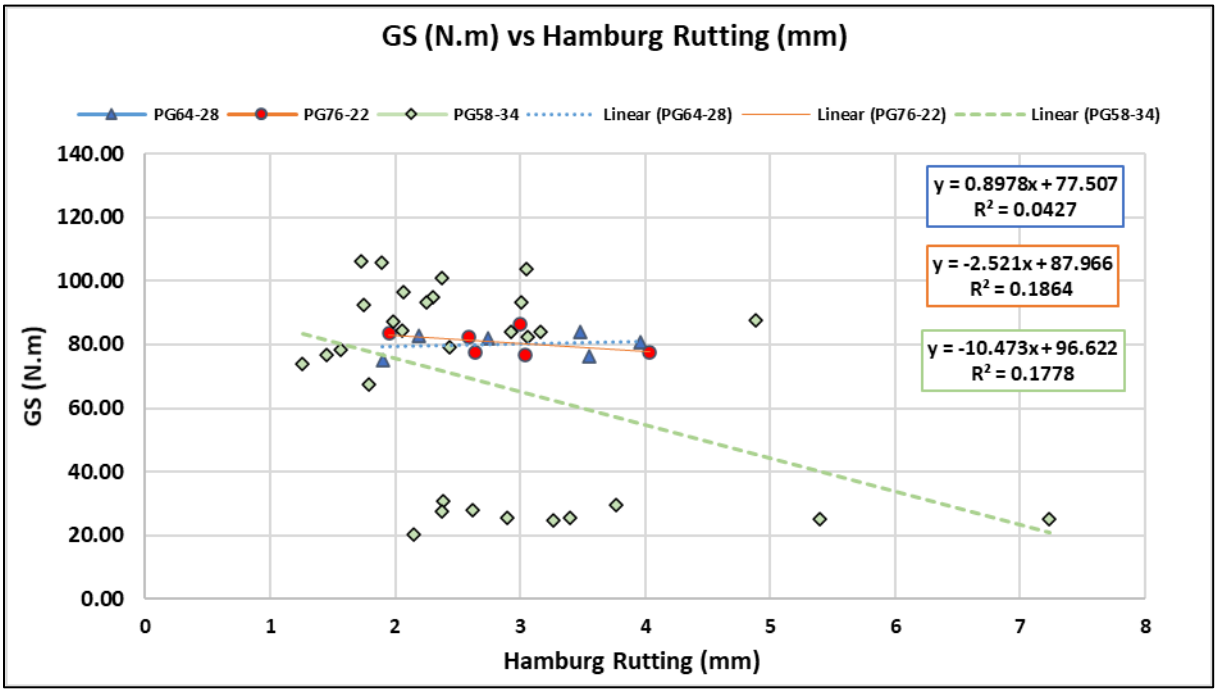

Figure 81. Correlation between GS and HWTT Rutting Data of LMLC Mixes

Construction Densification Index

There was a fair correlation (R^2 = 0.48) between CDI and APA rut depth values as shown in Figure 82. Higher CDI values were associated with small rut depths. The correlation was slightly improved when different binder grades were considered separately as shown in Figure 83. Mixes with higher CDI required more energy for compaction and exhibited less rutting compared to those with low CDI. Like the GS, the results showed no correlation between the CDI values and HWTT results (Figures 84 and 85). The HWTT is conducted at a constant temperature of 50°C and in wet conditions, while the CDI is calculated from the compaction data which is conducted at different temperatures based on the binder grade.

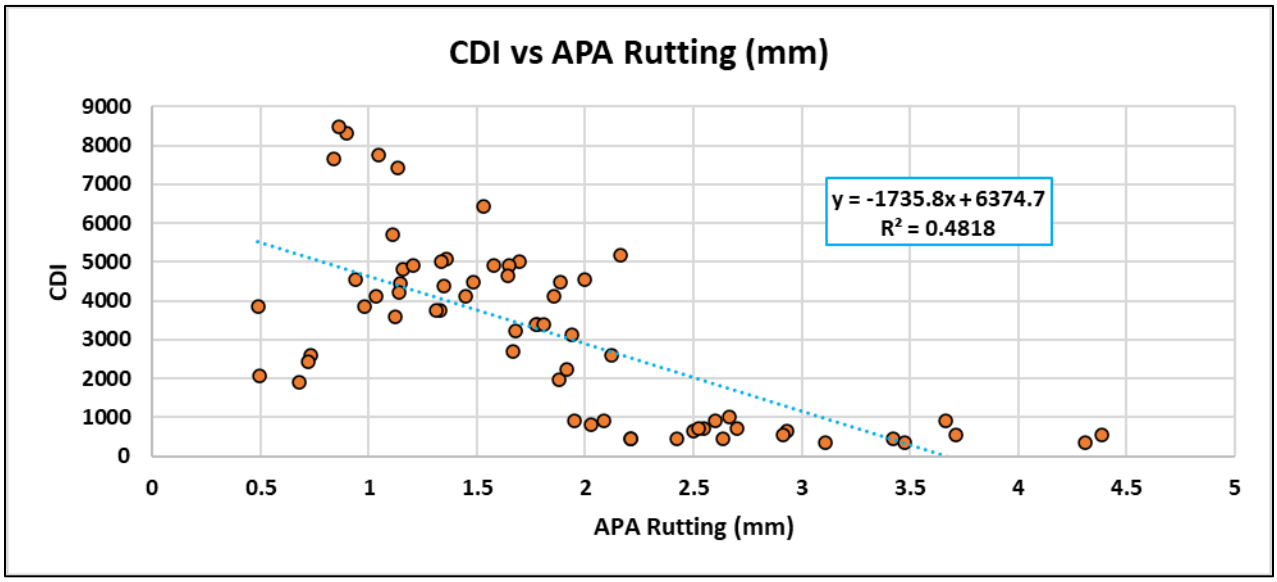

Figure 82. Correlation between CDI and APA Rutting Data of LMLC Mixes

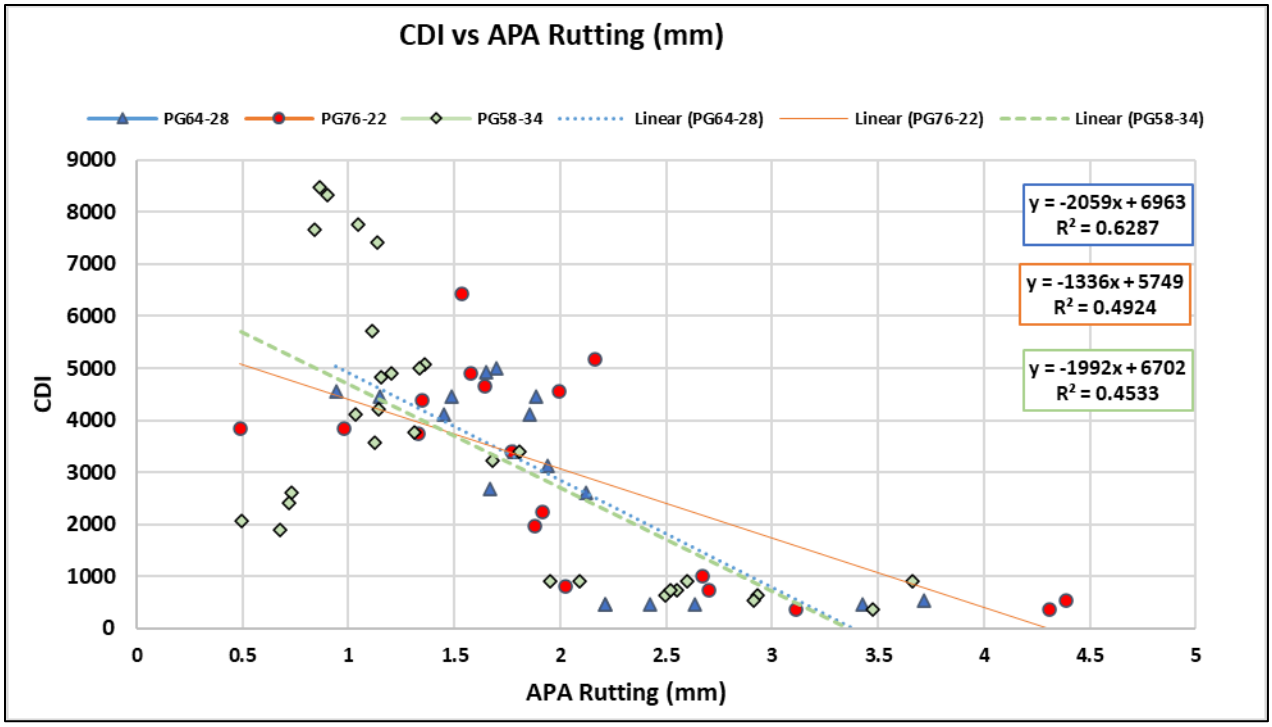

Figure 83. Correlation between CDI and APA Rutting Data of LMLC Mixes

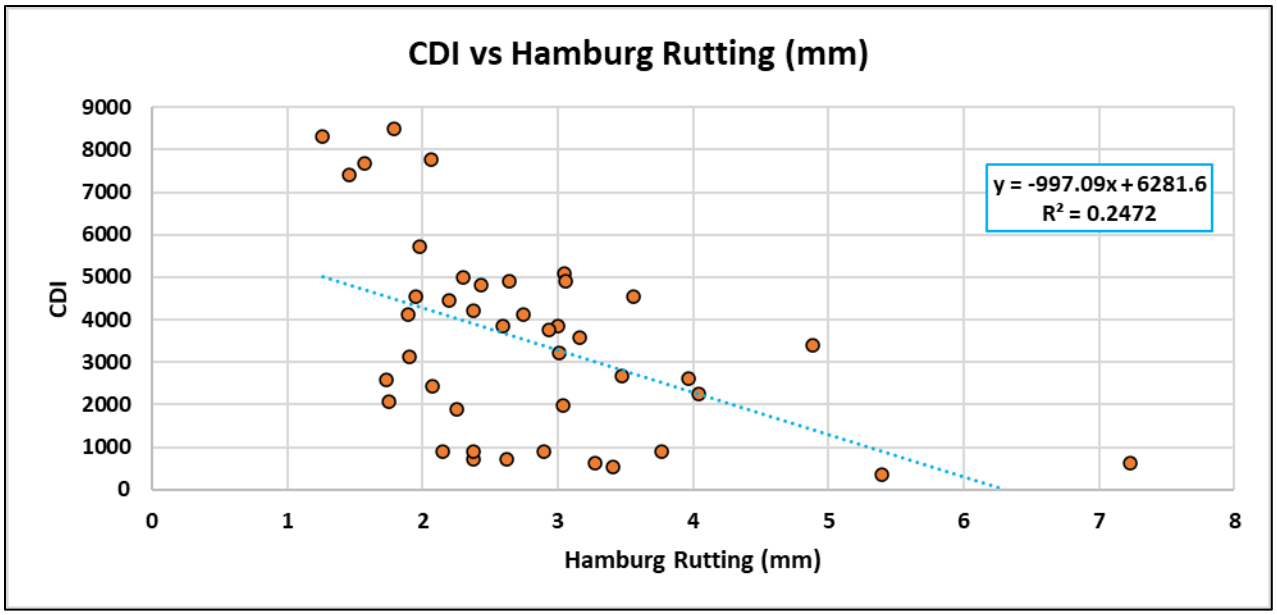

Figure 84. Correlation between CDI and HWTT Rutting Data of LMLC Mixes

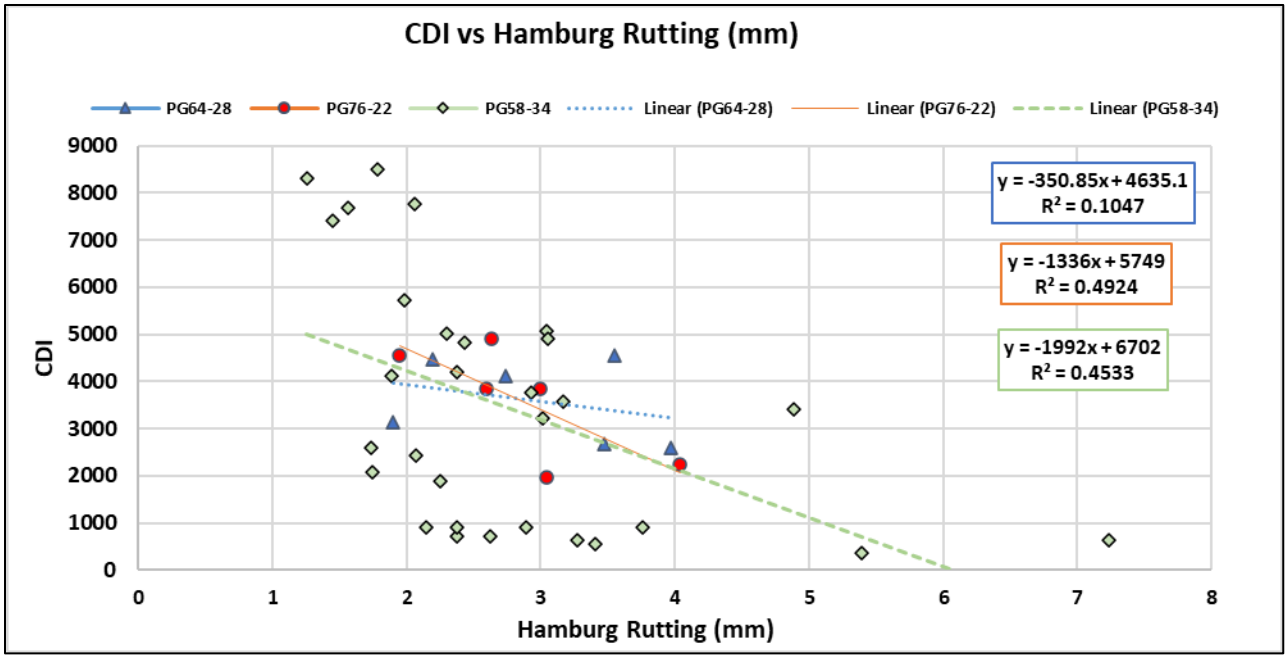

Figure 85. Correlation between CDI and HWTT Rutting Data of LMLC Mixes

Laboratory Compaction Index

The LCI was proposed by Kassem et al. (2012) to evaluate the compactability of asphalt mixtures in the laboratory. Higher LCI values indicate less resistance to densification and easy compaction. The assumption is that if the mixture exhibited less resistance to densification during laboratory compaction, it may experience higher permanent deformation or rutting under loading, especially at higher temperatures. In this study, the LCI was calculated for the test samples using Equation 8 and the results were correlated with the rut depth measured using APA and HWTT.

Figure 86 shows the correlation between the LCI and rut depth measured using the APA for the LMLC mixes. Higher LCI values were associated with less rutting, and vice versa. This is in good agreement with the assumption that mixtures with higher resistance to densification (low LCI) are more resistant to rutting. The correlation between LCI and APA rut depth had R^2 of 0.64. Such correlation is considered very good and promising given the inherent variability associated with evaluation of mix compactability and rutting resistance in the laboratory. Figure 87 shows the same relationship but for each binder grade separately, and its corresponding R^2 values. The LCI provided the best correlation with the APA rut depth compared to all other mix stability (e.g., GS) and compactability indices (e.g., CDI). This relationship can be used to assess the rutting resistance of asphalt mixtures during the mix design stage or during laboratory compaction of asphalt mixtures. The researchers developed a spreadsheet to facilitate the calculation of LCI as previously discussed in Chapter 4.

Figures 88 and 89 show the correlation between the LCI and HWTT rut depth for all LMLC mixes and for each binder grade, respectively. Similar to GS and CDI, there was no strong correlation between the LCI and HWTT. The reason is that the HWTT is conducted at constant temperature of 50°C and in wet

conditions and the LCI is calculated from the compaction data which is conducted at different temperatures based on the binder grade. Therefore, the comparison of LCI to APA rut depth is more appropriate as opposed to HWTT.

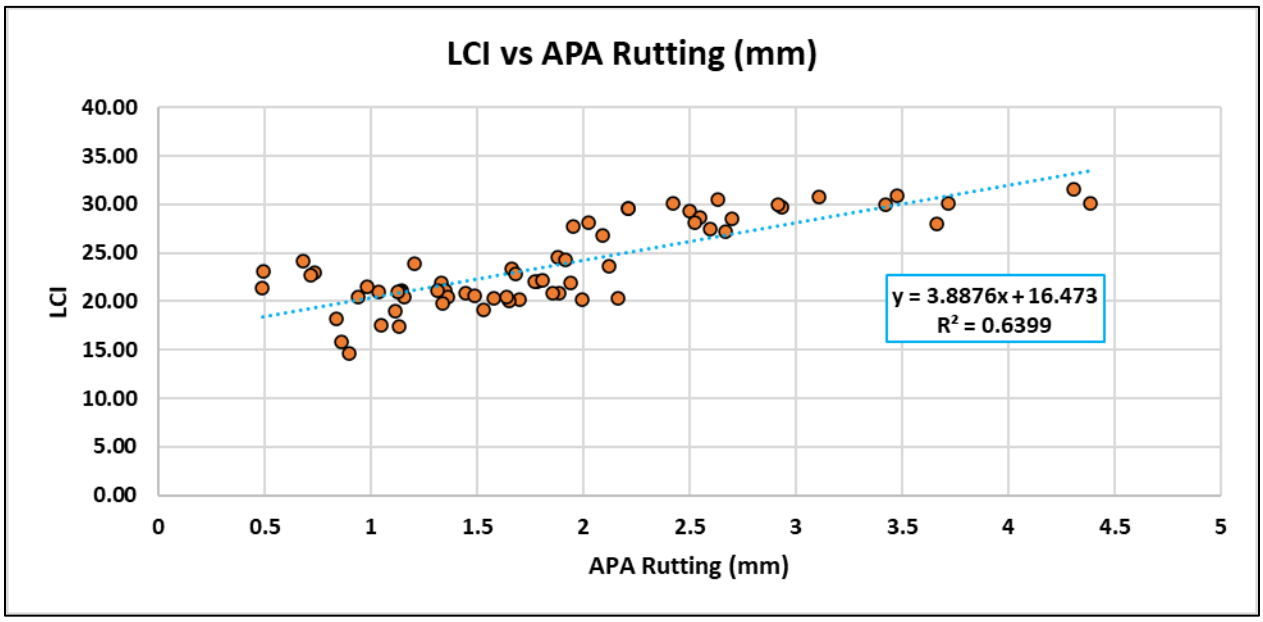

Figure 86. Correlation between LCI and APA Rutting Data of LMLC Mixes

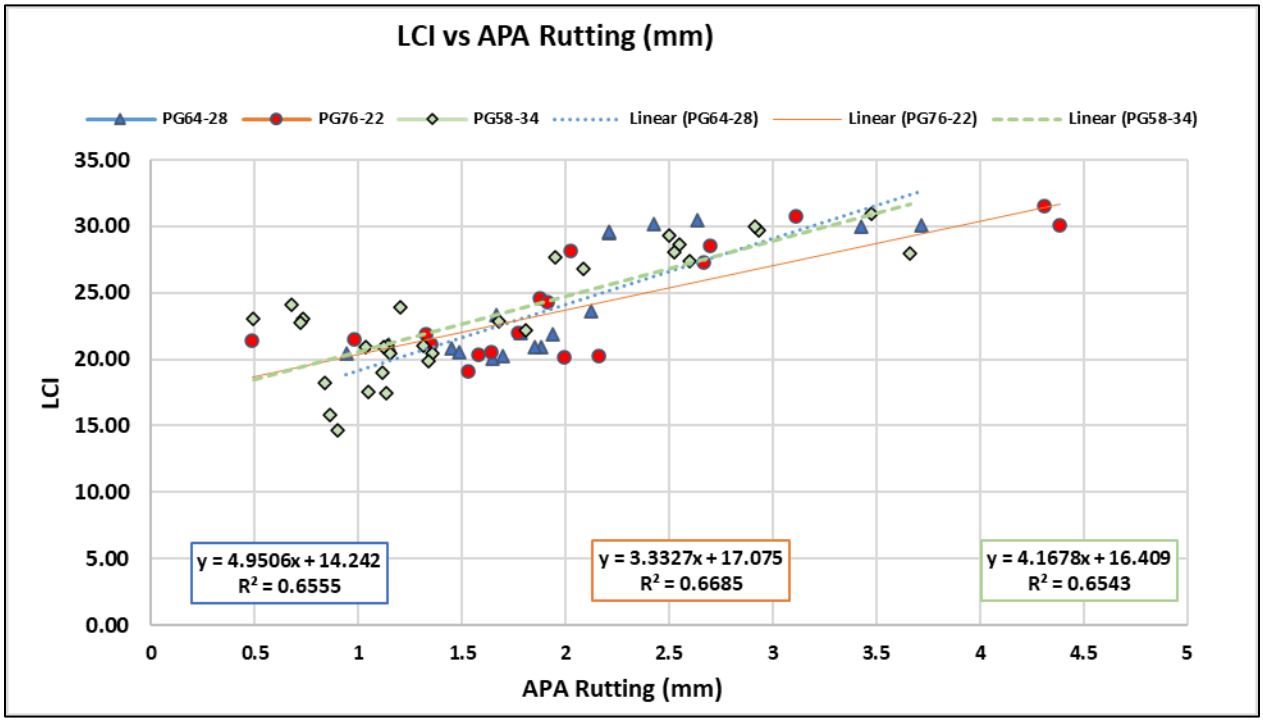

Figure 87. Correlation between LCI and APA Rutting Data of LMLC Mixes

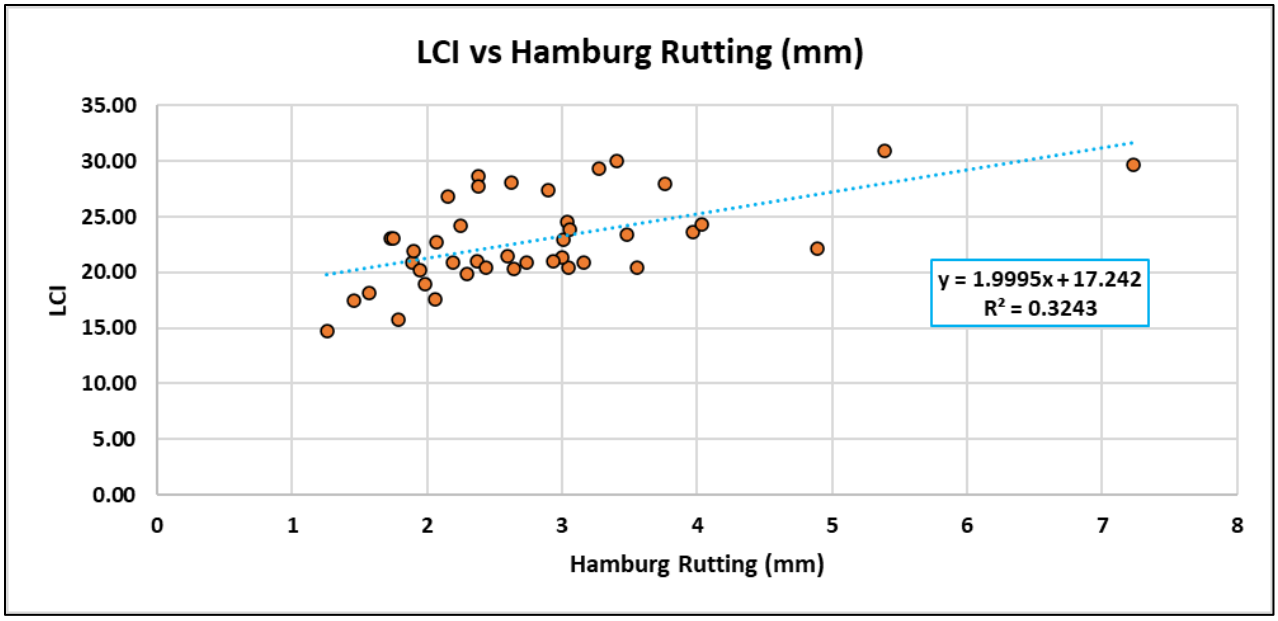

Figure 88. Correlation between LCI and HWTT Rutting Data of LMLC Mixes

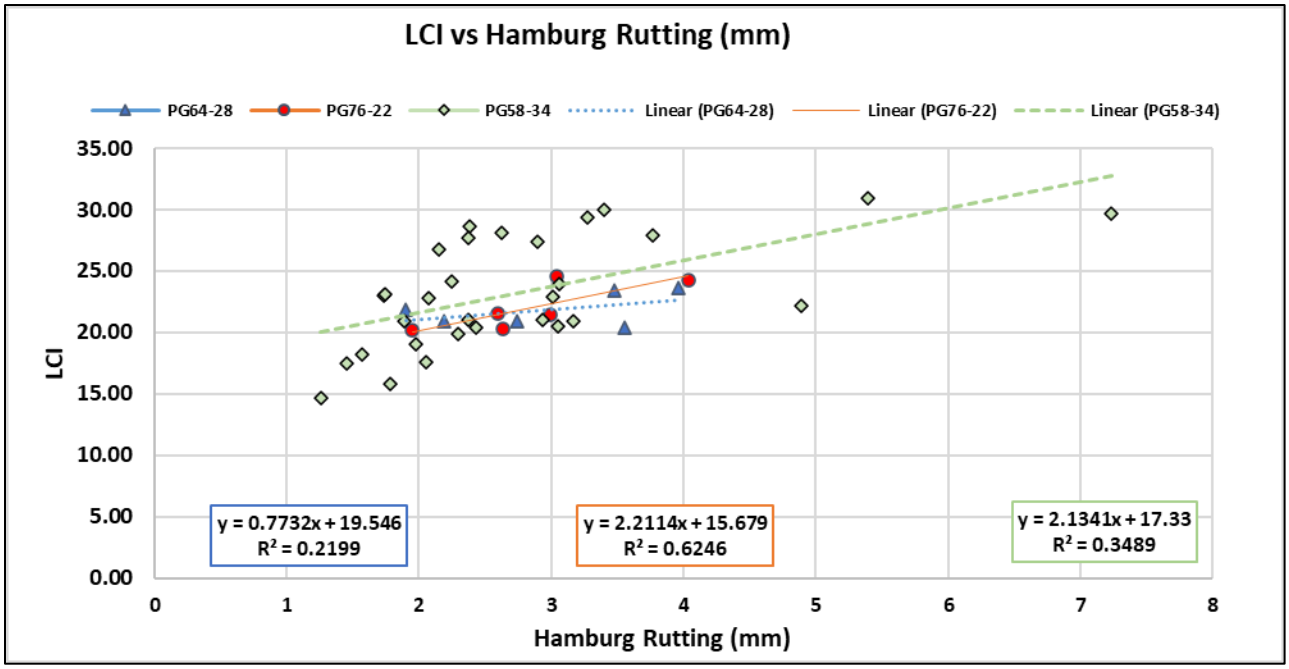

Figure 89. Correlation between LCI and HWTT Rutting Data of LMLC Mixes

Comparison between Stability Indices and HWTT of Field Mixes

As mentioned earlier, the researchers used the HWTT to evaluate the rutting resistance of the PMLC mixes since it can be used to assess both the moisture susceptibility and rutting. In addition, ITD is planning on implementing this test to evaluate the rutting resistance of asphalt mixtures in accordance with AASHTO T 324. The correlations between mix stability and compactability indices with HWTT rut depth results were examined for PMLC. Figures 90 through 92 show the correlation between HWTT and GS, CDI, and LCI, respectively. Like the findings of the LMLC mixes, there were no good correlation between HWTT and the stability and compactability indices. As discussed earlier, the GS, CDI, and LCI are calculated from the compaction curves which are obtained at various temperature depending on the binder grade, while HWTT is conducted at a fixed temperature of 122°F (50°C) in wet conditions.

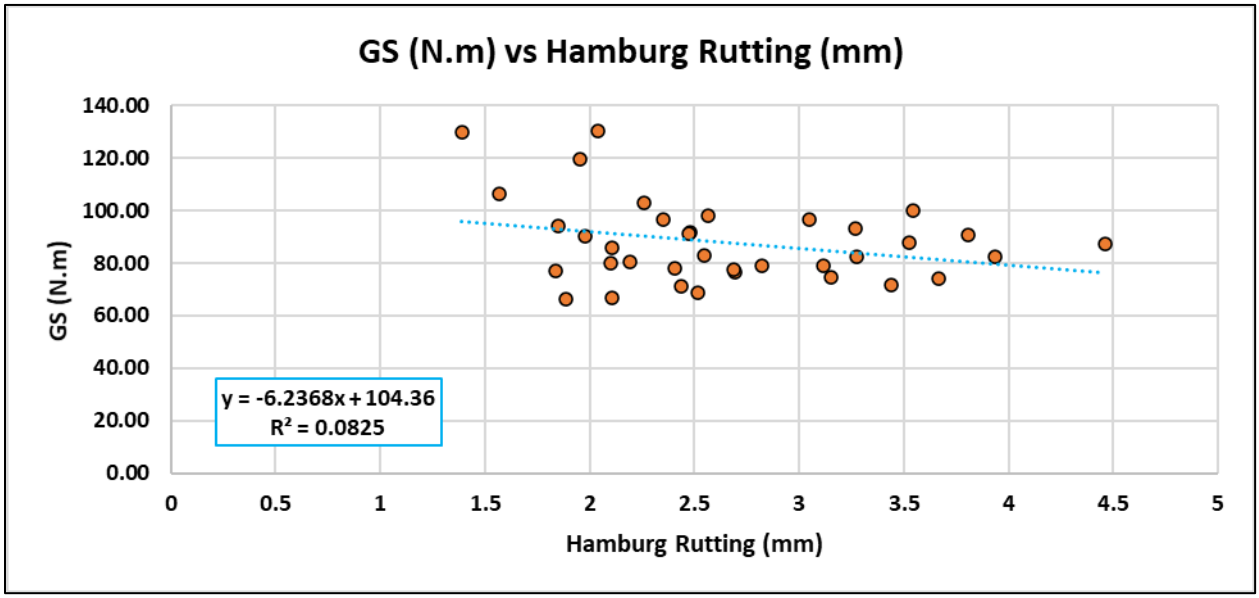

Figure 90. Correlation between GS and HWTT Rutting Data of PMLC Mixes

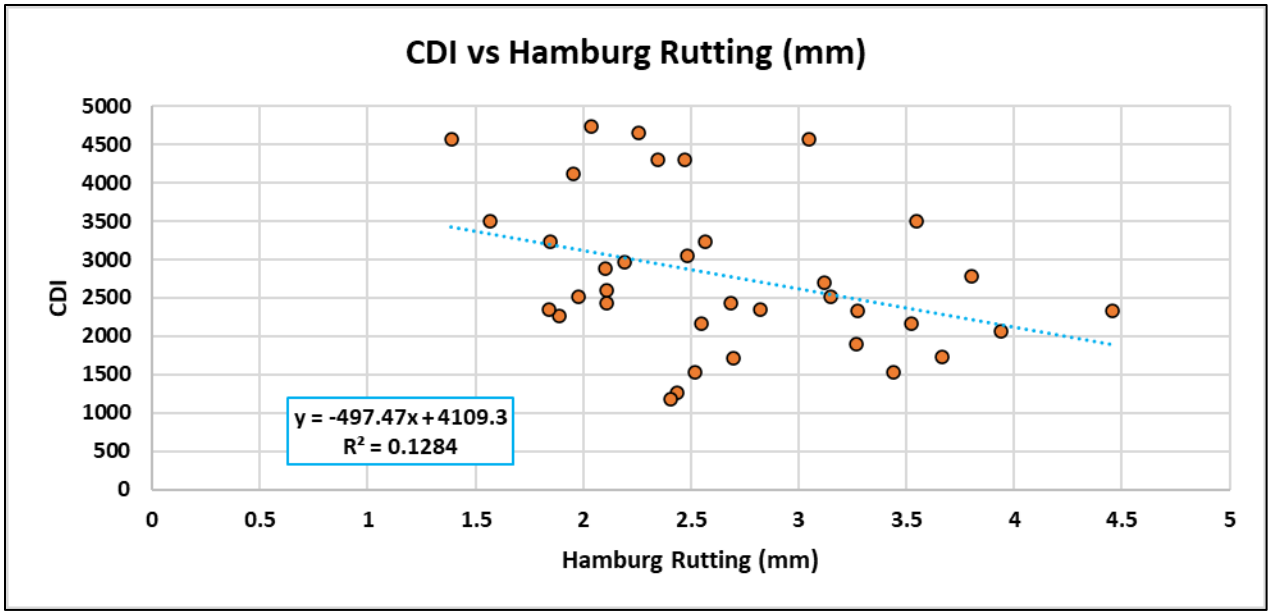

Figure 91. Correlation between CDI and HWTT Rutting Data of PMLC Mixes

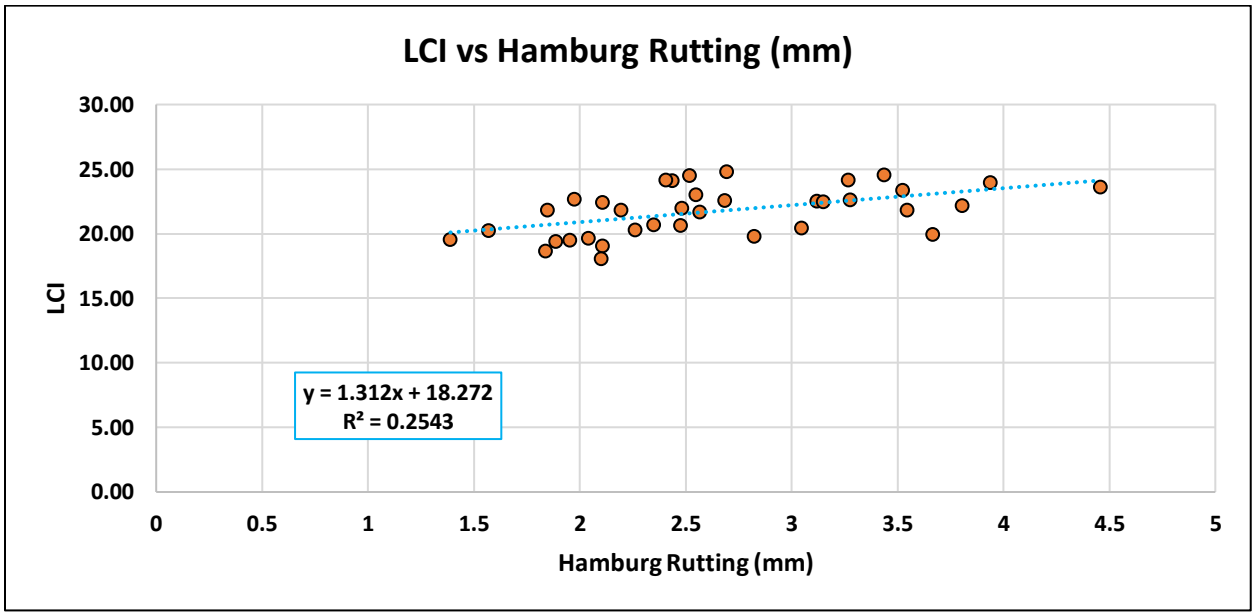

Figure 92. Correlation between LCI and HWTT Rutting Data of PMLC Mixes

Moisture Damage Evaluation

The researchers evaluated the moisture susceptibility of selected asphalt mixtures using the Lottman protocol in accordance with AASHTO T 283, Resistance of Compacted Bituminous Mixture to Moisture-Induced Damage," and ASTM D6931, Standard Test Method for Indirect Tensile (IDT) Strength of Asphalt Mixtures as discussed in Chapter 3. The test mixtures were prepared using river gravel rock, PG 58-34 at binder contents (i.e., 4.25 percent, 5.0 percent, and 5.75 percent), and RAP source No. 2 at three RAP contents (0 percent, 25 percent, and 50 percent). These mixtures were prepared with 0 percent and 1.5 percent of liquid anti-stripping agent (ASA). Typically, a TSR value of 0.80 or greater indicates good resistance to water damage. ASA is often used to improve the resistance to moisture damage when the TSR is less than 0.8. Moisture damage refers to the stripping of asphalt binder from the aggregates leading to raveling and premature pavement failure.

Figure 93 shows the TSR of the test samples prepared at different binder contents (4.25 percent, 5.0 percent, and 5.75 percent) with 0 percent and 1.5 percent ASA. The results showed that, the addition of ASA improved the TSR at 4.25 percent and 5.75 percent but not at 5.0 percent binder content. The use of ASA improves the adhesion between the asphalt binder and aggregates in the mix. The TSR was the lowest (TSR = 0.57 without ASA and 0.65 at 1.5 ASA) at 4.25 percent binder content. This could be due to less amount of binder coating the aggregates which could increase the moisture susceptibility of the mixtures. Meanwhile, the TSR was the highest (TSR = 0.99) at 5.75 percent with 1.5 percent SAS which could make it harder for water to strip the binder off the aggregates.

Figure 94 shows the effect of RAP content on the TSR. Overall, the use of RAP had a negative effect on moisture susceptibility and resulted in lower TSR values. Mixtures with RAP had TSR lower than 0.8 (0.60 at 25 percent RAP, and 0.68 at 50 percent RAP), which indicate these mixes are more susceptible to water damage. The addition of ASA improved the performance at 25 percent RAP where TSR increased from 0.60 to 0.82. However, the ASA did not enhance the resistance to moisture damage at 50 percent RAP (TSR = 0.69).

In addition to Lottman testing, the researchers evaluated the moisture susceptibility and rutting resistance of selected test mixtures using HWTT. This was performed to compare the findings from the TSR to HWTT results. Based on the TSR results, the team tested mixtures with two binder content (4.25 percent and 5.75 percent) with 0 percent and 1.5 percent ASA. Figure 95 shows the HWTT rut depth for the test samples. The addition of ASA slightly improved the resistance to rutting; however, there was no statistically significant difference between samples prepared with and without ASA at different binder contents. Test samples without ASA had good resistance to rutting and moisture damage based on the HWTT results, and this could reduce the effect of ASA on HWTT results. Overall, the HWTT did not provide comparable evaluation of the moisture susceptibility to that of TSR.

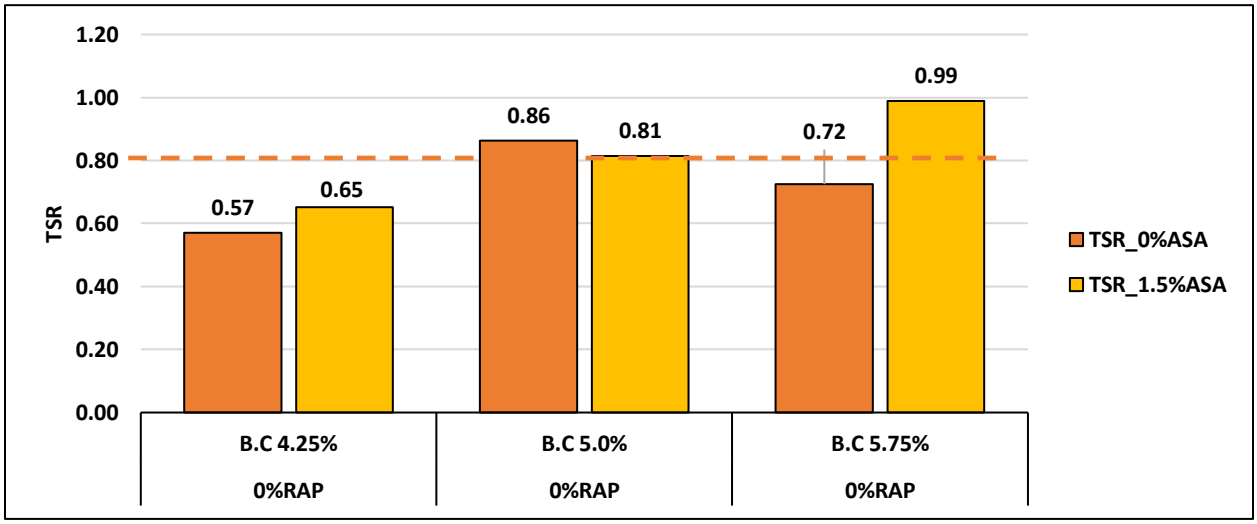

Figure 93. Effect of Binder Content on TSR

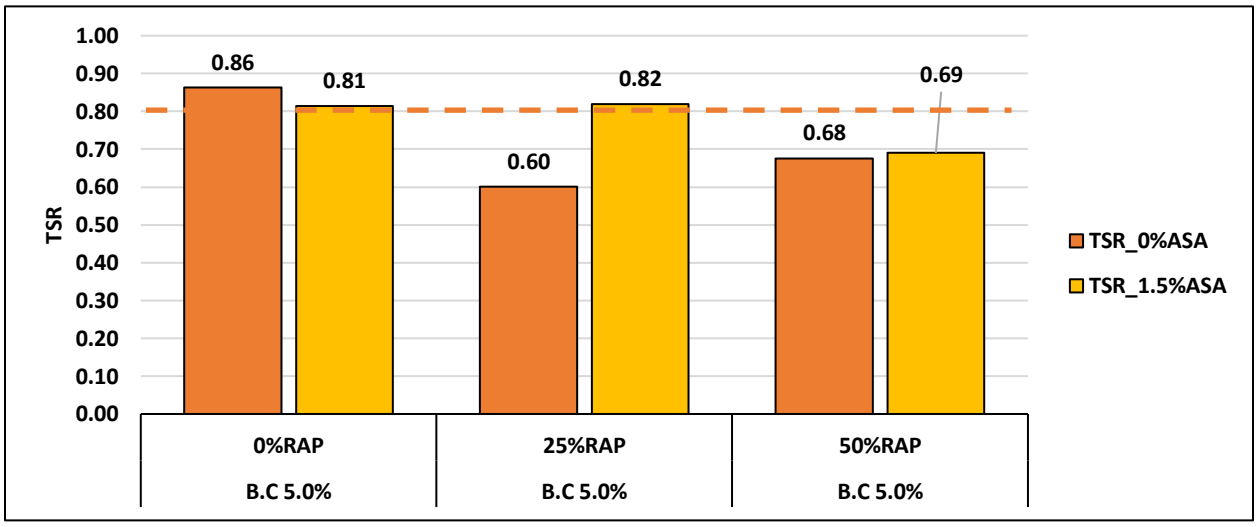

Figure 94. Effect of RAP Content on TSR

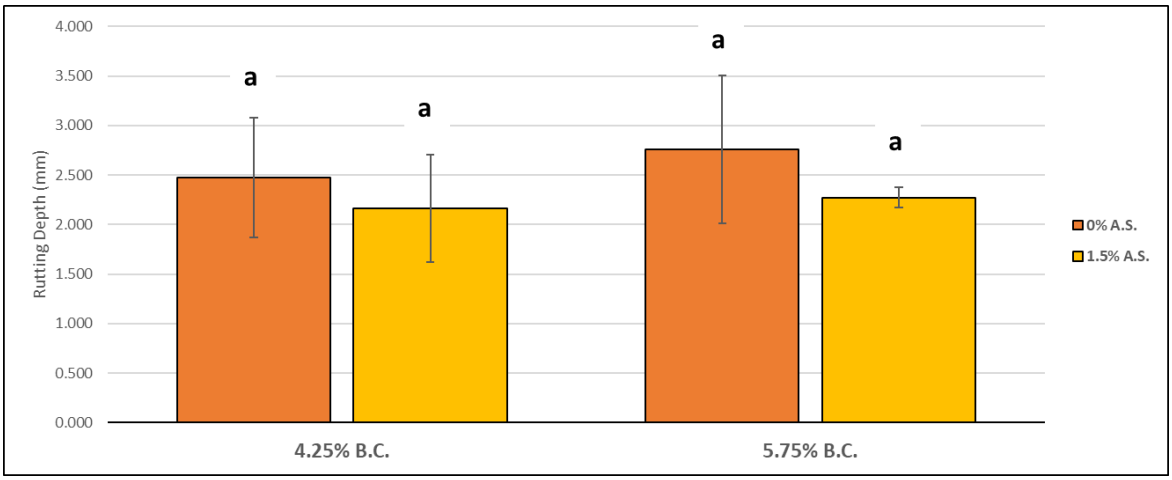

Figure 95. Effect of Anti-Stripping Agent on HWTT Rut Depth

6. Comprehensive Evaluation of Cracking Performance of RAP Mixes

Background

Chapter 6 evaluates the cracking resistance of LMLC and PMLC mixes. The researchers investigated the sensitivity of various monotonic cracking resistance indicators to the change in mix composition (e.g., binder content, binder grade, RAP content). In addition, they examined the cracking performance of the PMLC and the variation in the cracking resistance of various batches sampled throughout the construction of field projects. Furthermore, the researchers examined the correlation and variability of the results of various cracking resistance indicators.

Monotonic Cracking Resistance Indicators

In this study, several monotonic cracking indicators were used to analyze the load-displacement curve from the IDT test to assess the resistance of the mixes to cracking. These cracking performance indicators included IDEAL-CT_{Index}, CRI, N_{flex}, $Weibull_{CRI}$, G_f, $IDT_{Strength}$, $IDT_{Modulus}$, and FI. This section summarizes the equations used to calculate these cracking indicators. RP 261 research report (Kassem et al. 2019) provides further discussion on these indicators. The monotonic cracking indicators use one or more elements of the load-displacement curve of the IDT test to describe the mixture performance. In this study, the IDT test was conducted at 77°F (25°C) to assess the intermediate temperature cracking of the test mixtures.

The IDEAL-CT_{index} is calculated from the load-displacement curve by normalizing the total fracture energy with respect to the post-peak slope at 75 percent of the peak load multiplied by the normalized strain tolerance. The IDEAL-CT_{index} is calculated using Equation 26.

$$\mathrm{IDEAL-CT_{Index}} = \frac{G_{Fracture}^{Total}}{\left|m_{75\%}^{Post-peak}\right|} \times \frac{t}{62} \times \varepsilon_v \mathrm{tolerance} \qquad \text{..... Eqn.26}$$

where:

$\mathrm{IDEAL-CT_{Index}}$	= Cracking test index
$G_{Fracture}^{Total}$	= Total fracture energy (J/m^2)
$m_{75percent}^{Post-peak}$	= Post-peak slope at 75 percent of the peak load
t	= Specimen thickness (mm)
$\varepsilon_v$tolerance	= Strain tolerance

The CRI is also calculated from the load-displacement curve. The CRI is calculated by dividing the total fracture energy by the peak load as presented in Equation 27.

$$CRI = \frac{G_{Fracture}^{Total}}{P_{Peak}} \quad \text{..... Eqn.27}$$

where:

$G_{Fracture}^{Total}$ = Total fracture energy (J/m^2)

P_{Peak} = Peak load (N)

The N_{flex} parameter is the normalization of the toughness with respect to the tangent slope of the post-peak inflection point as presented in Equation 28.

$$N_{flex} = \frac{Toughness}{m} \quad \text{..... Eqn.28}$$

where:

N_{flex} = Total fracture energy (J/m^2)

$Toughness$ = Area under stress-strain curve until post peak inflection point

m = slope of the post-peak inflection point

The $Weibull_{CRI}$ is another indicator used to evaluate the cracking resistance of asphalt mixtures. The $Weibull_{CRI}$ was developed in RP 261 (Kassem et al. 2019) and was found to have a good correlation with field cracking performance. The $Weibull_{CRI}$ describes the entire load-displacement curve. Other cracking indicators (e.g., IDEAL-CT_{Index}, CRI, N_{flex}, $IDT_{modulus}$, FI, etc.) uses one or more elements of the load-displacement curve. This indicator uses the Weibull probability density function's fitting parameters to calculate the cracking resistance index. The $Weibull_{CRI}$ is calculated using Equation 29.

$$Weibull_{CRI} = \left(\frac{\eta}{\beta}\right) \times \log(A) \quad \text{.....Eqn.29}$$

where:

η = Scale parameter

β = Shape parameter (Weibull slope)

A = Scaling factor equals to the area under the load-displacement curve

Another cracking performance indicator is the total fracture energy (G_f) which is based on the area under the load-displacement curve over the crack face area presented Equation 30.

$$G_{Fracture}^{Total} = \frac{W_{Fracture}^{Total}}{Crack\ Face\ Area} \quad \text{.....Eqn.30}$$

where:

$G_{Fracture}^{Total}$ = Total fracture energy (J/m^2)

$W_{Fracture}^{Total}$ = The total work of fracture (J)

The $IDT_{strength}$ and $IDT_{modulus}$ are two parameters used in the literature to evaluate the cracking resistance of asphalt mixtures (Kassem et al. 2019). The $IDT_{strength}$ is calculated based on the peak load with respect to specimen geometry as shown in Equation 31. The $IDT_{modulus}$ uses the IDT tensile strength over the displacement at the peak load as presented in Equation 32.

$$IDT_{strenght} = \frac{2000 \times P_{Peak}}{\pi \times t \times D} \quad \text{.....Eqn.31}$$

$$IDT_{modulus} = \frac{\sigma_{Tensile}^{IDT}}{L_{Peak\ Load}} \quad \text{.....Eqn.32}$$

where:

$IDT_{strenght}$ = Tensile strength (kPa) determined from IDT test

P_{Peak} = Peak load (N)

t = Specimen thickness (mm)

D = Specimen diameter (mm)

$IDT_{modulus}$ = Ratio of tensile strength to displacement at peak load (MPa)

$\sigma_{Tensile}^{IDT}$ = IDT tensile strength (MPa)

$L_{Peak\ Load}$ = Displacement at the peak load (mm)

FI was also used in this study to assess the cracking resistance. This index is the fracture energy divided by the absolute value of the tangent of the slope of the post-peak inflection multiplied by a unit conversion

and scaling factor of 0.01 as shown in Equation 33. Hence, the FI was calculated in this study using the IDT test data, not a semicircular notched sample.

$$\mathrm{FI\ (IDT)} = 0.01 \times \frac{G_{\mathrm{Fracture}}^{\mathrm{Total}}}{\left|m_{\mathrm{Inflection}}^{\mathrm{Post-peak}}\right|}$$

……Eqn.33

where:

$G_{\mathrm{Fracture}}^{\mathrm{Total}}$ = Total fracture energy (J/m^2)

$m_{\mathrm{Inflection}}^{\mathrm{Post-peak}}$ = Post-peak inflection point

Cracking Resistance of Mixes with RAP Source No. 1

Mixtures prepared with the first source of RAP (RAP No. 1) at different RAP contents (0 percent, 25 percent, 50 percent) and using different binder grades (PG 58-34, PG 64-28, PG 76-22) were used to examine the effect of RAP content and binder grade on cracking resistance indicators (i.e., IDEAL-CT_{index}, $Weibull_{CRI}$, FI, CRI, N_{flex}, $IDT_{strength}$, $IDT_{Modulus}$, and G_f). These mixtures were prepared at an OBC of 5.0 percent. Figure 96 shows the IDEAL-CT_{index} results. Two thresholds were included on Figure 96 (i.e., 26.4 and 73.7). RP 261 suggested that mixes with IDEAL-CT_{index} greater than 73.7 to have good resistance to cracking, while mixtures with IDEAL-CT_{index} less than 26.4 to exhibit poor resistance to cracking. Mixtures with IDEAL-CT_{index} between 26.4 to 73.7 to show fair resistance to cracking; however, it is recommended to have higher IDEAL-CT_{index} (greater than 73.7) to ensure good cracking resistance.

Figure 96a shows the IDEAL-CT_{index} results for the test mixes. All mixes had higher IDEAL-CT_{index} (greater than 73.7) which means that all the mixtures are expected to exhibit good resistance to cracking. These results demonstrate that mixtures can utilize up to 50 percent of RAP No. 1 and still have good cracking resistance. However, this is not the case for mixtures prepared with RAP No. 2 as discussed in the next section. The results also showed that for PG 58-34 mixtures, 25 percent RAP and 50 percent RAP provided comparable IDEAL-CT_{index} results to those of the control mixture (0 percent RAP) and there was no statistically significant difference in the results. For PG 64-28 mixtures, 50 percent RAP provided higher IDEAL-CT_{index} compared to 0 percent and 25 percent RAP and there was a statistically significant difference in the results. For PG 76-22, mixtures with 50 percent and 25 percent RAP provided lower IDEAL-CT_{index} compared to 0 percent RAP content, and the difference was statistically significant between 0 percent and 25 percent RAP content. The adverse effect of RAP in mixes with PG 76-22 binder could be attributed to the use of a stiffer binder (PG 76-22). Overall, there is no consistent trend for the effect of RAP content on cracking resistance for all binder grades using the IDEAL-CT_{index} as indicator. Also, the results showed

that there was no clear trend or significant effect of binder grade at different RAP contents on the IDEAL-CT_{index} results as shown in Figure 96b.

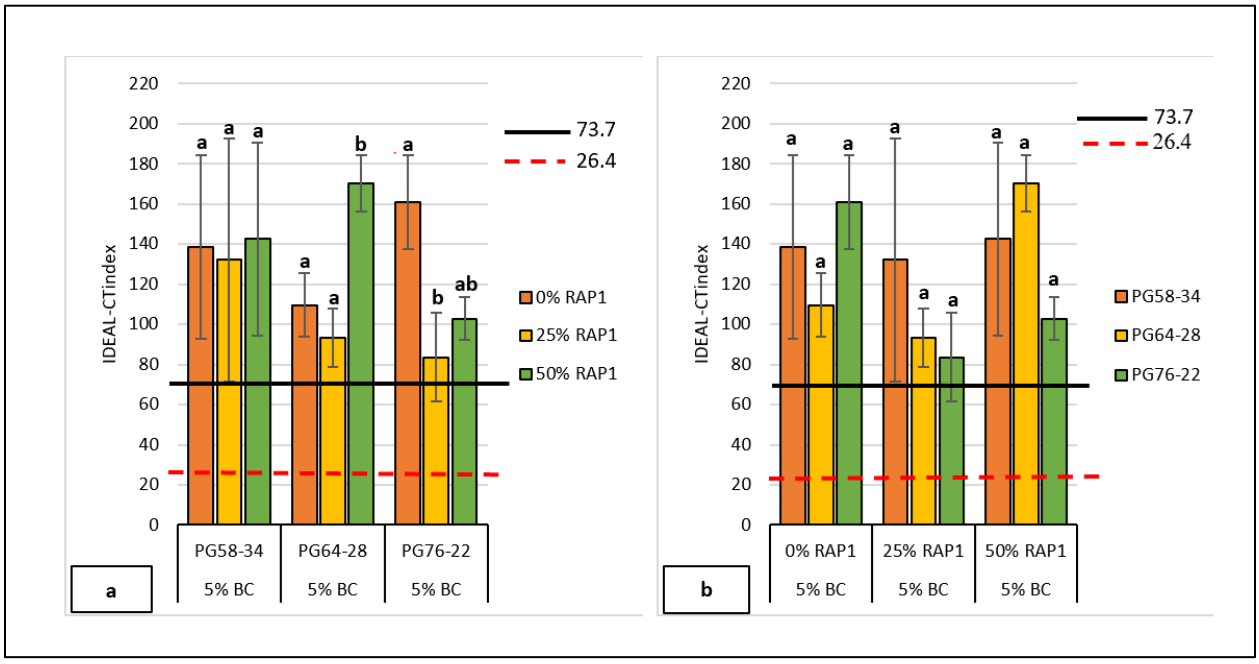

Figure 96. Effect of Binder Grade and RAP Content on IDEAL-CT_{Index}

Figure 97 illustrates the results of $Weibull_{CRI}$ at the OBC (5.0 percent) for mixes with three RAP contents and three binder grades. For PG 58-34 mixtures, 50 percent RAP provided higher $Weibull_{CRI}$ followed by 25 percent RAP then 0 percent RAP. However, there was no statistically significant difference in the results at various RAP contents. For PG 64-28, mixes with 0 percent and 25 percent RAP content had relatively comparable $Weibull_{CRI}$ while mixes with 50 percent RAP provided higher $Weibull_{CRI}$ than those with 0 percent and 25 percent RAP content, and the difference was statistically significant. Like IDEAL-CT_{index} results, for PG 76-22 mixtures, mixes with 25 percent and 50 percent RAP content had lower $Weibull_{CRI}$ compared to the control mixture (0 percent RAP), but the values were not not statistically significant different. Overall, all mixtures at different RAP contents and binder grades had $Weibull_{CRI}$ above 4.70 which indicates good cracking resistance. Also, similar to IDEAL-CT_{index}, there was no clear trend or significant effect for the effect of binder grade at different RAP contents on the $Weibull_{CRI}$ results as shown in Figure 97b.

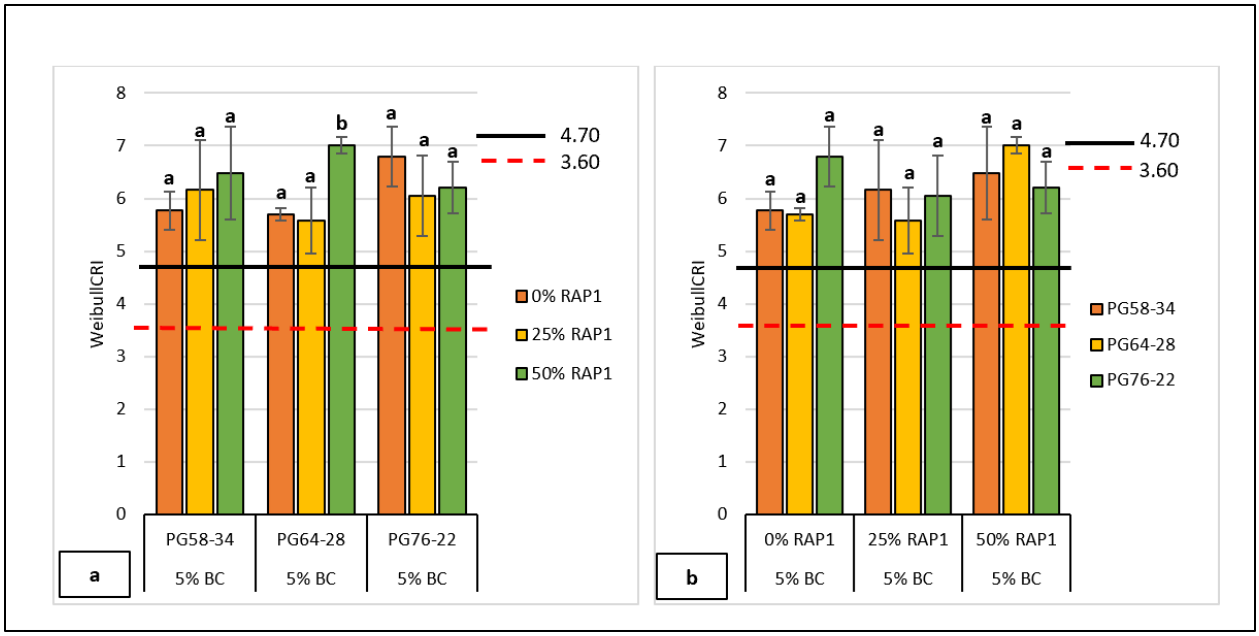

Figure 97. Effect of Binder Grade and RAP Content on $Weibull_{CRI}$

Figure 98 through 99 show the FI and N_{flex} results, respectively. All mixtures are expected to provide good cracking resistance since the FI and N_{flex} values were both above the indicator thresholds for good cracking performance. Like the IDEAL-CT_{index} and $Weibull_{CRI}$, there was no consistent trend for the effect of RAP content and binder grade on the results. Also, there was no statistically significant effect of the RAP content on FI and N_{flex} for PG 58-34 mixtures. While mixtures prepared with 50 percent RAP content provided higher FI and N_{flex} compared to those with 0 percent and 25 percent RAP content, and the difference was statistically significant for PG 64-28. For PG 76-22, mixtures 25 percent RAP content provided lower FI and N_{flex} compared to mixes with 0 percent and 50 percent RAP content, and the difference was significant for the FI results. Also, the results showed that there was no clear trend or significant effect for the binder grade on the FI and N_{flex} results.

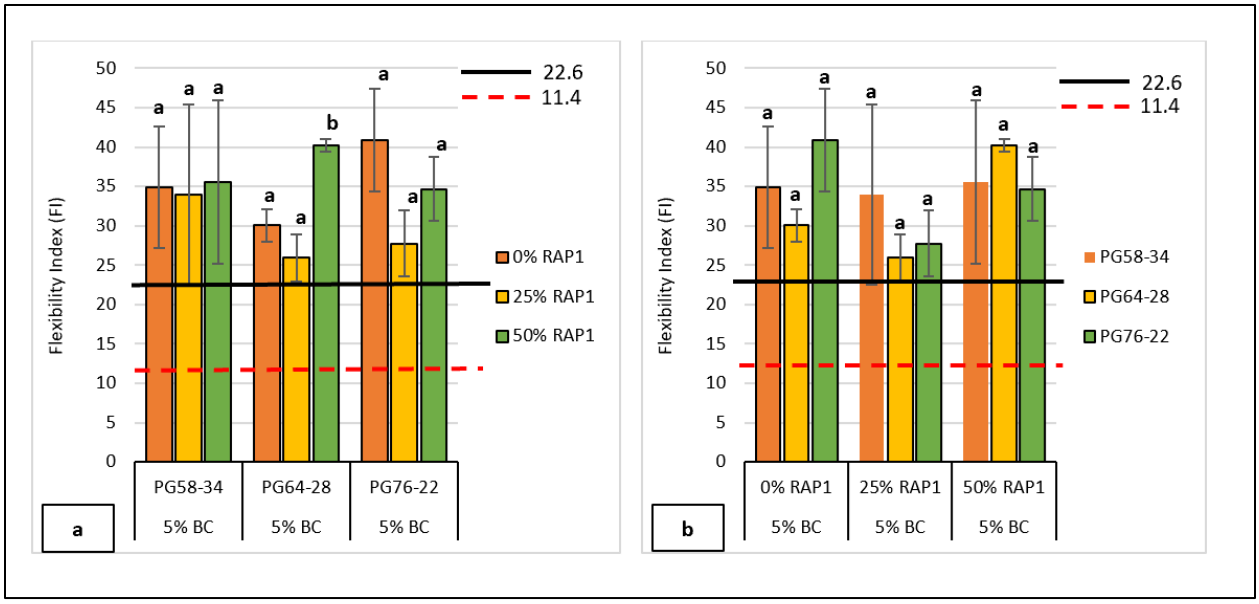

Figure 98. Effect of Binder Grade and RAP Content on FI

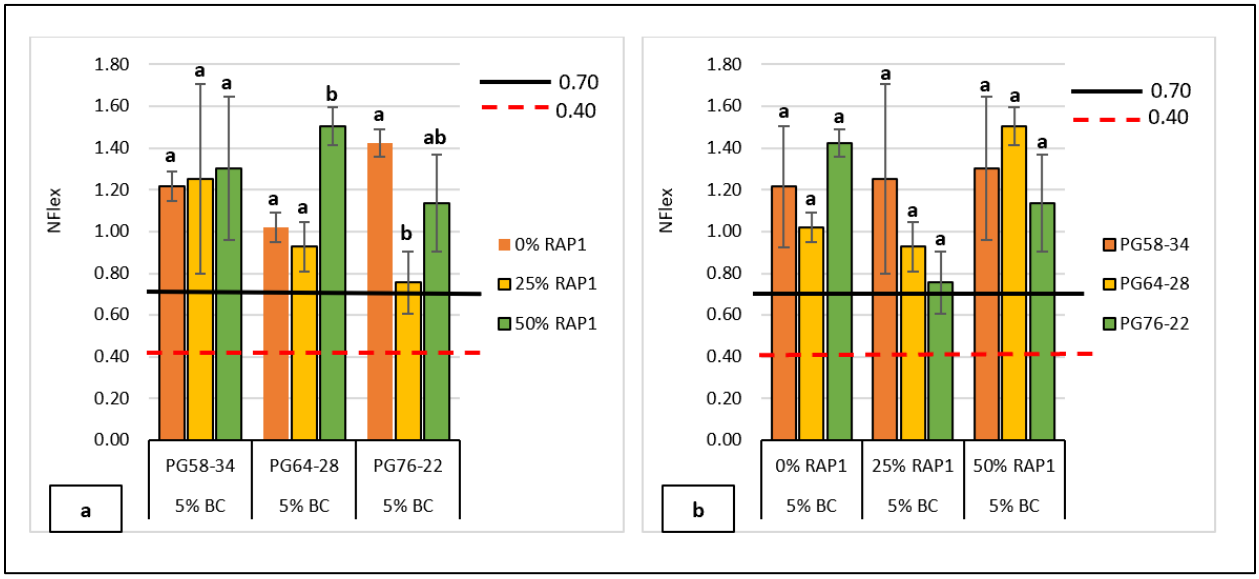

Figure 99. Effect of Binder Grade and RAP Content on N_{Flex}

Figure 100 shows the results of CRI for the test mixes. Some mixes are expected to provide fair cracking resistance (CRI between 614 and 466) (e.g., mixes with 0 percent RAP and 25 percent RAP content with PG 64-28; and mixes with 25 percent and 50 percent RAP content with PG 76-22). There was no statistically significant difference in the CRI results at different RAP contents except for mixes with 50 percent RAP using a PG 64-28 binder. Overall, this indicator was also less sensitive to the binder grade and RAP content.

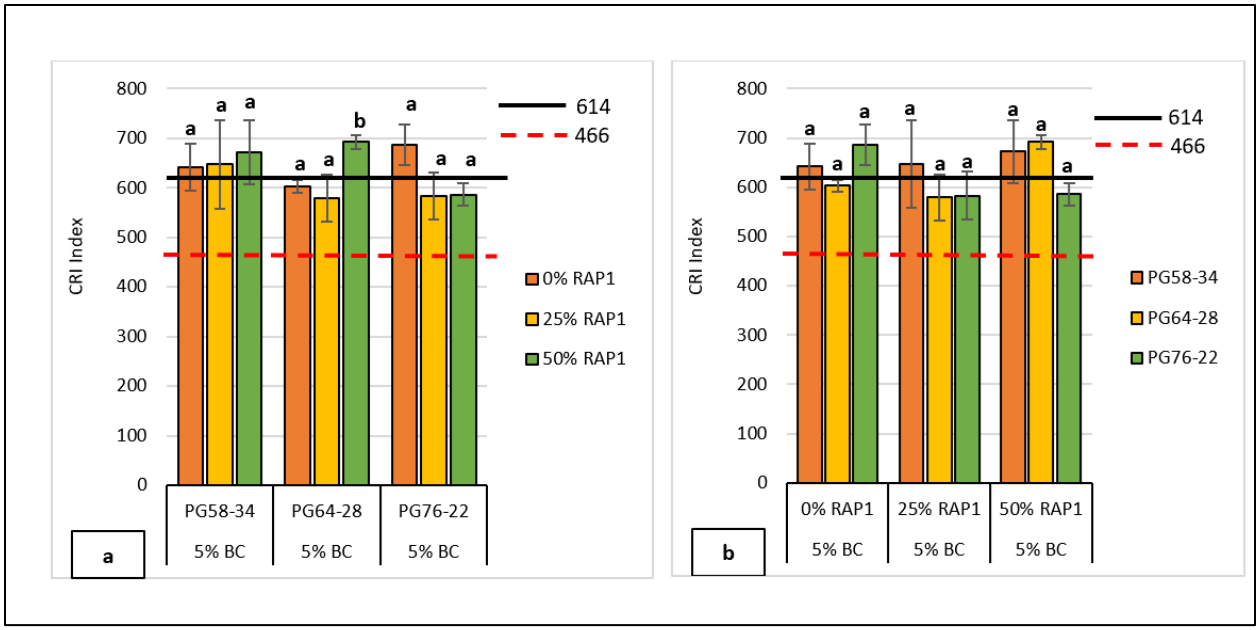

Figure 100. Effect of Binder Grade and RAP Content on CRI

Figure 101 shows the results of $IDT_{strength}$. IDT strength is a function of the peak load and the geometry of the test sample. Since the samples have the same diameter and height, the main variable of the calculated tensile strength is the maximum or peak load. The results demonstrated that mixes prepared with 25 percent and 50 percent RAP contents had higher $IDT_{strength}$ when compared to the control mixture (i.e., mix with 0 percent RAP content) and this difference was statistically significant. In addition, the results showed that mixtures prepared with PG 58-34 binder had lower $IDT_{strength}$ than mixes with either PG 64-28 or PG 76-22 binder at the corresponding RAP contents, and mixes with PG 76-22 binder had higher $IDT_{strength}$ when compared to mixes with PG 64-28 binder. The use of higher RAP content and stiffer binders required higher peak load to fracture the test samples.

Figures 102 and 103 show the results of $IDT_{modulus}$ and G_f, respectively. Like the $IDT_{strength}$, the same trend was also observed for $IDT_{modulus}$ and G_f. The $IDT_{modulus}$ and G_f increased with an increase in RAP content, at the same binder grade, and the value of these parameters was higher when a stiffer binder (i.e., PG 76-22) was used when compared to softer binders (e.g., PG 58-34). These three indicators (i.e., $IDT_{strength}$, $IDT_{modulus}$, and G_f) were more sensitive to the change in mix composition (e.g., RAP content and binder grade) and the results were more consistent compared to the other indicators (IDEAL-CT_{index}, $Weibull_{CRI}$, FI, CRI, N_{flex}). However, this is not necessarily related to cracking resistance based on the findings of RP 261 (Kassem et al. 2019).

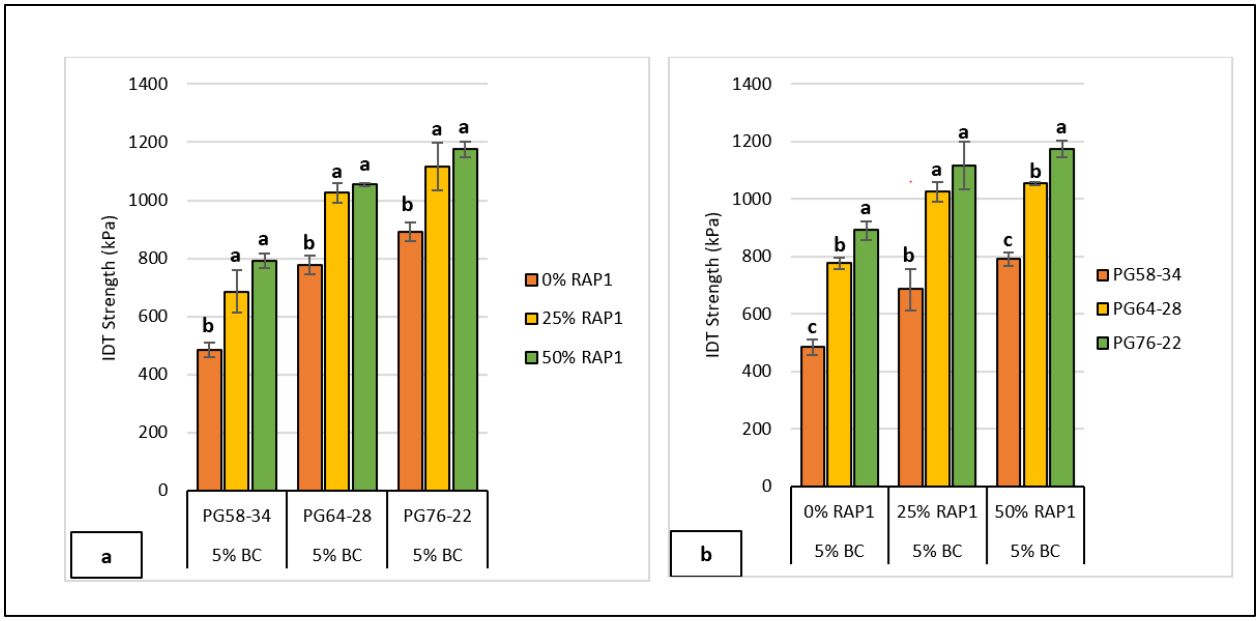

Figure 101. Effect of Binder Grade and RAP Content on $IDT_{Strength}$

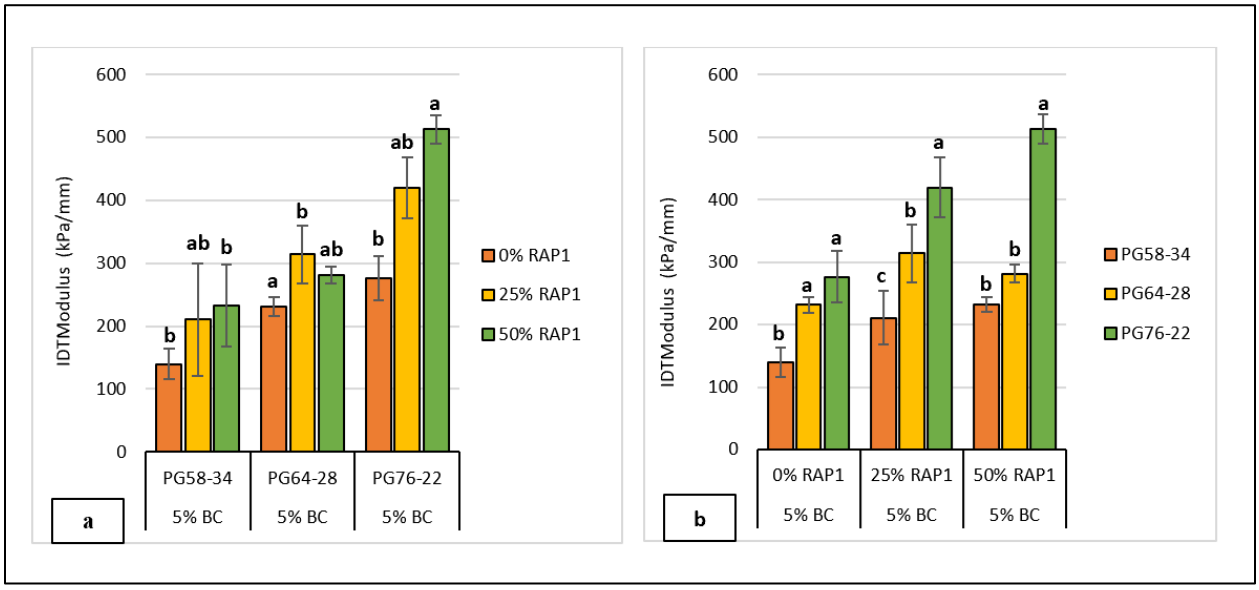

Figure 102. Effect of Binder Grade and RAP Content on $IDT_{Modulus}$

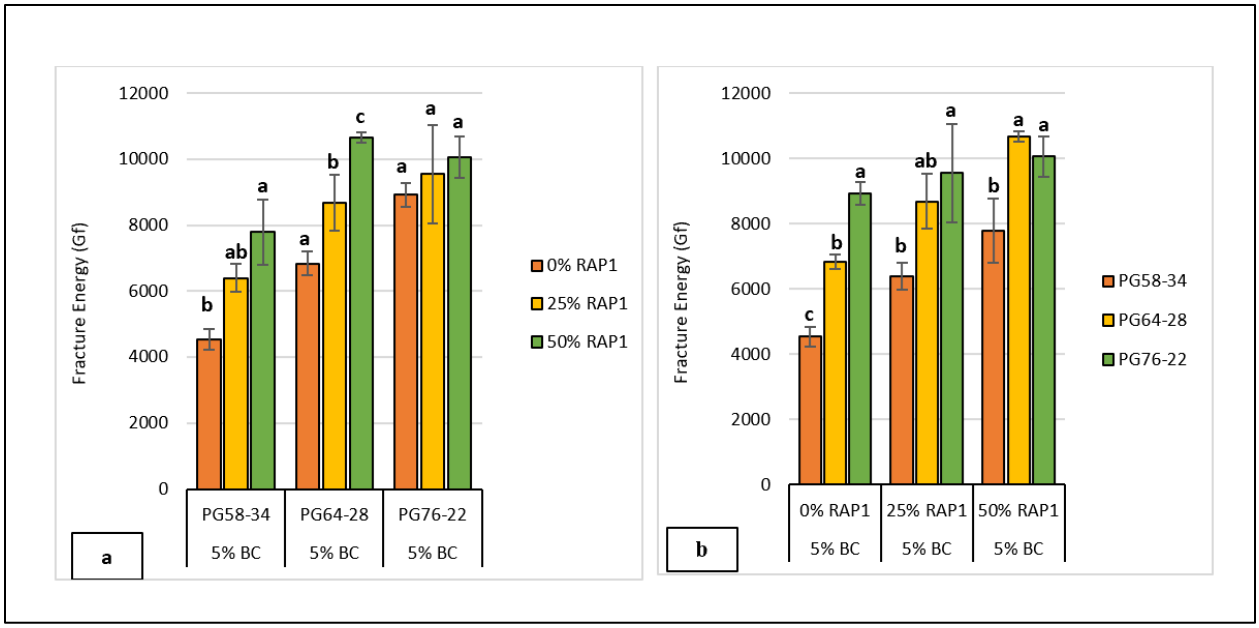

Figure 103. Effect of Binder Grade and RAP Content on Fracture Energy (G_f)

Cracking Resistance of Mixes with RAP Source No. 2

Test mixtures were prepared using the second source of RAP (RAP No. 2) at different RAP contents (0 percent, 25 percent, and 50 percent), and different binder contents (4.25 percent, 5.0 percent, and 5.75 percent). The same monotonic cracking resistance indicators (e.g., IDEAL-CT_{index}, $Weibull_{CRI}$, FI, CRI, N_{flex}, $IDT_{strength}$, $IDT_{Modulus}$, and G_f) were used to examine the effect of RAP and binder contents on cracking resistance.

Figure 104 shows the effect of binder content and RAP content on the IDEAL-CT_{index}. The results clearly demonstrate that the IDEAL-CT_{index} increased with binder content for all RAP contents, as expected. In addition, there was a statistically significant difference between 5.75 percent and both 4.25 percent and 5.0 percent binder contents. Higher IDEAL-CT_{index} is associated with improved cracking resistance. Also, the IDEAL-CT_{index} decreased with the increase in RAP content for all binder grades. Mixtures prepared using RAP No. 1 at different RAP contents did show such effect on IDEAL-CT_{index} as discussed earlier, and all mixtures prepared with RAP No. 1 had higher IDEAL-CT_{index}. These results suggested that RAP materials from source No. 2 could be more aged and stiffer when compared to the RAP materials from source No. 1 because of the reduced cracking resistance with increased RAP content.

Figure 104 also shows that mixtures with 0 percent RAP content and 5.75 percent binder content had the highest IDEAL-CT_{index} which indicates good cracking resistance, while mixture with 50 percent RAP at 4.25 percent binder content had the lowest IDEAL-CT_{index} which indicates poor cracking resistance. Mixes prepared with more binder provided good resistance to cracking when compared to mixtures prepared with less total binder, as expected. The results also illustrate that the cracking performance of mixtures prepared with RAP (up to 50 percent) can be improved by increasing the binder content. For example,

mixtures prepared with 50 percent RAP at OBC of 5.0 percent resulted in IDEAL-CT_{index} of 19 which indicates very poor cracking resistance while IDEAL-CT_{index} increased to 66 when the binder content was increased by 0.75 percent (i.e., 5.75 percent), which indicates a significant improvement in theresistance to cracking. Overall, the IDEAL-CT_{index} results were able to capture the change in binder content and RAP content in mixture prepared with RAP source No. 2.

Figure 105 illustrates the effect of the binder content and RAP content on $Weibull_{CRI}$. The results showed similar trends to IDEAL-CT_{index} where $Weibull_{CRI}$ increased with the increase in binder content and decrease in RAP content. The cracking resistance of mixtures with 25 percent and 50 percent RAP content can be improved by increasing the binder content (Figure 105a). Both $Weibull_{CRI}$ and IDEAL-CT_{index} were in good agreement in terms of cracking performance assessment of test mixtures, and $Weibull_{CRI}$ was also able to detect the change in binder content and RAP content for mixtures prepared with RAP source No. 2.

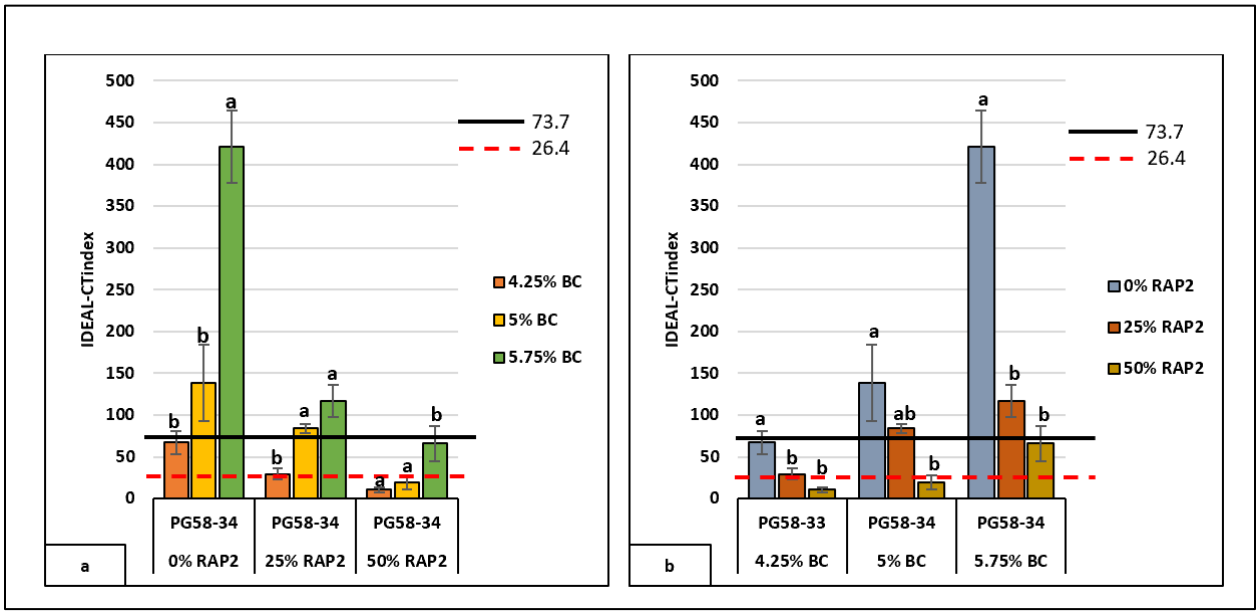

Figure 104. Effect of Binder Content and RAP Content on IDEAL-CT_{Index} for Mixes with RAP Source No. 2

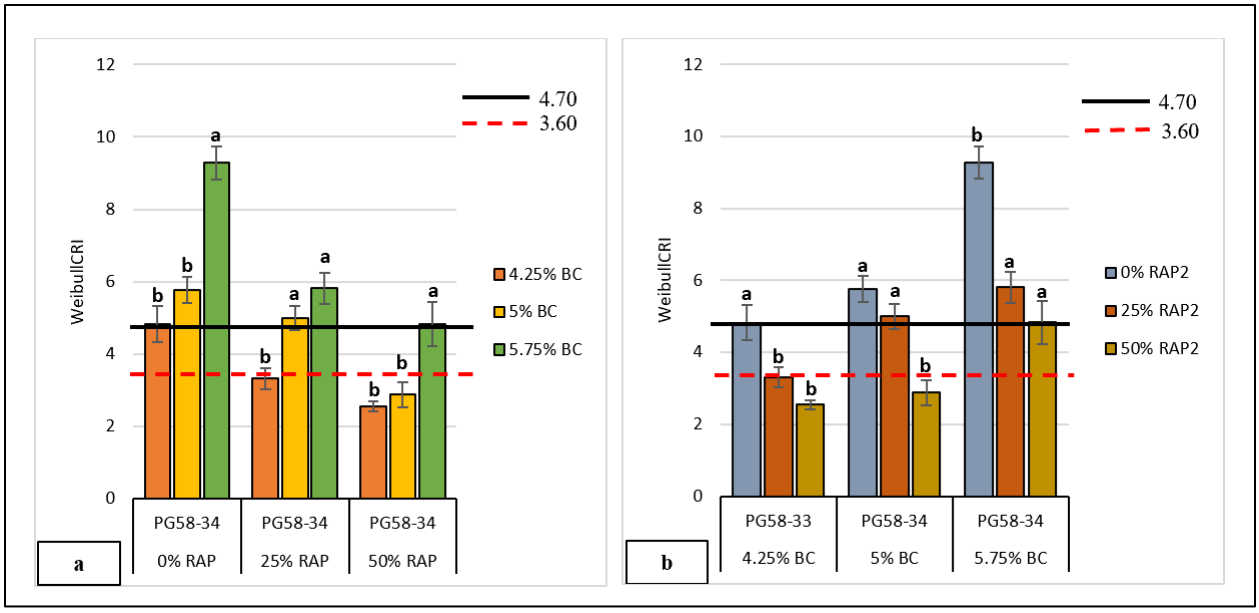

Figure 105. Effect of Binder Content and RAP Content on Weibull$_{CRI}$ for Mixes with RAP Source No. 2

Figures 106 through 108 show FI, CRI, and N_{Flex} results, respectively. The results of these cracking indicators showed the same trend as those of IDEAL-CT$_{index}$ and Weibull$_{CRI}$. The cracking resistance improved with the increase in binder content and decreased with the increase in RAP content. There was a statistically significant difference in the cracking performance using these indicators between mixtures with higher binder contents compared to mixtures with low binder contents at the corresponding RAP contents.

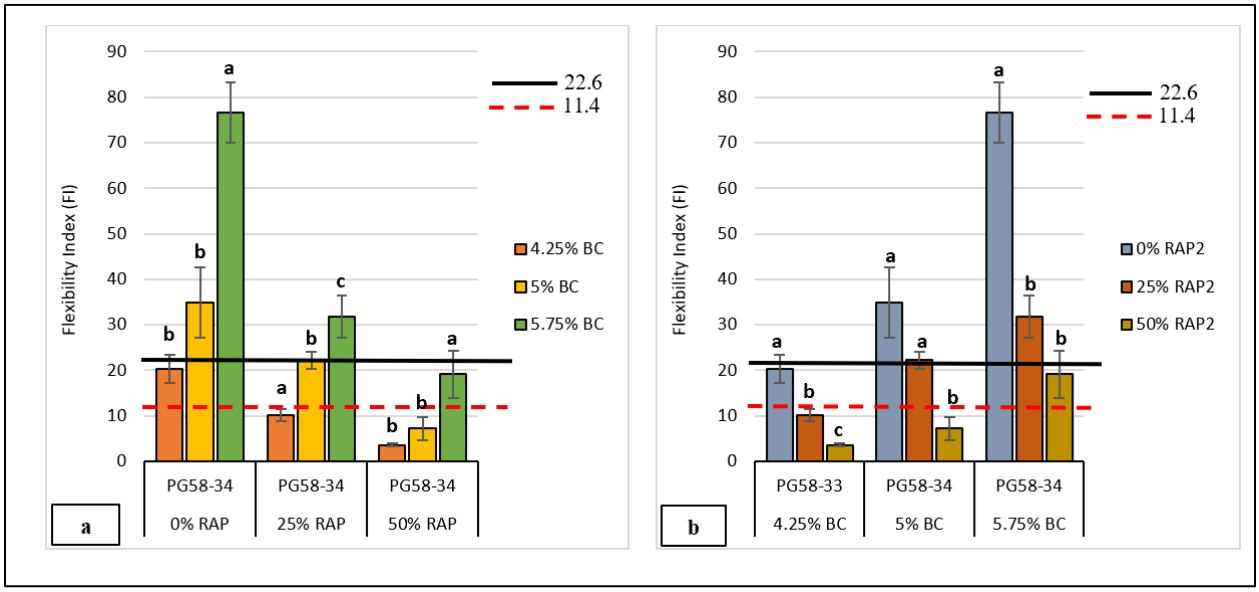

Figure 106. Effect of Binder Content and RAP Content on FI for Mixes with RAP Source No. 2

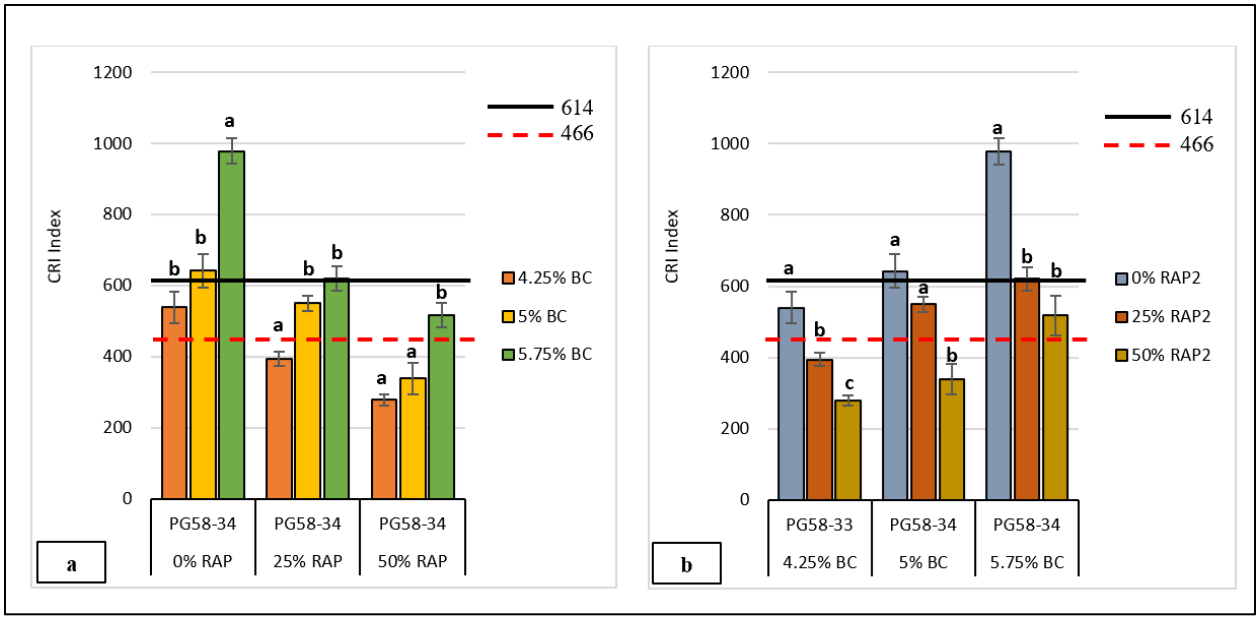

Figure 107. Effect of Binder Content and RAP Content on CRI for Mixes with RAP Source No. 2

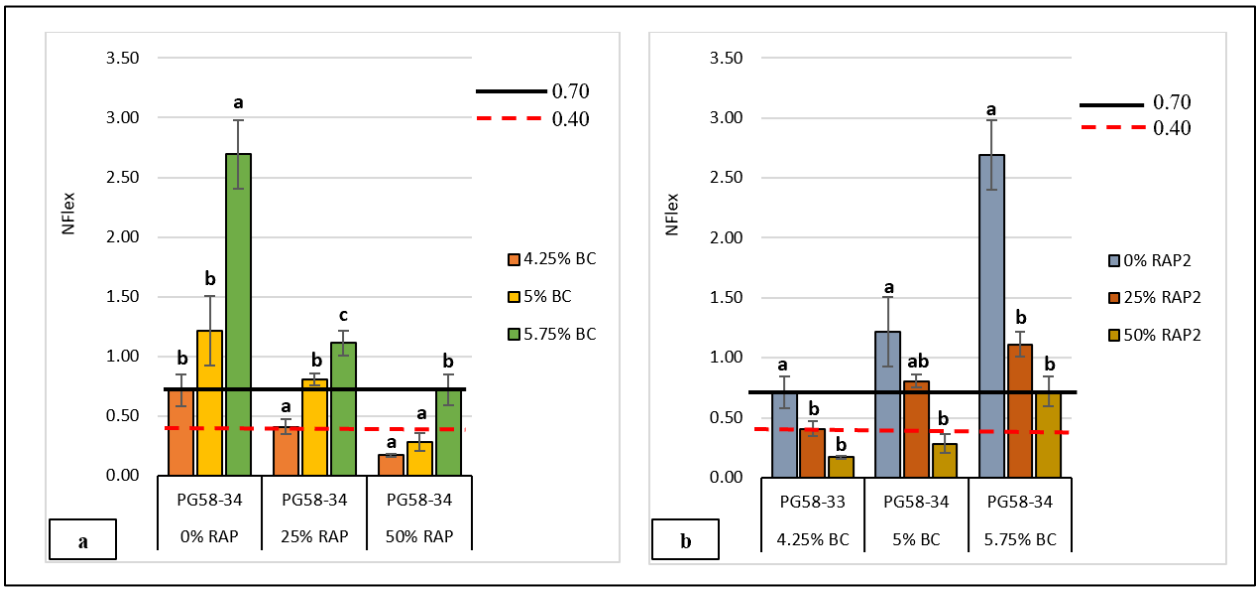

Figure 108. Effect of Binder Content and RAP Content on N_{Flex} for Mixes with RAP Source No. 2

Figure 109 shows the $IDT_{Strength}$ results. There was statistically significant difference in the $IDT_{Strength}$ results for all mixtures at different binder and RAP contents. The $IDT_{Strength}$ increased with the increase in RAP content, which indicates that mixes with higher RAP content become stiffer and brittle compared to the control mixtures (i.e., 0 percent RAP Content). In addition, the $IDT_{Strength}$ decreased with the increase in binder content. Similar to the findings of mixtures prepared using RAP source No. 1, the $IDT_{Strength}$ was able to capture the change in binder and RAP contents.

Figure 110 shows the $IDT_{Modulus}$ results $IDT_{Modulus}$ decreased with the increase in binder content and increased with the increase in RAP content. This is consistent with the $IDT_{Modulus}$ results shown in Figure 102 for mixtures prepared with RAP source No. 1. Stiffer mixtures had higher $IDT_{Modulus}$ results, and vice versa.

Figure 111 shows that the G_f did not exhibit a consistent trend with respect to binder content, and there was no statistically significant difference in most of the results. The fracture energy is the area under the load-displacement curve, the change in the peak load (maximum load) due to the change binder content could be associated with change in deformation which results in a small net variation in fracture energy. Therefore, the G_f is not an appropriate parameter to capture the change in binder content. Figure 111b illustrates the effect of RAP content on the G_f. The results showed that at 4.25 percent and 5.75 percent binder content, the G_f increased with the increase in RAP content, but it did not show a consistent trend at 5.0 percent binder content.

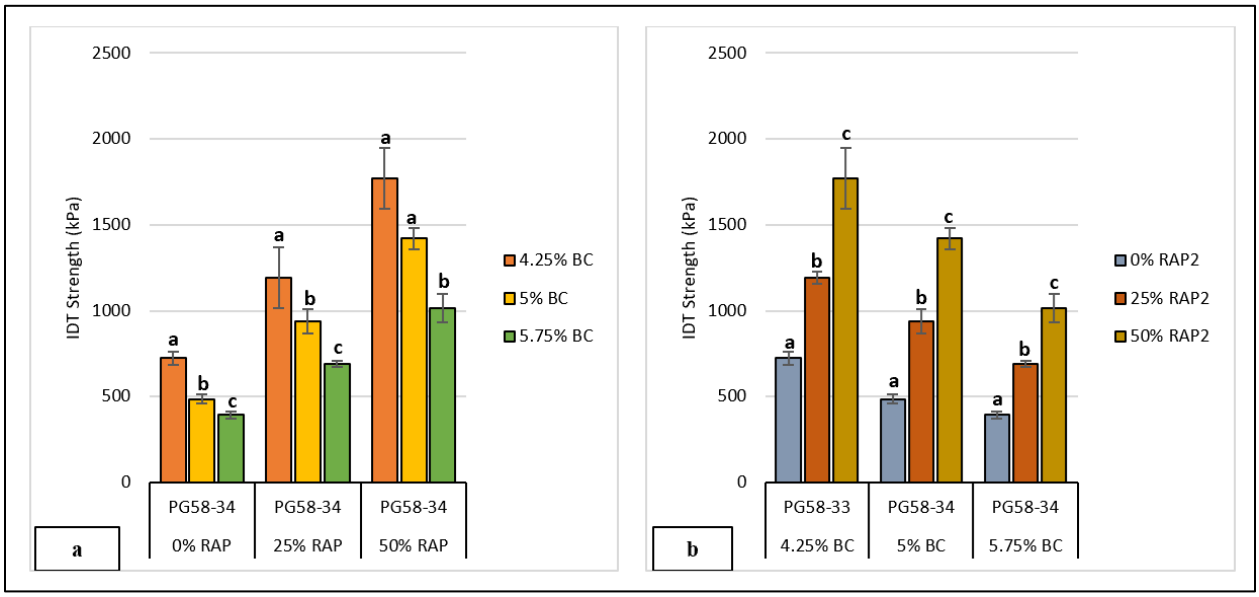

Figure 109. Effect of Binder Content and RAP Content on $IDT_{Strength}$ for Mixes with RAP Source No. 2

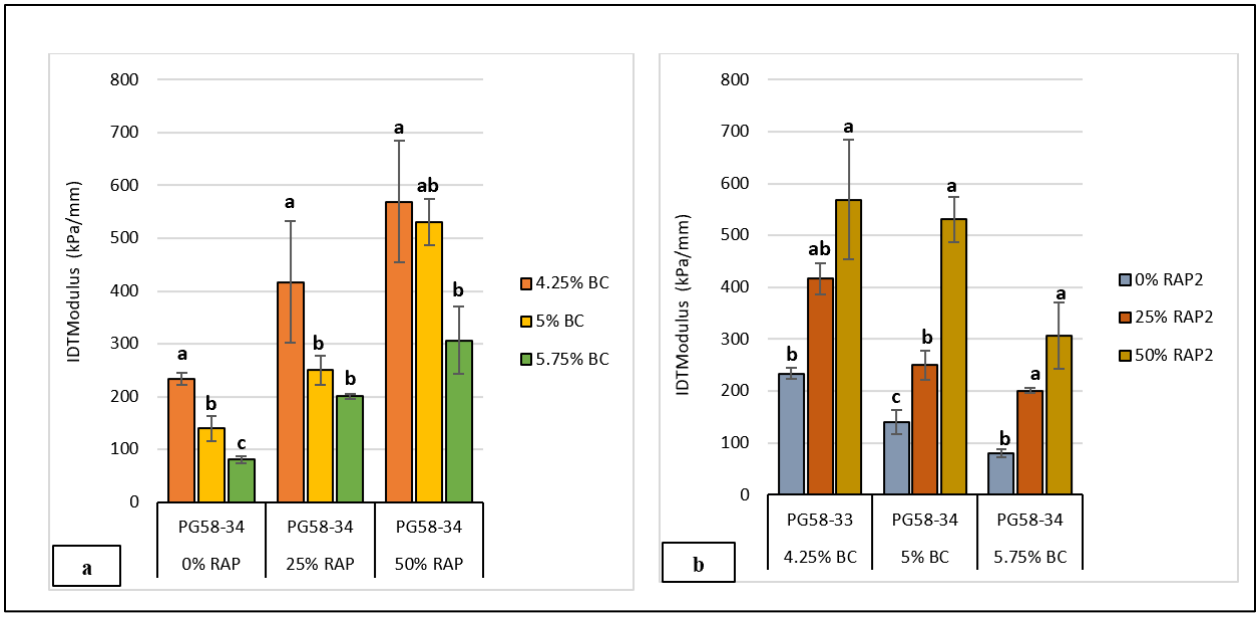

Figure 110. Effect of Binder Content and RAP Content on $IDT_{Modulus}$ for Mixes with RAP Source No. 2

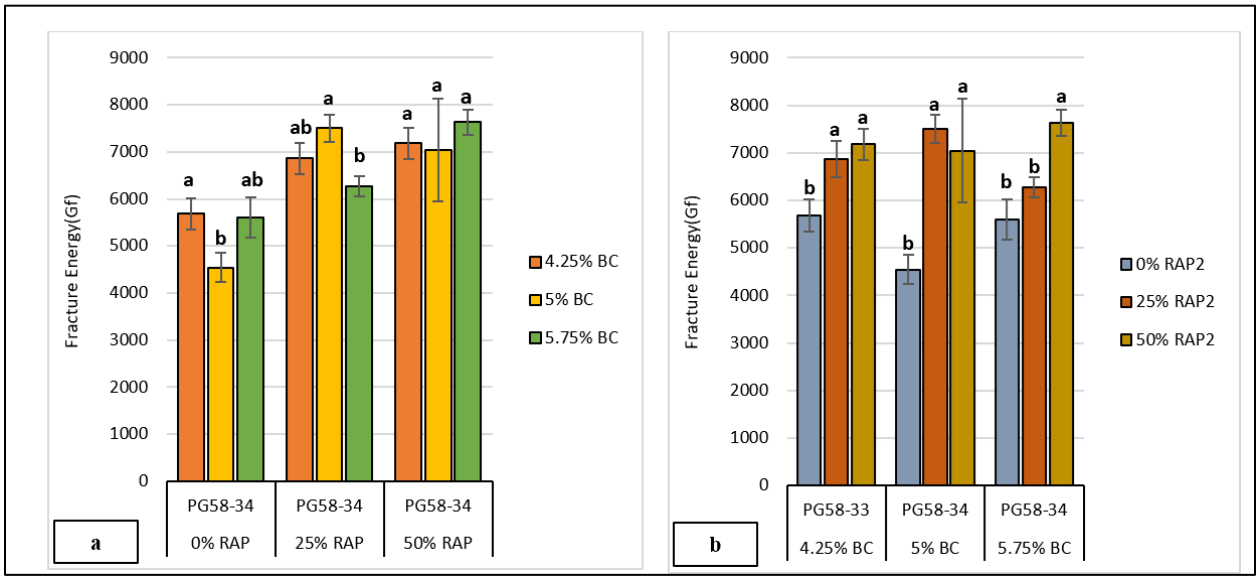

Figure 111. Effect of Binder Content and RAP Content on G_f for Mixes with RAP Source No. 2

Effect of Aggregate Type

The researchers evaluated mixtures prepared with another type of aggregate (i.e., river gravel). These mixtures were prepared using the RAP source No. 2 at three different RAP contents (0 percent, 25 percent, and 50 percent) and at OBC of 5.0 percent. The results of various cracking indicators were compared to those of basalt mixtures at the same binder and RAP contents.

Figure 112 shows the results for the IDEAL-CT_{index} for mixtures prepared with river gravel and basalt at different RAP contents. For the river gravel mixtures, the IDEAL-CT_{index} decreased with the increase in RAP content, which in agreement with the results of IDEAL-CT_{index} for mixtures prepared with basalt aggregates. In addition, the results demonstrated that mixtures with basalt had better cracking resistance at 0 percent and 25 percent RAP contents when compared to mixtures with river gravel. This could be attributed to strong interlocking between the particles for the basalt rock as compared to river gravel. Also, regardless of aggregate type, mixtures with 50 percent RAP showed poor cracking resistance (i.e., low IDEAL-CT_{index} values). Similar findings were observed for the other cracking indicators including $Weibull_{CRI}$, FI, CRI, and N_{flex} as presented Appendix C.

Figure 113 illustrates the results of the $IDT_{Strength}$. The $IDT_{Strength}$ increased with the increase in RAP content for both river gravel and basalt mixtures. Higher $IDT_{Strength}$ values indicate stiffer mixtures. There was a statistically significant difference in $IDT_{Strength}$ results at different RAP contents for basalt; however, there was no statistically significant difference between 25 percent and 50 percent RAP for the river gravel mixtures. Also, overall, the mixtures prepared with river gravel had higher $IDT_{Strength}$ compared to basalt at 0 percent and 25 percent RAP, while the $IDT_{Strength}$ results were comparable for both river gravel and basalt at 50 percent RAP content. Similar observations to those of $IDT_{Strength}$ were found for $IDT_{modulus}$ and G_f as presented in Appendix C.

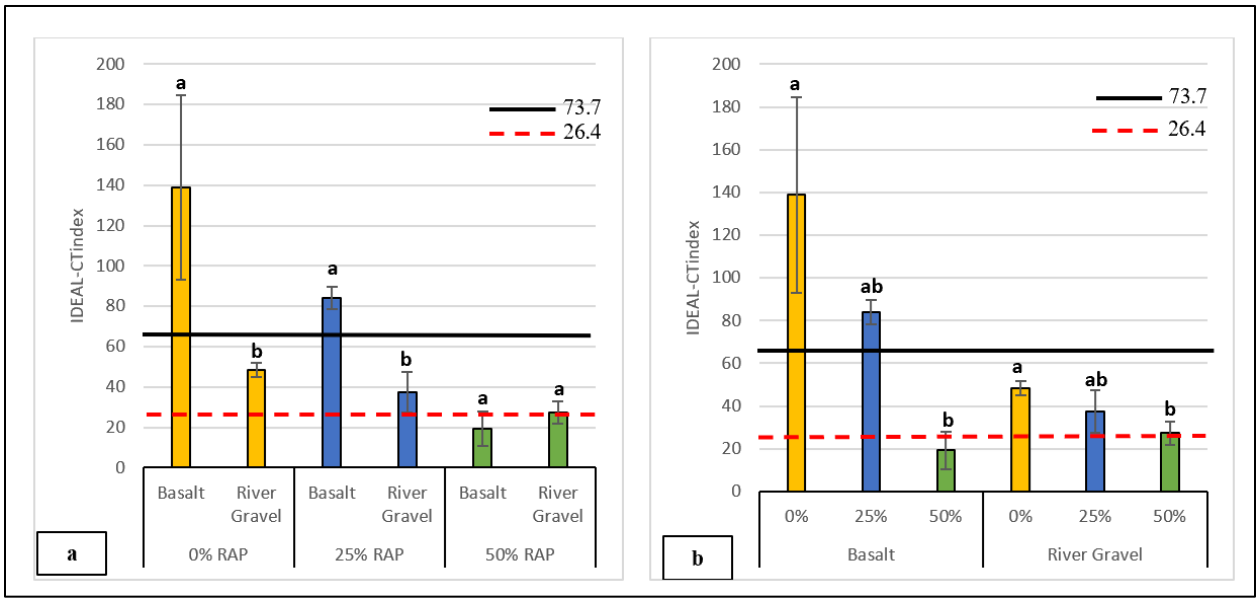

Figure 112. Effect of Aggregate Type on IDEAL-CT_{Index} for Mixes with RAP Source No. 2

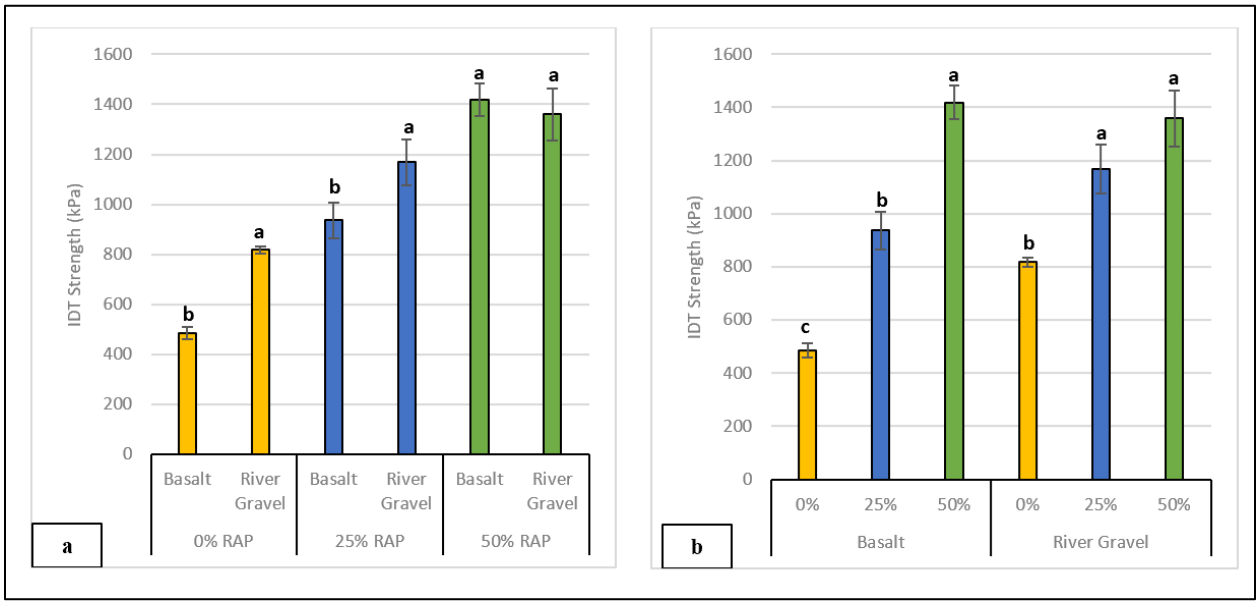

Figure 113. Effect of Aggregate Type on $IDT_{Strength}$ for Mixes with RAP Source No. 2

Evaluation of Cracking Resistance of Field Mixes

The researchers tested six PMLC mixes collected from new ITD paving projects distributed across the state as discussed in Chapter 3. Three batches were tested from each PMLC mixes to assess the variability in mix performance during production. Three batches (i.e., Batch No. 1, Batch No. 2, Batch No. 3) of loose mixes from each project were sampled throughout construction. A total of 54 PMLC samples (6 projects x 3 batches x 3 replicates) were prepared and tested in the laboratory to assess the cracking resistance. Several monotonic cracking indicators including IDEAL-CT_{Index}, $Weibull_{CRI}$, CRI, N_{flex}, FI, $IDT_{strength}$, $IDT_{modulus}$, and G_f were calculated. This section highlights the main findings of cracking resistance evaluation of PMLC mixes.

Figure 114 shows the IDEAL-CT_{Index} of the PMLC Mixes. The results demonstrate that there were some variations in the cracking resistance among project batches and in some cases such variation was statistically significant. For example, there was a statistically significant difference between Batch No. 1 and Batch No. 3 of D1-P1 project; Batch No. 3 versus both Batch No. 1 and Batch No. 2 of D3-P5 project; Batch No. 2 versus Batch No. 3 of D6-P1 project; Batch No. 2 versus both Batch No. 1 and Batch No. 3 of D1-P2 project; Batch No. 1 versus both Batch No. 2 and Batch No. 3 of D4-P1 project. Only one project (i.e., D4-P2) had no statistically significant difference in the IDEAL-CT_{Index} results between the three batches. The variation of IDEAL-CT_{Index} could be an indication of change in mix properties due to segregation or change in mix production. In addition, the results demonstrated that all batches of D1-P1, D1-P2, and D4-P2 projects showed good cracking resistance. D4-P2 had the highest average IDEAL-CT_{Index}, based on the three batches, compared to other projects. This could be due to the higher binder content (6.2 percent) and lower RAP content (17 percent) used in D4-P2. Higher binder content improves the

cracking resistance based on the LMLC results discussed earlier in this Chapter. D1-P1 and D1-P2 projects had 30 percent RAP content with binder content of 5.2 percent and 5.3 percent, respectively. All three batches of D3-P5 showed moderate cracking resistance (IDEAL-CT_{Index} between 73.7 and 26.4 based on the thresholds proposed by Kassem at al. [2019] in RP 261). This mix had 0 percent RAP and 5.4 percent binder content, but the researchers noticed that it was relatively dry during compaction, and this could be due to large quantity of fines (percent passing Sieve No. 200) in the mix. Also, the results of Figure 114 shows that there was a statistically significant difference among PMLC from the various field projects. For example, there was a statistically significant difference between D4-P2 versus D4-P1, D6-P1, D3-P5, and D1-P1; and D1-P2 versus D3-P5 and D4-P1.

The results of various compaction and stability indices, discussed in Chapter 4, demonstrated that Batch No. 2 of D1-P2 and Batch No. 1 of D4-P1 to require less energy to achieve 92 percent Gmm (less CDI values). In addition, the GS showed that these batches to have low GS compared to other batches in the project. Furthermore, these batches had higher LCI (easy to compact) compared to other batches. The variation in compaction and stability indices of these batches were also well captured and reflected in the IDEAL-CT_{Index} results.

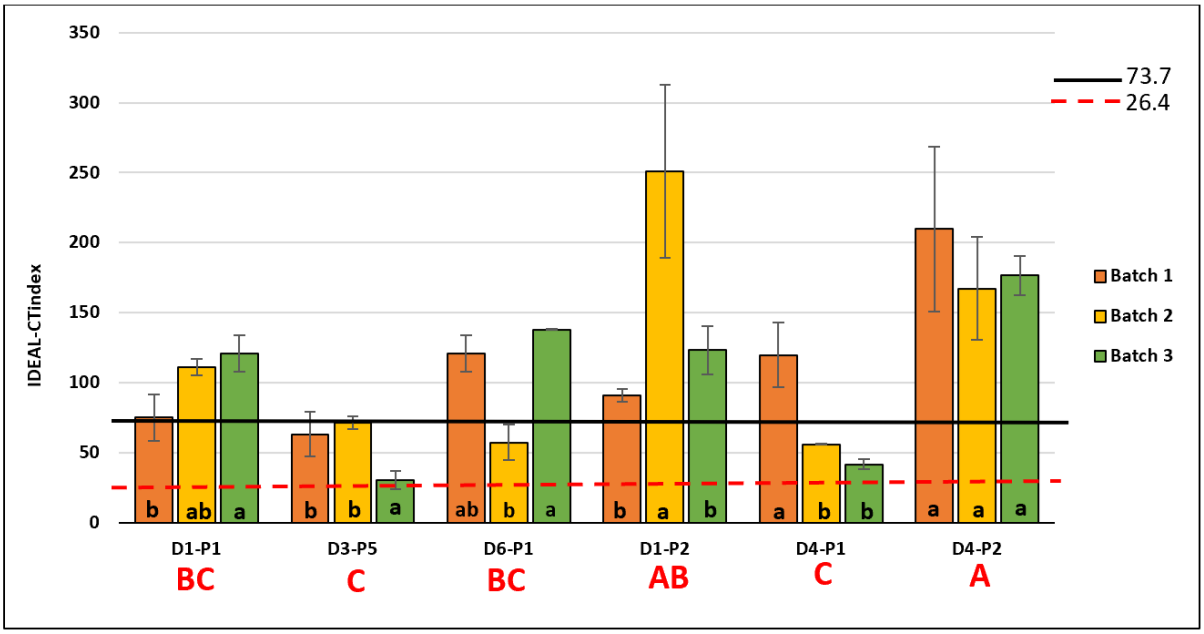

Figure 114. IDEAL-CT_{Index} of PMLC Mixes

Figure 115 shows the $Weibull_{CRI}$ results. The results showed that all batches of D1-P1, D1-P2, and D4-P2 to have good cracking resistance ($Weibull_{CRI}$ above 4.70), while all batches of D3-P5 are within moderate cracking resistance ($Weibull_{CRI}$ between 3.60 and 4.70 based on the thresholds proposed by Kassem at al. [2019] in RP 261). It is recommended that asphalt mixtures to have $Weibull_{CRI}$ of 4.70 and higher to ensure good cracking resistance. Also, D4-P2 had the highest average $Weibull_{CRI}$, based on all three batches, compared to other projects which could be due to the higher binder content of 6.2 percent in this mix. Overall, there was very good agreement between $Weibull_{CRI}$ and IDEAL-CT_{Index} in terms of evaluation of

cracking resistance of PMLC mixes. However, IDEAL-CT_{index} classified the mixes into three different statistical groups (A, B, and C), while $Weibull_{CRI}$ classified the PMLC mixes into four statistical groups (A, B, C, and D), as can be seen in Figures 114 and 115, respectively. This is due the higher variation in the test results of IDEAL-CT_{index} compared to $Weibull_{CRI}$, as discussed later in this chapter. Higher number of statistical groups provides the ability to distinguish between more mixes in terms of cracking resistance.

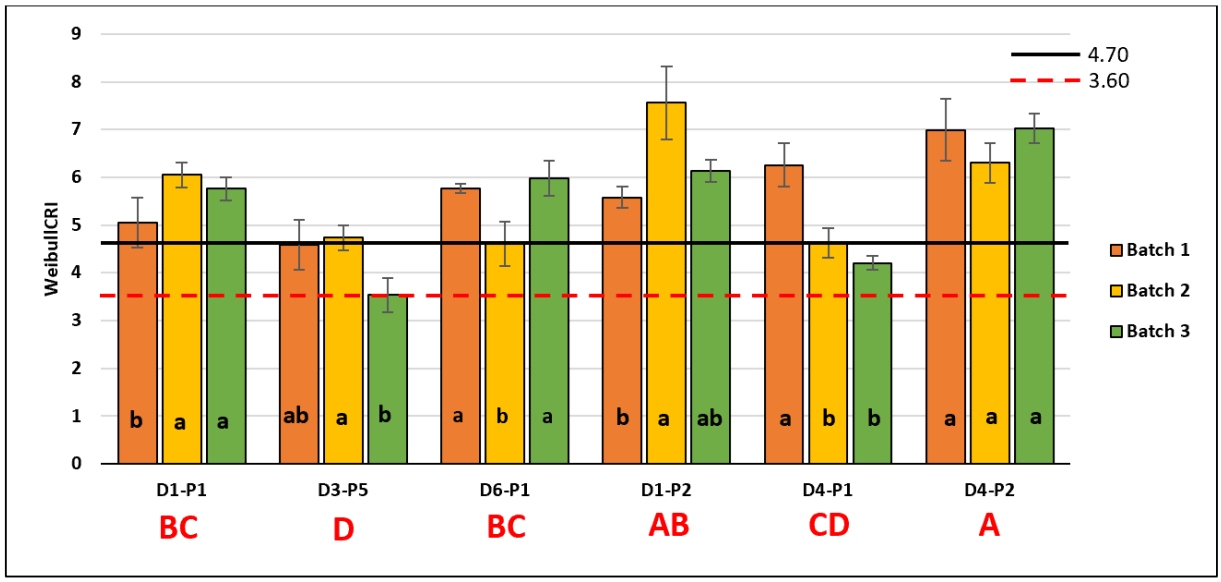

Figure 115. $Weibull_{CRI}$ of PMLC Mixes

Similar observations can be made from the results of FI, CRI, and N_{Flex} shown in Figures 116, 117, and 118, respectively. The results confirmed that some of the batches had different cracking resistance within the same field project, and the difference was statistically significant in some cases. Also, D4-P2 and D3-P5 should exhibit good cracking resistance and poor cracking resistance in the field, respectively, which supports the the findings obtained with of $Weibull_{CRI}$ and IDEAL-CT_{Index} parameters. Overall, similar trends were observed using the FI, CRI, and N_{Flex} cracking indicators compared to both $Weibull_{CRI}$ and IDEAL-CT_{Index}.

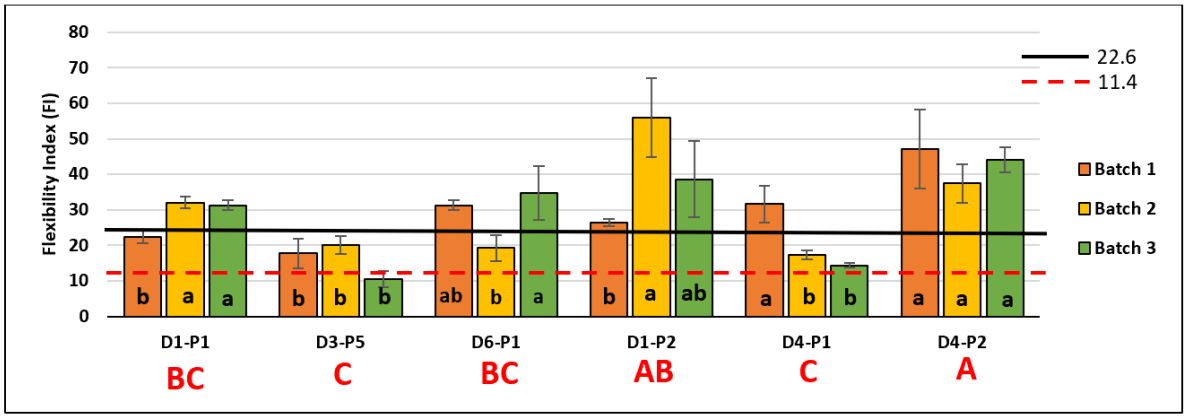

Figure 116. FI of PMLC Mixes

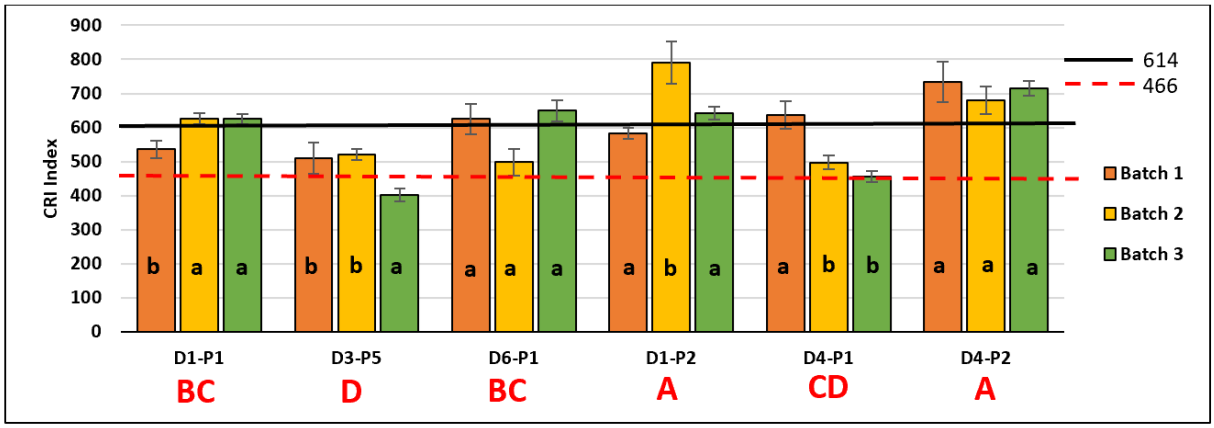

Figure 117. CRI of PMLC Mixes

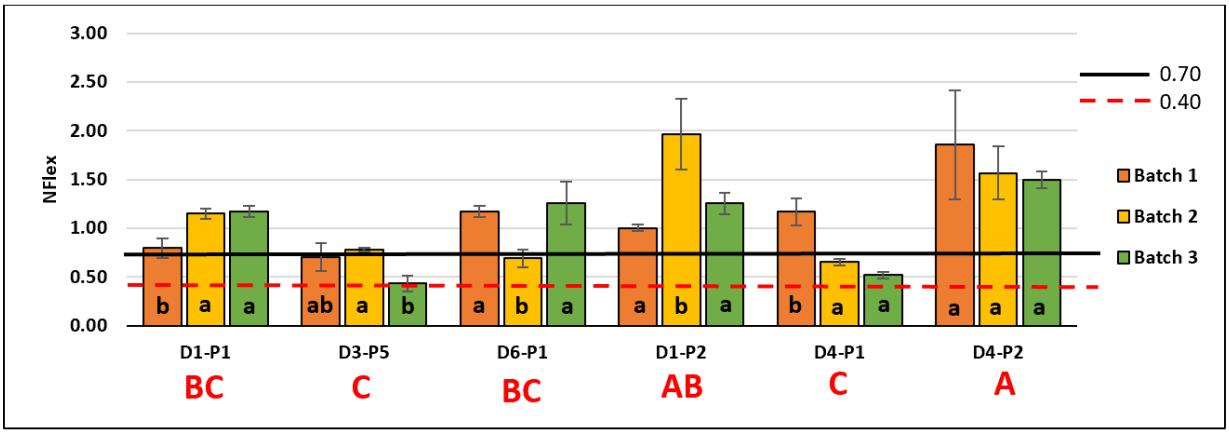

Figure 118. N_{Flex} of PMLC Mixes

Figure 119 shows the $IDT_{Strength}$ results of PMLC mixes. There was a statistically significant difference in $IDT_{Strength}$ results among different batches in some of the field projects (e.g., D1-P1, D3-P5, D6-P1, D1-P2). PMLC mixes from two projects (D4-P1 and D4-P2) had the highest average IDT strength when compared to PMLC mixes from other field projects mainly due to a stiffer binder grade (i.e., PG70-28) used in the mix. Overall, the $IDT_{Strength}$ was sensitive to the change in the binder grade and mix composition. The $IDT_{Strength}$ classified the mixes into two different statistical groups (A and B) only, which indicates that there was no significant difference in $IDT_{Strength}$ results given the variability in results among batches within the same project.

Figures 120 and 121 show the G_f and $IDT_{Modulus}$, respectively. D4-P1 had the highest G_f compared to other PMLC mixes due the use of PG 76-28 binder in this project, while other field projects used softer binder grades. $IDT_{Modulus}$ results illustrated that D4-P1 and D3-P5 had a significant difference in strength compared to D1-P1, D6-P1, D1-P2, and D4-P2 which agrees with $IDT_{Strength}$ results. Overall, there was some differences in G_f and $IDT_{Modulus}$ results among different batches within the same field project.

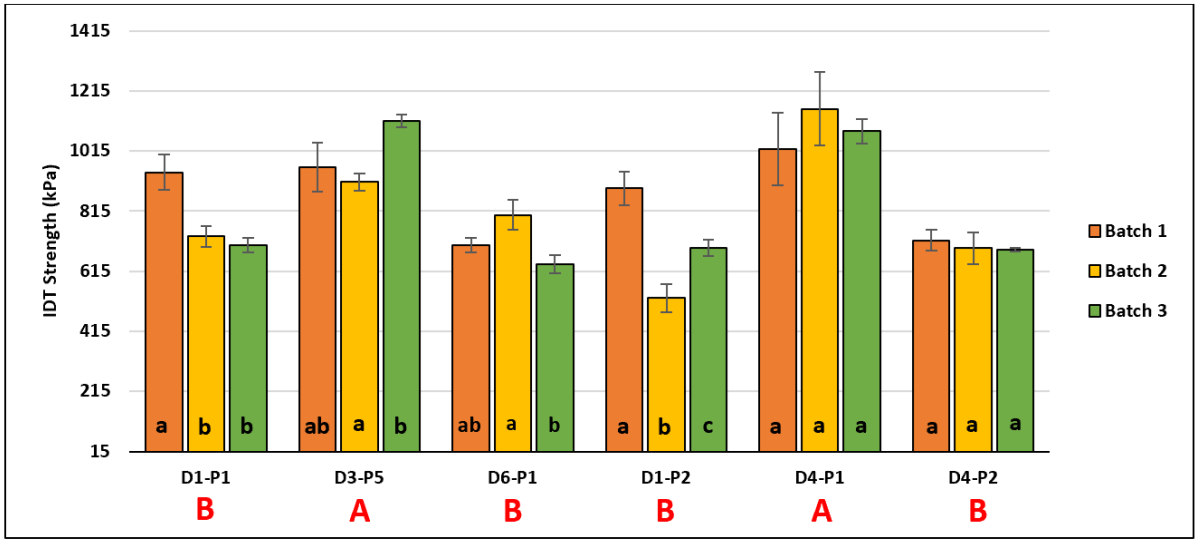

Figure 119. $IDT_{Strength}$ of PMLC Mixes

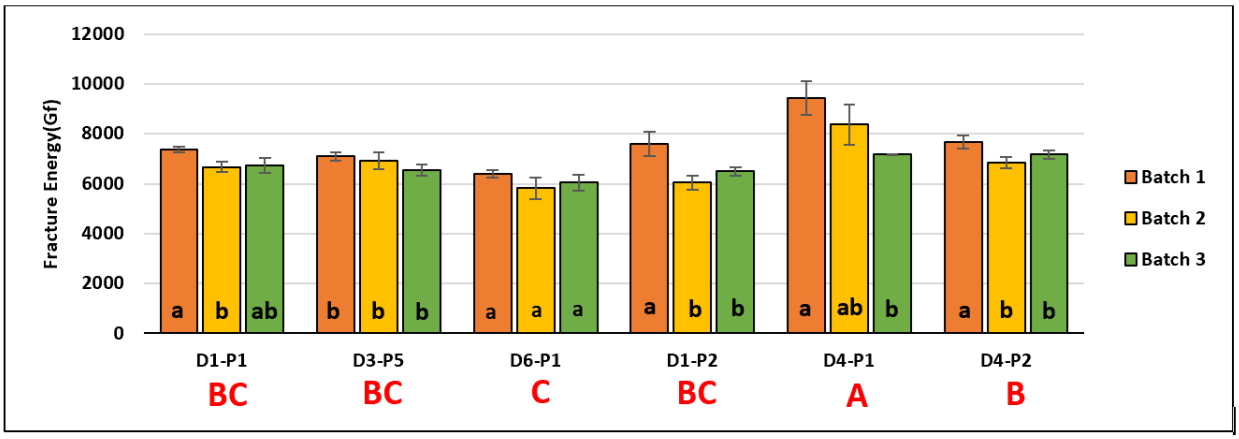

Figure 120. G_f of PMLC Mixes

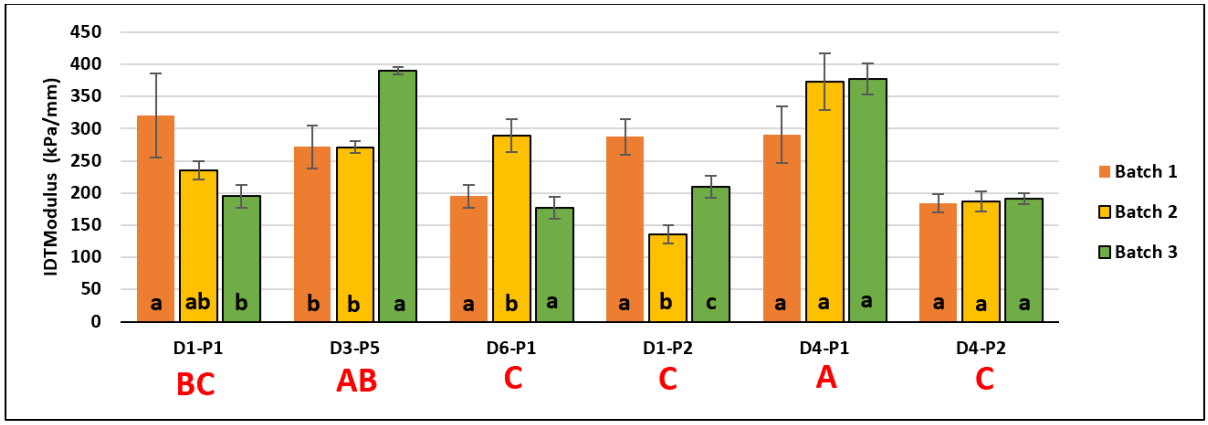

Figure 121. $IDT_{Modulus}$ of PMLC Mixes

Variability of the Cracking Performance Indicators

The researchers examined the variability of the test results of various cracking resistance indicators. They calculated the coefficient of variation (COV) of the test results for LMLC and PMLC mixes for each cracking resistance indicator. The COV is calculated by dividing the standard deviation by the average of three replicates for each cracking indicator. Figure 122 shows the range and average of COV for each cracking resistance indicator. Similar to RP 261, the indicators can be classified into three groups based on the average COV: low variability (COV < 10 percent), moderate variability (between 10 percent and 35 percent), and high variability (COV > 35 percent). The average COV of $IDT_{Strength}$, G_f, CRI, and $Weibull_{CRI}$ was 5.4 percent, 5.5 percent, 6.0p ercent, and 7.3 percent, respectively. This group is considered to have low variability in the test results. The average COV of $IDT_{Modulus}$, N_{Flex}, FI, and IDEAL-CT_{index} was 10.5 percent, 13.8 percent, 15.0 percent, and 19.2 percent, respectively. The IDEAL-CT_{index} was found to have the highest variability compared to all cracking resistance indicators evaluated in this study which agrees with the findings of RP 261 (Kassem et al. 2019).

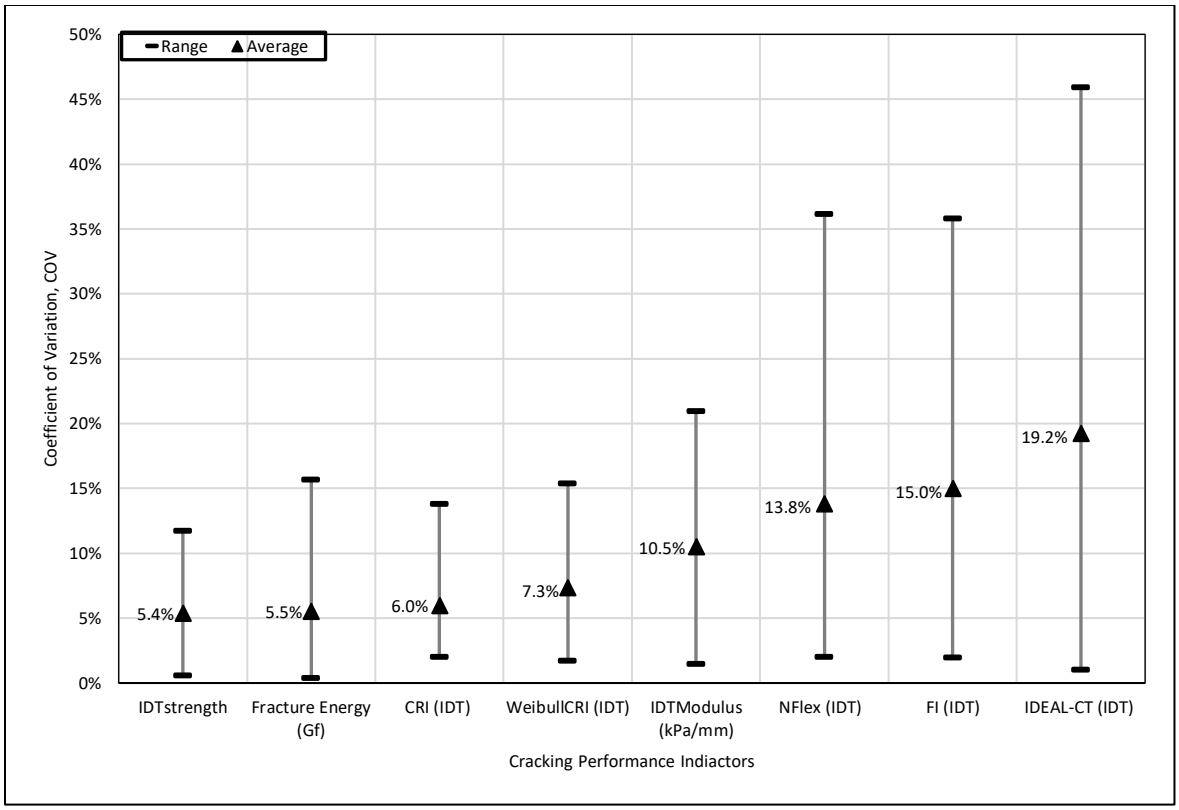

Figure 122. COV for Cracking Performance Indicators of LMLC and PMLC mixes

Correlation between Monotonic Performance Indicators

The researchers examined the correlation between various cracking performance indicators evaluated in this study. The Pearson product moment correlation coefficient (r) is used to examine the linear relationship between two indicators (Salkind 2010). The value of r ranges between -1 and +1. The sign indicates whether the relationship is direct (+) or inverse (-), while the magnitude describes the strength of the correlation. Higher magnitude indicates stronger correlation. Table 8 presents the value of r between various cracking performance indicators. The results demonstrated that $Weibull_{CRI}$, IDEAL-CT_{index}, N_{Flex}, CRI, and FI had direct strong correlations ($r > 0.90$). While $IDT_{Strength}$ and $IDT_{Modulus}$ had an inverse correlation with most indicators except between each other. G_f had inconsistent correlations with the other indicators. There was a strong direct correlation between $Weibull_{CRI}$ and IDEAL-CT_{index} ($r = 0.922$) and both of indicators were able to capture the change in mix composition; however, $Weibull_{CRI}$ had lower variability in the test results (average COV = 7.3 percent) compared to IDEAL-CT_{index} (average COV = 19.2 percent).

Table 8. Pearson Coefficient (r) for Cracking Performance Indicators

Pearson Coefficient	$Weibull_{CRI}$ (IDT)	IDEAL - CT (IDT)	NFlex (IDT)	CRI (IDT)	FI (IDT)	$IDT_{Strength}$	$IDT_{Modulus}$	Fracture Energy (Gf)
$Weibull_{CRI}$ (IDT)	1							
IDEAL -CT (IDT)	0.922	1						
NFlex (IDT)	0.959	0.978	1					
CRI (IDT)	0.987	0.947	0.976	1				
FI (IDT)	0.974	0.974	0.989	0.981	1			
IDT strength	-0.724	-0.695	-0.743	-0.800	-0.744	1		
IDTModulus	-0.723	-0.716	-0.758	-0.808	-0.737	0.956	1	
Fracture Energy (Gf)	0.065	-0.130	-0.085	-0.067	-0.076	0.549	0.500	1

Excellent Correlation ($r \geq 0.9$) Good Correlation ($0.7 < r < 0.9$) Fair Correlation ($0.5 < r \leq 0.7$) Poor Correlation ($0.1 < r \leq 0.5$) No Correlation

7. Conclusions, Implementation, and Recommendations

Summary and Conclusions

ITD Research Report RP 175 developed an algorithm for determining a Gyratory Stability (GS) for asphalt mixtures based on the Servopac gyratory compactor. The GS describes the ability of asphalt mixtures to resist rutting, and it can be determined during the mix design stage using the gyratory compaction data. The GS was recommended as a screening tool during mix design to evaluate the resistance of asphalt mixes to rutting. However, the current GS algorithm was developed for the Servopac gyratory compactor. Currently, ITD has adopted the use of Pine gyratory compactor in all districts and the headquarter labs. Since the previous GS model was developed by the Servopac compactor, the researchers developed a modified algorithm for GS applicable to Pine Gyratory compactor model AFG2AS. This study investigated the use of the GS, other gyratory compaction indices, and performance tests to detect the variability in mix composition (e.g., RAP content, RAP source, binder content, and binder grade). Several stability and compaction indices were examined including the GS, laboratory compaction index (LCI), construction densification index (CDI), compaction force index (CFI), locking point (LP), compactability energy index (CEI), and workability energy index (WEI).

The researchers prepared and tested laboratory-mixed laboratory-compacted (LMLC) mixes and plant-mixed laboratory-compacted (PMLC) mixes obtained from new ITD field projects. The LMLC mixes included three binder contents (4.25 percent, 5.0 percent, and 5.75 percent), three RAP contents (0 percent, 25 percent, 50 percent), three binder grades (PG 58-34, PG 64-28, PG 76-22), and two aggregate types (basalt and river gravel). The PMLC mixes were collected from six different field projects across the state. For each field project, three batches were selected to investigate changes in mix production during construction.

The rutting performance of the test mixtures was evaluated using two rutting tests: Hamburg wheel tracking test (HWTT) and asphalt pavement analyzer (APA). The HWTT is conducted in accordance with AASHTO T 324, while the APA rut test is conducted in accordance with AASHTO T 340. The HWTT was also used to evaluate mix resistance to moisture damage. Furthermore, this study assessed the resistance of asphalt mixes to cracking using several monotonic cracking indicators used to analyze the load-displacement curve from the indirect tension (IDT) test. These cracking performance indicators included IDEAL-CT_{Index}, cracking resistance index (CRI), N_{flex}, $Weibull_{CRI}$, fracture energy (G_f), $IDT_{Strength}$, $IDT_{Modulus}$, and flexibility index (FI). In addition, this study evaluated the moisture susceptibility using the Lottman procedure to examine the effect of change in mix properties and the use of anti-stripping agents on moisture damage. The main findings of this study are summarized in the next section.

Evaluation of Compaction and Stability Indices

- Different compaction indices including GS, LCI, CDI, CFI, LP, CEI, and WEI were calculated in this study from the compaction data. Based on the comprehensive evaluation of the results of these indices, the GS, CDI, and LCI were found to be sensitive to binder content; however, all the compaction indices

were less sensitive to the change in the RAP content and binder grade. The GS decreased with the increase in binder content for all mixes (with and without RAP) for different binder grades. Drier mixes required more energy for compaction than mixes with more binder content. The CDI decreased with the increase in binder content which indicates less energy was needed to compact the test samples. Mixes prepared at 4.25 percent binder content had higher CDI which indicates more energy was required to achieve 92 percent Gmm, while mixes at 5.75 percent binder content had the lowest CDI. In addition, the results showed that mixes with 5.75 percent binder content had higher LCI values that mixes with lower binder contents (i.e., 4.25 percent) and the difference was statistically significant. Higher LCI values indicate less compaction effort is needed to prepare a mix in the laboratory.

- The CDI, GS, and LCI indices can be used to assess the change in binder content, but they were not sensitive to the change in binder grade or RAP content, so it is recommended that other performance indicators be coupled with these compaction indices for quality control.

- The researchers developed an Excel spreadsheet to facilitate the calculations of the GS and LCI and incorporated these calculations in the *PineShear+* Excel spreadsheet. This utility allows the user to import the compaction data collected from the Pine compactor and provides charts for the GS and LCI indices like the ones already included in the *PineShear+*Excel spreadsheet. These charts enable the user to compare various groups of mixtures to assess changes in GS and LCI that may trigger changes in mix production due to segregation.

- The CDI, GS, and LCI of various batches of the PMLC mixes demonstrated that there was difference within batches for some field projects, which indicates variations in mix characteristics due to segregation or changes in mix production.

Evaluation of Rutting Performance and Moisture Susceptibility

- The rutting performance evaluation using the APA rut test and HWTT showed that all LMLC and PMLC mixes had good resistance to rutting. In addition, there was no sign for moisture damage for all mixtures tested using HWTT. The APA and HWTT rut depth increased with the increase in binder content as expected. However, there was a statistically significant difference in the APA rut depth results between mixtures with 5.75 percent binder content and 4.25 percent binder content, while the difference in the HWTT results was not statistically significant between 5.75 percent and 4.25 percent binder content.

- Overall, mixtures prepared with RAP tended to have slightly less rutting compared to mixtures without RAP at the corresponding binder contents, but the difference was not statistically significant.

- The researchers investigated the relationship between APA and HWTT rut depth for the LMLC mixes. Poor correlation was found between APA and HWTT rut depths. The reason for this observation is likely because both APA and HWTT tests are conducted under different conditions. The APA is

performed at different temperatures based on the binder grade, while the HWTT is conducted at a constant temperature of 50°C and in wet condition.

- The researchers investigated the relationship between the mix compaction indices and rutting. The GS and CDI showed fair correlations between the APA rut depth and mix stability. Mixes with higher rutting had lower GS and CDI values and vice versa. Higher GS and CDI values indicate higher resistance to densification and were found to be associated with less rutting. The LCI showed a better correlation with the APA rut depth ($R^2 = 0.64$). Such correlation is considered very good and promising given the inherent variability associated with evaluation of mix compactability and rutting resistance in the laboratory. Higher LCI values were associated with less rutting and vice versa. Mixtures with higher resistance to densification (i.e., low LCI) were found to have higher resistance to rutting. Also, all compaction indices had better correlation with the APA rut depth than HWTT since the compaction indices are calculated from the compaction data, which is conducted at different temperatures based on the binder grade, while the HWTT is conducted at a constant temperature of 50°C and in wet condition.

- The moisture damage evaluation using the Lottman procedure showed that the use of liquid anti-stripping agent (ASA) improved the TSR at 4.25 percent and 5.75 percent but not at 5.0 percent binder content. In addition, the use of RAP had an overall negative effect on moisture susceptibility and resulted in lower TSR values. Also, the results demonstrated that the HWTT did not provide comparable evaluation of the moisture susceptibility as compared to the assessment obtained with the TSR results.

Evaluation of Cracking Performance

- The research team also evaluated the cracking resistance of the test samples using the IDT test. Several monotonic cracking performance indicators can be calculated from the IDT load-displacement curve including IDEAL-CT_{Index}, CRI, N_{flex} factor, $Weibull_{CRI}$, G_f, $IDT_{Strength}$, $IDT_{Modulus}$, and FI. The results demonstrated that the $IDT_{Modulus}$ and $IDT_{Strength}$ were able to capture the change in binder content, binder grade, and RAP content. Other indices including IDEAL-CT_{Index}, $Weibull_{CRI}$, CRI, and N_{flex} factor were sensitive to binder content and RAP contents from the second source of RAP. Overall, the cracking resistance improved with the increase in binder content, as expected. Also, all mixtures prepared at different RAP contents (up to 50 percent) from the first source of RAP had good resistance to cracking; however, the mixtures prepared with the second source of RAP did not show this trend. The cracking resistance decreased with the increase in RAP content. These results suggested that RAP materials from the second source could be more aged and stiffer compared to the RAP materials from the first source, which resulted in reduced cracking resistance with increased RAP content. The source of RAP was found to be significant in this study which agrees with the findings of previous research (Sabahfar et al. 2014; Shu et al. 2008).

- The results also illustrated that the cracking performance of mixtures prepared with RAP (up to 50 percent) from the second source of RAP could be improved by increasing the binder content. This

indicates the importance of conducting a balanced mix design when incorporating RAP materials in asphalt mixes.

- The cracking resistance evaluation of PMLC mixes showed that all PLMC mixes met the minimum threshold values of all the cracking performance indicators and had good cracking resistance. Also, the PLMC mixes with higher binder content and lower RAP content (e.g., project D4-P2) provided better cracking resistance. Also, there was variability in the cracking resistance between batches obtained from the same field project, and in some cases the differences were statistically significant. This variation in cracking resistance could be an indication of change in mix properties due to segregation or change in mix production.

Implementation

The proposed mix compaction indices (GS, CDI, and LCI) accompanied with the modifications to the *PineShear+* Excel spreadsheets should be used as a screening tool to evaluate the change of mix composition. However, these indices were less sensitive to the change in RAP content and binder grade. In addition, the LCI can be used to assess the rutting resistance during the mix design stage or during laboratory compaction of asphalt mixes.

It is recommended to conduct the IDT and calculate both $IDT_{Modulus}$ and $IDT_{Strength}$ to capture the change in mix composition during mix production. These two parameters were found to provide consistent results in terms of sensitivity to binder content, binder grade, and RAP content in the mix. However, these parameters (i.e., $IDT_{Modulus}$ and $IDT_{Strength}$) were not necessarily related to cracking resistance based on the findings of RP 261 (Kassem et al. 2019). Instead, it is recommended to use IDEAL-CT_{Index} and $Weibull_{CRI}$, as quality control indicators to ensure that the mixes have adequate resistance to cracking. Meanwhile, $Weibull_{CRI}$ was found to have less variability in the test results compared to IDEAL-CT_{Index} based on the results of this study, which is consistent with the findings of RP 261 (Kassem et al. 2019).

The national asphalt landscape is changing with balanced mix design, and the future of asphalt mix development, where the asphalt mix is optimized to balance rutting and cracking susceptibility. ITD should consider implementing and applying a balanced (engineered) mix design concept for asphalt mixes prepared with high RAP content to ensure that such mixtures have adequate resistance to cracking and rutting and are comparable or superior to the control mix. The results of this study showed that adjusting the binder content improved the cracking performance of mixtures prepared with up to 50 percent RAP content.

Recommendations for Future Research

- Based on the results of this study, the use of high RAP content (up to 50 percent) can still provide comparable performance results to the control mixture (i.e., 0 percent RAP content) depending on the RAP source. RAP materials from different sources have different characteristics and implementing cracking assessment test and performance indicator would enable the materials

engineers to optimize the mix design with high RAP content. Incorporating high RAP content in asphalt mixtures with adequate cracking resistance would contribute to significant economic savings.

- Further research is recommended to investigate the correlation between various compaction and stability indices and rutting performance in the field. Historical compaction data and field performance collected by ITD could be used for this purpose.

8. Cited Works

Abdo, A., Bayomy, F., Nielsen, R., Jung, S. J., and Santi, M."Development and evaluation of hot mix asphalt stability index." *Int. J. Pavement Eng.*, 11(6), 529–539, 2010.

Advanced Asphalt Technologies, LLC. *Precision of the Dynamic Modulus and Flow Number Tests Conducted with the Asphalt Mixture Performance Tester.* Washington, D.C.: Transportation Research Board, NCHRP Report 702, 2011.

Al-Qadi, I. L., Q. Aurangzeb, S. H. Carpenter, W. J. Pine and J. Trepanier. *Impact of High RAP Content on Structural and Performance Properties of Asphalt Mixtures.* Urbana, IL: Illinois Center for Transportation, University of Illinois, FHWA-ICT-12-002, 2012. https://www.ideals.illinois.edu/bitstream/handle/2142/45810/FHWA-ICT-12-002.pdf?sequence=2. Accessed May 2020.

Al-Qadi, I.L., Carpenter, S.H., Roberts, G.L., Ozer, H., Aurangzeb, Q., Elseifi, M.A., and Trepanier, J. Determination of Usable Residual Asphalt Binder in RAP. Report No. ICT-R27-11. Rantoul, IL: Illinois Center for Transportation, 2008

American Association of State Highway and Transportation Officials. *AASHTO T308-10: Standard Method of Test for Determining the Asphalt Binder Content of Hot Mix Asphalt (HMA) by the Ignition Method.* Washington, D.C.: American Association of State Highway and Transportation Officials, 2015.

American Association of State Highway and Transportation Officials. *AASHTO T164-14: Standard Method of Test for Quantitative Extraction of Asphalt Binder from Hot Mix Asphalt (HMA)*. Washington, D.C.: American Association of State Highway and Transportation Officials, 2015.

American Association of State Highway and Transportation Officials. *AASHTO T319-14: Standard Method of Test for Quantitative Extraction and Recovery of Asphalt Binder from Asphalt Mixtures. Washington*, D.C.: American Association of State Highway and Transportation Officials, 2015.

American Association of State Highway and Transportation Officials. *AASHTO T85-14: Standard Method of Test for Specific Gravity and Absorption of Coarse Aggregate.* Washington, D.C.: American Association of State Highway and Transportation Officials, 2015.

American Association of State Highway and Transportation Officials. *AASHTO T84-13: Standard Method of Test for Specific Gravity and Absorption of Fine Aggregate*. Washington, D.C.: American Association of State Highway and Transportation Officials, 2015.

American Association of State Highway and Transportation Officials. *AASHTO M323-13: Standard Specification for Superpave Volumetric Mix Design*. Washington, D.C.: American Association of State Highway and Transportation Officials, 2015.

American Association of State Highway and Transportation (AASHTO). *Standard Method of Test for Determining the Rutting Susceptibility of Asphalt Paving Mixtures Using the Asphalt Pavement Analyzer (APA) (AASHTO T340)*. *AASHTO specifications and test Method* (2015).

Apeagyei, A. K., B. K. Diefenderfer, and S. D. Diefenderfer. "Rutting Resistance of Asphalt Concrete Mixtures that Contain Recycled Asphalt Pavement." *Transportation Research Record: Journal of the Transportation Research Board,* No. 2208 (2011): 9 - 16.

Bahia, H., T. Friemel, P. Peterson, J. Russell, and B. Poehnelt. "Optimization of Contractibility and Resistance to Traffic: A New Design Approach for HMA Using the Superpave Compactor." *Journal of Association of Asphalt Paving Technologists*, Vol. 72, 2003.

Bayomy, F., E. Masad, and S. Dessouky. "Development and Performance Prediction of Idaho Superpave Mixes," Interim Report ITD-NIATT Project KLK464, National Institute for Advanced Transportation Technology, University of Idaho, Moscow, Idaho, 2002

Bayomy, F.B. and A. Abu Abdo. "Performance Evaluation of Idaho HMA Mixes Using Gyratory Stability." Final Report ITD-NIATT Project KLK482, National Institute for Advanced Transportation Technology, University of Idaho, Moscow, Idaho, 2007.

Beeson, M., Prather, M., and Huber, G. A. "Characterization of reclaimed asphalt pavement in Indiana: Changing INDOT specifications for RAP." Transportation Research Board 90th Annual Meeting (No. 11-1055), Transportation Research Board, Washington, DC, 2011

Brown, E.R., Newcomb, D., and Epps J.A. Designing HMA Mixtures with High RAP Content: A Practical Guide, Quality Improvement Series 124, National Asphalt Pavement Association, Lanham, MD, 2007

Butcher, M., "Determining Gyratory Compaction Characteristic Using Servopac Gyratory Compactor." *Transportation Research Record 1630*, TRB, Washington, D.C., 1998.

Carvalho, R. L., H. Shirazi, M. Ayres, and O. Selezneva. "Performance of Recycled Hot-Mix Asphalt Overlays in Rehabilitation of Flexible Pavements." *Transportation Research Record: Journal of the Transportation Research Board,* No. 2155 (2010): 55 - 62.

Colbert, B. and Z. You. "The Determination of Mechanical Performance of Laboratory Produced Hot Mix Asphalt Mixtures Using Controlled RAP and Virgin Aggregate Size Fractions." *Construction and Building Materials*, Vol. 26, No. 1 (Jan. 2012): 655 - 662.

Copeland, A. *Reclaimed Asphalt Pavement in Asphalt Mixtures: State of the Practice.* McLean, VA: Federal Highway Administration, FHWA-HRT-11-021, 2011.

Daniel, J. S. and A. Lachance. "Mechanistic and Volumetric Properties of Asphalt Mixtures with Recycled Asphalt Pavement." *Transportation Research Record: Journal of the Transportation Research Board*, No. 1929 (2005): 28 - 36.

DeSombre, R., B. Chadbourn, D.E. Newcomb, and V. Voller. “Parameters to Define the Laboratory Compaction Temperature Range of Hot-Mix Asphalt.” *Journal of Association of Asphalt Paving Technologists*, Vol. 67, 1998

Dessouky S, Masad E, Bayomy F. “Evaluation of asphalt mix stability using compaction properties and aggregate structure analysis.” *International Journal of Pavement Engineering*. 2003 Jun 1;4(2):87-103.

Dessouky S, Pothuganti A, Walubita LF, Rand D. “Laboratory evaluation of the workability and compactability of asphaltic materials prior to road construction.” *Journal of Materials in Civil Engineering*. 2012 Aug 29; 25(6):810-8.

Dessouky, S., E. Masad, and F. Bayomy. “Prediction of Hot Mix Asphalt Stability Using the Superpave Gyratory Compactor,” *Journal of Materials in Civil Engineering*, Vol. 16, No. 6, 2004.

Estakhri, E., C. Spiegelman, B. Gajewski, G. Yang, and D. Little. *Recycled Hot-Mix Asphalt Concrete in Florida: a Variability Study.* Austin, TX: International Center for Aggregate Research, ICAP-401-1/98, 1999.

Hajj, E. Y., P. E. Sebaaly, R. West, N. Morian, and L. Loria. “Recommendations for the Characterization of RAP Aggregate Properties Using Traditional Testing and Mixture Volumetrics.” *Road Materials and Pavement Design*, Vol. 13, No. S1 (June 2012): 209 - 233.

Hassan, R. “Feasibility of Using High RAP Contents in Hot Mix Asphalt.” *Proceedings of the 13th International Flexible Pavements Conference*. Queensland, Australia: Australian Asphalt Pavement Association, 2009.

Idaho Transportation Department. *Standard Specification for Highway Construction*. Boise, Idaho: Idaho Transportation Department, 2021. http://itd.idaho.gov/manuals/Manualpercent20Production/SpecBook/SpecHome.htm Accessed in May 2020.

Idaho Transportation Department. 2007. RP175 *Idaho Transportation System Pavement Performance Report.* Idaho Transportation Department, Boise, Idaho.

Kandhal, P. S., S. S. Rao, D. E. Watson, and B. Young. *Performance of Recycled Hot Mix Asphalt Mixtures.* Auburn, AL: National Center for Asphalt Technology, Auburn University, NCAT Report 95-01, 1995.

Kingery, W. R. “Laboratory Study of Fatigue Characteristics of HMA Surface Mixtures Containing Recycled Asphalt Pavement (RAP).” Master’s Thesis, University of Tennessee - Knoxville, 2004.

Kumar A., and W. Goetz. “The Gyratory Testing Machine as a Design Tool and Instrument for Bituminous Mixture Evaluation.” *Asphalt Paving Technology*, Vol. 43, 1974.

Kvasnak, A., R. West, J. Michael, L. Loria, E. Y. Hajj and N. Tran. “Bulk Specific Gravity of Reclaimed Asphalt Pavement Aggregate: Evaluating the Effect on Voids in Mineral Aggregate.” *Transportation Research Record: Journal of the Transportation Research Board*, No. 2180 (2010): 30 - 35.

Li, X., T. R. Clyne, and M. O. Marasteanu. *Recycled Asphalt Pavement (RAP) Effects on Binder and Mixture Quality*. Minneapolis, MN: University of Minnesota, MnDOT 2005-02, 2004.

Mallick, R. "Use of Superpave Gyratory Compactor to Characterize Hot Mix Asphalt." *Transportation Research Record 1681*, TRB, Washington, D.C., 1999.

Masad, E., "The Development of A Computer Controlled Image Analysis System for Measuring Aggregate Shape Properties." NCHRP-IDEA Project 77 Final Report, Transportation Research Board, Washington,D.C., 2003.

Mahmoud A., Faheem, A., and Bahia, H. *Using gyratory compactor to measure mechanical stability of asphalt mixtures*. Wisconsin highway research program, 2004.

Maupin, G. W., S. D. Diefenderfer, and J. S. Gillespie. *Evaluation of Using Higher Percentages of Recycled Asphalt Pavement in Asphalt Mixes in Virginia.* Charlottesville, VA: Virginia Transportation Research Council, VTRC 08-R22, 2008.

McDaniel, R. S., A. Shah, G. A. Huber, and A. Copeland. "Effects of Reclaimed Asphalt Pavement Content and Virgin Binder Grade on Properties of Plant Produced Mixtures." *Road Materials and Pavement Design*, Vol. 13, No. S1 (June 2012): 161 - 182.

McDaniel, R. S., A. Shah, G. A. Huber, and A. Copeland. "Effects of Reclaimed Asphalt Pavement Content and Virgin Binder Grade on Properties of Plant Produced Mixtures." *Road Materials and Pavement Design*, Vol. 13, No. S1 (June 2012): 161 - 182.

McRea, J.L., "Gyratory Compaction Method for Determining Density Requirements for Subgrade and Base of Flexible Pavements." Miscellaneous paper No. 4-494, U.S. Army Engineering Waterways Experiment Station, Corps of Engineering, Vicksburg, MS., 1962.

McRea, J.L., "Gyratory Testing Machine Technical Manual." Engineering Developments Company Inc., Vicksburg, MS, 2, 1965.

Minitab. 2019. *Data Analysis, Statistical & Process Improvement Tools*. [online] Available at: <https://www.minitab.com/en-us/> [Accessed 5 March 2021].

Mogawer, W., T. Bennert, J. S. Daniel, R. Bonaquist, A. Austerman, and A. Booshehrian. "Performance Characteristics of Plant Produced High RAP Mixtures." *Road Materials and Pavement Design*, Vol. 13, No. 1 (June 2012): 183 - 208.

Nady, R. M. "The Quality of Random RAP: Separating Fact from Supposition." *HMAT: Hot Mix Asphalt Technology*, Vol. 2, No. 2 (1997): 14 - 17.

NAPA. "Recycling." Recycling - National Asphalt Pavement Association, 2019, www.asphaltpavement.org/expertise/sustainability/sustainability-resources/recycling.

Hicks, R.G. (1991). *NCHRP Synthesis of Highway Practice 175: Moisture Damage in Asphalt Concrete*. Transportation Research Board, National Research Council. Washington, D.C

Paul, H. R. *Evaluation of Recycled Projects for Performance.* Baton Rouge, LA: Louisiana Department of Transportation and Development, Louisiana Transportation Research Center, LTRC Research Project No. 83-1B, 1995

Pine Test Equipment, *AFLS1 - Rapid Angle Measurement (RAM) Kit Operation Manual*, LMAFS!, Version 012, Copyright © 2003-2017 Pine Test Equipment, Inc, March 10, 2017

Pine Test Equipment, *AFG2AS /AFG2CS PineShear+ User Guide, V002*, Copyright 2010-2017 Pine Instrument Company, June 29, 2017

Prowell, B. and C. B. Carter. *Evaluation of the Effect on Aggregate Properties of Samples Extracted Using the Ignition Furnace, Interim Report.* Charlottesville, VA: Virginia Transportation Research Council, VTRC 00-IR1, 2000.

Putman, B. J., J. Aune, and S. N. Amirkhanian. *Recycled Asphalt Pavement (RAP) Used in Superpave Mixes Made with Rubberized Asphalt.* Clemson, SC: Clemson Univeristy, http://www.clemson.edu/ Accessed June 2020.

Ruth, B., X. Shen, and L. Wang. "Gyratory Evaluation of Aggregate Blends to Determine their Effects on Shear Resistance and Sensitivity to Asphalt Content." *American Society for Testing and Materials*, 1147, 1991.

Sabahfar, N., S. R. Aziz,M. Hossain and G. Schieber. "Evaluation of Superpave Mixtures with High Percentages of Reclaimed Asphalt Pavement." *93rd Annual Meeting of the Transportation Research Board*, Washington, D.C.: Transportation Research Board, 2014.

Santos, L., A. Baptista, and S. Capitão. "Assessment of the Use of Hot-Mix Recycled Asphalt Concrete in Plant." *Journal of Transportation Engineering*, Vol. 136, No. 12 (Dec. 2010): 1159 - 1164.

Shirodkar, P., Y. Mehta, A. Nolan, K. Sonpal, A. Norton, C. Tomlinson, E. Dubois, P. Sullivan and R. Sauber. "A Study to Determine the Degree of Partial Blending of Reclaimed Asphalt Pavement (RAP) Binder for High RAP Hot Mix Asphalt." *Construction and Building Materials,* Vol. 25, No. 1 (Jan. 2011): 150 - 155.

Shu, X., B. Huang, and D. Vukosavljevic. "Laboratory Evaluation of Fatigue Characteristics of Recycled Asphalt Mixture." *Construction and Building Materials*, Vol. 22 (2008): 1323 - 1330.

Sigurjonsson, S., B. Ruth. "Use of Gyratory Testing Machine to Evaluate Shear Resistance of Asphalt Paving Mixture." *Transportation Research Record 1259*, TRB, Washington, D.C., 1990.

Solaimanian, M. and M. Tahmoressi. "Variability Analysis of Hot Mix Asphalt Concrete Containing High Percentages of Reclaimed Asphalt Pavement." *Transportation Research Record: Journal of the Transportation Research Board, No. 1543 (1996): 89 - 96.*

Sondag, M. S., B. A. Chadbourn, and A. Drescher. *Investigation of Recycled Asphalt Pavement (RAP) Mixture.* St. Paul, MN: Minnesota Department of Transportation, Report MnDOT 2002-15, 2002.

Stroup-Gardiner, M. and C. Wagner. “Use of Reclaimed Asphalt Pavement in Superpave Hot-Mix Asphalt Applications.” *Transportation Research Record: Journal of the Transportation Research Board*, No. 1681 (1999): 1 - 9.

Vavrik, W. R., S. H. Carpenter, S. Gillen, J. Behnke and F. Garrott. *Evaluation of Field-Produced Hot Mix Asphalt (HMA) Mixtures with Fractionated Recycled Asphalt Pavement (RAP), 2007 Illinois Tollway Field Mix Trials*. Champaign, IL: Illinois Center for Transportation, ICT-08-030, 2008.

Vukosavljevic, D. “Fatigue Characteristics of Field HMA Surface Mixtures Containing Recycled Asphalt Pavement (RAP).” Master’s Thesis, University of Tennessee - Knoxville, 2006.

West, R. C. “Keys to Managing RAP Variability.” *Better Roads*, Vol. 15 (Oct. 2009): 12 - 15.

West, R. C. *Reclaimed Asphalt Pavement Management: Best Practices*. Auburn, AL: National Center for Asphalt Technology, Auburn University, 2010. http://www.morerap.us/files/rap-best-practices.pdf Accessed May 2020.

West, R. C. *Summary of NCAT Survey on RAP Management Practices and RAP Variability.* Auburn, AL: National Center for Asphalt Technology, 2008. http://www.morerap.us/files/rap-field-projects/summary-survey-rap-mgt-variablity.pdf Accessed June 2020.

West, R. C., A. N. Kvasnak, N. H. Tran, R. L. Powell, and P. Turner. “Testing of Moderate and High Reclaimed Asphalt Pavement Content Mixes: Laboratory and Accelerated Field Performance Testing at the National Center for Asphalt Technology Test Track.” *Transportation Research Record: Journal of the Transportation Research Board*, No. 2126 (2009): 100 - 108.

West, R., J. R. Willis, and M. Marasteanu. *Improved Mix Design, Evaluation, and Materials Management Practices for Hot Mix Asphalt with High Reclaimed Asphalt Pavement Content*. Washington, D.C.: Transportation Research Board, NCHRP Report 752, 2013

Yousefi Rad, F. “Estimating Blending Level of Fresh and RAP Binders in Recycled Hot Mix Asphalt.” Master’s Thesis, University of Wisconsin, 2013.

Zhao, S., B. Huang, X. Shu, X. Jia, and M. Woods. “Laboratory Performance Evaluation of Warm-Mix Asphalt Containing High Percentages of Reclaimed Asphalt Pavement.” *Transportation Research Record: Journal of the Transportation Research Board*, No. 2294 (2012): 98 - 105.

Zhou, F., G. Das, T. Scullion, and S. Hu. *RAP Stockpile Management and Processing in Texas: State of the Practice and Proposed Guidelines.* College Station, TX: Texas Transportation Institute, FHWA/TX-10/0-6092-1, 2010

Appendix A: Mix Design Summary

Design Specifications: Blend 3 / 100 Gyrations @ N Design (PG 70-34) Binder Bump PG 64-34

	Gyratory Compactor: Model # AFGB1A Serial # 5443	Job Mix Formula	Spec
1	Percent Asphalt by Weight of Total Mix	**5.0**	--
2	Percent Asphalt by Weight of Aggregate	5.3	--
3	Virgin Asphalt by Weight of Mix	3.72	--
4	Virgin Asphalt by Weight of Aggregate	3.92	--
5	Percent Air Voids (Pa)	4.0	4.0
6	Voids in Mineral Aggregate (VMA)	14.3	14min
7	Compacted Unit Weight Gmb, pcf	2.497 155.4	--
8	Theoretical Maximum Density Gmm, pcf	**2.602 162.0**	--
9	Percent Effective Asphalt Content (Pbe)	4.2	--
10	Percent Absorbed Asphalt (Pba)	0.83	--
11	Specific Gravity of Binder (Gb)	**1.028**	--
12	Percent Gmm @ N Initial (8 Gyrations)	85.5	≤ 89.0
13	Percent Gmm @ N Design (100 Gyrations)	96.0	96.0
14	Percent Gmm @ N Max (160 Gyrations)	97.4	≤ 98.0
15	Dust to Asphalt Ratio (DP)	1.4	0.8-1.5
16	Percent Passing #200 Sieve	6.0	2.0-10.0
17	Voids Filled w/ Asphalt (VFA)	72	65-75
18	Laboratory Mixing Temperature for Design (°F)	312	304-312
19	Laboratory Compaction Temperature for Design (°F)	**290**	283-291
20	Laboratory Sample Weight for Volumetric Testing (g)	**4950**	--
21	Ignition Oven (NCAT) Correction Factor @ 538 °F	**0.86**	--
22	Sand Equivalent	66	45 Min
23	Fracture Face Count (%)	99/98	98/98 Min
24	Fine Aggregate Angularity (%)	49.1	45 Min
25	Flat and Elongated Particles in Coarse Aggregates (%)	4.0	10 Max
	Recycled Asphalt Pavement (RAP) Properties		
26	Percentage of Asphalt in RAP (Wt. of Mix)	4.3	--
27	Percentage of RAP by Total Weight of Aggregate	30	--
28	Percent of RAP Binder by Weight of Total Binder	25.7	30 Max
29	RAP Contribution by Mix	1.28	--
30	RAP Contribution by Aggregate	1.34	--
31	RAP NCAT Correction Factor	1.57	--

Figure A.1. Mix Design for the LMLC Mixes

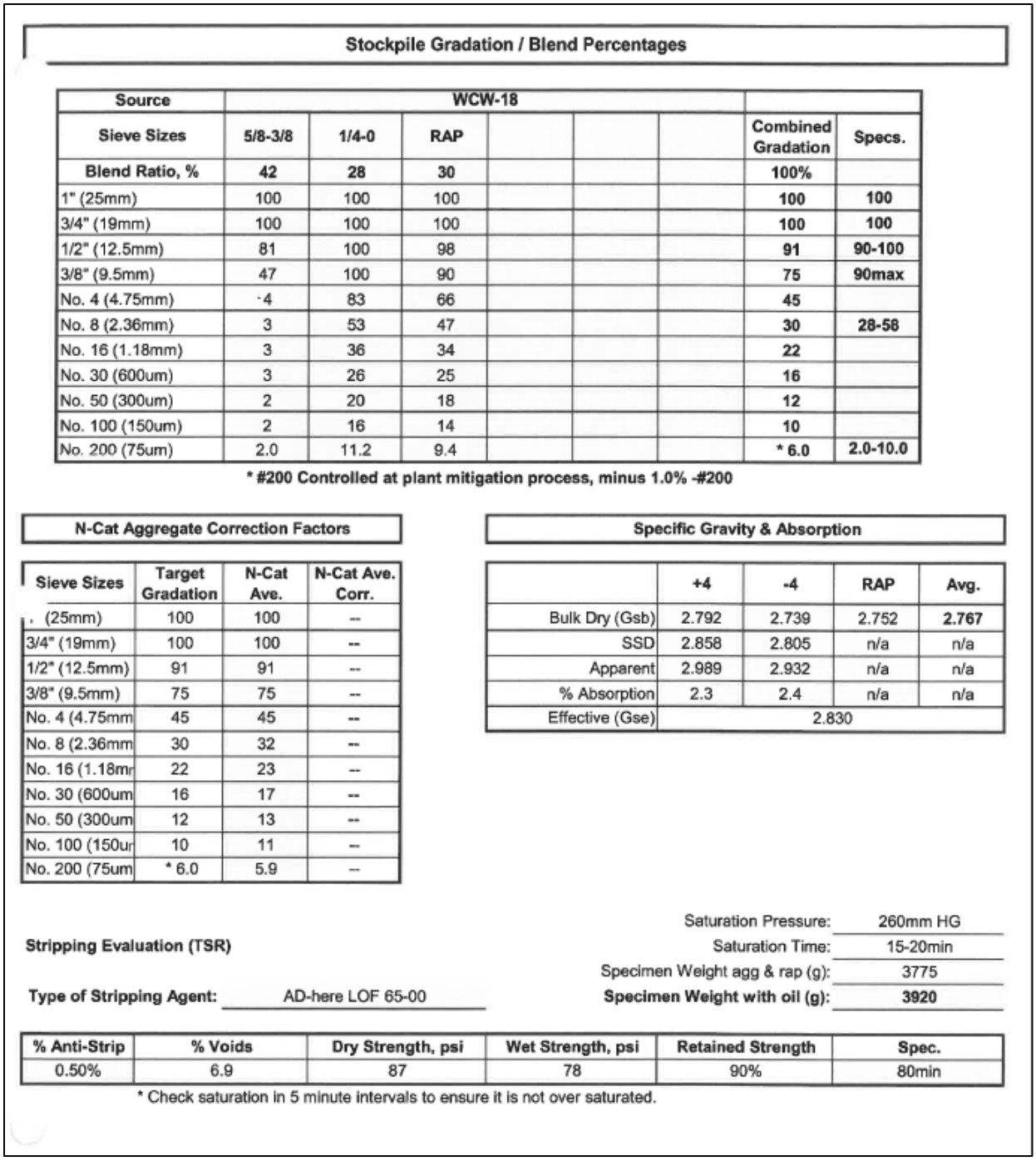

Stockpile Gradation / Blend Percentages

Source	WCW-18							
Sieve Sizes	5/8-3/8	1/4-0	RAP				Combined Gradation	Specs.
Blend Ratio, %	42	28	30				100%	
1" (25mm)	100	100	100				100	100
3/4" (19mm)	100	100	100				100	100
1/2" (12.5mm)	81	100	98				91	90-100
3/8" (9.5mm)	47	100	90				75	90max
No. 4 (4.75mm)	4	83	66				45	
No. 8 (2.36mm)	3	53	47				30	28-58
No. 16 (1.18mm)	3	36	34				22	
No. 30 (600um)	3	26	25				16	
No. 50 (300um)	2	20	18				12	
No. 100 (150um)	2	16	14				10	
No. 200 (75um)	2.0	11.2	9.4				* 6.0	2.0-10.0

* #200 Controlled at plant mitigation process, minus 1.0% -#200

N-Cat Aggregate Correction Factors

Sieve Sizes	Target Gradation	N-Cat Ave.	N-Cat Ave. Corr.
(25mm)	100	100	--
3/4" (19mm)	100	100	--
1/2" (12.5mm)	91	91	--
3/8" (9.5mm)	75	75	--
No. 4 (4.75mm	45	45	--
No. 8 (2.36mm	30	32	--
No. 16 (1.18mr	22	23	--
No. 30 (600um	16	17	--
No. 50 (300um	12	13	--
No. 100 (150ur	10	11	--
No. 200 (75um	* 6.0	5.9	--

Specific Gravity & Absorption

	+4	-4	RAP	Avg.
Bulk Dry (Gsb)	2.792	2.739	2.752	2.767
SSD	2.858	2.805	n/a	n/a
Apparent	2.989	2.932	n/a	n/a
% Absorption	2.3	2.4	n/a	n/a
Effective (Gse)	2.830			

Stripping Evaluation (TSR)

Type of Stripping Agent: AD-here LOF 65-00

Saturation Pressure: 260mm HG
Saturation Time: 15-20min
Specimen Weight agg & rap (g): 3775
Specimen Weight with oil (g): 3920

% Anti-Strip	% Voids	Dry Strength, psi	Wet Strength, psi	Retained Strength	Spec.
0.50%	6.9	87	78	90%	80min

* Check saturation in 5 minute intervals to ensure it is not over saturated.

Figure A.2. Mix Design for the LMLC Mixes (cont.)

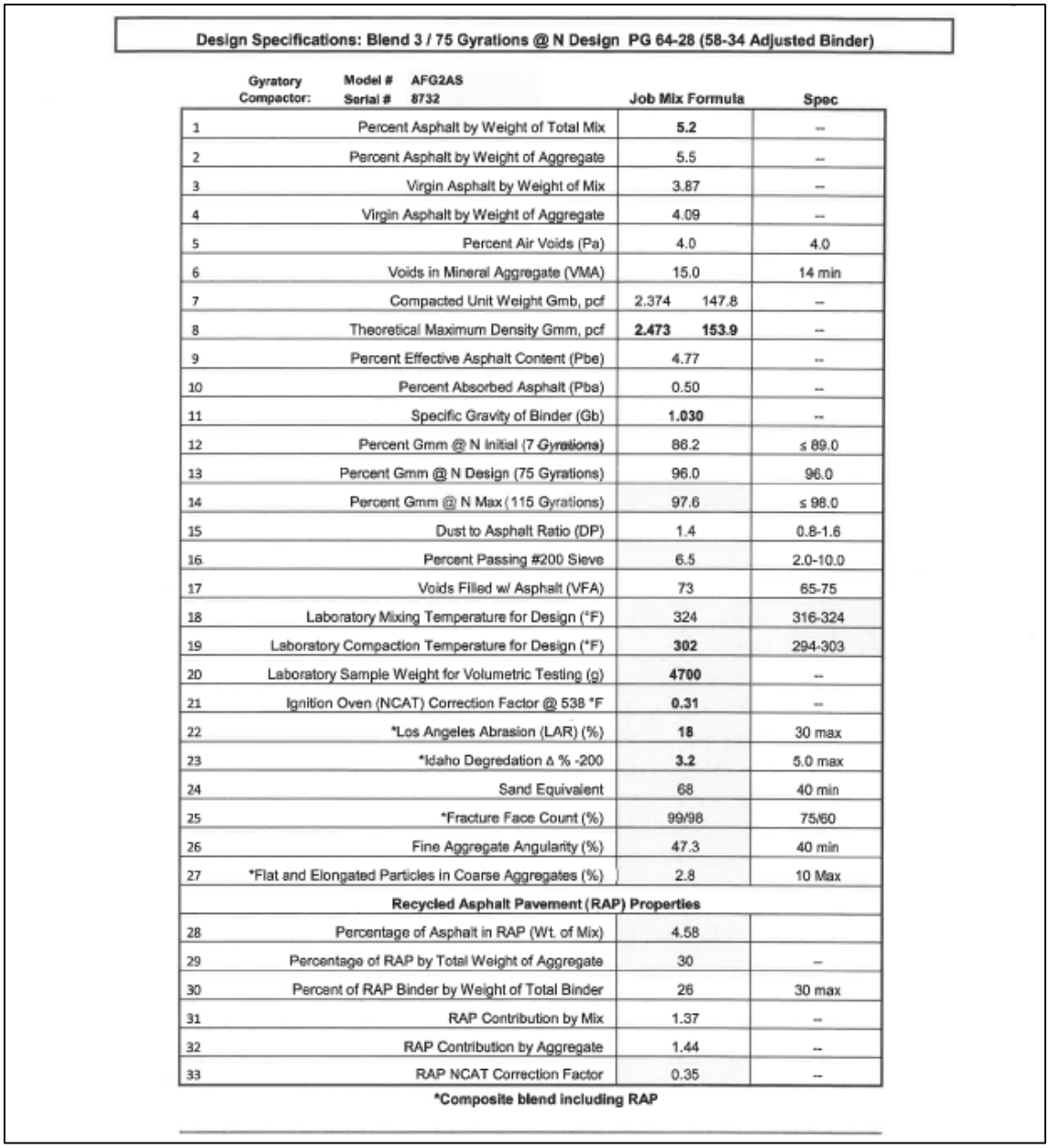

Design Specifications: Blend 3 / 75 Gyrations @ N Design PG 64-28 (58-34 Adjusted Binder)

	Gyratory Compactor: Model # AFG2AS Serial # 8732	Job Mix Formula	Spec
1	Percent Asphalt by Weight of Total Mix	**5.2**	--
2	Percent Asphalt by Weight of Aggregate	5.5	--
3	Virgin Asphalt by Weight of Mix	3.87	--
4	Virgin Asphalt by Weight of Aggregate	4.09	--
5	Percent Air Voids (Pa)	4.0	4.0
6	Voids in Mineral Aggregate (VMA)	15.0	14 min
7	Compacted Unit Weight Gmb, pcf	2.374 147.8	--
8	Theoretical Maximum Density Gmm, pcf	**2.473 153.9**	--
9	Percent Effective Asphalt Content (Pbe)	4.77	--
10	Percent Absorbed Asphalt (Pba)	0.50	--
11	Specific Gravity of Binder (Gb)	**1.030**	--
12	Percent Gmm @ N Initial (7 Gyrations)	86.2	≤ 89.0
13	Percent Gmm @ N Design (75 Gyrations)	96.0	96.0
14	Percent Gmm @ N Max (115 Gyrations)	97.6	≤ 98.0
15	Dust to Asphalt Ratio (DP)	1.4	0.8-1.6
16	Percent Passing #200 Sieve	6.5	2.0-10.0
17	Voids Filled w/ Asphalt (VFA)	73	65-75
18	Laboratory Mixing Temperature for Design (°F)	324	316-324
19	Laboratory Compaction Temperature for Design (°F)	**302**	294-303
20	Laboratory Sample Weight for Volumetric Testing (g)	**4700**	--
21	Ignition Oven (NCAT) Correction Factor @ 538 °F	**0.31**	--
22	*Los Angeles Abrasion (LAR) (%)	**18**	30 max
23	*Idaho Degredation Δ % -200	**3.2**	5.0 max
24	Sand Equivalent	68	40 min
25	*Fracture Face Count (%)	99/98	75/60
26	Fine Aggregate Angularity (%)	47.3	40 min
27	*Flat and Elongated Particles in Coarse Aggregates (%)	2.8	10 Max
	Recycled Asphalt Pavement (RAP) Properties		
28	Percentage of Asphalt in RAP (Wt. of Mix)	4.58	
29	Percentage of RAP by Total Weight of Aggregate	30	--
30	Percent of RAP Binder by Weight of Total Binder	26	30 max
31	RAP Contribution by Mix	1.37	--
32	RAP Contribution by Aggregate	1.44	--
33	RAP NCAT Correction Factor	0.35	--

***Composite blend including RAP**

Figure A.3. District 1 – JMF P1

Design Specifications: Blend 1 / 75 Gyrations @ N Design PG 64-28 (58-34 Adjusted Binder)

	Gyratory Compactor: Model # AFG2AS Serial # 8436	Job Mix Formula	Spec
1	Percent Asphalt by Weight of Total Mix	**5.3**	--
2	Percent Asphalt by Weight of Aggregate	5.64	--
3	Virgin Asphalt by Weight of Mix	4.08	--
4	Virgin Asphalt by Weight of Aggregate	4.32	--
5	Percent Air Voids (Pa)	4.0	4.0
6	Voids in Mineral Aggregate (VMA)	15.6	14 min
7	Compacted Unit Weight Gmb, pcf	2.366 147.3	--
8	Theoretical Maximum Density Gmm, pcf	**2.465 153.4**	--
9	Percent Effective Asphalt Content (Pbe)	5.04	--
10	Percent Absorbed Asphalt (Pba)	0.32	--
11	Specific Gravity of Binder (Gb)	**1.028**	--
12	Percent Gmm @ N Initial (7 Gyrations)	86.8	≤ 89.0
13	Percent Gmm @ N Design (75 Gyrations)	96.0	96.0
14	Percent Gmm @ N Max (115 Gyrations)	97.3	≤ 98.0
15	Dust to Asphalt Ratio (DP)	1.1	0.6-1.4
16	Percent Passing #200 Sieve	5.6	2.0-10.0
17	Voids Filled w/ Asphalt (VFA)	74	65-75
18	Laboratory Mixing Temperature for Design (°F)	320	316-324
19	Laboratory Compaction Temperature for Design (°F)	**299**	295-303
20	Laboratory Sample Weight for Volumetric Testing (g)	**4720**	--
21	Ignition Oven (NCAT) Correction Factor @ 538 °F	**0.30**	--
22	*Los Angeles Abrasion (LAR) (%)	24	30 max
23	*Idaho Degradation Δ % -200	3.5	5.0 max
24	Sand Equivalent	66	40 min
25	*Fracture Face Count (%)	98/96	75/60
26	Fine Aggregate Angularity (%)	47.2	40 min
27	*Flat and Elongated Particles in Coarse Aggregates (%)	0.3	10 max
	Recycled Asphalt Pavement (RAP) Properties		
28	Percentage of Asphalt in RAP (Wt. of Mix)	4.20	
29	Percentage of RAP by Total Weight of Aggregate	30	--
30	Percent of RAP Binder by Weight of Total Binder	24	30 max
31	RAP Contribution by Mix	1.26	--
32	RAP Contribution by Aggregate	1.32	
33	RAP NCAT Correction Factor	0.36	--

***Composite blend including RAP**

Figure A.4. District 1- JMF P2

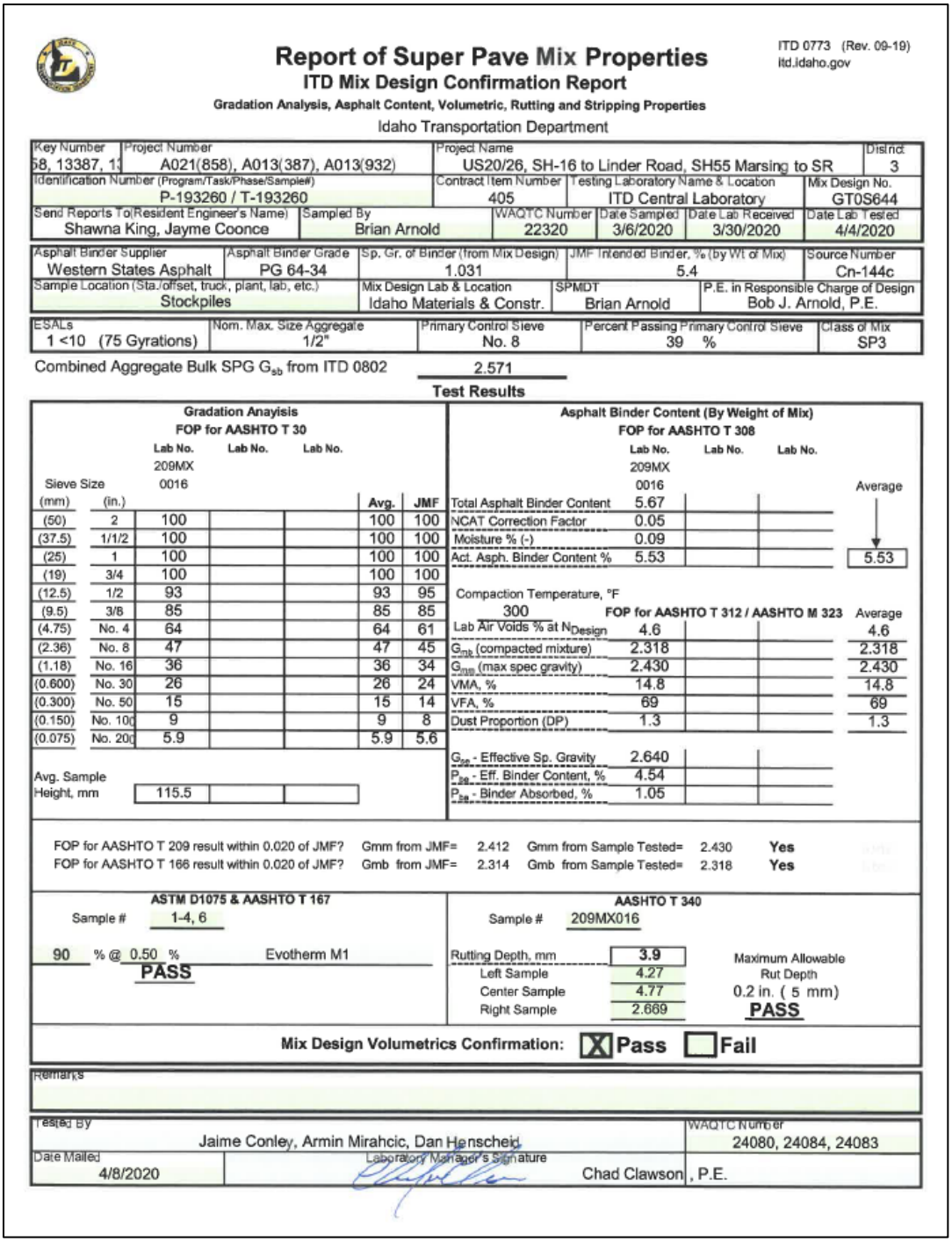

Report of Super Pave Mix Properties

ITD 0773 (Rev. 09-19)
itd.idaho.gov

ITD Mix Design Confirmation Report

Gradation Analysis, Asphalt Content, Volumetric, Rutting and Stripping Properties

Idaho Transportation Department

Key Number	Project Number	Project Name	District
58, 13387, 1	A021(858), A013(387), A013(932)	US20/26, SH-16 to Linder Road, SH55 Marsing to SR	3

Identification Number (Program/Task/Phase/Sample#)	Contract Item Number	Testing Laboratory Name & Location	Mix Design No.
P-193260 / T-193260	405	ITD Central Laboratory	GT0S644

Send Reports To(Resident Engineer's Name)	Sampled By	WAQTC Number	Date Sampled	Date Lab Received	Date Lab Tested
Shawna King, Jayme Coonce	Brian Arnold	22320	3/6/2020	3/30/2020	4/4/2020

Asphalt Binder Supplier	Asphalt Binder Grade	Sp. Gr. of Binder (from Mix Design)	JMF Intended Binder, % (by Wt of Mix)	Source Number
Western States Asphalt	PG 64-34	1.031	5.4	Cn-144c

Sample Location (Sta./offset, truck, plant, lab, etc.)	Mix Design Lab & Location	SPMDT	P.E. in Responsible Charge of Design
Stockpiles	Idaho Materials & Constr.	Brian Arnold	Bob J. Arnold, P.E.

ESALs	Nom. Max. Size Aggregate	Primary Control Sieve	Percent Passing Primary Control Sieve	Class of Mix
1 <10 (75 Gyrations)	1/2"	No. 8	39 %	SP3

Combined Aggregate Bulk SPG G_{sb} from ITD 0802: 2.571

Test Results

Gradation Anayisis
FOP for AASHTO T 30

Sieve Size (mm)	(in.)	Lab No. 209MX 0016	Lab No.	Lab No.	Avg.	JMF
(50)	2	100			100	100
(37.5)	1/1/2	100			100	100
(25)	1	100			100	100
(19)	3/4	100			100	100
(12.5)	1/2	93			93	95
(9.5)	3/8	85			85	85
(4.75)	No. 4	64			64	61
(2.36)	No. 8	47			47	45
(1.18)	No. 16	36			36	34
(0.600)	No. 30	26			26	24
(0.300)	No. 50	15			15	14
(0.150)	No. 100	9			9	8
(0.075)	No. 200	5.9			5.9	5.6
Avg. Sample Height, mm		115.5				

Asphalt Binder Content (By Weight of Mix)
FOP for AASHTO T 308

	Lab No. 209MX 0016	Lab No.	Lab No.	Average
Total Asphalt Binder Content	5.67			
NCAT Correction Factor	0.05			
Moisture % (-)	0.09			
Act. Asph. Binder Content %	5.53			5.53

Compaction Temperature, °F: 300

FOP for AASHTO T 312 / AASHTO M 323

				Average
Lab Air Voids % at N_{Design}	4.6			4.6
G_{mb} (compacted mixture)	2.318			2.318
G_{mm} (max spec gravity)	2.430			2.430
VMA, %	14.8			14.8
VFA, %	69			69
Dust Proportion (DP)	1.3			1.3
G_{se} - Effective Sp. Gravity	2.640			
P_{be} - Eff. Binder Content, %	4.54			
P_{ba} - Binder Absorbed, %	1.05			

FOP for AASHTO T 209 result within 0.020 of JMF? Gmm from JMF= 2.412 Gmm from Sample Tested= 2.430 **Yes**

FOP for AASHTO T 166 result within 0.020 of JMF? Gmb from JMF= 2.314 Gmb from Sample Tested= 2.318 **Yes**

ASTM D1075 & AASHTO T 167

Sample # 1-4, 6

90 % @ 0.50 % Evotherm M1

PASS

AASHTO T 340

Sample # 209MX016

Rutting Depth, mm	3.9
Left Sample	4.27
Center Sample	4.77
Right Sample	2.669

Maximum Allowable Rut Depth: 0.2 in. (5 mm)

PASS

Mix Design Volumetrics Confirmation: [X] **Pass** [ ] **Fail**

Remarks

Tested By	WAQTC Number
Jaime Conley, Armin Mirahcic, Dan Henscheid	24080, 24084, 24083

Date Mailed	Laboratory Manager's Signature
4/8/2020	Chad Clawson, P.E.

Figure A.5. District 3 – Field JMF P5

Design Specifications: Blend 1 / 75 Gyrations @ N Design PG 64-34

	Gyratory Compactor: Model # AFG2AS Serial # 8436	Job Mix Formula	Spec
1	Percent Asphalt by Weight of Total Mix	**6.2**	--
2	Percent Asphalt by Weight of Aggregate	6.66	--
3	Virgin Asphalt by Weight of Mix	5.21	--
4	Virgin Asphalt by Weight of Aggregate	5.58	--
5	Percent Air Voids (Pa)	4.0	4.0
6	Voids in Mineral Aggregate (VMA)	14.5	14 min
7	Compacted Unit Weight Gmb, pcf	2.204 137.2	--
8	Theoretical Maximum Density Gmm, pcf	**2.296 142.9**	--
9	Percent Effective Asphalt Content (Pbe)	4.90	--
10	Percent Absorbed Asphalt (Pba)	1.43	--
11	Specific Gravity of Binder (Gb)	**1.029**	--
12	Percent Gmm @ N Initial (7 Gyrations)	86.7	≤ 89.0
13	Percent Gmm @ N Design (75 Gyrations)	96.0	96.0
14	Percent Gmm @ N Max (115 Gyrations)	97.2	≤ 98.0
15	Dust to Asphalt Ratio (DP)	1.3	0.6-1.4
16	Percent Passing #200 Sieve	6.5	2.0-10.0
17	Voids Filled w/ Asphalt (VFA)	72	65-75
18	Laboratory Mixing Temperature for Design (°F)	327	320-333
19	Laboratory Compaction Temperature for Design (°F)	**299**	291-306
20	Laboratory Sample Weight for Volumetric Testing (g)	**4365**	--
21	Ignition Oven (NCAT) Correction Factor @ 538 °F	**0.38**	--
22	Sand Equivalent	45	40 min
23	Fracture Face Count (%)	100/100	75/60
24	Fine Aggregate Angularity (%)	45.2	40 min
25	Flat and Elongated Particles in Coarse Aggregates (%)	0.0	10 Max
	Recycled Asphalt Pavement (RAP) Properties		
26	Percentage of Asphalt in RAP (Wt. of Mix)	5.40	--
27	Percentage of RAP by Total Weight of Aggregate	19	--
28	Percent of RAP Binder by Weight of Total Binder	17	17 max
29	RAP Contribution by Mix	1.03	--
30	RAP Contribution by Aggregate	1.08	--
31	RAP NCAT Correction Factor	0.47	--

Figure A.6. District 4 -Field JMF P2

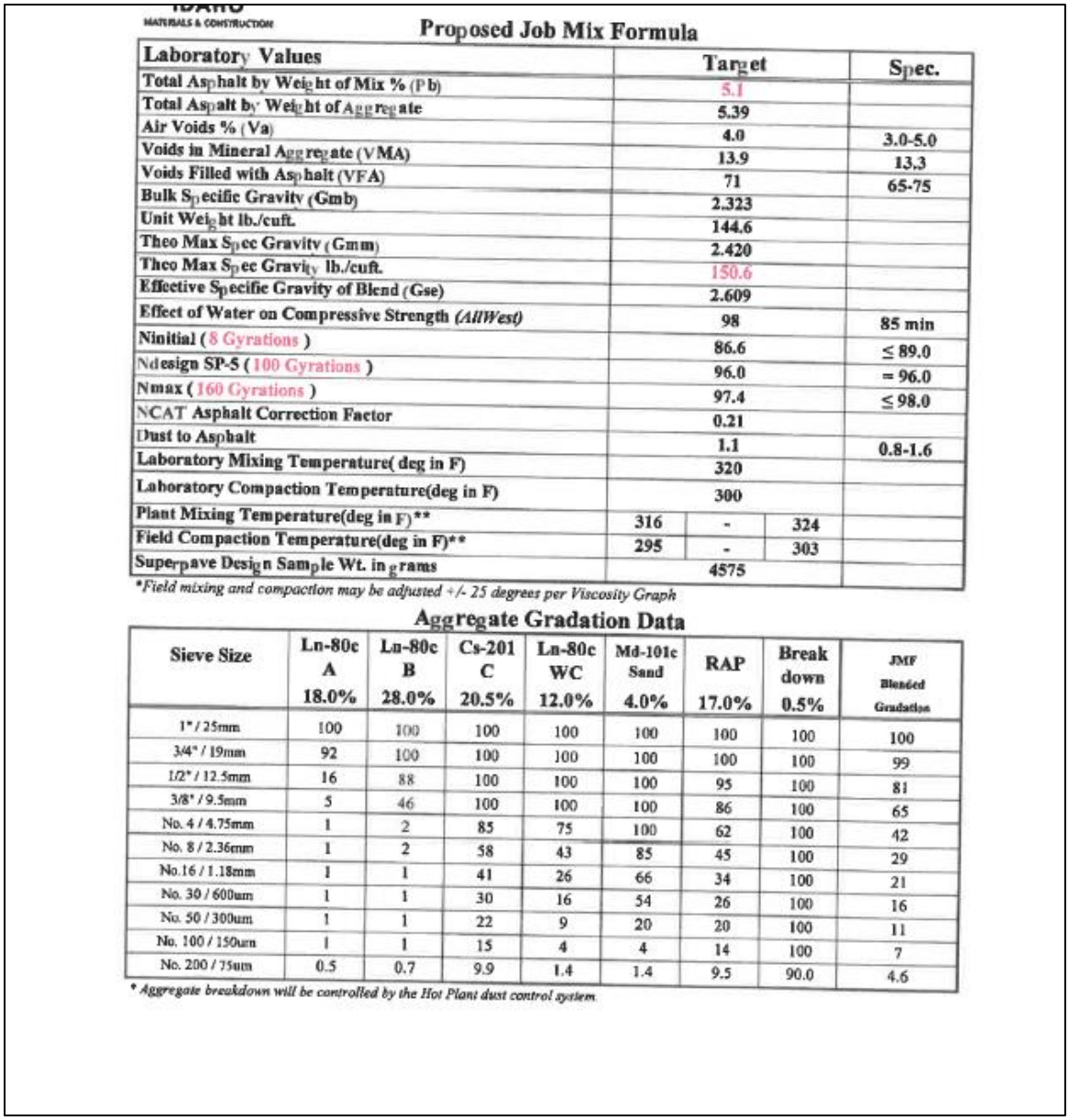

IDAHO
MATERIALS & CONSTRUCTION

Proposed Job Mix Formula

Laboratory Values	Target			Spec.
Total Asphalt by Weight of Mix % (Pb)	5.1			
Total Asphalt by Weight of Aggregate	5.39			
Air Voids % (Va)	4.0			3.0-5.0
Voids in Mineral Aggregate (VMA)	13.9			13.3
Voids Filled with Asphalt (VFA)	71			65-75
Bulk Specific Gravity (Gmb)	2.323			
Unit Weight lb./cuft.	144.6			
Theo Max Spec Gravity (Gmm)	2.420			
Theo Max Spec Gravity lb./cuft.	150.6			
Effective Specific Gravity of Blend (Gse)	2.609			
Effect of Water on Compressive Strength *(AllWest)*	98			85 min
Ninitial (8 Gyrations)	86.6			≤ 89.0
Ndesign SP-5 (100 Gyrations)	96.0			= 96.0
Nmax (160 Gyrations)	97.4			≤ 98.0
NCAT Asphalt Correction Factor	0.21			
Dust to Asphalt	1.1			0.8-1.6
Laboratory Mixing Temperature(deg in F)	320			
Laboratory Compaction Temperature(deg in F)	300			
Plant Mixing Temperature(deg in F)**	316	-	324	
Field Compaction Temperature(deg in F)**	295	-	303	
Superpave Design Sample Wt. in grams	4575			

**Field mixing and compaction may be adjusted +/- 25 degrees per Viscosity Graph*

Aggregate Gradation Data

Sieve Size	Ln-80c A 18.0%	Ln-80c B 28.0%	Cs-201 C 20.5%	Ln-80c WC 12.0%	Md-101c Sand 4.0%	RAP 17.0%	Break down 0.5%	JMF Blended Gradation
1" / 25mm	100	100	100	100	100	100	100	100
3/4" / 19mm	92	100	100	100	100	100	100	99
1/2" / 12.5mm	16	88	100	100	100	95	100	81
3/8" / 9.5mm	5	46	100	100	100	86	100	65
No. 4 / 4.75mm	1	2	85	75	100	62	100	42
No. 8 / 2.36mm	1	2	58	43	85	45	100	29
No.16 / 1.18mm	1	1	41	26	66	34	100	21
No. 30 / 600um	1	1	30	16	54	26	100	16
No. 50 / 300um	1	1	22	9	20	20	100	11
No. 100 / 150um	1	1	15	4	4	14	100	7
No. 200 / 75um	0.5	0.7	9.9	1.4	1.4	9.5	90.0	4.6

** Aggregate breakdown will be controlled by the Hot Plant dust control system.*

Figure A.7. District 4 – Field JMF P5

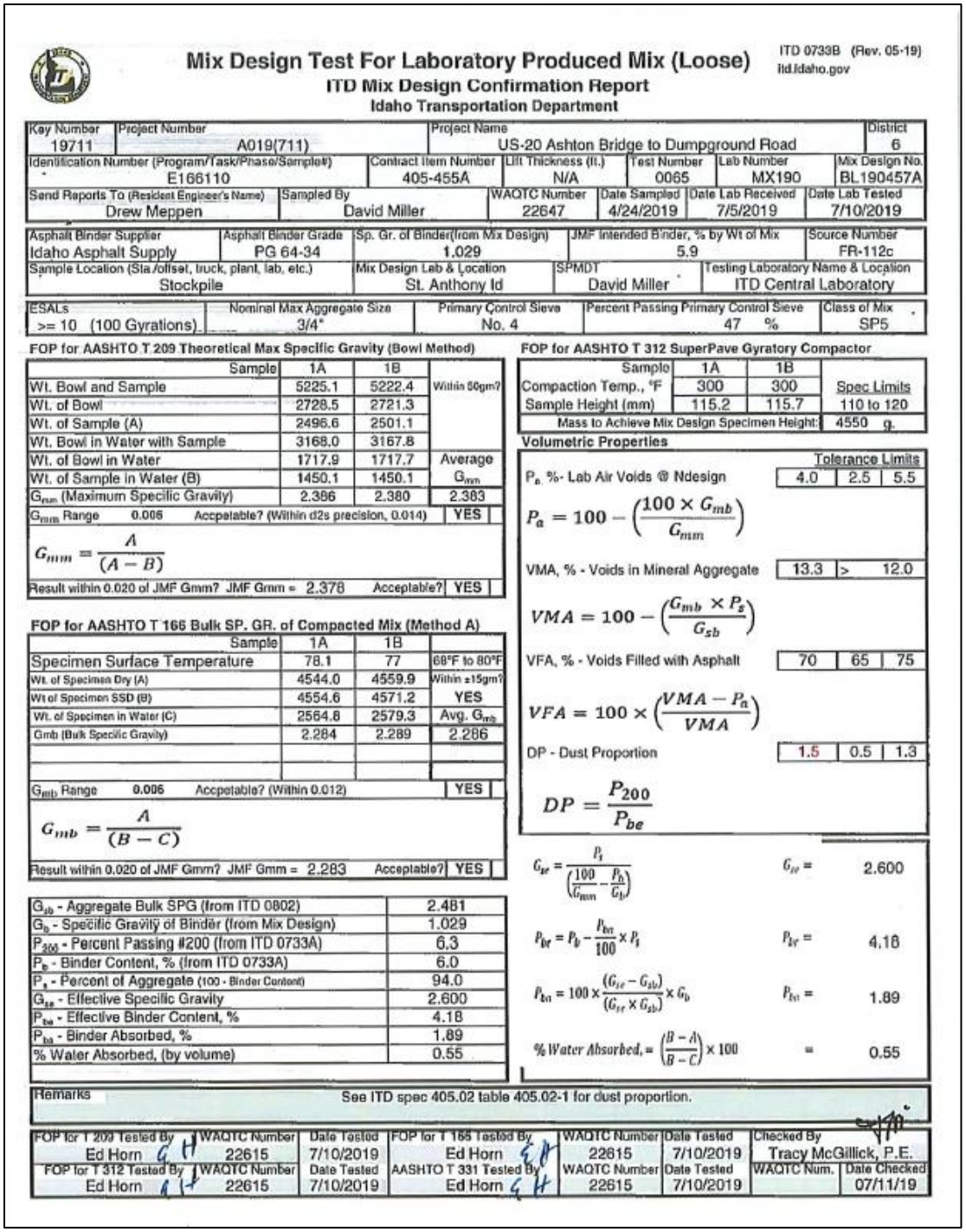

Mix Design Test For Laboratory Produced Mix (Loose)

ITD 0733B (Rev. 05-19)
itd.idaho.gov

ITD Mix Design Confirmation Report

Idaho Transportation Department

Key Number	Project Number	Project Name	District
19711	A019(711)	US-20 Ashton Bridge to Dumpground Road	6

Identification Number (Program/Task/Phase/Sample#)	Contract Item Number	Lift Thickness (ft.)	Test Number	Lab Number	Mix Design No.
E166110	405-455A	N/A	0065	MX190	BL190457A

Send Reports To (Resident Engineer's Name)	Sampled By	WAQTC Number	Date Sampled	Date Lab Received	Date Lab Tested
Drew Meppen	David Miller	22647	4/24/2019	7/5/2019	7/10/2019

Asphalt Binder Supplier	Asphalt Binder Grade	Sp. Gr. of Binder(from Mix Design)	JMF Intended Binder, % by Wt of Mix	Source Number
Idaho Asphalt Supply	PG 64-34	1.029	5.9	FR-112c

Sample Location (Sta./offset, truck, plant, lab, etc.)	Mix Design Lab & Location	SPMDT	Testing Laboratory Name & Location
Stockpile	St. Anthony Id	David Miller	ITD Central Laboratory

ESALs	Nominal Max Aggregate Size	Primary Control Sieve	Percent Passing Primary Control Sieve	Class of Mix
>= 10 (100 Gyrations)	3/4"	No. 4	47 %	SP5

FOP for AASHTO T 209 Theoretical Max Specific Gravity (Bowl Method)

Sample	1A	1B	
Wt. Bowl and Sample	5225.1	5222.4	Within 50gm?
Wt. of Bowl	2728.5	2721.3	
Wt. of Sample (A)	2496.6	2501.1	
Wt. Bowl in Water with Sample	3168.0	3167.8	
Wt. of Bowl in Water	1717.9	1717.7	Average
Wt. of Sample in Water (B)	1450.1	1450.1	G_{mm}
G_{mm} (Maximum Specific Gravity)	2.386	2.380	2.383
G_{mm} Range 0.006	Acceptable? (Within d2s precision, 0.014)		YES

$$G_{mm} = \frac{A}{(A - B)}$$

Result within 0.020 of JMF Gmm? JMF Gmm = 2.378 Acceptable? YES

FOP for AASHTO T 166 Bulk SP. GR. of Compacted Mix (Method A)

Sample	1A	1B	
Specimen Surface Temperature	78.1	77	68°F to 80°F
Wt. of Specimen Dry (A)	4544.0	4559.9	Within ±15gm?
Wt of Specimen SSD (B)	4554.6	4571.2	YES
Wt. of Specimen in Water (C)	2564.8	2579.3	Avg. G_{mb}
Gmb (Bulk Specific Gravity)	2.284	2.289	2.286
G_{mb} Range 0.006	Acceptable? (Within 0.012)		YES

$$G_{mb} = \frac{A}{(B - C)}$$

Result within 0.020 of JMF Gmm? JMF Gmm = 2.283 Acceptable? YES

G_{sb} - Aggregate Bulk SPG (from ITD 0802)	2.481
G_b - Specific Gravity of Binder (from Mix Design)	1.029
P_{200} - Percent Passing #200 (from ITD 0733A)	6.3
P_b - Binder Content, % (from ITD 0733A)	6.0
P_s - Percent of Aggregate (100 - Binder Content)	94.0
G_{se} - Effective Specific Gravity	2.600
P_{be} - Effective Binder Content, %	4.18
P_{ba} - Binder Absorbed, %	1.89
% Water Absorbed, (by volume)	0.55

FOP for AASHTO T 312 SuperPave Gyratory Compactor

Sample	1A	1B	
Compaction Temp., °F	300	300	Spec Limits
Sample Height (mm)	115.2	115.7	110 to 120
Mass to Achieve Mix Design Specimen Height:			4550 g.

Volumetric Properties

	Tolerance Limits		
P_a %- Lab Air Voids @ Ndesign	4.0	2.5	5.5

$$P_a = 100 - \left(\frac{100 \times G_{mb}}{G_{mm}}\right)$$

VMA, % - Voids in Mineral Aggregate	13.3	>	12.0

$$VMA = 100 - \left(\frac{G_{mb} \times P_s}{G_{sb}}\right)$$

VFA, % - Voids Filled with Asphalt	70	65	75

$$VFA = 100 \times \left(\frac{VMA - P_a}{VMA}\right)$$

DP - Dust Proportion	1.5	0.5	1.3

$$DP = \frac{P_{200}}{P_{be}}$$

$$G_{se} = \frac{P_s}{\left(\frac{100}{G_{mm}} - \frac{P_b}{G_b}\right)} \qquad G_{se} = 2.600$$

$$P_{be} = P_b - \frac{P_{ba}}{100} \times P_s \qquad P_{be} = 4.18$$

$$P_{ba} = 100 \times \frac{(G_{se} - G_{sb})}{(G_{se} \times G_{sb})} \times G_b \qquad P_{ba} = 1.89$$

$$\%\ Water\ Absorbed, = \left(\frac{B - A}{B - C}\right) \times 100 \qquad = 0.55$$

Remarks: See ITD spec 405.02 table 405.02-1 for dust proportion.

FOP for T 209 Tested By	WAQTC Number	Date Tested	FOP for T 166 Tested By	WAQTC Number	Date Tested	Checked By
Ed Horn	22615	7/10/2019	Ed Horn	22615	7/10/2019	Tracy McGillick, P.E.
FOP for T 312 Tested By	**WAQTC Number**	**Date Tested**	**AASHTO T 331 Tested By**	**WAQTC Number**	**Date Tested**	**WAQTC Num. / Date Checked**
Ed Horn	22615	7/10/2019	Ed Horn	22615	7/10/2019	07/11/19

Figure A.8. District 6 – Field JMF P1

Appendix B: Mix Stability Testing Results

Table B.1 Summary of Mix Stability Indices for SP5 Mix Design @ 0.0 percent RAP Content

Summary Report	0 percent RAP@ 4.25 B.C.	0 percent RAP@ 5 B.C.	0 percent RAP@5.75 B.C.
CDI (Average)	4640	3307	501
CDI (Std. Dev.)	622	127	192
CEI (Average)	0.37	0.56	2.90
CEI (Std. Dev.)	0.05	0.04	0.48
L.P. (Average)	54	57	0
L.P. (Std. Dev.)	4	0	0
WEI (Average)	3.96	5.11	10.59
WEI (Std. Dev.)	0.19	0.25	0.78
CFI (Average)	2387	1351	387
CFI (Std. Dev.)	58	61	97
GSI (1) (Average)	0.61	0.76	4.87
GSI (1) (Std. Dev.)	0.12	0.09	0.70
GSI (2) (Average)	0.64	0.76	4.98
GSI (2) (Std. Dev.)	0.16	0.07	0.55
LCI (4 percent) (Average)	20.74	22.53	30.32
LCI (4 percent) (Std. Dev.)	0.40	0.52	0.86
LCI (7 percent) (Average)	21.52	23.14	28.19
LCI (7 percent) (Std. Dev.)	0.23	0.36	0.50

Table B.2 Summary of Mix Stability Indices for SP5 Mix Design @ 25.0 percent RAP Content

Summary Report	25 percent RAP@ 4.25 B.C.	25 percent RAP@ 5 B.C.	25 percent RAP@ 5.75 B.C.
CDI (Average)	7713	4864	593
CDI (Std. Dev.)	64	67	64
CEI (Average)	0.16	0.32	2.65
CEI (Std. Dev.)	0.01	0.01	0.21
L.P. (Average)	56	57	0
L.P. (Std. Dev.)	3	1	0
WEI (Average)	2.78	3.84	10.11
WEI (Std. Dev.)	0.02	0.09	0.31
CFI (Average)	3445	1851	426
CFI (Std. Dev.)	126	10	3
GSI (1) (Average)	0.20	0.40	2.98
GSI (1) (Std. Dev.)	0.02	0.01	0.25
GSI (2) (Average)	0.25	0.42	4.38
GSI (2) (Std. Dev.)	0.03	0.02	0.55
LCI (4 percent) (Average)	17.89	22.17	29.69
LCI (4 percent) (Std. Dev.)	0.41	2.45	0.47
LCI (7 percent) (Average)	25.03	22.66	27.90
LCI (7 percent) (Std. Dev.)	0.08	1.74	0.26

Table B.3 Summary of Mix Stability Indices for SP5 Mix Design @ 50 percent RAP Content

Summary Report	50 percent RAP@ 4.25 B.C.	50 percent RAP@ 5 B.C.	50 percent RAP@ 5.75 B.C.
CDI (Average)	4561	3671	906
CDI (Std. Dev.)	630	126	1
CEI (Average)	0.35	0.43	1.90
CEI (Std. Dev.)	0.07	0.01	0.08
L.P. (Average)	52	51	0
L.P. (Std. Dev.)	2	4	0
WEI (Average)	3.90	4.44	8.81
WEI (Std. Dev.)	0.36	0.18	0.22
CFI (Average)	2296	1542	643
CFI (Std. Dev.)	416	23	34
GSI (1) (Average)	0.57	0.55	2.46
GSI (1) (Std. Dev.)	0.15	0.02	0.02
GSI (2) (Average)	0.61	0.59	3.61
GSI (2) (Std. Dev.)	0.12	0.01	0.22
LCI (4 percent) (Average)	20.38	20.99	27.69
LCI (4 percent) (Std. Dev.)	0.75	0.10	0.36
LCI (7 percent) (Average)	21.25	21.86	26.50
LCI (7 percent) (Std. Dev.)	0.53	0.19	0.37

Table B.4 Summary of Mix Stability Indices for SP3 Mix Design @ 0.0percent RAP Content

Summary Report	0 percent RAP@ 4.25 B.C.	0 percent RAP@ 5.0 B.C.	0 percent RAP@5.75 B.C.
CDI (Average)	4640	3307	501
CDI (Std. Dev.)	622	127	192
CEI (Average)	0.37	0.56	2.90
CEI (Std. Dev.)	0.05	0.04	0.48
L.P. (Average)	54	57	0
L.P. (Std. Dev.)	4	0	0
WEI (Average)	3.91	5.11	10.59
WEI (Std. Dev.)	0.12	0.25	0.78
CFI (Average)	2387	1351	387
CFI (Std. Dev.)	58	61	97
GSI (1) (Average)	0.61	0.76	4.87
GSI (1) (Std. Dev.)	0.12	0.09	0.70
GSI (2) (Average)	0.64	0.76	4.98
GSI (2) (Std. Dev.)	0.16	0.07	0.55
LCI (4 percent) (Average)	20.77	22.56	30.11
LCI (4 percent) (Std. Dev.)	0.44	0.47	0.82
LCI (7 percent) (Average)	21.53	23.14	28.08
LCI (7 percent) (Std. Dev.)	0.22	0.36	0.66

Table B.5 Summary of Mix Stability Indices for SP3 Mix Design @ 25percent RAP Content

Summary Report	25 percent RAP@ 4.25 B.C.	25 percent RAP@ 5.0 B.C.	25 percent RAP@ 5.75 B.C.
CDI (Average)	6564	2244	817
CDI (Std. Dev.)	1199	502	129
CEI (Average)	0.19	0.78	1.98
CEI (Std. Dev.)	0.05	0.16	0.31
L.P. (Average)	54	54	0
L.P. (Std. Dev.)	3	2	0
WEI (Average)	3.70	6.06	9.24
WEI (Std. Dev.)	0.58	0.65	0.49
CFI (Average)	3280	1237	570
CFI (Std. Dev.)	473	237	73
GSI (1) (Average)	0.25	1.26	3.40
GSI (1) (Std. Dev.)	0.10	0.18	0.58
GSI (2) (Average)	0.32	1.34	3.51
GSI (2) (Std. Dev.)	0.11	0.23	0.42
LCI (4 percent) (Average)	18.23	23.58	28.17
LCI (4 percent) (Std. Dev.)	1.08	0.80	0.65
LCI (7 percent) (Average)	19.90	23.83	27.01
LCI (7 percent) (Std. Dev.)	0.89	0.62	0.24

Table B.6 Summary of Mix Stability Indices for SP3 Mix Design @ 50 percent RAP

Summary Report	50 percent RAP@ 4.25 B.C.	50 percent RAP@ 5.0 B.C.	50 percent RAP@ 5.75 B.C.
CDI (Average)	8403	2247	817
CDI (Std. Dev.)	121	250	126
CEI (Average)	0.08	0.70	1.73
CEI (Std. Dev.)	0.01	0.05	0.20
L.P. (Average)	55	51	0
L.P. (Std. Dev.)	1	1	4
WEI (Average)	2.48	5.88	9.09
WEI (Std. Dev.)	0.05	0.28	0.52
CFI (Average)	4079	1252	558
CFI (Std. Dev.)	3	129	88
GSI (1) (Average)	0.08	1.08	2.61
GSI (1) (Std. Dev.)	0.02	0.05	0.52
GSI (2) (Average)	0.13	1.22	3.00
GSI (2) (Std. Dev.)	0.03	0.10	0.35
LCI (4 percent) (Average)	15.22	22.92	27.43
LCI (4 percent) (Std. Dev.)	0.77	0.23	0.93
LCI (7 percent) (Average)	18.61	23.47	26.66
LCI (7 percent) (Std. Dev.)	0.26	0.21	0.75

==========

File Name: FEB20_05.DAT

Time: 20:56 RP280_50%RAP PG58-34_5%BC Time:

Date: 02/19/2020 Axial Force Axial Displacement 11/30/2020 16:45

Diameter: 150 mm lbf in 35.97363 Sec

S/N: 8835

==========

Gyration (#)	Height (mm)	Angle (Deg Int)	Pressure (kPa)	Moment (N-m)
0	140.1	----	597	0.0
1	135.3	1.17	575	654.0
2	132.4	1.16	575	759.9
3	130.3	1.15	580	813.6
4	128.7	1.15	594	844.8
5	127.4	1.16	599	862.8
6	126.3	1.16	601	871.8
7	125.4	1.16	601	877.6
8	124.6	1.15	601	881.4
9	123.9	1.15	601	885.3
10	123.3	1.16	601	890.2
11	122.7	1.16	601	893.6
12	122.2	1.16	601	894.4
13	121.7	1.16	601	894.6
14	121.3	1.16	601	896.5
15	120.9	1.16	601	896.2
16	120.5	1.16	601	896.4
17	120.2	1.16	601	896.2
18	119.9	1.16	601	896.3
19	119.6	1.16	601	897.9
20	119.3	1.16	601	900.7
21	119.0	1.16	601	900.9
22	118.8	1.16	601	901.8
23	118.5	1.16	600	901.2
24	118.3	1.16	600	900.0
25	118.1	1.16	600	899.3
26	117.9	1.16	600	897.5
27	117.7	1.16	600	896.5

Figure B.1 Sample of Compaction Data for PG 58-34 (50 percent RAP-5.0 percent B.C.)

File Name: FEB20_05.DAT
RP280_50%RAP PG58-34_5%BC
Axial Displacement

S/N: 8835

Gyration (#)	Height (mm)	Angle (Deg Int)	Pressure (kPa)	Moment (N-m)
34	116.6	1.16	599	887.4
35	116.4	1.16	599	885.5
36	116.3	1.16	600	884.2
37	116.2	1.16	600	882.6
38	116.0	1.16	600	881.9
39	115.9	1.16	600	881.4
40	115.8	1.16	600	880.4
41	115.7	1.16	600	880.4
42	115.6	1.16	600	880.7
43	115.5	1.16	600	881.0
44	115.4	1.16	600	880.0
45	115.3	1.16	600	879.2
46	115.2	1.16	600	879.4
47	115.1	1.16	600	879.0
48	115.0	1.16	600	877.6
49	114.9	1.16	601	876.4
50	114.8	1.16	601	876.2
51	114.7	1.16	601	874.2
52	114.6	1.16	601	873.0
53	114.5	1.16	601	871.3
54	114.5	1.16	601	869.3
55	114.4	1.16	601	867.5
56	114.3	1.16	601	867.1
57	114.2	1.16	601	866.4
58	114.2	1.16	601	866.2
59	114.1	1.16	601	865.7
60	114.0	1.16	601	865.8
61	114.0	1.16	601	865.0
62	113.9	1.16	601	864.4
63	113.8	1.16	601	864.2

Figure B.1 Sample of Compaction Data for PG 58-34 (50 percent RAP-5.0 percent B.C.) (cont.)

==========

File Name: FEB20_05.DAT
RP280_50%RAP PG58-34_5%BC
Axial Displacement

S/N: 8835

==========

Gyration	Height	Angle	Pressure	Moment
64	113.8	1.16	601	863.2
65	113.7	1.16	601	862.8
66	113.6	1.16	601	861.5
67	113.6	1.16	601	861.5
68	113.5	1.16	601	860.8
69	113.5	1.16	601	860.3
70	113.4	1.16	601	859.8
71	113.3	1.16	601	859.9
72	113.3	1.16	601	859.4
73	113.2	1.16	601	859.4
74	113.2	1.16	602	858.8
75	113.1	1.16	602	857.7
76	113.1	1.16	602	857.2
77	113.0	1.16	602	856.8
78	113.0	1.16	602	856.1
79	112.9	1.16	602	855.6
80	112.9	1.16	602	854.4
81	112.8	1.16	602	853.3
82	112.8	1.16	602	852.3
83	112.7	1.16	602	851.6
84	112.7	1.16	602	850.8
85	112.6	1.16	602	849.8
86	112.6	1.16	602	850.3
87	112.6	1.16	602	849.6
88	112.5	1.16	602	848.5
89	112.5	1.16	602	848.3
90	112.4	1.16	602	848.1
91	112.4	1.16	602	846.0

Figure B.1 Sample of Compaction Data for PG 58-34 (50 percent RAP-5.0 percent B.C.) (cont.).

==========

File Name: FEB20_05.DAT
RP280_50%RAP PG58-34_5%BC
Axial Displacement

S/N: 8835

==========

Gyration	Height	Angle	Pressure	Moment
92	112.4	1.16	602	844.9
93	112.3	1.16	602	843.2
94	112.3	1.16	602	842.1
95	112.2	1.16	602	842.0
96	112.2	1.16	602	840.4
97	112.2	1.16	602	840.5
98	112.1	1.15	602	834.7
99	112.1	1.15	602	834.7
100	112.0	1.15	602	834.9
101	112.0	1.15	602	835.3
102	112.0	1.15	602	835.3
103	111.9	1.15	602	834.6
104	111.9	1.15	602	834.5
105	111.9	1.15	602	834.0
106	111.8	1.15	602	833.3
107	111.8	1.15	602	833.0
108	111.8	1.15	602	832.3
109	111.7	1.15	602	831.8
110	111.7	1.15	602	832.2
111	111.7	1.15	602	831.9
112	111.7	1.15	602	831.0
113	111.6	1.15	602	830.1
114	111.6	1.15	602	828.8
115	111.6	1.16	602	829.0
116	111.5	1.15	602	829.4
117	111.5	1.16	602	828.6
118	111.5	1.16	602	828.6

Figure B.1 Sample of Compaction Data for PG 58-34 (50 percent RAP-5.0 percent B.C.) (cont.)

==========

File Name: FEB20_05.DAT
RP280_50%RAP PG58-34_5%BC
Axial Displacement

S/N: 8835

==========

Gyration (#)	Height (mm)	Angle (Deg Int)	Pressure (kPa)	Moment (N-m)
147	110.8	1.16	603	821.2
148	110.7	1.16	602	820.3
149	110.7	1.16	602	820.0
150	110.7	1.16	602	819.7
151	110.7	1.16	603	819.4
152	110.6	1.16	603	819.0
153	110.6	1.16	603	818.6
154	110.6	1.16	603	818.6
155	110.6	1.16	603	817.9
156	110.6	1.16	603	817.9
157	110.5	1.16	603	817.5
158	110.5	1.16	603	816.6
159	110.5	1.16	603	816.7
160	110.5	1.16	603	816.5
161	110.5	1.16	603	816.3
162	110.5	1.16	603	816.1
163	110.4	1.16	603	816.4
164	110.4	1.16	603	817.3
165	110.4	1.16	603	818.1
166	110.4	1.16	603	817.8
167	110.4	1.16	603	816.8
168	110.3	1.16	603	817.4
169	110.3	1.16	603	817.1
170	110.3	1.16	603	816.6
171	110.3	1.16	603	816.3
172	110.3	1.16	603	815.3
173	110.3	1.16	603	814.6
174	110.2	1.16	603	813.9
175	110.2	1.16	603	813.9
176	110.2	1.16	603	813.2
177	110.2	1.16	603	812.4
178	110.2	1.16	603	812.1

Figure B.1 Sample of Compaction Data for PG 58-34 (50 percent RAP-5.0 percent B.C.) (cont.)

==========

File Name: FEB20_05.DAT

RP280_50%RAP PG58-34_5%BC

Axial Displacement

S/N: 8835

==========

Gyration	Height	Angle	Pressure	Moment
179	110.2	1.16	603	812.2
180	110.1	1.16	603	812.3
181	110.1	1.16	603	811.8
182	110.1	1.16	603	811.9
183	110.1	1.16	603	810.8
184	110.1	1.16	603	810.3
185	110.1	1.16	603	809.8
186	110.0	1.16	603	809.4
187	110.0	1.16	603	808.2
188	110.0	1.16	603	807.4
189	110.0	1.16	603	807.0

Figure B.1 Sample of Compaction Data for PG 58-34 (50 percent RAP-5.0 percent B.C.) (cont.)

Appendix C: Rutting and Cracking Samples

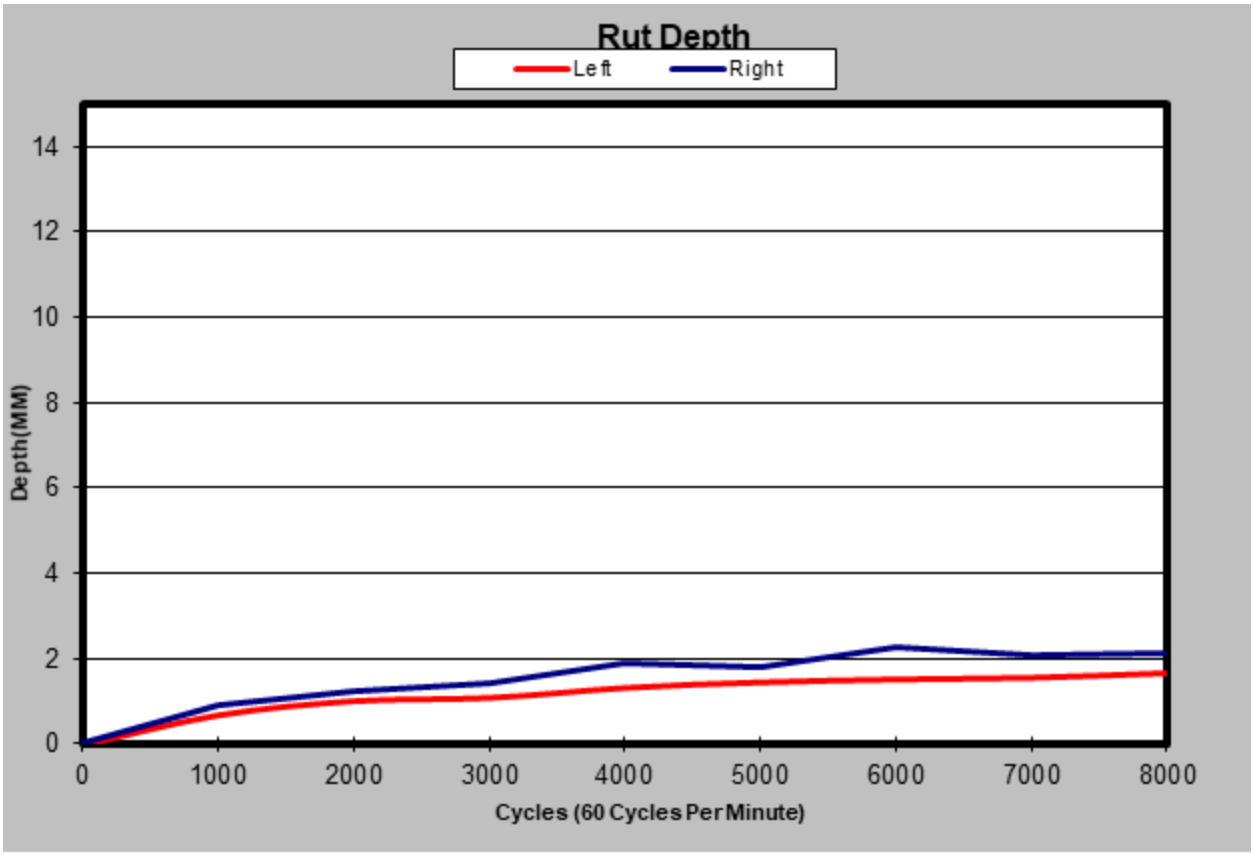

Figure C.1. APA Rutting Data Sample PG 64-28 (0 percent RAP-5.0 percent B.C)

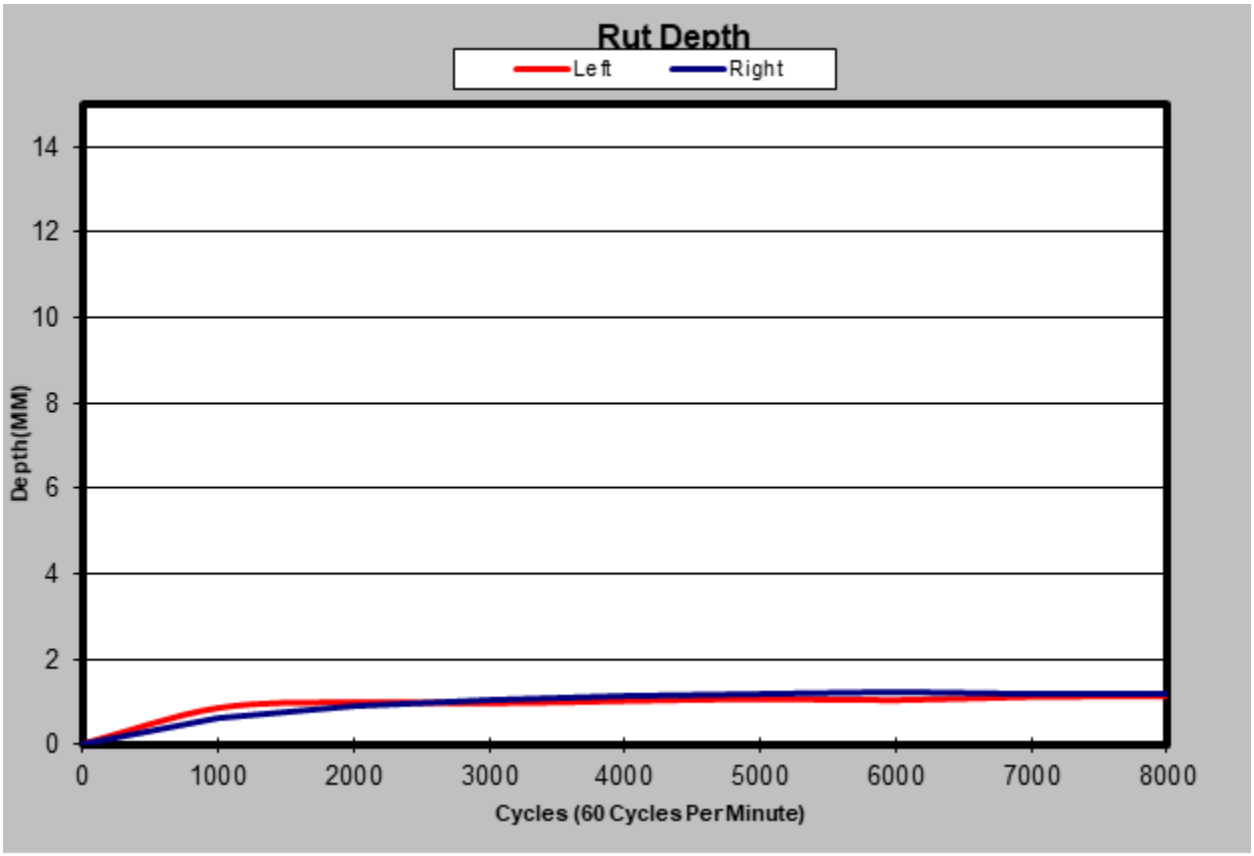

Figure C.2. APA Rutting Data Sample PG 58-34 (25 percent RAP-5.0 percent B.C)

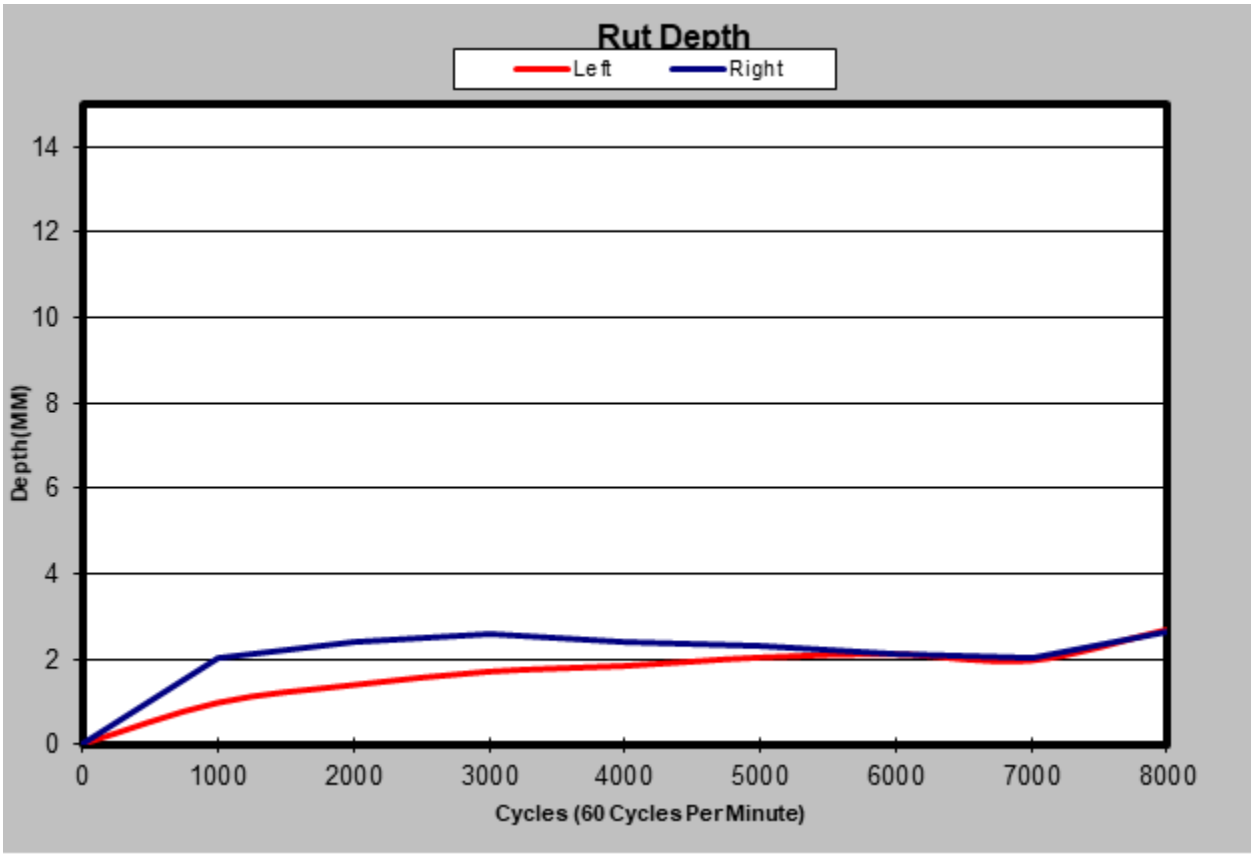

Figure C.3. APA Rutting Data Sample PG 76-22 (50 percent RAP-5.75 percent B.C)

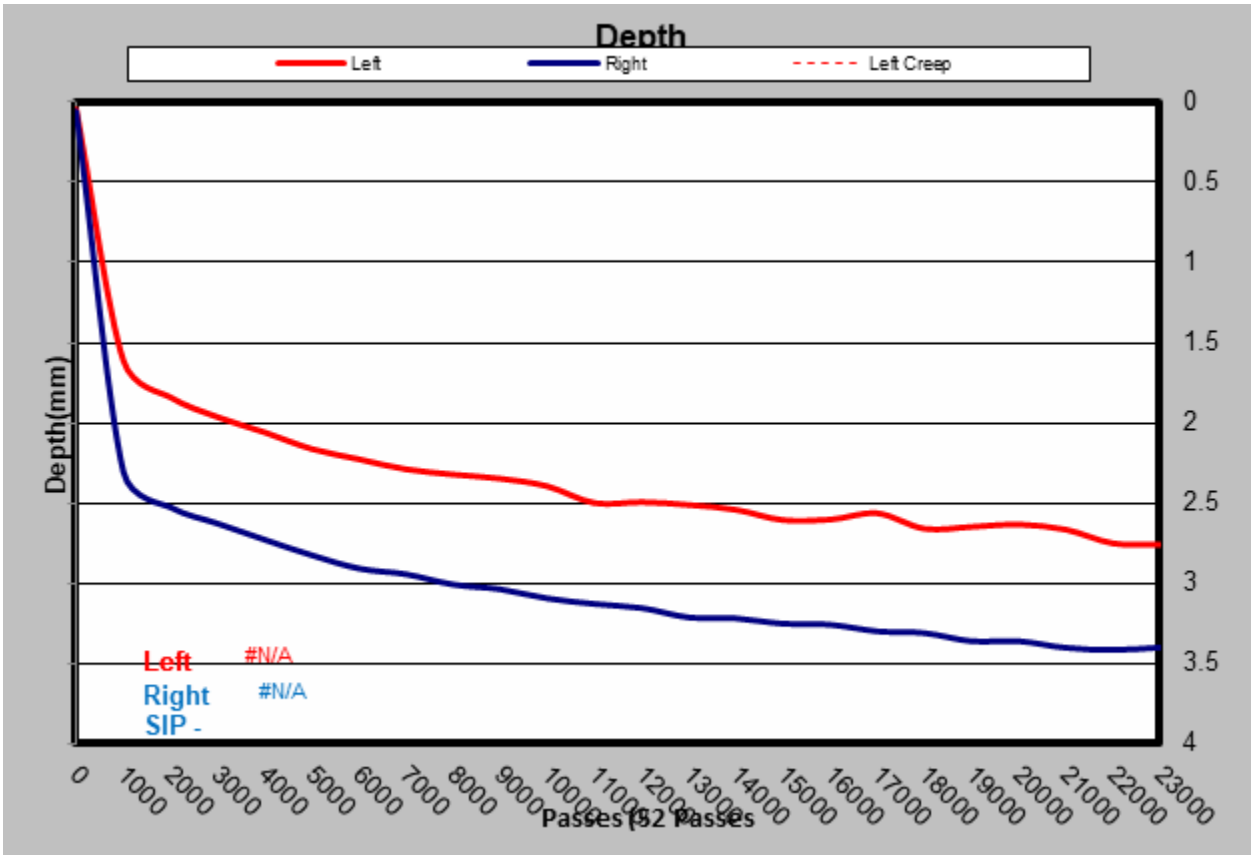

Figure C.4. HWTT Rutting Data Sample PG 58-34 (0 percent RAP-4.25 percent B.C)

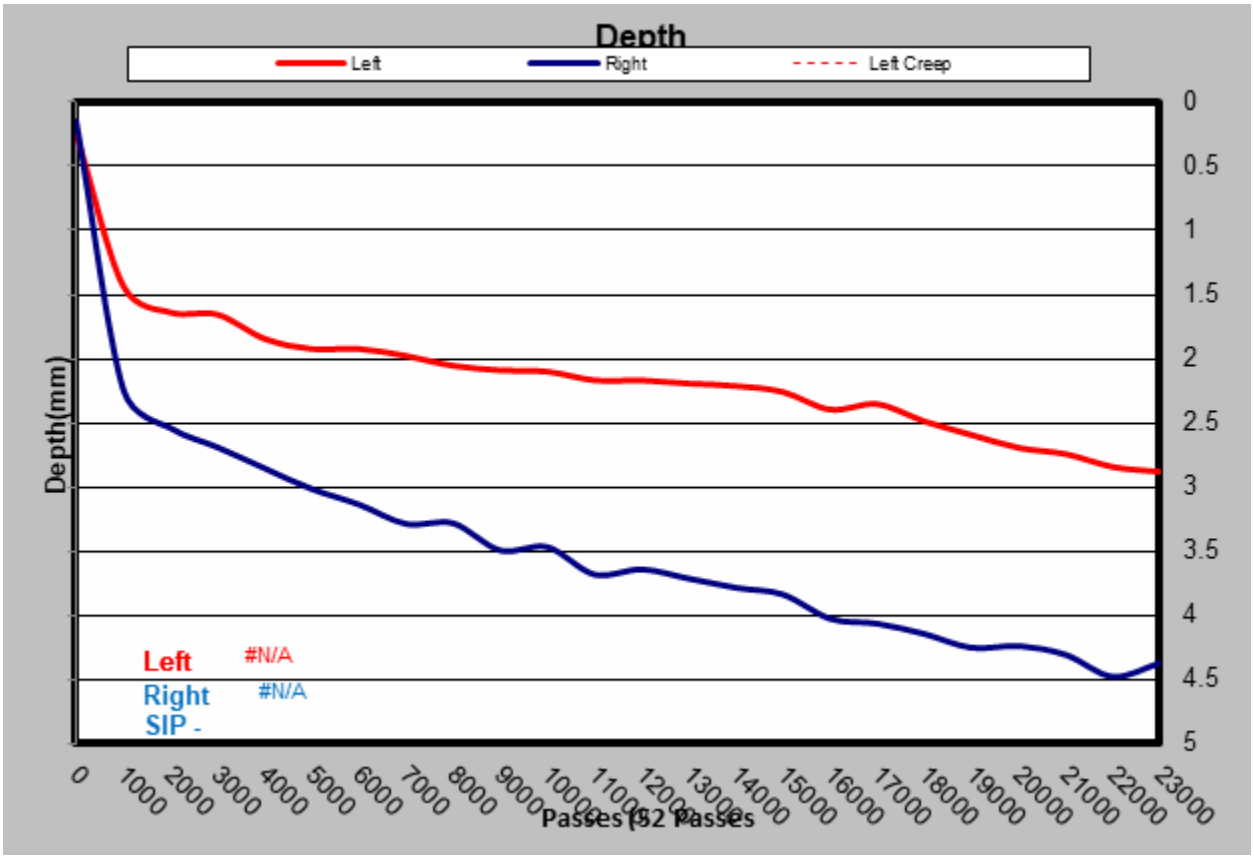

Figure C.5. HWTT Rutting Data Sample PG 64-28 (25 percent RAP-5.0 percent B.C)

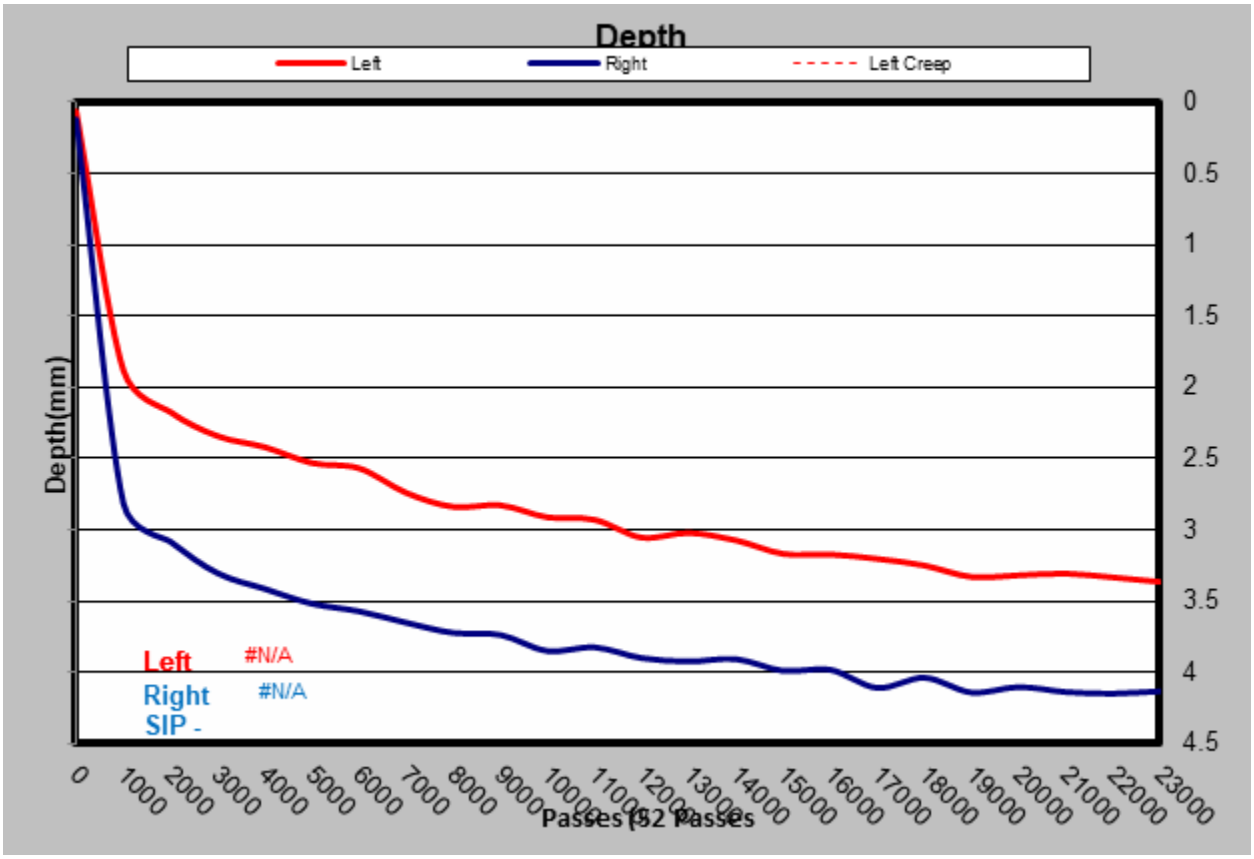

Figure C.6. HWTT Rutting Data Sample PG 58-34 (50 percent RAP-5.75 percent B.C)

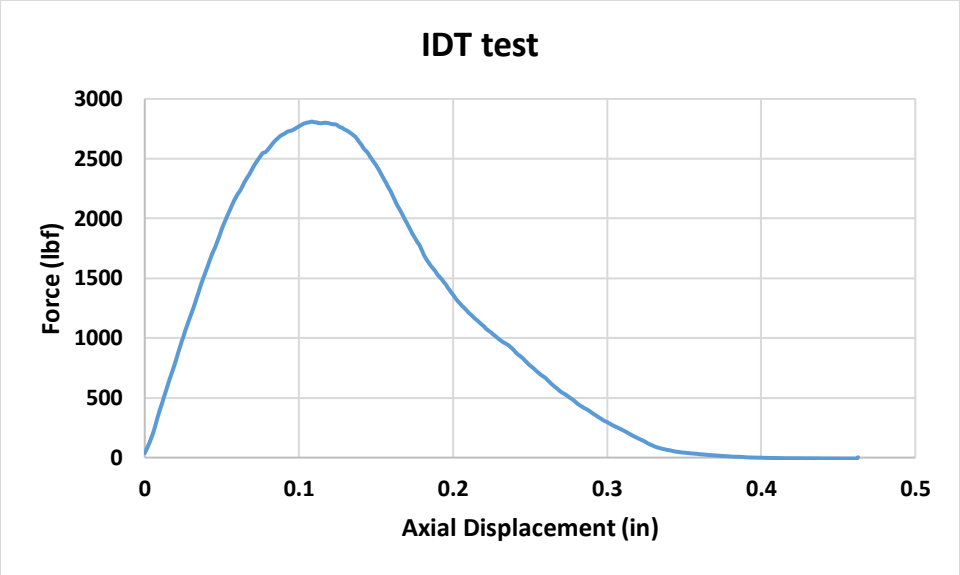

Figure C.7. Dry IDT Test Sample 0 percent RAP, 0 percent ASA, 5.0 percent B.C.

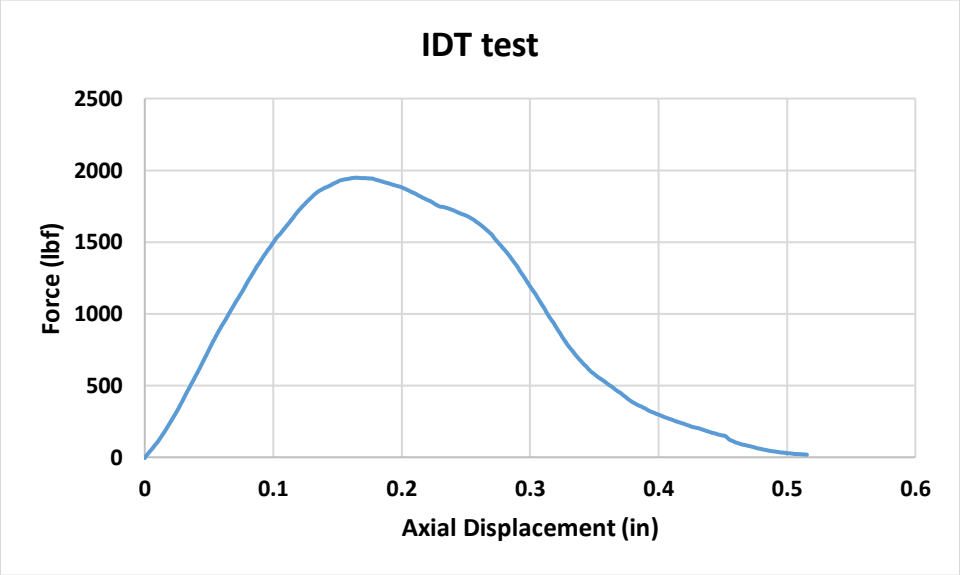

Figure C.8. Wet IDT Test Sample 0 percent RAP, 0 percent ASA, 5.0 percent B.C.

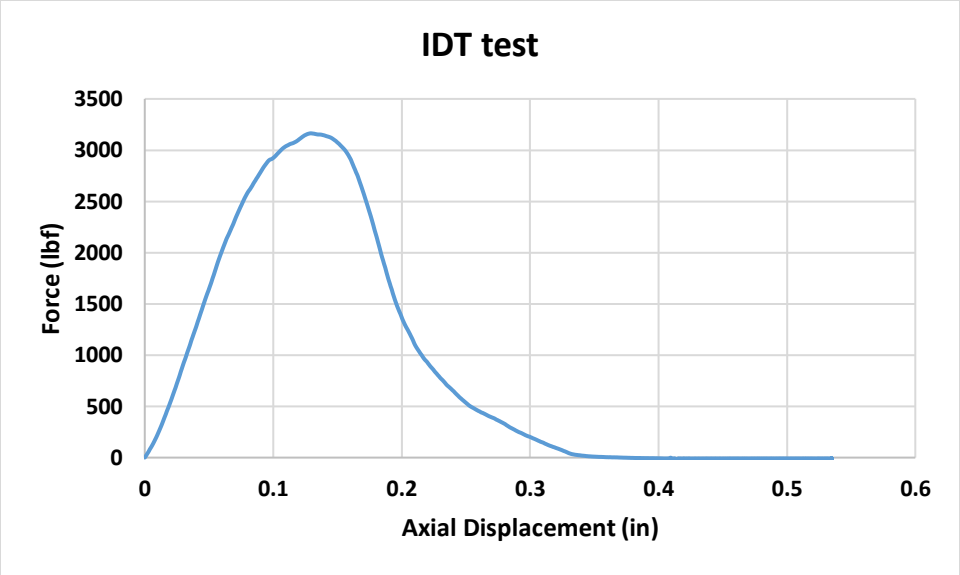

Figure C.9. Dry IDT Test Sample 0 percent RAP, 0 percent ASA, 4.25 percent B.C.

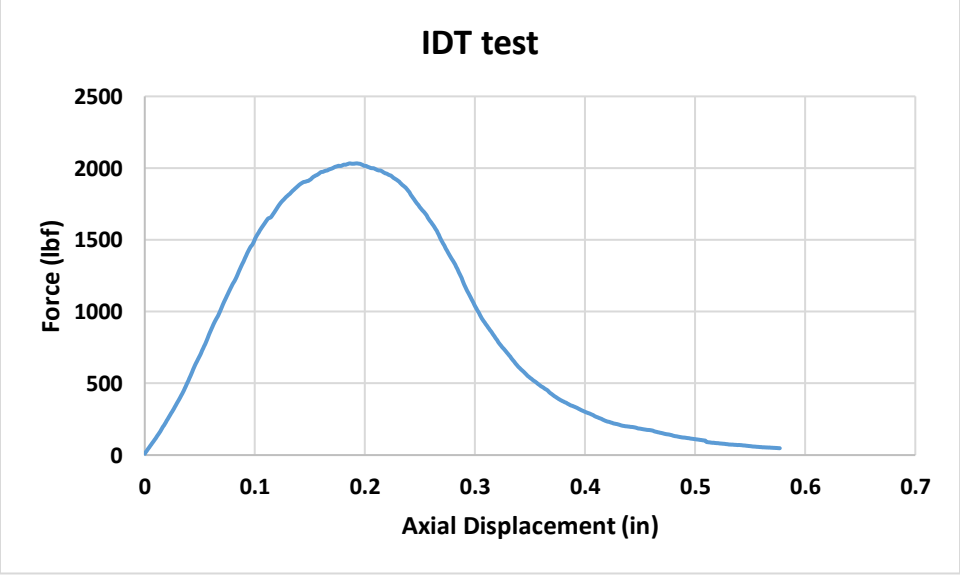

Figure C.10. Wet IDT Test Sample 0 percent RAP, 0 percent ASA, 4.25 percent B.C.

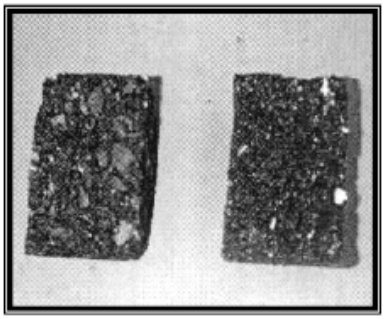

Figure 4
Specimen Broken for Observation

Calculations

The tensile strength is calculated using the following equation:

English units:

$$S_t = \frac{2P}{\pi t D}$$

where:
S_t = tensile strength, psi
P = maximum load, lbs
t = specimen thickness, in.
D = specimen diameter, in.

SI units:

$$S_t = \frac{2000P}{\pi t D}$$

where:
S_t = tensile strength, kPa
P = maximum load, Newtons
t = specimen thickness, mm
D = specimen diameter, mm

The tensile strength ratio is calculated as follows:

$$\text{Tensile Strength Ratio (TSR)} = \frac{S_2}{S_1}$$

where:
S_1 = average tensile strength of the dry subset, psi (kPa)
S_2 = average tensile strength of the conditioned subset, psi (kPa)

Figure C.11. TSR Calculations from AASHTO T 283

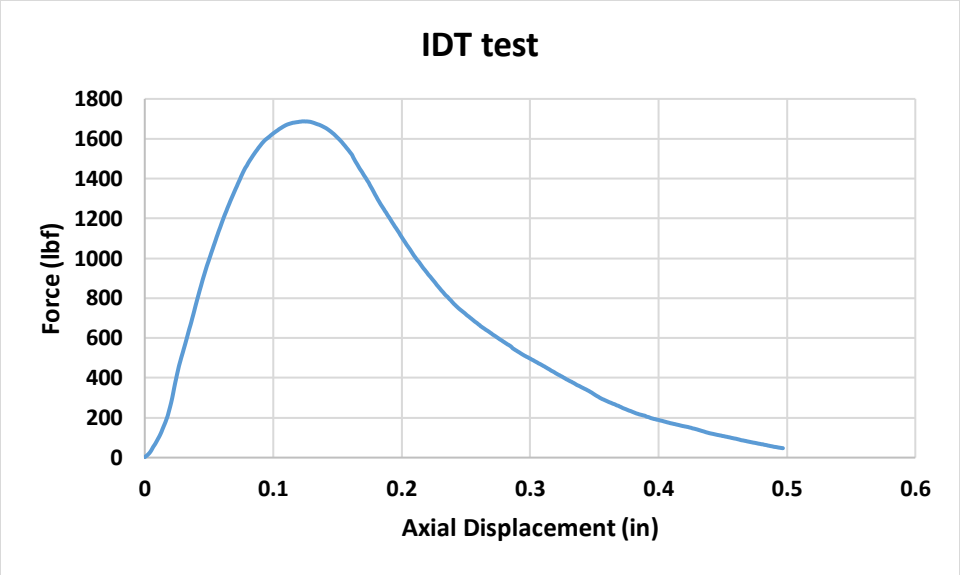

Figure C.12. IDT Crack Test Sample PG 58-34, 0 percent RAP, 5.0 percent B.C.

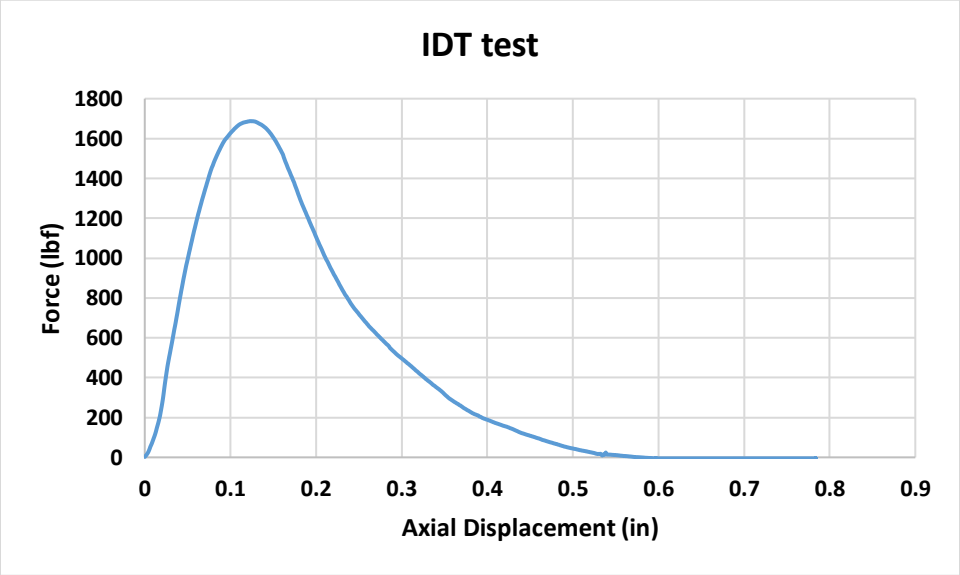

Figure C.13. IDT Cracking Test Sample 2 PG 58-34, 0 percent RAP, 5.0 percent B.C.

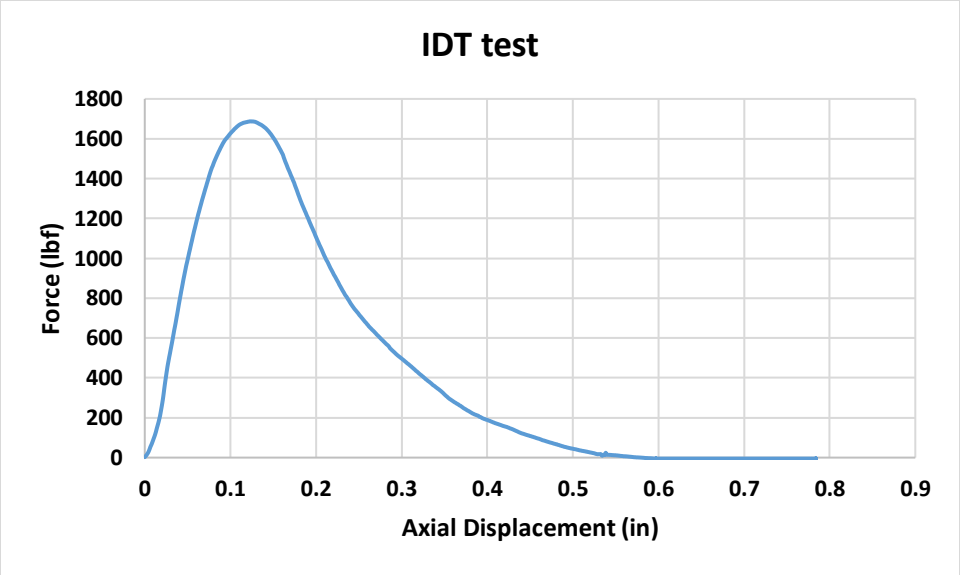

Figure C.14. IDT Cracking Test Sample 3 PG58-34, 0 percent RAP, 5.0 percent B.C.

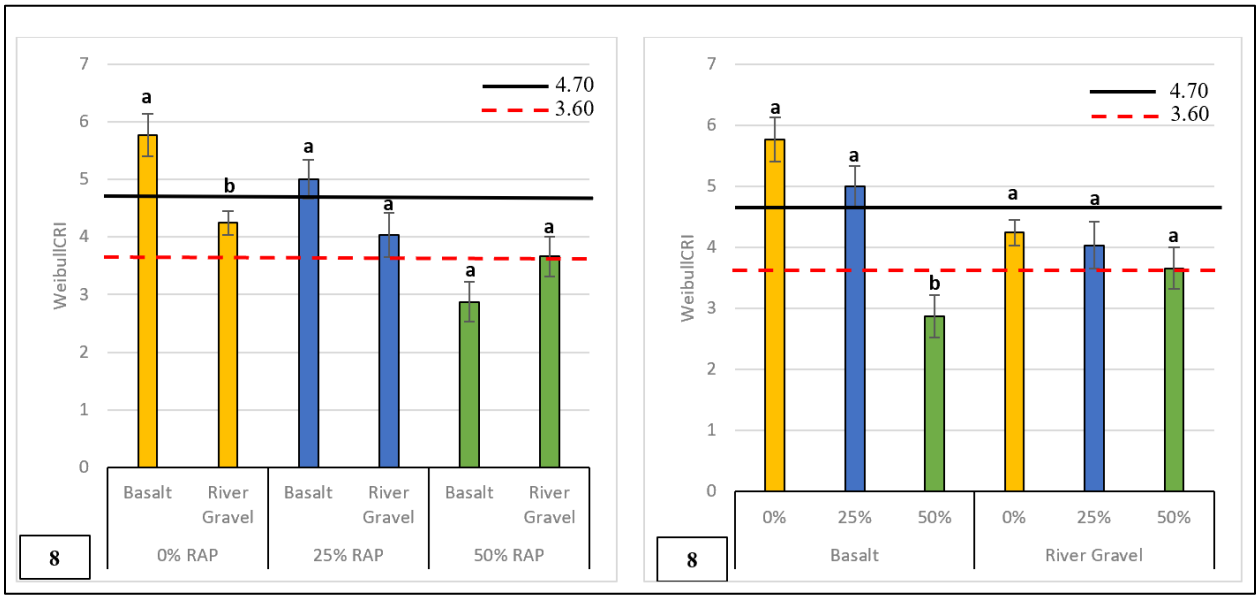

Figure C.15. Weibull$_{CRI}$ of Basalt and River Gravel

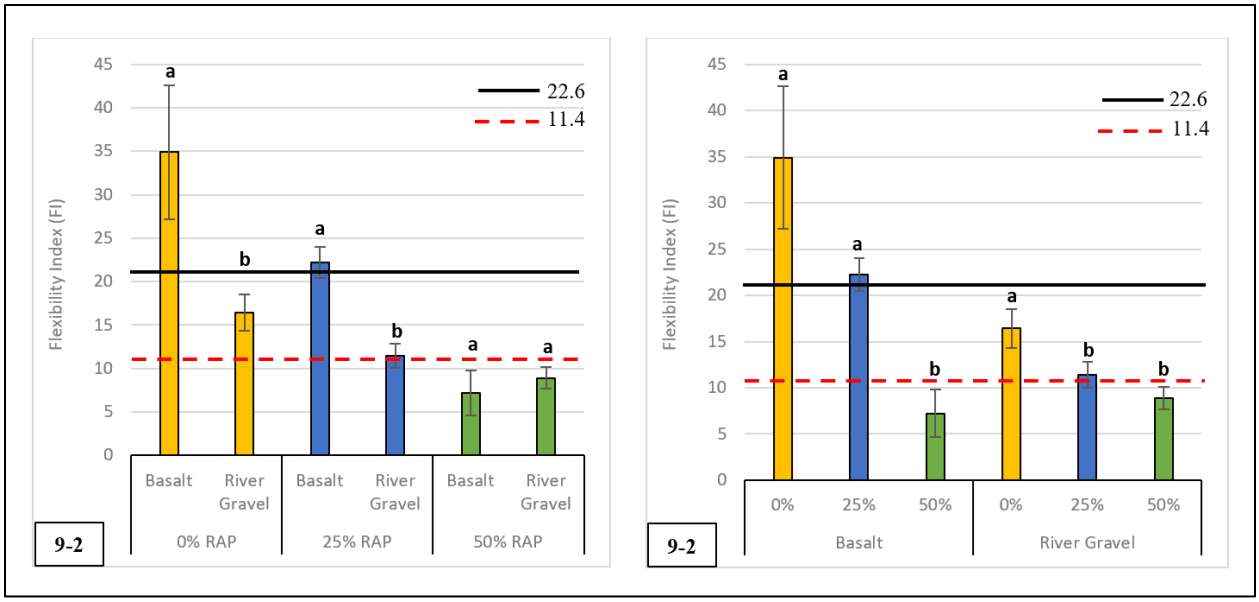

Figure C.16. FI of Basalt and River Gravel

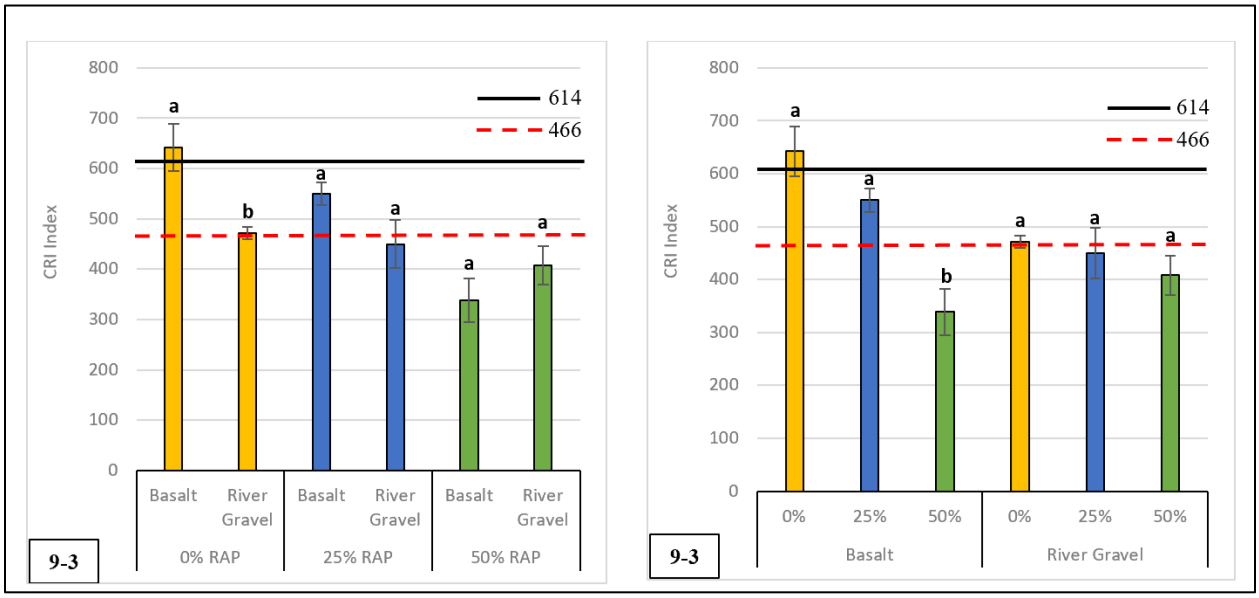

Figure C.17. CRI of Basalt and River Gravel

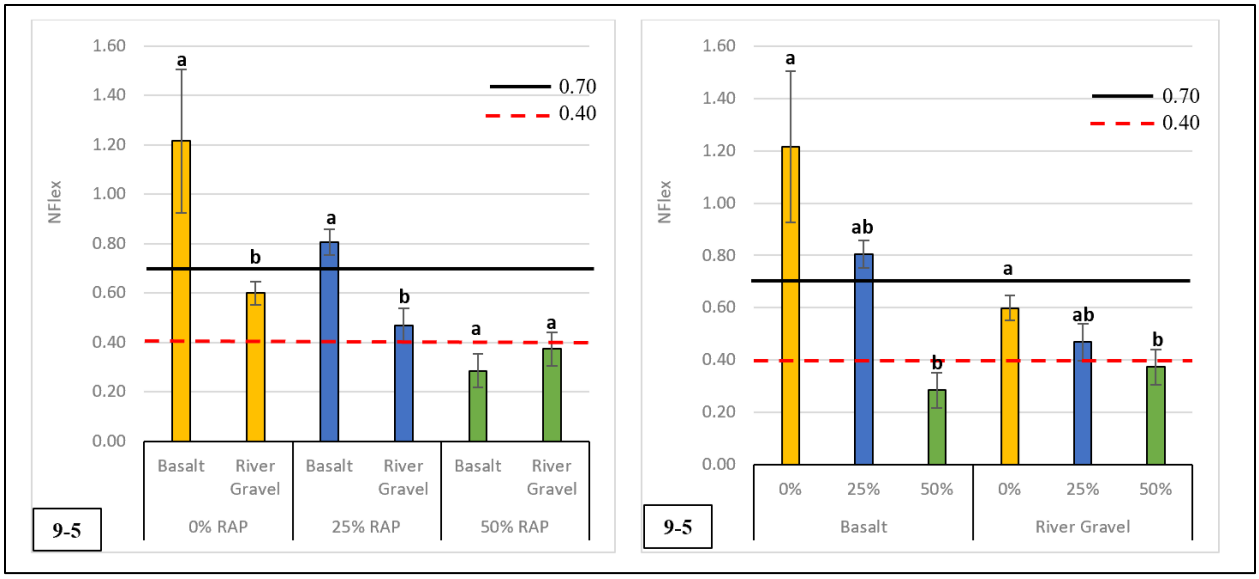

Figure C.18. N_{Flex} of Basalt and River Gravel

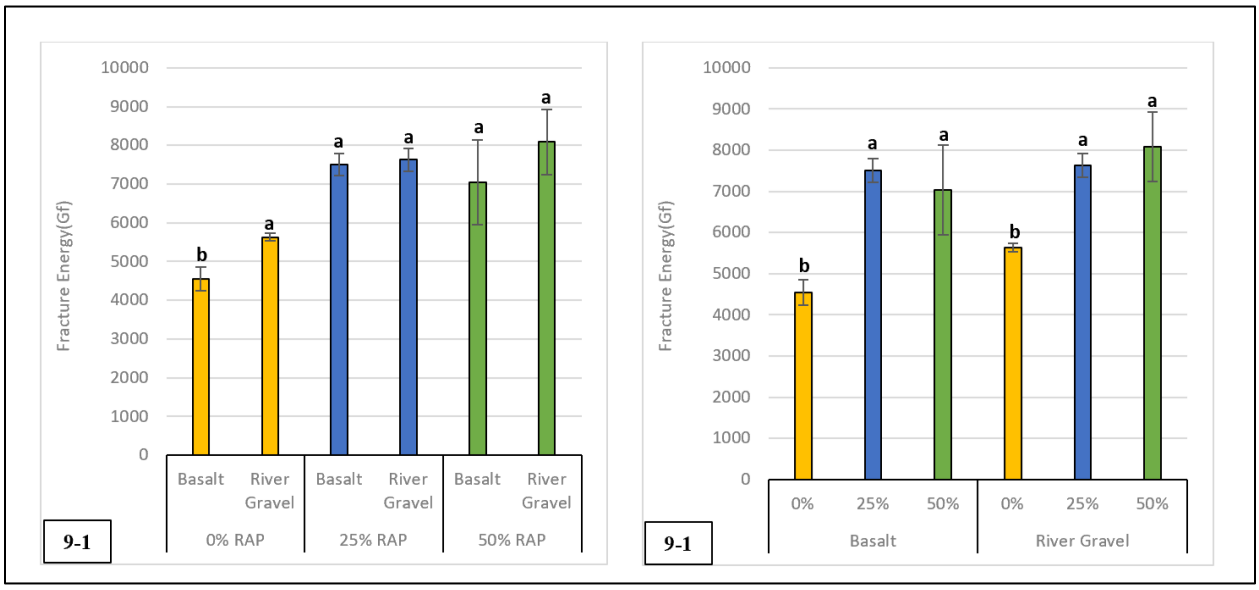

Figure C.19. G_f of Basalt and River Gravel

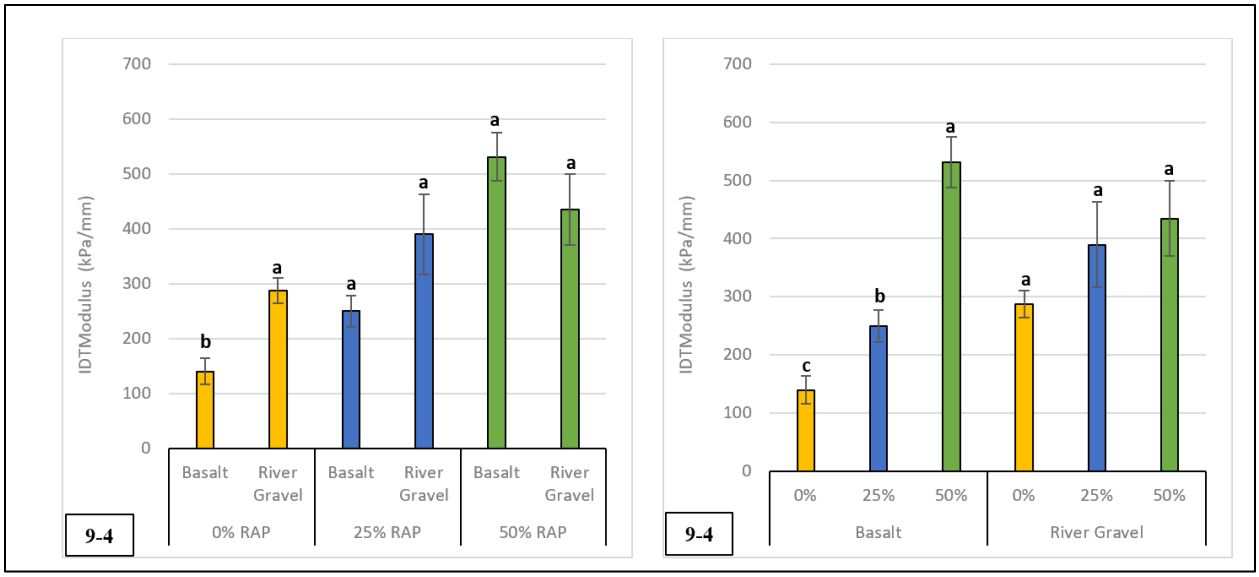

Figure C.20. IDT Modulus (kPa/mm) of Basalt and River Gravel